FUNCTIONAL CHARACTERIZATION OF THE NIPAH VIRUS NUCLEOCAPSID PROTEIN AND ITS IMPLICATIONS ON NIPAH VIRUS REPLICATION

BY

CHARLENE RANADHEERA

B.SC. (MICROBIOLOGY) UNIVERSITY OF MANITOBA 2002

A THESIS SUBMITTED TO THE FACULTY OF GRADUATE STUDIES OF THE UNIVERSITY OF MANITOBA IN PARTIAL FULFILLMENT OF THE REQUIREMENTS FOR THE DEGREE OF

DOCTOR OF PHILOSOPHY

IN

MEDICAL MICROBIOLOGY AND INFECTIOUS DISEASES
UNIVERSITY OF MANITOBA
WINNIPEG, MANITOBA

THE UNIVERSITY OF MANITOBA

FACULTY OF GRADUATE STUDIES

*****

COPYRIGHT PERMISSION

FUNCTIONAL CHARACTERIZATION OF THE NIPAH VIRUS NUCLEOCAPSID PROTEIN AND ITS IMPLICATIONS ON NIPAH VIRUS REPLICATION

BY

Charlene Ranadheera

A Thesis/Practicum submitted to the Faculty of Graduate Studies of The University of Manitoba in partial fulfillment of the requirement of the degree

DOCTOR OF PHILOSOPHY

ABSTRACT

FUNCTIONAL CHARACTERIZATION OF THE NIPAH VIRUS NUCLEOCAPSID PROTEIN AND ITS IMPLICATIONS ON NIPAH VIRUS REPLICATION

By

Charlene Ranadheera

University of Manitoba, January 2008

Nipah virus (NiV) was identified as the causative agent for outbreaks of meningitis, encephalitis, and respiratory disease in Malaysia, Singapore, Bangladesh, and India. Due to the ease in transmission, high fatality rates and lack of preventative or therapeutic treatments NiV has been classified as a biosafety level 4 agent. This emphasizes the need for research focusing on the development of effective vaccines and/or antiviral therapies against NiV infections. The objective of this study was to determine whether interfering with normal interactions between the NiV nucleocapsid protein (N) and the NiV phosphoprotein (P) would result in the disruption of viral replication.

Together with NiV P and the NiV polymerase protein (L), NiV N forms a replicase that generates full-length anti-genomic and genomic RNA. The newly synthesized full-length genomic viral RNA is encapsidated by NiV N as a fundamental step in virus particle formation. For both of these processes to occur, it is essential that NiV N interacts with NiV P. In the absence of NiV N, NiV P along with NiV L forms a transcriptase, which is responsible for the synthesis of viral mRNA. I hypothesized that transient recombinant expression of NiV N would interact with virally-expressed NiV P, causing a functional transformation of the transcriptase into a replicase. This hypothetical change in function, the transcriptase to a replicase, would lead to the impairment of viral transcription and translation, thereby causing an overall disruption to viral replication.

The work presented here demonstrates that increased expression of recombinant NiV N correlated with a 74% and 98% decrease in viral transcription and translation, respectively, and a 94% decrease in the production of full-length genomic RNA. As a result, infectivity levels decreased by 4 orders of magnitude in cells expressing recombinant NiV N when compared to those of control cells. Similar results were obtained when using truncated NiV N peptides containing the binding domains for NiV P. These findings provide a novel target for the development of antivirals aimed at disrupting the viral polymerase complex of negative-stranded viruses.

ACKNOWLEDGMENTS

I have so many people to thank who have contributed to my training over the past five and a half years. I hope that I can honour them appropriately.

I would like to begin by thanking my supervisor Markus Czub. Your mentorship and support over the last years have meant so much to me. Your excitement and passion for science was infectious and I have learned so much from you. You have inspired me and provoked my curiosity, which I have no doubt will continue to help me in my future scientific endeavours. Thank you for seeing the potential and taking a chance on me. I look forward to new and exciting future endeavours together.

To my graduate committee, Kevin, Dave, and Tom thank you for your continued encouragement and guidance, your insights were truly helpful. You pushed me to be better and to look a little bit deeper and for that, I am most grateful. To the department of Medical Microbiology and Infectious Disease and the Faculty of Graduate Studies at the University of Manitoba I appreciate all of the dedication and support you showed to me over the years.

I have to extend a special thank you to Hana Weingartl. I appreciate your ongoing willingness to assist me with anything I need, whether theoretical or technical. You insights and expertise over the years have been so appreciated and I have learned so much from you.

John Rutherford, thank you so much for lending me your time, help, and expertise using the confocal microscope. I would also like to thank Lynn Burton for dedicating her time to assisting me with the electron microscopy imaging.

I have to convey my sincere thanks and appreciation for Michael Carpenter. Thank you so much for your help, support and generosity over the years. You have taught me so much about proteomics and I truly appreciate that. I look forward to our future collaborations together.

I would also like to extend my appreciation to Krystal Rypien for her assistance with the statistical analysis of the data within this thesis.

To my Special Pathogens family, you have made these past five years exciting, interesting and never boring. Getting to know all of you has been an amazing experience for me. It has been such a privilege to have work with so many amazing people. The knowledge and expertise you have are incredible and thank you for sharing it with me. I have to pay a special thank you to Heinz Feldmann. It has been a pleasure to work with you. Your guidance, insights and help over the years has been most rewarding. Your ongoing support was truly appreciated and I look forward to working with you again.

Now to the Nipah Group... what can I say... Allen, I am so grateful for you patience and your brain... especially in those first few months, where all you heard was "Allen, can you help me?", "Allen, what should I do now?", "Allen, can you fix this?" You have taught me so much and you will always be my Superhero Tech! Nina, life in the lab with the two of us was never boring, from our 80's tunes, to our Western blot dancing, to festive lab decorating skills and most importantly our tag-team skills... thank you for your friendship and support over the years! Bevan, thanks for always supporting me, your willingness help whenever I needed you, and of course for your endless ability to listen to me whine and complain. Bevan I have always appreciated your brain and thank you for sharing it with me, I appreciate that you were will to proofread my thesis for me. I will miss working with you and I wish you all the best in the future. Roxy, you kept me sane throughout the insanity. I do not know how to thank you for everything. Your insights, your help in and out of level four, your support, your encouragement, and most of all your friendship means so much to me. Last but by no means least, Shane. You never fail to amaze me, you make me laugh, you make me cry, and sometimes you even make me angry. But no matter what you always supported me and were always willing to help me even if it meant endless hours in level four. I do not know how to thank you enough.

To my friends, you know who you are, thank you for your continued support, love and encouragement. I would not have survived the last five years without you. My "DITES" sisters, Candace, Adrienne and Roxanne, we have seen each other through the best and worst of it and I can hardly wait to see what the future has for us. Lisa, your friendship over the past few years, your help, and encouragement to me has meant so much to me and has helped me through some hard times. Andrea, Carla, and Andrea, how can I say thank you enough, you have been with me since the beginning, I love you guys and could never have done this without you cheering me on.

Finally, and most importantly, I would like to thank my family. I could never have accomplished my goals and so much more without you. You always had faith in me and supported me through anything and everything. You held me accountable and encouraged me to strive for more. More importantly, you have instilled in me values, which will help me in my life and future scientific career. You have been such a blessing to me and there are no words that can convey my appreciation and love for you

There are so many other people who have inspired me and have contributed to this dissertation, to all of you I extend me sincere thanks and gratitude.

This is what the Lord says, He who made the earth, the Lord who formed it and established it - the Lord is his name. 'Call to me and I will answer you and tell you great and unsearchable things you do not know'

Jeremiah 33:2-3 (NIV)

TABLE OF CONTENTS

LIST OF TABLES

LIST OF FIGURES

PAGE

ABBREVIATIONS

293T	Human embryonic kidney cells
aa	Amino acid
ATP	Adenosine triphosphate
BDV	Borna disease virus
BME	β-mercaptoethanol
BSA	Bovine Serum Albumin
BSL	Biosafety Level
$C0_2$	Carbon dioxide
CFP	Cyan fluorescent protein
CL	Containment level
CMV	Cytomegalovirus
CNS	Central Nervous System
CPE	Cytopathic effect
C-terminal	Carboxyl-terminal
Da	Dalton
ddH_20	Double distilled water
DMEM	Dulbecco's Modified Eagles Medium
DNA	Deoxyribonucleic acid
dNTP	Deoxyribonucleotide triphosphate
et al	et alli (latin for "and others")
E.coli	*Escherichia coli*
EDTA	Ethylenediamine tetraacetic acid
ER	Endoplasmic reticulum
F	Fusion Protein
FBS	Fetal Bovine Serum
FITC	Fluorescein Isothiocynate
G	Attachment Glycoprotein
g	Gravitational force
GAPDH	Glyceraldehyde-3-phosphate dehydrogenase
GFP	Green fluorescent protein
H_20	Water
HA	Hemagglutinin
HeV	Hendra virus
HPIV3	Human parainfluenza virus 3
HRP	Horseradish peroxidase
i.e.	id est (latin for "that is")
IFA	Immunofluorescence Assay
IFN	Interferon
IFU	Infectious unit
IgG	Immunoglobulin G
IRES	Internal ribosomal entry site
kb	Kilobase

kDa	Kilodalton
L	L protein
LB	Luria-Bertani
M	Matrix Protein
mA	Milliamp
MeV	Measles virus
$MgCl_2$	Magnesium chloride
min	Minute
ml	Millilitre
mM	Millimolar
MOI	Multiplicity of infection
mRNA	Messenger RNA
N	Nucleocapsid protein
NaCl	Sodium chloride
NC	Nucleocapsid
NDV	Newcastle disease virus
NES	Nuclear export signal
NiV	Nipah virus
NLS	Nuclear localization signal
nm	Nanometer
NP-40	Nonidet-P40
N-terminal	Amino-terminal
NTR	Non-translated Region
°C	Degrees celsius
OD	Optical density
ORF	Open reading frame
P	Phosphoprotein
PAGE	Polyacrylamide gel electrophoresis
PARP	Poly-ADP-ribose polymerase
PBS	Phosphate buffered saline
PCR	Polymerase chain reaction
PFU	Plaque forming unit
PVDF	Polyvinylidene fluoride
RNA	Ribonucleic acid
RNP	Ribonucleoprotein
rpm	Revolutions per minute
RPV	Rinderpest virus
RSV	Respiratory syncytial virus
RT	Reverse transcription
RT-PCR	Reverse transcription polymerase chain reaction
RV	Rabies virus
RVFV	Rift Valley Fever Virus
SDS	Sodium dodecyl sulphate
Sec	Seconds
SeV	Sendai virus
SSC	Sodium chloride sodium citrate

SV40	Simian virus 40
TAE	Tris-acetate-EDTA
$TCID_{50}$	Tissue culture infectivity dose 50
TNE	Tris-NaCl-EDTA
UV	Ultraviolet
V	Volts
VeroE6	African green monkey cells
VSV	Vesicular stomatitis virus
α	Alpha
β	Beta
µg	Microgram
µl	Microlitre
µM	Mircromolar

1.0 Introduction

Henipavirus represents a newly formed genus within the subfamily: *Paramyxovirinae,* family: *Paramyxoviridae* and order: *Mononegavirales.* This genus contains two recently emerged members, Hendra virus (HeV), the prototypic virus, which emerged in Australia, and Nipah virus (NiV), which emerged in Southeast Asia. Unlike other paramyxoviruses, Henipaviruses have been classified as biosafety level four (BSL-4) containment viruses due to their ability to cause a life threatening disease in both humans and animals with no preventative vaccines and/or therapeutic treatments. Furthermore, the possibility of human-to-human transmission increases the risk factors of weaponizing this virus as a bioterrorism agent. Henipaviruses are transmitted from animals to humans. Pteropid fruit bats are suspected to be the natural reservoir for these viruses and have a direct role in the transmission of Henipaviruses to their host. Other paramyxoviruses, such as Menangle and Tioman viruses, have also been shown to use similar bats as their natural reservoirs (31;79;114).

1.1 Emergence and Epidemics of Henipaviruses

1.1.1 Emergence and Viral Transmission of HeV

In 1994, a number of horses in Australia presented with a pulmonary disease (58;136;140;164;184). It was found that individuals working closely together with these animals, such as veterinarians and trainers, were later inflicted with similar respiratory ailments (58;81;184). An unknown infectious agent was isolated from the kidney of a horse trainer who died during the course

of infection (164). Ultrastructure analysis of this infectious agent revealed typical features typical of viruses within the order Mononegavirales: herringbone nucleocapsids (NC), pleomorphic shapes, and surface protein spike projections (129). Serological tests demonstrated that the unknown virus cross-reacted with convalescent sera from infected patients and horses. However, anti-sera derived from other paramyxoviruses such as measles virus (MeV), canine distemper virus (CDV) and rinderpest virus (RPV) were unable to neutralize it. Further characterization classified this virus as HeV (129). Since the initial outbreak in 1994, HeV has re-emerged sporadically throughout Australia (58;59). Currently, the only method of controlling and containing the spread of infection is through the euthanization of suspected animals and the isolation of infected individuals. Viral transmission is believed to occur through close contact with infected bodily secretions and fluids (81;192). Since HeV infections in humans have been limited, case fatality rates are unknown.

1.1.2 Emergence and Viral Transmission of NiV

In 1998 and early 1999, reports surfaced of an epidemic of respiratory disease in pigs and acute febrile encephalitis in humans. Initial evidence indicated that Japanese encephalitis virus was the causative agent for this disease in humans. However, after vaccination campaigns and mosquito control, the disease was still rampant (184). Within the same period, there was an outbreak of respiratory illness in pigs, initially believed to be caused by classical swine fever virus. However, it was soon discovered that the disease in pigs

correlated with the disease in humans and the infectious agent responsible for these diseases was identified as a novel virus: NiV, a close relative of HeV (24;25;33). For some time, it was unknown how pigs and/or humans became exposed to NiV. It soon became evident that fruit bats were a potential transmission factor for NiV. Initially, Henipavirus epidemics were correlated with the birthing patterns of fruit bats, since Henipaviruses have been isolated from bat uterine fluid and aborted fetal tissue (80;124). However, the birthing period for fruit bats (late spring, early summer) did not seem to correlate with all of the observed Henipavirus outbreak periods. A more likely theory suggests that animals contracted the virus from exposure to contaminated bat secretions/excretion (117). Consequently, humans became exposed to NiV through contact with bodily excretions and fluids of infected animals, such as pigs. During 1998, viral spread was aided by the transfer of infected pigs to other farms where new outbreaks subsequently occurred (24;25). Attempts to control the spread of NiV led to the culling of over a million pigs. During this outbreak, approximately 40% of humans infected with NiV individuals succumbed to the infection.

Following the initial outbreak of NiV in Southeast Asia, a number of smaller NiV outbreaks were reported in regions in and surrounding India and Bangladesh. During a 2004 NiV outbreak in Bangladesh, researchers were able to make several distinctions between the present epidemic and the initial outbreak in 1998. Differences observed included: increased neurological complications, increased mortality rates upwards to 70%, and potential human-

to-human transmission. It was suggested that the increased rate of mortality in 2004, as compared to 1998, was attributed to the higher proportion of individuals experiencing severe neurological symptoms. Another factor attributing to the higher mortality rates observed may have been the lack of an animal intermediate, such as pigs, which would have been involved in the transmission of NiV from its natural reservoir into humans. It could be speculated that passaging this virus through an animal intermediate, such as pigs, could render the virus less virulent; thereby, explaining the lower mortality rates seen in the Malaysian 1998 outbreak. Sequence comparison between the Malaysian strain and the Bangladeshi strain demonstrated a nucleotide identitiy of approximately 92%, with changes found within both the open reading frames (ORF), resulting in amino acid (aa) changes in almost all viral proteins, and the non-translated regions (NTR) (82). These changes supported the idea that the sequence variation between the two strains had an effect on virus pathogenesis. As previously mentioned, this outbreak also provided the evidence that NiV could be transmitted human-to-human. In Meherpur and Naogaon districts, clusters of cases were reported which occurred within families, indicating that exposure to infected individuals and their secretions were possible risk factors of virus transmission (93). Throughout this outbreak, it was believed that humans were initially infected through exposure to materials contaminated with infectious bat urine/excreta such as contaminated food. Once the individual became ill, they passed it on to family members. The onset of illness within family members occurred over an extended period of time, suggesting that

individual family members were not infected from the same source of NiV but rather from multiple sources (93). One likely source of exposure included caring for sick family members, suggesting that NiV was transmitted from patient-to-patient (93). Figure 1 demonstrates the similarities and differences seen between NiV-transmission during the two major outbreaks of NiV.

1.2 Natural Reservoir of Henipaviruses

There are 58 species of flying foxes and a variety of these species has been screened for the presence of Henipaviruses. The presence of antibodies against Henipaviruses and/or isolation of live virus were used as indicators for Henipavirus infections, since the infection in bats is sub-clinical (58). During the Malaysian outbreak of NiV, bats from the following species were found to be serologically positive for NiV-specific antibodies: *Cynopterus brachyotis, Eonyveteris spelaea, Scotophuilus kuhli, Pteropus vampyrus* and *Pteropus hypomelanus* (201), with NiV specifically isolated from *Pteropus hypomelanus* (30). During the NiV epidemic in Bangladesh, bats of the species *Pteropus giganteus* were positive for NiV-specific antibodies (93). A epidemiological study conducted in Cambodia in 2005 revealed bats of the species *Pteropus lylei* to be serologically-positive against NiV, with NiV successfully isolated from two of the infected bats (137;156). Finally, a study in Papua New Guinea demonstrated the presence of bats, which were sero-positive for HeV-antibodies (79). Currently, eight species of fruit bats are known to be sero-positive for Henipavirus-specific antibodies. These epidemiological studies provided evidence that fruit bats or

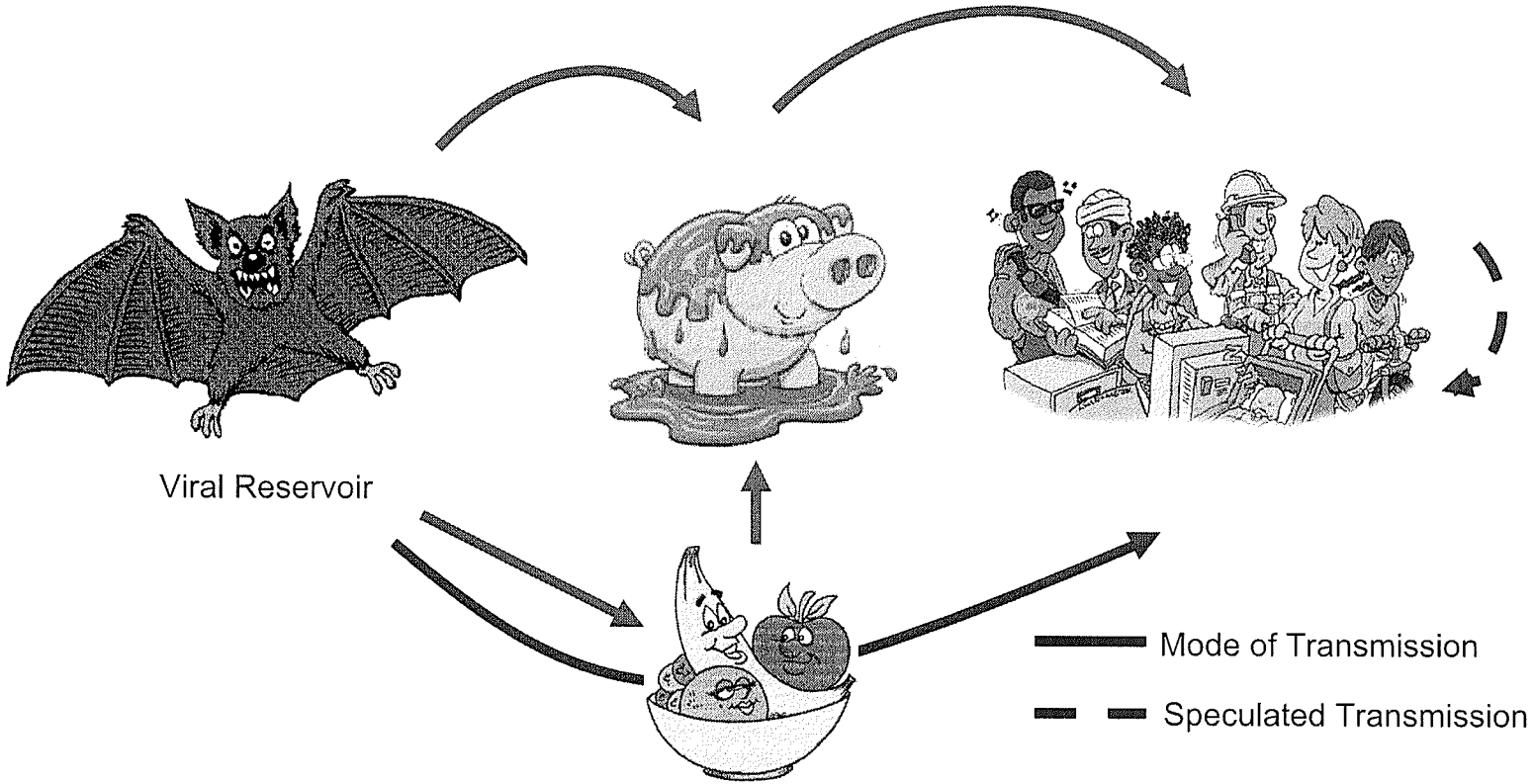

Figure 1: Mechanisms of Transmission for NiV. The Malaysian outbreak of 1998 demonstrated the presence of a porcine intermediate, which was essential for the transmission of NiV from its natural reservoir into humans. However, the more recent Bangladesh outbreak of 2004 demonstrated a higher mortality rate and the direct transmission of NiV from bats to humans, with possible human to human transmission.

flying foxes, of the suborder *Megachiroptera*, were the natural reservoir for HeV and NiV (30;80;137;165;201).

Flying foxes have a vast geographic distribution spanning from Madagascar, South and Southeast Asia, the Philippines, the Pacific Islands, and Australia. Accordingly, Henipavirus outbreaks have occurred within these regions: Australia, Malaysia, Bangladesh, North and West Bengal, India, and Uttar Pradesh. However, there have been no reported cases of NiV infections in Africa. Furthermore, previously mentioned screening expeditions have demonstrated the presence of Henipaviruses within regions where human outbreaks have not yet occurred. These findings suggest that the distribution of Henipaviruses is far greater than the observed outbreak locations, and as such carry the potential for epidemics to occur in new regions.

1.3 Henipavirus Infection

1.3.1 Clinical Signs and Disease

Upon infection with NiV or HeV there is an incubation period, which ranges from days to three weeks in both animals and humans (73). Experimentally infected pigs (125;191), hamsters (196), cats (89;125;128;193) and horses (88;195) demonstrated similar incubation periods.

Horses showed signs and symptoms characteristic of a severe pulmonary disease and pulmonary oedema: severe pneumonia, high respiratory rate, fever, increased heart rate, lethargy, and anorexia. Another symptom observed in HeV-infected horses was a frothy nasal discharge, which led to airway blockages

(81;140;164;192). In addition to the apparent respiratory disease, a neurological disease was also observed in 2 out of 22 horses infected with HeV. In humans, the HeV infection was associated with a severe respiratory disease with additional neurological symptoms. There has been one documented case of meningoencephalitis (136;140). Since the initial outbreak in 1994, four individuals have been identified as being infected with HeV, and two of the four succumbed to the infection. The two survivors developed a milder disease mainly presenting with respiratory symptoms (136;140;164).

Symptoms associated with NiV infection during the Malaysian outbreak were primarily respiratory symptoms in pigs, while infections in humans demonstrated both respiratory and neurological signs. The NiV infection in pigs was mainly asymptomatic; however approximately 10-20% of infected pigs presented with a disease characterized by respiratory complications, with a small percentage of pigs developing a neurological illness. These findings were also verified experimentally (191). The NiV-associated disease in humans was described mainly by pulmonary symptoms and more severe cases included the development of neurological complications, cough, dyspnea, fever, headache, dizziness, vomiting, seizures, reduced levels of consciousness and prominent brain stem dysfunction. Features of this disease included segmental myoclonus, areflexia and hypotonia, hypertension and tachycardia, suggesting that the brainstem and upper cervical spinal cord were involved. A follow-up study with 116 of the NiV-infected patients confirmed that the spinal cord was damaged due to the NiV infection (73;115).

1.3.2 Henipavirus Persistence

A relapse of clinical signs associated with both HeV and NiV infections has been documented. An Australian male who was infected with HeV and recovered from meningitis, died one year later due to progressive encephalitis (136;140). Symptomatic relapse of a NiV-associated disease has also been reported in 12 out of 64 patients surviving the Malaysian outbreak. Patients demonstrated a long latency period, on average 8.3 months between detection of initial symptoms and the reappearance of neurological symptoms (73;179;180). Furthermore at the late-onset of disease, a significant increase in NiV/HeV-specific antibodies was observed, indirectly indicating the presence of replicating virus (136;197). This finding was similar to MeV-infected patients experiencing late-onset of subacute sclerosing panencephalitis (197). Taken together, the relapse in neurological symptoms and the increasing antibody titres suggest the presence of replicating virus and therefore viral persistence for both HeV and NiV is a possibility.

1.3.3 NiV Pathology

In humans, the main histopathological findings were systemic vasculitis, meningitis, and encephalitis. Respiratory and lymphatic organs were also damaged either directly or indirectly. Experimental studies in pigs have demonstrated that viral replication occurs within blood vessels, trachea, lymph nodes, and the central nervous system (CNS) (191). In pigs, it appears that NiV infects the olfactory and respiratory cells, cranial nerves and immune cells such

as peripheral mononuclear blood cells. Infection of these cells cause the initiation of viremia and the further spread into the reticuloendothelial system, including replication in the endothelial cells of the blood and lymphatic vessels (191). Viremia is implied by positive immunostaining of the lymphocytes and monocytes/macrophages. A small percentage of these infected pigs displayed signs of neurological illness. The presence of a neurological illness could be inadvertently caused by the host defence system responding to the NiV infection or due to the presence of NiV replicating in the brain. Experimental studies were conducted to provide further insights into these two possibilities. It has been demonstrated that NiV was able to gain access to the CNS via the olfactory nerves, although other mechanisms of invading that CNS were also possible (191). These findings indicated that NiV was able to replicate in the brain and was subsequently responsible for the neurological symptoms observed.

1.4 Henipavirus Biology

Henipaviruses closely resemble other paramyxoviruses. They are spherical viruses and range in size from 120nm to 500nm (32). As with all members of the order *Mononegavirales*, NiV and HeV are enveloped viruses containing a negative-sense single-stranded RNA genome. While members within the family *Paramyxoviridae* have relatively uniform genome sizes, 15-16kb (84), NiV and HeV have two of the larger genomes within this group of viruses, 18,246 and 18,234 nucleotides respectively (83;84;189), with only the recently discovered J virus having a larger viral genome (97).

Henipavirus genomes consists of six genes in the order, 3' – N – P/V/W/C – M – F – G – L – 5' (Figure 2a), which are similarly organized like morbilliviruses and Respiroviruses. The six genes encode at least six structural proteins, the nucleocapsid (N) protein, the phosphoprotein (P), the matrix (M) protein, the fusion (F) protein, the attachment (G) glycoprotein and the viral RNA-dependant RNA polymerase (L) protein. Viral membranes are studded with two glycoproteins, the G protein, which is involved in viral attachment to the cellular receptor, and the F protein, which is involved in the fusion of the viral and cellular membranes. The M protein mediates viral assembly by interacting with the viral glycoproteins and the viral core, the ribonucleoprotein (RNP) complex, initiating viral egress while also providing structural support. The RNP complex consists of all of the factors necessary for transcription and replication of viral gene products and genome: the viral genome, the N protein, which encapsidates the viral genome and the polymerase complex, consisting of the L protein and its co-factor the P protein. A diagrammatical representation of the virion is demonstrated in Figure 2b.

1.5 Viral Life Cycle

Currently, little is known about the NiV- or HeV-life cycle. Therefore, models have been adopted from other paramyxoviruses as well as from other negative-stranded RNA viruses. An overview of the Henipavirus-life cycle is diagrammatically represented in Figure 3, (Adapted from (110)).

A

B

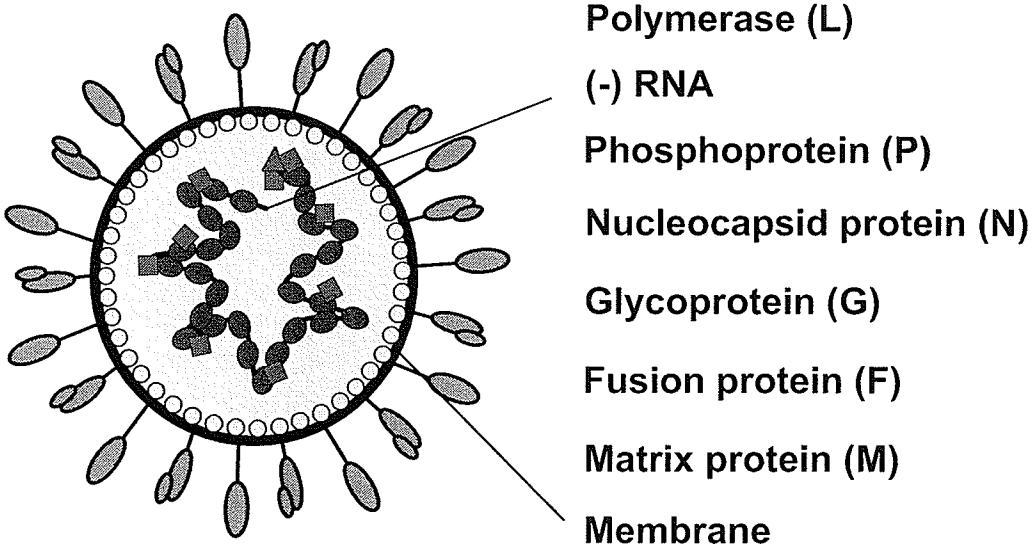

Figure 2: Henipavirus Structure and Organization. (A) A diagrammatical representation of the Henipavirus genetic structure. (B) A diagrammatical representation of Henipavirus virion structure and organization.

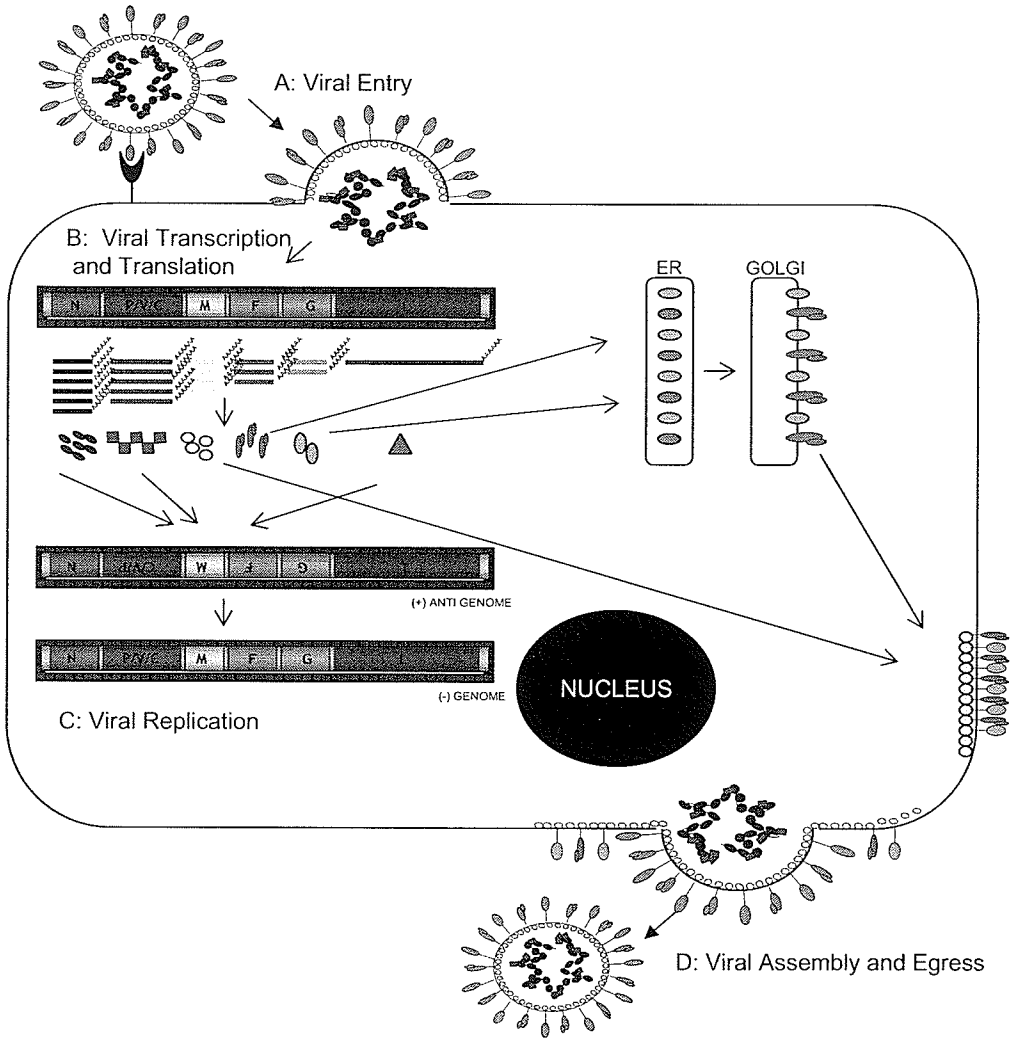

Figure 3: Henipavirus Life Cycle. A general schematic of the proposed Henipavirus life cycle. (A) Viral Entry- Henipaviruses bind the cellular receptor, Ephrin B2, via the G protein. F and G proteins mediate fusion of the viral and plasma membranes allowing the release of the viral RNP complex into the cytoplasm of cells. (B) Viral Transcription and Translation- the polymerase complex or the transcriptase, comprised of L and P proteins, transcribe viral mRNA from the template genomic RNA and cellular ribosomal machinery synthesize viral proteins. Viral proteins are further post-translationally modified, if necessary, and are recruited to specific sub-cellular locations in order to mediate viral egress. (C) Viral Replication- upon synthesis of viral proteins, the N protein binds to the polymerase creating a replicase complex. This complex is necessary for the production of viral genomic RNA. The template negative-sense genomic RNA is used to synthesize positive-sense anti-genome, which further acts to synthesize viral negative-sense genomic RNA. (D) Viral egress- M proteins mediate viral assembly and egress. The M protein mediates recruitment of viral proteins and genomic RNA to the plasma membrane where virus assembly and egress from the plasma membrane occurs.

1.5.1 Viral Entry

The attachment of NiV or HeV to cells and the subsequent release of NiV- and HeV-RNP complexes into cells is dependant upon the presence of specific cellular receptors. Recently, two studies using distinct experimental approaches simultaneously identified the use of Ephrin B2 as the major cellular attachment protein for NiV and HeV (14;133). It is believed that through binding this cellular receptor a conformational change is induced in the G protein, which activates the F protein (110). Subsequently, the activated F protein mediates the fusion of the viral and cellular membranes allowing entry of the viral RNP complex into the cytoplasm of cells (110).

1.5.2 Viral Replication

Replication studies focusing specifically on HeV or NiV are limited. However, based on evolutionary relatedness to other negative-stranded RNA viruses, NiV and HeV are believed to carry out similar methods of replication. The initial step in viral replication is the production of viral mRNA followed by the subsequent production of viral proteins. Upon the accumulation of viral proteins, the second stage of viral replication begins to emerge, more specifically the production of full-length anti-genomic and genomic RNA. Figure 4 diagrammatically represents the various stages observed during Henipavirus replication (110).

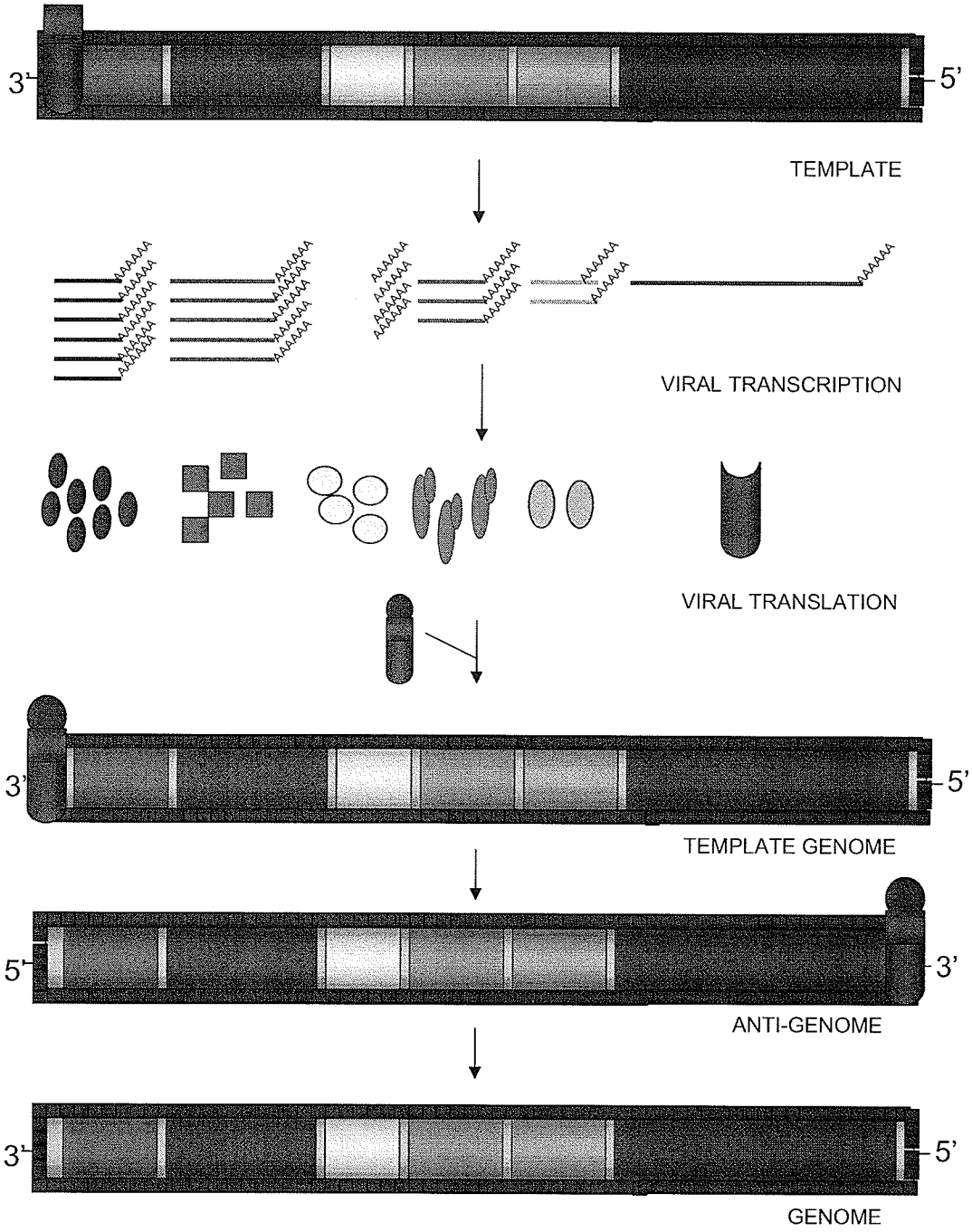

Figure 4: General Strategies of Viral Replication for Most Negative-Stranded RNA Viruses. The transcriptase complex, P and L proteins, mediates the production of viral transcripts. Cellular machinery is responsible for the translation of viral proteins. Upon the synthesis of viral proteins, the N protein is able to bind to the transcriptase complex forming a replicase complex, N, P and L. The replicase complex mediates the production of viral (anti-) genomic RNA.

1.5.2.1 Viral Transcription

After viral attachment, membrane fusion and the subsequent release of the RNP into the cytoplasm of cells, the first step of viral replication is the transcription of viral genes. The transcriptase, a viral polymerase complex consisting of the P and L proteins, is believed to bind and scan through the leader region of the template RNA, Figure 5. This region is represented by the first 52 nucleotides of the viral genome containing various polymerase-binding sites and packaging signals. The signals within the leader region likely direct viral transcription at the first viral gene, the N gene. In the past, it was believed that a "Single Initiation Stop-Start Model" was responsible for the transcription of viral mRNAs (55). This theory proposed that the polymerase complex positioned itself at position 1 of the 3' end of the genome, transcribed a leader region and then subsequent downstream genes (55). Once the polymerase complex reached the end of the gene, it ceased transcription of the viral RNA, "scanned" the intergenic region, and reinitiated transcription at the next gene consensus sequence.

However, recent studies with vesicular stomatitis virus (VSV) have begun to question aspects of this hypothesis. VSV, a related virus found within the family *Rhabdoviridae* and order *Mononegavirales,* is believed to have similar replication strategies as paramyxoviruses. Using a UV mapping technique it was demonstrated that VSV N mRNA transcripts, representing the first gene, were present in infected cells without the requirement for the transcription of the leader RNA (194). In 2004, another group more directly

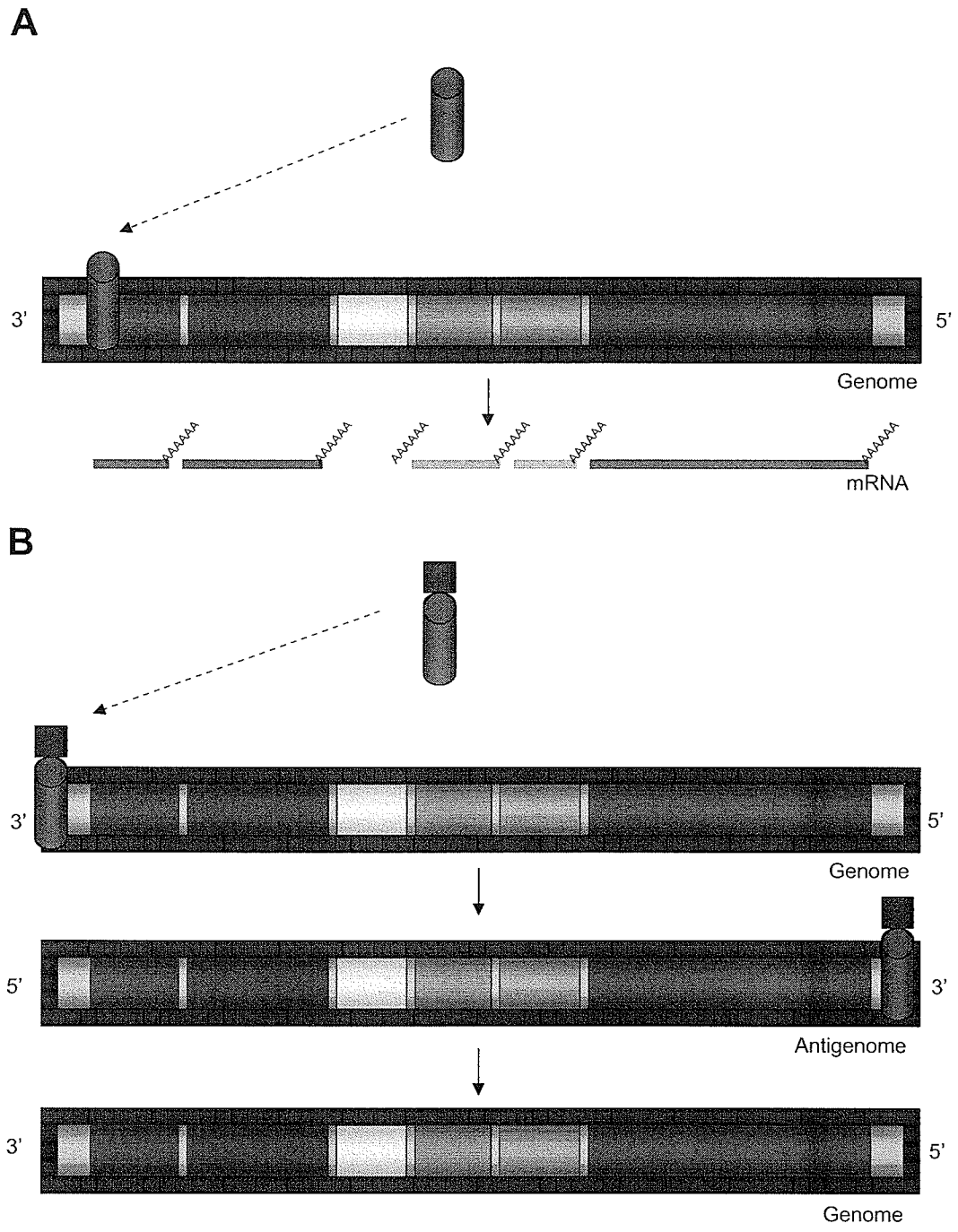

Figure 5: Schematic Representation of the Proposed NiV Polymerase Complexes: a Transcriptase and a Replicase. (A) Diagramatical representation of the NiV Transcriptase. The polymerase complex consists of the P and L proteins, which produces viral mRNA. (B) Diagrammatical representation of the NiV Replicase. The polymerase complex consists of N, P and L proteins, which synthesizes full-length genomic RNA.

identified the initiation point of the transcriptase. They purified viral transcriptases from infected cells and used them to synthesize viral transcripts *in vitro* (154). They also observed the presence of viral mRNA whereas leader RNA was not present (154). These results led to a modified version of the previously described theory: the transcriptase will bind to the genome at the 3' end but will only initiate transcription at the transcriptional start signal in the N gene, which is 56 nucleotides downstream of the 3' genomic end (154;194). The difference regarding the presence of the leader RNA is significant in understanding the different stages of replication. It is not the transcriptase, which is responsible for the synthesis of the leader sequence but rather the replicase (see Section 1.5.2.2).

Production of all viral mRNA is believed to occur through the stuttering of the viral transcriptase along the viral RNA template in a start-stop manner (55). This suggests that the polymerase complex has the tendency to "fall off" the viral template as it gets further away from the 3' end of the genome. A stepwise decrease in viral transcripts occurs as the genes to be transcribed approach the 5' end of the genome. This may be due to the differences in transcriptional regulation at various gene boundaries and/or polyadenylation signals (100;198). Currently, there are a number of studies to support the idea that there are more transcripts produced from the 3' end of the genome than the 5' end of the genome (23;86). More specifically one study analyzing HeV transcripts, using quantitative real-time PCR to demonstrate the relative presence of viral transcripts, indicated two points of attenuation during viral transcription (198).

Levels of viral transcripts for HeV N, P, and M were relatively equivalent (198). A 5.5 fold decrease in the level of F transcripts was seen in comparison to M transcripts (198). The level of viral transcripts for F and G were relatively stable, and then a second point of attenuation with a 2.2 fold decrease was observed between the levels of G and L transcripts (198). These results demonstrated a gradient production of viral transcripts (albeit not a linear gradient) as the transcriptase progressed along the viral genome, with viral genes found closer to the 3' end of the genome being transcribed more readily than genes found at the 5' end of the genome. Interestingly, viral proteins that are needed in large amounts, such as the N protein, are located towards the 3' end of the genome; while proteins that are needed at lower levels, such as the L protein, are located at the 5' end of the genome. Therefore, it appears that the virus has positioned its genes within the genome depending on the relative amounts of proteins needed to propagate viral replication. Viral transcripts are further translated using the host's ribosomal cellular machinery producing the necessary viral proteins that are essential for the subsequent production of anti-genomic and genomic RNA, and virion assembly.

1.5.2.2 Synthesis of Viral Full-length Genome

Upon production of viral proteins, specifically the RNP complex proteins (N, P and L proteins), the production of full-length viral anti-genome and genome is possible. Currently, there are many uncertainties as to what is truly happening at the transition from transcription of viral mRNA to synthesis of viral anti-genome

and genome. Historically, the most commonly accepted theory of replication was focused around the expression of the viral N proteins. It was believed that as the amount of the N protein accumulated in a cell and reached a certain threshold it would mask the intergenic regions on the genomic template strand, allowing the polymerase complex (P and L proteins) to read-through the genomic template and synthesize full-length anti-genomic RNA rather than mRNA. Anti-genomic RNA would subsequently be used as a template to create full-length genomic RNA in the same manner. N proteins alone, and their ability to mask the intergenic regions on the template strand, were believed to mediate the transition from viral transcription to viral genome replication (110). However, recent studies with VSV have modified this hypothesis of replication. Gupta *et al*, found that a trimeric polymerase complex or more specifically a replicase complex, made up of N, P and L proteins, was essential in producing viral genomes; whereas, the transcriptase complex, made of only P and L proteins but not the N protein, was necessary for the production of viral mRNA (78;154), Figure 5. This modified hypothesis fits into the historically accepted hypothesis of replication except rather than N proteins masking the intergenic regions of the template strand and regulating the production of full-length viral RNA, N proteins have a role in the formation of the trimeric replicase complex (N-P-L), which go on to regulate viral genome synthesis. From these findings, Gupta *et al* suggested that the N protein has the ability to bind and modify the transcriptase complex into a replicase complex (78). The replicase then has the ability to bind at position 1 of the 3' end of the genome and read-through the intergenic regions on the genomic template

without falling off and produce anti-genomic RNA. The replicase complex will then use the anti-genome as a template for the synthesis of genomic RNA.

These recent insights into viral replication have led to a "Two Polymerase Entry Model of Replication" theory (34). Production of viral transcripts or full-length viral RNA is predetermined based upon the formation of a transcriptase complex (P-L) (41;44;64;65;78;154) or a replicase complex (N-P-L) (39;78;90;154;186;187), respectively. The levels of N proteins still play an important role in the synthesis of genomic RNA; increased levels of N proteins have the potential to increase the tendency towards formation of the replicase complex but do not solely contribute to the transition from viral transcription to replication of the viral genome.

Additional modifications to this hypothesis have also been made due to the recent studies with VSV. It was found that the transcriptase may have entered the genome at the 3' end but it did not initiate transcription until reaching the transcriptional start sequence found in the N gene (194); however, the replicase entered and initiated viral replication at the 3' most end of the genome, position 1 (154;194). In the event that sufficient amounts of the N-P protein complexes were not available for encapsidation, the replicase only produced leader RNA (194). The production of only leader RNA demonstrates premature initiation of viral replication. The replicase likely terminates viral replication until sufficient amounts of N-P protein complexes are present for encapsidation and then production of full-length genome will proceed (154). These findings demonstrated that the leader region contains two distinctive initiation sites for

viral RNA synthesis, one for viral transcription and the other for viral genome and anti-genome production. These results also support the theory that there are two structurally and functionally distinct viral polymerases.

1.5.2.3 Encapsidation of the Viral Genome

Apart from the synthesis of the viral genome, increased expression levels of the N protein are also essential for encapsidation of the newly synthesized viral genome. Due to the cytoplasmic-based replication strategy of these viruses, it is necessary for the viral full-length RNA to be protected from the harsh cytoplasmic environment and RNA digestion. Therefore, upon synthesis of anti-genomic and genomic RNA, the RNA is encapsidated within a protective shell composed of N proteins. N proteins make a number of important interactions throughout the viral life cycle, two of which are the interaction with other N molecules and viral RNA. However, N proteins are also able to bind non-specifically to cellular RNA rendering the N proteins unavailable for viral replication. In an attempt to direct N proteins towards viral replication, newly synthesized P proteins were found to be important to maintain N proteins in a useable manner for viral replication, Figure 6 (91;144). The P protein will bind the N protein and act as a chaperone to enhance the specificity of the N protein towards binding viral RNA versus non-specific cellular RNA (8;29;42;43;45;56;66;134;143;153;172;200;205). Upon contact with the viral RNA, the N protein will dissociate from the P protein. The P protein will then go

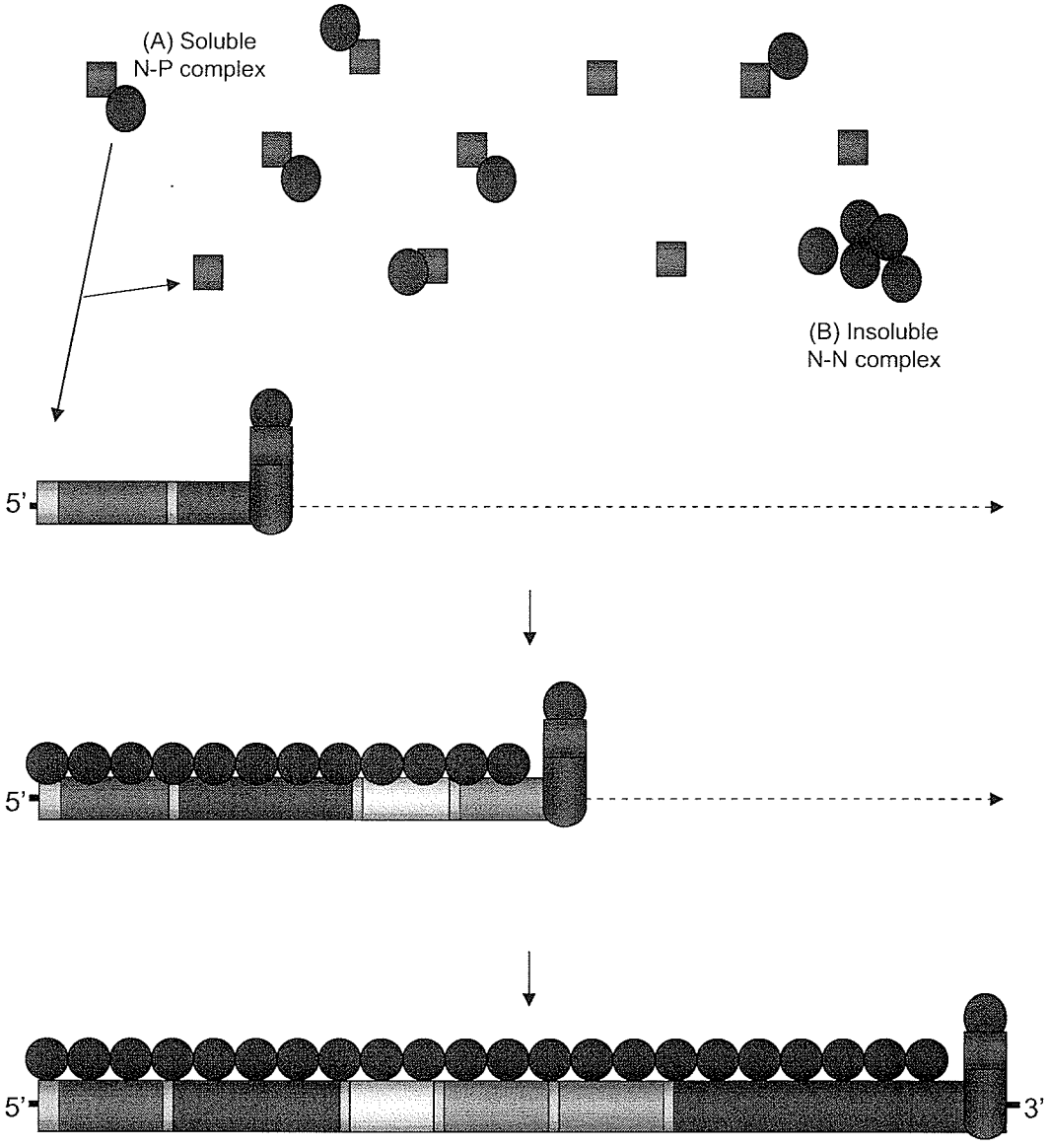

Figure 6: Mechanisms of Viral Encapsidation. The N protein is essential for viral encapsidation. (A) The P protein is believed to associate with N proteins and act as a chaperone to direct binding of the N protein to viral RNA. (B) In the absence of P proteins, the N protein is able to interact with other N proteins, bind cellular RNA and become unavailable for viral encapsidation.

on to bind other N proteins and direct them towards the specific encapsidation of viral RNA (40;42;60;87;90;173).

1.5.3 Viral Assembly and Egress

Upon production of the viral proteins and viral genome encapsidation, the M protein mediates assembly of these viral components into a virion (110;177). M proteins are membrane-associated proteins which have been suggested to crosslink the viral core (the RNP complex) and the viral surface glycoproteins (36;126;161;176;204). In the absence of virus assembly and egress, the M protein is believed to localize around the perinuclear region of the cell, awaiting contact with the RNP (46;71;120;150;160;176). Upon binding the RNP, the RNP-M protein complex translocates to the plasma membrane to interact with the cytoplasmic tails of the viral surface glycoproteins (46;71;120;150;160;176). The M protein concentrates the surface glycoproteins into patches on the plasma membrane in order to mediate efficient virus assembly and to optimize the number of glycoprotein surface spikes found on the newly produced virion (131;176;203). Upon interactions between the RNP-M complex with the surface glycoproteins, the M protein provides the driving force, which will initiate viral egress or budding from the plasma membrane (36;67;110;121;177). An essential component for M proteins to generate this driving force is the presence of late domains. These motifs interact with cellular factors, which are crucial to mediate the release of the virion from the cell membrane (61;127). Recently, it was discovered that the presence of a late domain (YPDL), which is similar to the

late domain found within equine infectious anaemia virus, was found within the NiV M protein and was responsible for virus budding (35). By creating a recombinant system and a series of mutations within the M protein, these authors were able to demonstrate that the late domain found within the NiV M protein was essential to viral egress (35).

1.6 Structural Characterization of N proteins

There have been very few structural studies investigating the various N proteins within the order *Mononegavirales.* Currently, there are three groups, which have reported the N protein crystal structure for various members of the order *Mononegavirales*: Borna Disease Virus (BDV), rabies virus (RV) and VSV. These findings provided some suggestions to describe the structural and functional domains within the N protein, specifically focusing on how the N protein interacted with viral RNA and other N protein molecules.

The analysis of the BDV N crystal structure demonstrated the presence of a novel fold, which divided the N proteins into two distinct halves: an amino-terminal (N-terminal) half and a carboxyl-terminal (C-terminal) half (159). This structural moiety was primarily composed of alpha- (α) helices; however, the presence of two beta- (β) strands was the important component that provided the division of the two distinct regions (159). Additionally, the N proteins are able to self-assemble and form an elongated cube structure, which likely represented the oligomerization of a NC structure (159). Each layer of this structure contained four N proteins and then each layer was subsequently stacked one on top of the

other (159). This protein formation created a positively-charged central channel (159). This channel was large enough to accommodate a single-strand of RNA and its positive charge was complementary to binding RNA, due to the negative charge of the sugar-phosphate backbone of RNA. On the other hand, a large positively-charged cleft was found running diagonally across the surface of the protein, which was also suitable for binding single-stranded RNA (159). These findings suggested two potential locations, which could be responsible for the binding of RNA. However, it remained unclear where the viral RNA would be situated. If RNA were bound within the central channel, it would be completely surrounded by N proteins and protected from RNase degradation. However, it would be necessary for N proteins to dissociate from the viral RNA so that the polymerase complex could gain access to the viral RNA during viral replication (159). If RNA were bound within the positively-charged groove running diagonally across the tetramer surface, it would be more accessible to the viral polymerase complex; however, at the same time exposed to RNase digestion (159). There are advantages and disadvantages to either of the potential binding sites; however, this experimental setup was not able to deduce the region critical for RNA binding. Thus, further investigations were needed to answer this question.

Analysis of the RV and VSV N protein structure revealed similar findings when compared to the protein structure of BDV N. It was observed that 10 and 11 N proteins formed circular rings, for VSV and RV respectively (6;76). These rings were then packed head-to-head forming cylindrical cores containing a

hollow inner channel (6), similar to the cuboid structure described for BDV N proteins (76). The structural analysis of BDV N indicated there could be two potential sites that could accommodate viral RNA. The studies with VSV and RV N proteins helped to determine whether RNA was bound within the central channel, or within a cleft on the outer surface. Unlike the BDV N crystal structure, the crystal structures of RV and VSV N proteins were done in association with synthetic pieces of viral RNA. When crystallized, the synthetic RNA was found present within the inner channel. This finding suggests that under infectious conditions, the viral genome would also be found within the inner core of the protein structure and subsequently would be protected from cellular RNAses (6;76). Similar to the BDV study, the crystal structures of RV and VSV N proteins demonstrated that each monomer was divided into two domains: an N-terminal domain and a C-terminal domain (6;76). More importantly, the junction at which the N-terminal domain met the C-terminal domain was capable of tightly binding synthetic RNA (6;76).

The crystal structures presented for BDV N, VSV N, and RV N proteins provided clues as to the conformation and structure of the N proteins when bound to RNA, with specific emphasis on the junction between the N- and C-terminal halves. However, these studies were not able to shed any insight into how N proteins associated with P proteins and whether there were any important changes to the protein structure. It could be speculated that since the central region of the N protein was necessary for binding RNA, the N- and C-terminal ends of the protein could be important for binding P proteins and interacting with

other N protein. Further structural studies analyzing the interactions between N proteins and P proteins would provide interesting insights into further understanding various aspects of viral replication. Overall, a common structural design was observed for the N proteins of three different viruses; therefore, it could be assumed that N proteins from other member of the order *Mononegavirales* could take on similar structural features.

1.7 Functional domains of paramyxovirus N proteins – Interactions between P and N proteins

The interactions between N and P proteins of paramyxoviruses are necessary for forming an active replicase complex with the L protein and maintaining N proteins in a soluble state to mediate encapsidation of the viral genome. However, there is currently no structural information characterizing these interactions. Therefore, mutagenesis studies were employed in order to determine regions on the N protein, which may contain regions necessary for interacting with the P protein.

The C-terminal end of the N protein is an essential target for binding P proteins for many paramyxoviruses (9;19;40;85;135). The P binding domain of SeV N was localized to aa 463-488 (19;26;87). Similarly, (9;17)aa 304-374, 489-504, 517, and 525 on the MeV N protein were essential for binding MeV P proteins (9;17;105). Structural studies have confirmed these findings by demonstrating the ability of the N protein-binding domain of the MeV P protein to bind C-terminal peptides (aa 489-506) of the MeV N protein (104). Finally,

studies on Newcastle Disease virus (NDV) N proteins have shown that aa 440-489 were needed for binding P proteins (102). However, residues 1-26 also contained both essential and highly interactive domains for NDV P proteins (102). Interestingly, the N-terminal portion of the protein was seen to be more significant when compared with the C-terminal portion of the protein (102). Similarly, residues 4-188 of the MeV N protein was identified being capable of interacting with MeV P (9), and aa 1-400 of the SeV N protein contained an alternative SeV P protein-binding domain (20;87). A previous report described the presence of a NiV P protein-binding domain found at the C-terminal end of the N protein, between aa 468 and 496 (27). The authors utilized a protein-blot-protein overlay assay in order to analyze the interactions between NiV N and NiV P proteins, using a variety of denatured truncated proteins, which were expressed in a bacterial system. This assay was useful to analyze protein-protein interactions; however, was limited to analyzing the interaction between denatured proteins that may represent non-native conformations. Additionally, the use of a bacterial expression system, which alters the co- and post-translational modification scheme of the viral proteins, may also not represent an accurate picture. Since this system used less than optimal conditions, this brings about the question of whether the apparent P protein-binding domain was an artefact of this system. Therefore, determining the NiV P protein-binding domains based on the protein's native structure may be more biologically relevant. These findings were compiled using a ClustalW alignments program

(3) and a schematic was created to easily visualize the regions of the N protein which were important to binding P proteins, Figure 7.

Overall, these studies demonstrated the importance that the N- and C-terminal ends of the N protein have in binding P proteins for a variety of paramyxoviruses. These results suggested the presence of multiple functional P protein-binding sites, which may be used to explain the various roles that an N-P complex has in facilitating the replication cycle.

1.8 Rationale and Hypothesis

The N proteins of negative-stranded viruses play pivotal roles throughout the virus life cycle. They function in viral assembly and egress through an interaction of the RNP complex and the M protein, and contributes to the production and encapsidation of viral genomic and anti-genomic RNA. NiV N proteins are believed to have these same responsibilities. NiV N proteins may also interact with specific cellular factors, which could have an impact throughout the viral life cycle. In the presence of NiV N proteins, it is believed that the transcriptase complex (P-L) can be converted into a replicase complex (N-P-L), which would subsequently activate the synthesis of viral full-length RNA (not viral mRNA). Simultaneously, NiV N proteins would also be responsible for encapsidating this newly synthesized viral (anti-)genome. As N proteins increase, there will be a tendency towards the formation of a viral replicase; however, upon depletion of the N protein through viral encapsidation, the

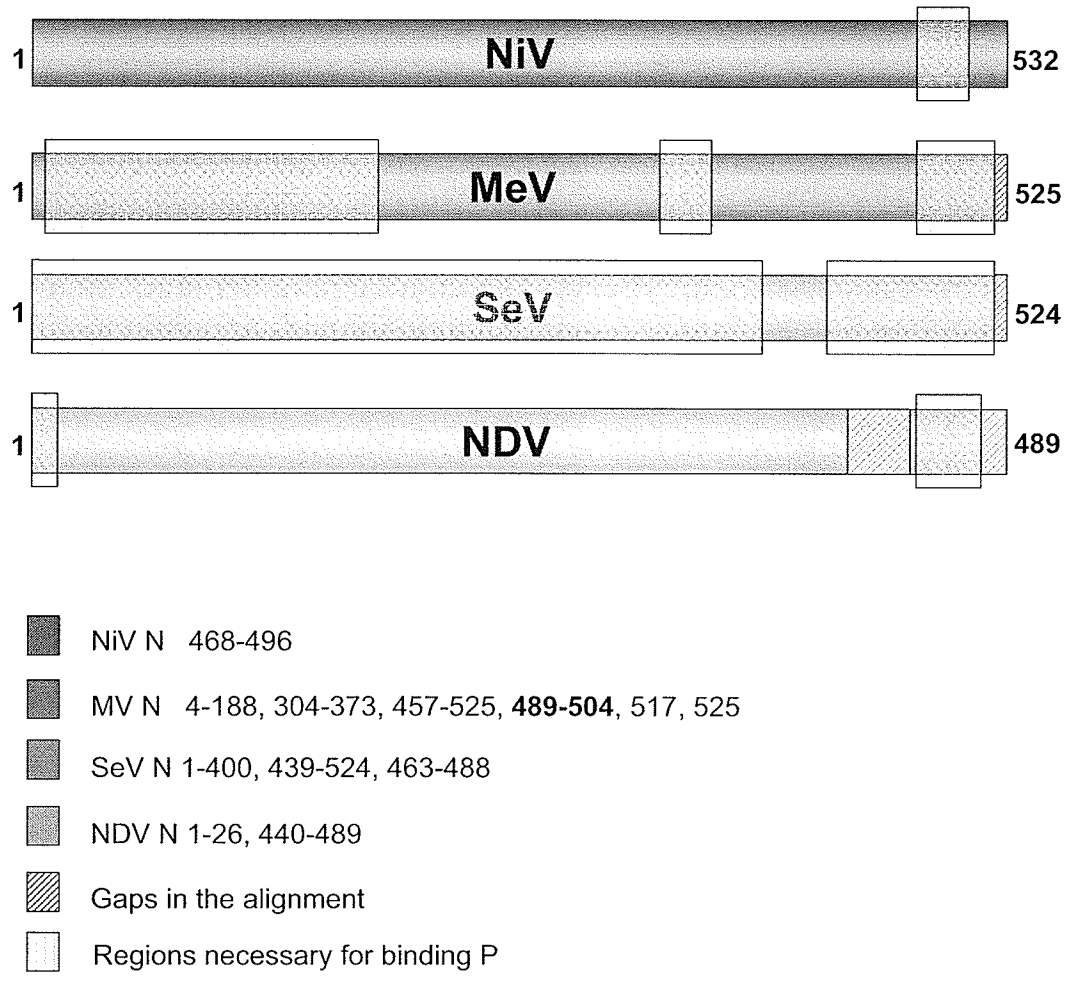

Figure 7: Comparison of the P Binding Sites Found on N proteins From Various Paramyxoviruses. A schematic diagram was compiled from various published data describing the P binding sites found on NiV, MeV, SeV and NDV N proteins (9,15,16,17,23,24,37,81,83,98,100,101). The N- and C-terminal ends of the N protein seem to be necessary for the binding of P proteins. Hashed regions indicate gaps found in the alignments and highlighted regions indicate areas necessary for binding P proteins.

production of a transcriptase would be favoured. This would suggest that the synthesis and encapsidation of the viral genome would provide a method of regulating the amounts of N protein produced. If there is no regulation of the amount of N proteins produced, a disproportionate presence of NiV N proteins could favour the synthesis of full-length viral RNA and potentially stall viral transcription.

The intent of this present research is to analyze the role of the NiV N protein during viral replication and to characterize the specific interaction between NiV N and NiV P proteins. I hypothesize that excess expression of recombinant full-length NiV N proteins will cause an imbalance in viral replication, enabling the premature formation of the replicase complex (N-P-L), through an interaction with the NiV P protein of the transcriptase complex (P-L). This result would thereby limit the availability of the transcriptase. It is expected that by favouring the formation of a premature replicase complex, a negative impact on viral transcription will be observed thus causing an overall decline of viral proteins. A decline in the production of viral proteins will eventually lead to a decline in the production of viral full-length viral RNA, since the products necessary for viral replication specifically the L protein would not be synthesized. Therefore, a decrease in both the production of viral mRNA and full-length (anti-) genomic RNA will occur when there is a disproportionate amount of NiV N proteins present. Furthermore, I believe that the NiV P protein-binding domains found on the NiV N proteins would be sufficient to disable viral replication. The NiV P protein-binding domains alone have the potential to occupy the binding site

on the transcriptase (via the P protein) and disable the function of the viral polymerases. The interaction between recombinant NiV N peptides and the NiV transcriptase may inhibit or alter an essential protein conformation, which is necessary for viral transcription and at the same time preventing the binding of viral full-length NiV N proteins to the transcriptase complex and thereby inhibiting the production of a functional replicase complex. Overall, it is speculated that the over-expression of the NiV N protein or a component of the NiV N protein will be sufficient to abrogate viral replication.

This study has three main objectives: (1) to identify the NiV P binding domains within the NiV N protein, (2) to determine whether the NiV N protein can have a negative impact on NiV replication and (3) to determine whether the NiV P binding domains found within the NiV N protein are capable of interfering with NiV replication. By completing these objectives, insights into NiV replication can be made and the antiviral potential of NiV N proteins assessed.

2.0 Materials and Methods

2.1 Cells and Viruses

293T (human embryonic kidney) cells were cultured in Dulbecco's modified Eagle's medium (DMEM, Sigma®) with 10% heat inactivated fetal bovine serum (FBS). Tissue culture dishes were coated with poly-D-lysine (1mg/ml, Sigma®) for 30 minutes (min) at 37°C to enhance cell attachment. Dishes were subsequently washed with sterile water prior to seeding of cells.

Vero-E6 (African green monkey) cells were cultured in DMEM supplemented with 10% FBS.

All cells were incubated in 5% CO_2 and H_20-saturated atmosphere conditions at 37°C. Cells were passaged by treatment with trypsin [0.25% Trypsin-EDTA (ethylenediamine tetraacetic acid), Gibco™] and diluted in culture medium every two to three days.

Escherichia coli (*E.coli*) Top 10 chemically competent cells (Invitrogen™) were made in house by growing 4ml of an overnight culture in 2 000ml (1:500 dilution) of Luria-Bertani (LB) broth at 37°C with shaking until the optical density (OD) at 660 nm (OD_{660}) wavelength was within 0.4-0.6. Cells were then pelleted by centrifugation at 2 000rpm at 4°C for 15 min and re-suspended in 300ml of Solution A (Appendix 1). Cells were incubated on ice for 20 min and pelleted by centrifugation at 2 000rpm for 15 min at 4°C. The pellet was then re-suspended in 60ml of Solution B (Appendix 1), aliquoted at stored at -80°C.

NiV was a kind gift from the Centers for Disease Control and Prevention (Atlanta, GA). Virus stocks were prepared by infecting a 70% sub-confluent monolayer of Vero-E6 cells in a 150cm^2 flask with NiV at a multiplicity of infection (MOI) of 0.01 (approximately 3x10^5 infectious units (IFU)/flask). Once the cells demonstrated a cytopathic effect (CPE) of +3 out of a +5 scale (approximately three days post-infection), the supernatants were collected and clarified by centrifugation at 1 000xg for 10 min to remove any residual cell debris. Virus stocks were aliquoted and then frozen in liquid nitrogen. NiV infectivity titres of the aliquoted stock were determined to be 2 x10^7 IFU/ml in 293T cells using a tissue culture infectivity dose 50 ($TCID_{50}$,) assay, Section 2.24. Handling of NiV was done under containment level 4 (CL-4) conditions as outlined in the Health Canada Laboratory Bio-safety Guidelines CL-4 handling procedures (www.hc-sc.gc.ca/pphb-dgspsp/publicat/lbg-ldmbl-96/index.html) and Center for Disease Control Material Safety Data Sheet.

2.2 Antibodies and Primers

See Appendix 2 for a list of primary and secondary antibodies used. NiV specific antibodies were a kind gift from Dr. Hana Weingartl from the Canadian Food Inspection Agency, Winnipeg, Canada.

See Appendix 3 for a list of primers used. Primers designed against NiV were based on sequences from genbank, ascension number: NC002728.

2.3 RNA Extraction

Viral RNA extractions of NiV stocks were carried out to generate template for RT-PCR reactions. Viral stocks, described in Section 2.1, were treated with TRIzol LS® (GibcoBRL) and RNA was extracted using a modified version of the TRIzol LS® protocol (GibcoBRL). In brief, viral RNA was isolated from supernatants of infected cells in the following manner: 1) Homogenization of the extract in TRIzol LS®. 2) Phase separation of RNA, DNA and proteins with the addition of chloroform. RNA is found in the aqueous phase, DNA is found in the interphase and the phenol phase, and protein is found in the phenol phase. 3) Precipitation of RNA, with the addition of 20-40µg/ml of glycogen to act as a carrier molecule to increase RNA precipitation from supernatants, followed by the addition of isopropyl alcohol. 4) RNA wash with 75% ethanol and 5) Re-dissolving RNA in DNase/RNase free water.

2.4 Polymerase Chain Reaction (PCR)

PCR reactions described in this manuscript were preformed using Pfu Ultra Hotstart™ DNA polymerase (Stratagene®) in a Whatman Biometra® TGradient thermocycler. Pfu Ultra Hotstart™ DNA polymerase was chosen since it has been shown to have robust PCR product yields at the same time as having proofreading activity resulting in lower error rates. PCR was used to amplify viral genes from plasmid DNA. In general, a typical 150µl reaction consisted of 15µl of 10x PfuUltra™ HF reaction buffer, 6.0µl of deoxynucleotide triphosphate (dNTP) solution (10mM each) (Invitrogen™), 3.0µl of 20µM forward primer, 3.0µl

of 20µM reverse primer, 150ng of DNA plasmid, 3ul (7.5 units) of PfuUltra™ Hotstart DNA polymerase and the volume was brought up to 150µl with sterile water. All reactions were set up on ice. See Appendix 3 for a list of primers used and inserts created using PCR. General cycling conditions are outlined in Table 1.

Table 1: General thermocycling parameters for PCR

Number of cycles	Time	Temperature	Cycle Description
1x	15 min	95°C	Activation of DNA polymerase
30-50x	1 min 1 min 1-3 min	95°C 50-60°C 68-72°C	Denaturation Annealing Elongation
1x	7 min	68-72°C	Final elongation
1x	hold	4°C	Final cooling

2.4.1 Reverse Transcription Polymerase Chain Reaction (RT-PCR)

RT-PCR reactions were conducted using Qiagen One-Step RT-PCR™ kit and performed in a Whatman Biometra® TGradient Thermocycler. See Appendix 3 for a list of primers and inserts which were created using RT-PCR. RT-PCR was used to amplify viral genes from viral RNA. A 50µl reaction was prepared: 10µl of 5x RT-PCR buffer, 2µl of 10mM dNTP solution, 1µl of 20µM forward primer, 1µl of 20µM reverse primer, 2µl One-step RT-PCR Enzyme Mix™, a varying amount of RNA, and the volume was brought up to 50µl with sterile water. All reactions were set up on ice. A general outline of cycling conditions is presented in Table 2.

Table 2: General thermocycling parameters for RT-PCR

Number of Cycles	Time	Temperature	Cycle Description
1x	30 min	50°C	Reverse transcription
1x	15 min	95°C	Activation of HotstarTaq™ polymerase
50x	2 min 1 min 1-5 min	95°C 50-55°C 68°C	Denaturation Annealing Elongation
1x	7 min	68°C	Final elongation
1x	hold	4°C	Final cooling

2.4.2 Amplicon Analysis

Production of all amplicons was verified for size and quality by running a sample of the DNA on a 1.0% agarose gel, followed by gel electrophoresis and visualization by UV illumination. Gels were made with and run in 1x Tris acetate EDTA (TAE) buffer, and contained 0.002% ethidium bromide, which was used to stain DNA. Typically one sixth (5µl) of the reaction was mixed with 6x Gel loading buffer (Appendix 1). A molecular weight marker, 2 log DNA ladder™ (New England Biolabs, Appendix 4), was also included when loading the gel to verify the size of the amplicon. Gel electrophoresis was carried out at 100 volts (V) for 40 min and DNA was visualized with a MacroVue UV-25 Hoefer transilluminator.

2.5 Cloning

Sequence specific primers were used to generate inserts by PCR or RT-PCR (Section 2.4). Amplicon size was verified by 1% agarose gel electrophoresis (Section 2.4.2). All amplicons were purified using a QIAquick® PCR purification kit (Qiagen), and eluted in 30µl of Elution Buffer, supplied with kit.

2.5.1 DNA Digestion

Amplified DNA inserts were digested in parallel with appropriate vector constructs and restriction enzymes (New England Biolabs). A typical 30µl digestion was prepared: 3µl of restriction enzyme buffer, 0.5µg of vector DNA / 25µl insert DNA, 10 units of restriction enzyme 1 (typically 0.5-1µl), 10 units of restriction enzyme 2 (typically 0.5-1µl), Xµl of water. Digestions were incubated at 25°C or 37°C for 2–24 hours. DNA was purified using either a QIAquick® PCR purification kit or QIAquick® gel extraction kit (Qiagen).

2.5.2 DNA Ligation

Following DNA digestion, 5µl of the reaction mixture was loaded onto a 1% agarose gel, underwent gel electrophoresis, and UV illumination to estimate the quality and quantity of digested DNA present. The insert and vector was ligated using T4 DNA ligase (5 units/µl, Roche). A typical 20µl DNA ligation reaction consisted of 2µl of 10x ligation buffer, 1.0µl of digested vector DNA, 5-

15µl of digested insert DNA, 1.0µl of T4 DNA ligase and Xµl of water. Ligation reactions were incubated at 16°C overnight.

2.5.3 DNA Plasmid Transformation

E.coli Top 10 chemically competent cells were transformed by thawing cells on ice, addition of 50% of the ligation reaction, followed by a 30 min incubation on ice. Cells were heat shocked at 42°C for 45 seconds (sec), SOC medium (Appendix 1) was added and cells were then incubated at 37°C with horizontal shaking for 1 hour. The bacterial culture was then plated on LB + Ampicillin (100 µg/ml) or LB + Kanamycin (35 µg/ml) plates and incubated for 16 hours at 37°C.

2.5.4 Digestion Screen and Verification of the Construct

Bacterial colonies were cultured in 2ml of LB broth (Appendix 1) overnight at 37°C with shaking and plasmid DNA was subsequently extracted using a plasmid DNA miniprep kit (QIAprep Spin Miniprep Kit, Qiagen). Extracted plasmid DNA was digested with specific restriction enzymes (New England Biolabs) in order to verify the presence of the insert. Positive screened colonies were then sequenced, using the dideoxy technique based on Sanger et al., (1977) and ABI3100 Genetic Analyzer, in order to ensure the presence and quality of the insert. Sequencing was graciously carried out by an in-house DNA core facility.

2.5.5 Site-Directed Mutagenesis

If necessary, site directed mutagenesis (QuikChange™ Site-Directed Mutagenesis Kit, Stratagene®) was carried out to correct any point mutations incurred by the DNA polymerase. In brief, primers were designed to adjust any mutations (Appendix 3) and used to PCR amplify the plasmid. Amplified DNA was then treated with Dpn1 restriction enzyme digestion for 1 hour at 37°C, to digest any methylated DNA i.e. the parental strand. The DNA was then transformed into *E.coli* XL1-Blue Supercompetant Cells (Stratagene®) as previously described in Section 2.5.3. A random selection of colonies were picked and grown up in 2ml of LB broth overnight at 37°C with shaking and plasmid DNA was purified using a miniprep kit (QIAprep Spin Miniprep Kit, Qiagen). Extracted plasmid DNA was sent for DNA sequencing to verify the incorporation of the correct nucleotide changes and to verify the sequence of the insert.

2.6 Cloning Strategy – Creation of NiV N-IRES-CMV

Internal ribosomal entry site (IRES) is a nucleotide structure with very complex secondary and tertiary structures. These structures resemble the 5' cap structure of mRNA and can enhance the translation of proteins. To enhance the expression levels of recombinantly expressed NiV N proteins, a human IRES was cloned in between the cytomegalovirus (CMV) promoter and the NiV N ORF. The IRES was PCR amplified from a synthetic oligo template, whose sequence was taken from the eukaryotic initiation factor 4 gamma gene (Accession #

D12686), as described in Section 2.4 (Appendix 3). The amplicon was subsequently cloned into the NiV N-CMV constructs, as describe in Section 2.5, creating a construct called NiV N-IRES-CMV.

2.7 Cloning Strategy - Creation of ΔNiV N-IRES-CMV

Site directed mutagenesis was carried out on the NiV N-IRES-CMV construct in order to prevent translation of the NiV N ORF. Two in-frame translational start sites were mutated from ATG to TTG, as described in Section 2.5.5 (Appendix 3). This construct, ΔNiV N-IRES-CMV, was created to produce a plasmid that was transcriptionally active, allowing the production of NiV N mRNA, but preventing expression of the NiV N protein.

2.8 Cloning Strategy – Creation of Truncated NiV N Constructs

Various truncated versions of the NiV N gene were created in order to assess the various functional domains it may possess. The NiV N ORF was systematically truncated from the 3' and/or the 5' ends.

Full-length constructs were cloned into two separate expression plasmids, pBK-CMV-IRES and pECFP-N1 (Clontech) (Figure 8), as described in Section 2.4 and Section 2.5. Both of these expression plasmids are driven by CMV promoters and can be used in a variety of eukaryotic tissue culture expression systems. The vector, pBK-CMV-IRES, includes an IRES directly after the CMV promoter in order to enhance expression of the adjacent gene (Figure 8). The

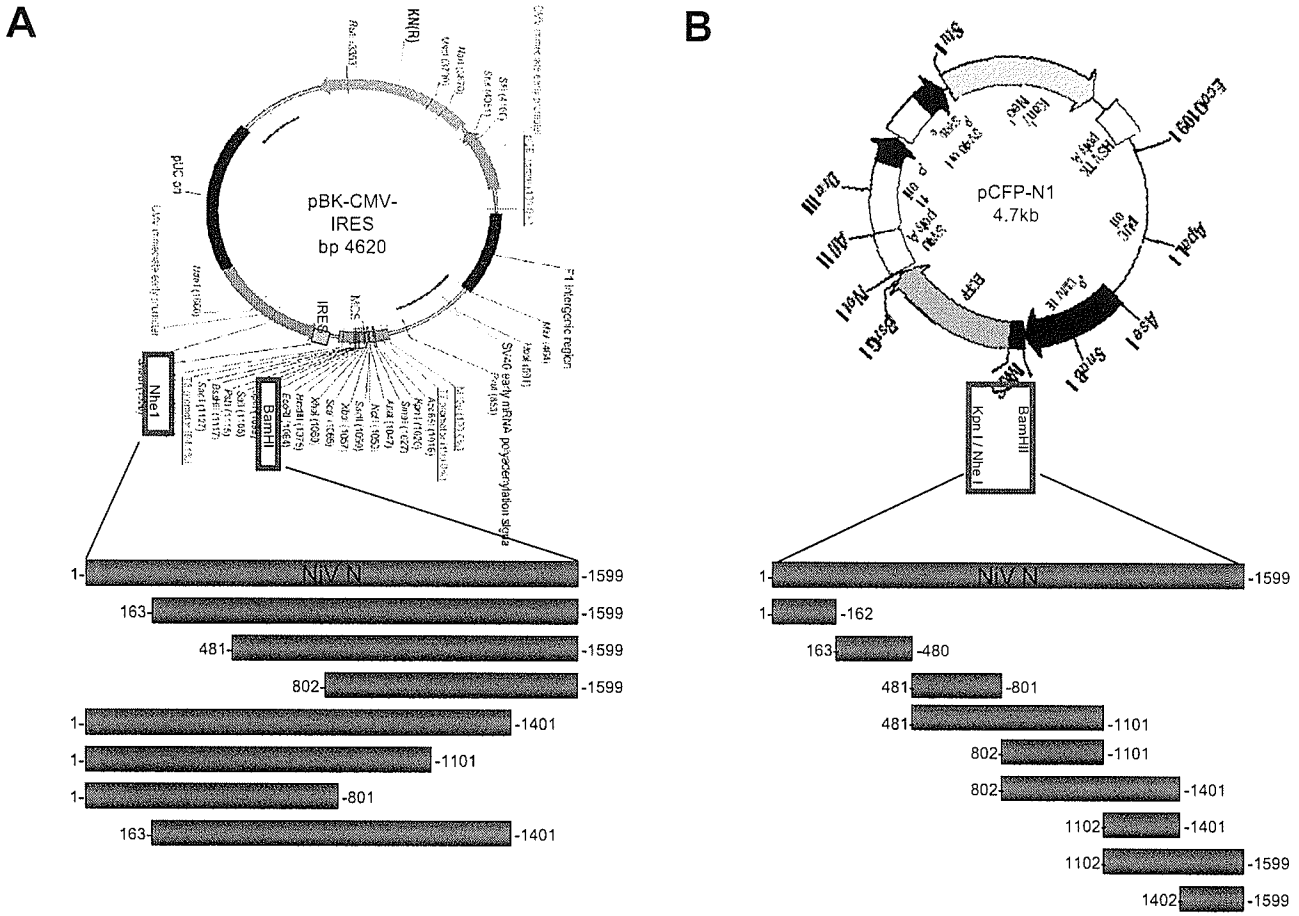

Figure 8: Cloning Strategies for the Creation of Truncated NiV N Constructs. (A) Various truncated NiV N constructs were PCR amplified with a C-terminal HA-tag and cloned into pBK-CMV-IRES using restriction sites NheI and BamHI. (B) Various truncated NiV N constructs were PCR amplified and cloned into pECFP-N1, creating a fusion protein with a C-terminal CFP tag using restriction sites KpnI/NheI and BamHI.

vector, pECFP-N1, encodes a gene for the cyan fluorescent protein (CFP), which is a variant of the *Aequorea victoria* green fluorescent protein (GFP), containing 6 aa substitutions. CFP is antigenically similar to GFP thereby allowing the use of anti-GFP antibodies to detect CFP. This CFP variant has fluorescence excitation major peak at 475nm and a minor peak at 501nm, which is also similar to the excitation wavelengths of GFP, and therefore, can be visualized by using the UV channel on a fluorescent microscope.

N- and C-terminal deletions were systematically designed, where three constructs were truncated up to 50% of the NiV N protein from the N-terminal end and three constructs were truncated up to 50% from the C-terminal end of the NiV N protein, Figure 8, left panel. All of these constructs also include a Hemagglutinin (HA) tag on the C-terminal end, which was incorporated by PCR and subsequently cloned into pBK-CMV-IRES, as described in Section 2.4 and 2.5. Inclusion of an HA-tag was essential for the detection of these proteins by immunoblot and immunofluorescence assays (IFA). Larger truncations were designed specifically containing the various regions, which were deleted from the aforementioned HA-tagged constructs, Figure 8, right panel. In order to create a fusion protein with the CFP gene found in the vector, it was necessary to design primers, which would incorporate an extra nucleotide after the truncated NiV N gene during PCR amplification, to facilitate in-frame translation of the NiV N gene and the CFP gene, Appendix 3. These constructs would be then cloned into pECFP-N1 creating a fusion protein with CFP, as described in Section 2.4 and 2.5. Creation of a fusion protein was ideal for detection of the proteins by

fluorescence microscopy, as well as increasing the molecular weight to sizes, which can be more effectively separated and visualized by SDS-PAGE gel electrophoresis and immunoblot. In addition, antibodies against GFP could be used to detect the presence of the CFP fusion constructs. Primers designed to amplify these regions, as well as other properties are found in Appendix 3.

2.9 Cloning Strategies – Creation of NiV P constructs

In order to analyze the interaction between NiV N and NiV P proteins, a cloning strategy for the expression of a recombinant NiV P protein was designed. The NiV P ORF was cloned into the eukaryotic expression vector pBK-CMV (Stratagene), a CMV driven vector, with and without a FLAG-tag (Figure 9). A FLAG-tag was incorporated onto the 3' end of the NiV P gene, by incorporating its nucleotide sequence onto the 5' end of the reverse NiV P specific primer, Appendix 3. Cloning of the NiV P constructs were carried out as described in Section 2.4, Section 2.5.

2.10 Cloning Strategy – Creation of NiV P-NiV N-CMV

A dual promoter construct, NiV P-NiV N-CMV, was designed in order to express the NiV N protein as well as the NiV P protein from one construct. This construct was used to ensure that every cell transfected is expressing both of these proteins. The dual promoter system was created by PCR amplifying the CMV promoter, the NiV N ORF and the simian virus 40 (SV40) poly A termination

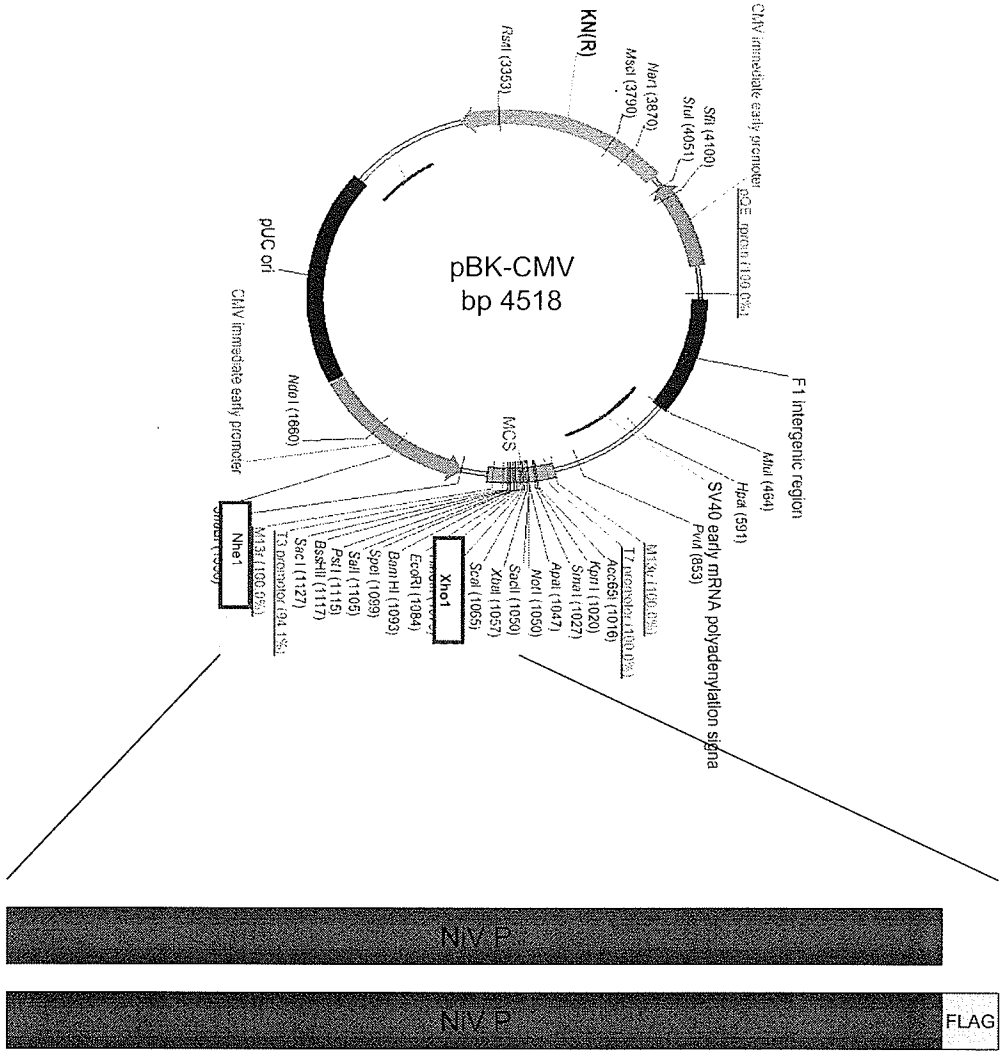

Figure 9: Cloning Strategy for the Creation of NiV P Constructs. The NiV P ORF was PCR amplified with and without a C-terminal FLAG tag. It was subsequently cloned into pBK-CMV using restriction sites, NheI and XhoI.

signals found in the NiV N-CMV construct (Section 2.4, Appendix 3) and was cloned downstream of the NiV P ORF (Section 2.5), Figure 10.

2.11 Transfections

Cells were transfected with plasmid DNA in order to express recombinant proteins. Typically, 293T cells were seeded into 35mm dishes at a dilution of 1:5 from a T75 stock flask, in order that the next day cells were approximately 60% sub-confluent. Lipofectamine™ 2000 (Invitrogen™) was the transfection reagent of choice. In brief, 4µg of plasmid DNA was added to a tube containing 250µl of Opti-MEM®I Reduced Serum Media (Opti-MEM, Gibco®). In another tube, 5µl of Lipofectamine™ 2000 was added to 250µl of Opti-MEM. Reactions were incubated for 5 min at room temperature, then mixed together and incubated for a further 15 min at room temperature. Finally, the volume in each tube was adjusted to 1ml with Opti-MEM. The spent media on 293T cells was removed and was replaced by the transfection reaction. Cells were incubated for 24 hours at 37°C with 5% CO_2 and H_20-saturated atmospheric conditions. The transfection reagent was then removed and fresh DMEM supplemented with 2% FBS was added to the cells and allowed to incubate a further 24 hours.

2.12 Sodium Dodecyl Sulphate Polyacrylamide Gel Electrophoresis (SDS PAGE) Gels and Semi-Dry Transfer

Cell supernatants from a 35mm dish were harvested in an equal amount of 4X SDS Gel loading buffer (Appendix 1). Cells were then washed once with

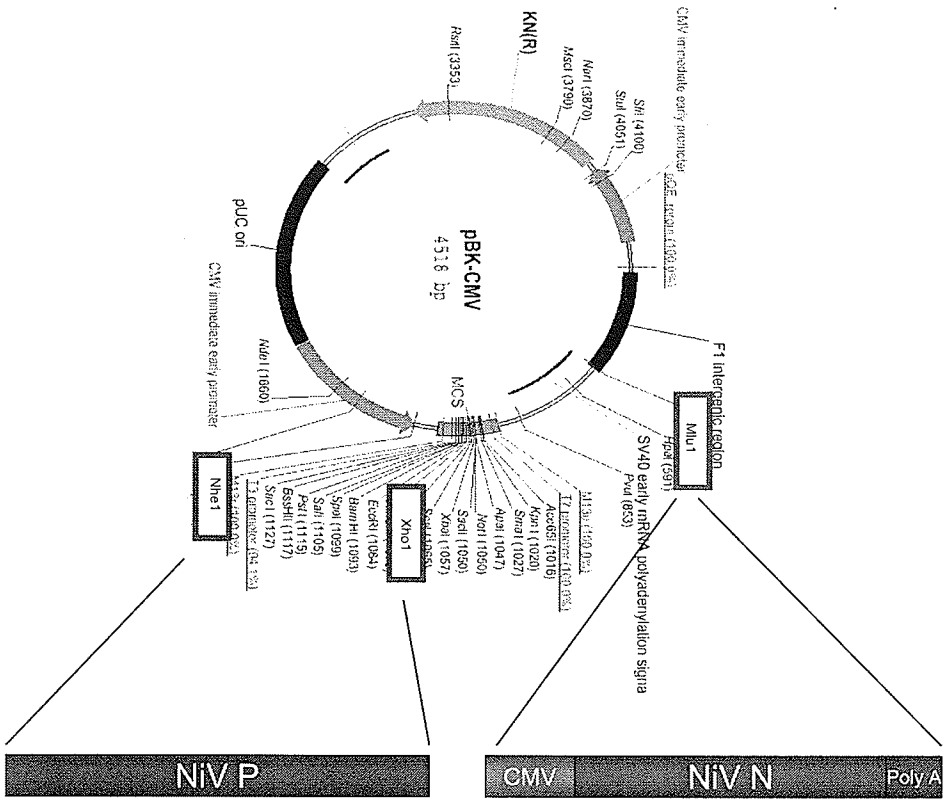

Figure 10: Cloning Strategy for the Creation of NiV P-NiV N-CMV Dual Promoter Construct. A schematic diagram demonstrates the cloning strategy used to create a NiV N and NiV P dual promoter construct. The CMV promoter, NiV N gene and SV40 poly A tail was PCR amplified using NiV N-CMV as a template. The construct was digested with Mlu1 and cloned into NiV P-CMV.

PBS to remove residual growth media, and then lysed with 250µl of 2X SDS Gel loading buffer (Appendix 1). Cell lysates were run on a miniature SDS-PAGE gel to resolve proteins based on molecular weight. All gels included two molecular weight markers, to help verify protein size, See Blue Plus 2 (Invitrogen™) and Magic Mark™ XP (Invitrogen™), Appendix 5. The former ladder is visualized as the proteins undergo electrophoresis and transfer and the latter ladder is visualized on an immunoblot. Magic Mark™ XP (Invitrogen™) contains 9 protein standards, which were made from *E. coli* using a fusion construct containing an immunoglobulin G (IgG) binding site. This IgG binding site on the protein standards interact with the secondary antibody thereby allowing visualization by immunoblot. Protein samples were electrophoresed using the Protean III mini-gel system (Bio-Rad) at 100V for 1-1.5 hours. Proteins were resolved on 7-12% SDS-PAGE gels (Appendix 1) and then transferred onto to a polyvinylidene fluoride (PVDF) membrane (Hybond P, Amersham Pharmacia Biotech) using a Trans-blot SD semi-dry transfer apparatus (Bio-Rad). Following electrophoresis, the gels were soaked in semi-dry transfer buffer (Appendix 1) for 15 min and the PVDF membrane was activated by treatment in methanol for 30 sec and extensively washed with semi-dry transfer buffer for another 15 min. The semi-dry transblot anode plate was wet with transfer buffer and a pre-soaked extra thick filter paper was placed on the wet surface. The membrane was then placed on top of the filter paper and the air bubbles were removed by rolling a wet pipette across the surface of the membrane. The stacking gel of the SDS-PAGE gel was discarded and the resolving gel was placed on top of the membrane.

Another pre-soaked extra thick filter paper was then placed on top of the growing sandwich. The cathode plate was wet with transfer buffer and placed on top of the sandwich. Proteins were transferred for 90 min at 60mA per gel.

2.13 Immunoblot

Following the transfer of proteins from the SDS-PAGE gel onto the PVDF membrane, the membrane was blocked with 5% skim milk + 0.1% Tween-20 overnight at 4°C or for 1 hour at room temperature to reduce non-specific binding of the protein. The blot was then incubated in primary antibody, which was diluted in blocking buffer, for 1 hour with rocking (Appendix 2). The blot was then washed three times in phosphate buffered saline (PBS) + 0.1% Tween-20 for 10 min each at room temperature and incubated in the secondary antibody diluted in blocking buffer for another 1 hour at room temperature with rocking (Appendix 2). Following the final incubation with antibody, the blot was washed three times in PBS + 0.1% Tween-20 for 10 min each at room temperature. The proteins of interest were visualized using the ECL+plus Western Blotting Detection System (Amersham Biosciences). Following detection, blots were maintained in PBS or stored at -20°C for long-term storage. If necessary blots were stripped of antibodies in order to be probed using another set of antibodies. In this case, blots were incubated with stripping buffer (Appendix 1) for 30 min at 50°C. Blots were thoroughly washed three times with PBS + 0.1% Tween-20 and immunoblots were preformed again as just described. If necessary, blots were quantified using spot densitometry and AlphaEaseFC^{TM} software, standardized

against the expression of actin and normalized to either 0% or 100% dependant upon the assay. In general, if recombinant protein expression was being quantified, then the negative control or mock-transfected cells (0µg of plasmid DNA) was normalized to 0%, whereas, if viral protein expression was being quantified, then the positive control (infected cells without other treatments) was normalized to 100%. Standard deviations of the mean were calculated.

2.14 Separation of Soluble Proteins from Insoluble Proteins

293T cells were seeded into 35mm^2 dishes at a ratio of 1:5 24 hours prior to transfection. Cells were transfected as described in Section 2.11, with either 4µg of NiV N-IRES-CMV or 4µg of NiV P-NiV N-CMV. Following transfection cells were washed three times with sterile PBS and lysed in 200µl of Nonidet P40 (NP-40) Lysis Buffer (Appendix 1) for 1 hour at 4°C with end-over-end rotation. The cell lysate was clarified by centrifugation at 19 000xg for 15 min. The supernatants were then added to 1.3ml of a 20% sucrose solution (dissolved in Tris-NaCl-EDTA (TNE) buffer). The cushion was spun at 130 000xg for 1 hour at 4°C in a Beckman Optima^{TM} TLX Ultracentrifuge. The supernatant was collected (1.3ml) and the pellet was brought up in 1.3ml of sterile PBS. 375µl of 4X SDS Gel Loading Buffer + 10% BME was added to each sample. Samples were loaded onto a 10% SDS PAGE gel. Gel electrophoresis, transfer, and immunoblot were carried out as described in Sections 2.12 and 2.13.

2.15 Cellular Fractionation of 293T Cells into Nuclear and Cytoplasmic Fractions

35mm dishes were seeded with 293T cells at a ratio of 1:5 24 hours prior to transfection. Cells were co-transfected each, with 4µg of truncated NiV N-IRES-CMV-HA tagged constructs and/or NiV P-CMV, using procedures described in Section 2.11. Cells were lysed in 200µl of Cell Fractionation Lysis Buffer (Appendix 1) for 10 min at room temperature and then spun at 19 000xg (13 000 rpm) for 30 min to separate the nuclear fraction from the cytoplasmic fraction. The cytoplasmic fraction (supernatant) was removed and 50µl of 4X Gel Loading Buffer + 10% BME was added. The nuclear fraction was washed with sterile PBS three times and lysed in 250µl of 1X Gel Loading Buffer + 10% BME. 10µl of these reactions were loaded onto a 10% SDS PAGE gel for electrophoresis and transfer (Section 2.12). Blots were probed with antibodies in order to visualize specific proteins (Section 2.13 and Appendix 2)

Immunoblots were quantified using AlphaEaseFC^{TM} software. Standard deviations were calculated from the mean value. In order to assess the statistical significance between value points obtained, a variety of statistical analyses were employed using JMP version 7.0 (2007 SAS Institute Inc) programming and a 2-way ANOVA (analysis of variance) test (116). Data were initially checked for normality, using the Shapiro-Wilk test (107). The null hypothesis is that the data are normal, therefore, if the P-value<0.05 then the data will have to be transformed. The data have a P-value=0.0103, therefore the data were transformed for normal distribution using a BOXCOX transformation (18). A

Shapiro-Wilk test was applied to determine the P-value after transformation, and was calculated to be 0.3337 (107). There were two treatments, NiV N proteins alone and NiV N proteins in conjunction with NiV P proteins. The response variable was the percentage of NiV N proteins within the nuclear fraction. P-values were calculated and P-values<0.05 were considered significant. The presence of NiV P proteins were found to significantly effect the amount of NiV N proteins found within the nuclear fraction (P-value<0.0001). As well, the different NiV N truncated proteins were found to significantly effect the distribution of the NiV N truncated protein to the nuclear fraction (P-value<0.0001). Finally, there was a significant interaction between NiV P proteins and the different truncated proteins (P value=0.0013), meaning that different truncated proteins responded differently to the presence of NiV P proteins. The data were then analyzed using a Tukey HOC test, in order to determine which constructs were significantly different to NiV N proteins or NiV N proteins co-expressed with NiV P proteins.

2.16 Co-Immunoprecipitation Assay

35mm dishes were seeded with 293T cells at a ratio of 1:5 24 hours prior to transfection. Table 3 describes the constructs transfected, as described in Section 2.11, for various co-immunoprecipitation experiments.

Table 3: Details of constructs and amounts of plasmid DNA transfected into 293T cells for various immunoprecipitation assays

Construct	Amount of DNA (µg)	Section
NiV P-FLAG and truncated NiV N-HA	2 and 4	4.0
NiV P and truncated NiV N-HA	2 and 4	4.0
NiV P and truncated NiV N-CFP	2 and 4	4.0
NiV P and truncated NiV N-CFP	2 and 4	5.0

Transfected cells were washed with PBS and lysed in 1ml of NP-40 lysis buffer for 1 hour at 4°C with end-over-end rotation. Lysates were cleared of cellular debris by centrifuging samples at 19 000xg for 15 min. 50µl of immobilized protein A/G resin (Pierce) was used per reaction. Beads were washed with Equilibration Buffer (Appendix 1) and then spun at 2 500xg for 3 min. This step was repeated two times. Cell lysates were pre-cleared by addition of the lysate to the empty resin and incubation for 2 hours at room temperature with end-over-end rotation. The pre-cleared lysate was removed by centrifugation at 2 500xg for 3 min. 50µl of immobilized resin was equilibrated, as previously described. Table 4 provides details on the resin and antibodies used for each experiment.

Table 4: Details of resin and antibodies used in immunoprecipitation assays

Resin Properties	Company	Antibody Properties	Quantity added to reaction	Company	Immunoppt *	Co-immunoppt **
HA Affinity Matrix	Roche	Rat monoclonal anti HA	N/A	N/A	NiV N-HA	NiV P
Anti-GFP conjugated agarose	Santa Cruz Biotech.	Mouse monoclonal anti-GFP	N/A	N/A	NiV N-CFP	NiV P
Immobilized Protein A/G resin	Pierce	Mouse monoclonal anti-FLAG® M2	4.9µg	Sigma®	NiV P-FLAG	NiV N-HA
Immobilized Protein A/G resin	Pierce	Mouse monoclonal anti NiV P	5.0µg	In House	NiV P	NiV N-CFP

* Describes which protein was immunoprecipitated using the specified antibodies/resin

** Describe which protein was co-immunoprecipitated using the specified antibodies/resin

The pre-cleared supernatants were added to the antibody-resin mixture and incubated overnight at 4°C. The matrix was washed three times with NP-40 lysis buffer and spun at 2 500xg for 3 min each time to remove wash buffer. Proteins bound to the beads were eluted by boiling in 20µl of 2X SDS Gel loading buffer for 5 min. Beads were spun down at 2 500xg for 5 min and the supernatants were added to fresh tubes. BME was then added to the supernatants at a final concentration of 10% and the entire sample was loaded onto a 10 or 12% SDS-PAGE gels for electrophoresis and transfer, as previously described in Section 2.12. Immunoblots were carried out to visualize the proteins immunoprecipitated and co-immunoprecipitated, Section 2.13 and Appendix 2.

2.17 Visualization of Nucleocapsid-like Structures

Three 35mm dish seeded with 293T cells were transfected with NiV N-IRES-CMV as described in Section 2.11. 293T cells were washed with sterile PBS and lysed in a final volume of 300µl of NP-40 lysis buffer (Appendix 1). The lysate was clarified by spinning the lysates at 2 500xg for 15 min. The clarified samples were analyzed by negative staining electron microscopy using a Philips CM120 Transmission Electron Microscope.

2.18 Immunofluorescence Assay (IFA) – Confocal Fluorescent Microscopy

293T cells were chosen to analyze the expression and staining characteristics of the NiV N truncated proteins, since these cells were consistently used throughout this thesis. 293T cells were seeded onto 0.8cm^2-well chamber slides at a ratio of 1:5 24 hours prior to transfection. Plasmid DNA was transfected into cells using Lipofectamine 2000^{TM} transfection reagent. In brief, 0.5µg of plasmid DNA was diluted in 25µl of Opti-MEM and 0.5µl of Lipofectamine^{TM} 2000 was diluted in 25µl of Opti-MEM. Reactions were incubated for 5 min at room temperature, then mixed together and incubated for a further 15 min at room temperature. Spent media was removed from cells and washed one time with Opti-MEM. The transfection mix was then brought up to 200µl with Opti-MEM and added to cells. Cells were incubated for 24 hours at 37°C with 5% CO_2 and H_20-saturated atmosphere conditions. Following transfection, cells were prepared for IFA staining. Cells were fixed and

permeabilized in 4.0% paraformaldehyde-PBS + 0.6% Triton®-X-100 (Fisher Scientific) for 30 min at 37°C. Cells were washed three times with sterile PBS for 5 min and then blocked in 1% Bovine Serum Albumin-PBS + 0.6% Triton®-X-100 (BSA-Triton-X-100) for another 30 min at 37°C. Cells were incubated with primary antibodies (Appendix 2), diluted in BSA-Triton-X-100 for 1 hour at room temperature. Following incubation with the primary antibody, cells were washed three times with BSA-Triton-X-100. Cells were incubated with AlexaFluor® conjugated secondary antibodies (Appendix 2) diluted in BSA-Triton-X-100, at room temperature in the dark. Cells were washed three times with BSA-Triton-X-100 and fixed once more with 2% paraformaldehyde-PBS for 10 min. Cells were washed three times with sterile PBS for 5 min and were immediately visualized with an Olympus IX70 confocal microscope and Fluoview 2.1 software. Cells were visualized at 60X magnification. Controls to ensure that cross-reactivity between antibodies or cells was not occurring were carried out for each experiment, data not shown.

2.19 Immunofluorescence Assay – Visualization of NiV P and NiV N Protein Expression

293T cells were seeded into 0.8cm^2-well chamber slides 24 hours prior to transfection or infection at a ratio of 1:10. Cells were transfected with 0.5µg of plasmid DNA as described in Section 2.18. A modified version of the IFA protocol described in Section 2.18 was employed in order to visualize the expression of NiV N and NiV P. A monoclonal antibody against the NiV P protein

was added for 1 hour at room temperature, Appendix 2. Cells were washed three times in BSA-Triton-X-100 for 5 min each. The secondary antibody, goat anti-mouse-AlexaFluor® 568 (Appendix 2), was added for 1 hour at room temperature. Cells were washed three times in BSA-Triton-X-100 for 5 min each. Finally, a monoclonal antibody, mouse anti NiV N-FITC (Appendix 2), against the NiV N protein was added to the cells for 1 hour at room temperature. The remaining protocol was carried out as described in Section 2.18. An Olympus IX70 confocal microscope and Fluoview 2.1 software were used for acquisition of images. Cells were visualized at 60X magnification. Controls to ensure that cross-reactivity between antibodies or cells was not occurring were carried out for each experiment, data not shown.

2.20 Immunofluorescence Assay – Co-localization of NiV N Proteins to the Nucleus and Cytoplasm

293T cells were seeded into 0.8cm^2-well chamber slides 24 hours prior to transfection or infection at a ratio of 1:12. Cells were transfected with 0.5µg of plasmid DNA as described in Section 2.18. A modified version of the IFA protocol described in Section 2.18 was employed in order to visualize the expression of NiV N proteins within the nuclear or cytoplasmic compartments. A monoclonal antibody against Poly-ADP-Ribose Polymerase (PARP), a nuclear protein, was added for 1 hour at room temperature, Appendix 2. Cells were washed 3 times with BSA-Triton-X-100 for 5 min each. The secondary antibody, an antibody conjugated with AlexaFluor®647 fluorochrome and the primary

monoclonal antibody against NiV N conjugated with a FITC fluorochrome was added for 1 hour at room temperature in the dark. Cells were washed 3 times with BSA-Triton-X-100 for 5 min each. Finally, phalloidin conjugated with the AlexaFluor®568 fluorochrome, which binds F-actin, was added to cells for 15 min at room temperature in the dark. The remaining protocol was carried out as described in Section 2.18. An Olympus IX70 confocal microscope and Fluoview 2.1 software were used for acquisition of images. Cells were visualized at 60X magnification. One specific advantage is the use of lasers rather than filters when visualizing IFAs for co-localization studies. Green fluorescence visualized at a wavelength of 488nm is excited by the use of an argon laser, while red fluorescence, visualized at a wavelength of 568nm, and far-red fluorescence, visualized at a wavelength of 647nm, can be visualized using the krypton laser. Using a fluorescent microscope, a common problem, which needs to be compensated for, is the possibility of green emissions bleeding into the red spectrum, thereby skewing the immunofluorescence results. However, the krypton laser will not cause excitation within the green spectrum, thereby, preventing the problems of bleed-through, which would have a negative impact on co-localization studies. Controls to ensure that cross-reactivity between antibodies or cells was not occurring were carried out for each experiment, data not shown.

2.21 Visualization of NiV F and G Protein-Mediated Fusion

293T cells were transfected in a 35mm dish with either NiV N-CFP or pECFP-N1, or plasmids expressing NiV F and G proteins, as described in Section 2.11. Six hours post-transfection media was removed, cells were washed with PBS, and 250µl of Accumax™ (Chemicon International) was added to cells to create a single cell suspension. NiV N-CFP expressing cells or CFP only expressing cells were mixed with cells expressing NiV F and G proteins at a ratio of 1:3 and reseeded into a 12-well dish with DMEM supplemented with 2% FBS. Cells were incubated for 24 hours at 37°C with 5% CO_2 and H_20-saturated conditions. Cells expressing both NiV F and G proteins fused with adjacent cells and formed multi-nucleated giant cells. If cells expressing NiV F and G proteisn were able to fuse with cells expressing NiV N-CFP, this would demonstrate that the expression of NiV N proteins is not affecting virus-mediated fusion and therefore entry. The fusion between cells expressing NiV F and G proteins and NiV N-CFP would be observed by the presence of fluorescent multi-nucleated giant cells. Formation of multi-nucleated giant cells was visualized with fluorescent microscopy using a Zeiss model Axiovert 100 fluorescent microscopy and software. Cells were visualized at a magnification of 32X.

2.22 NiV Infections

293T cells were seeded into 35mm dishes, at a cell density of 70-80% sub-confluency (approximately $2x10^6$ cells), 24 hours prior to infection. Cells were infected with NiV at an MOI of 1 ($2x10^6$ IFU/well); NiV was added to cells

and allowed to adsorb for 1 hour. Virus was removed and replaced with fresh medium, DMEM supplemented with 2% FBS. Cells and supernatants were harvested at various time points: 3, 6, 9, 12, 18, 24, 36, and 48 hours post-infection. Total cell lysates were collected by re-suspending cell pellets in 500µl of 2X SDS Gel loading buffer and supernatants were harvested by adding 250µl of supernatants to 250µl of 4X SDS Gel loading buffer for viral protein analysis. SDS samples were boiled for 15 min at 100°C in CL-4 and another 15 min at 100°C in CL-2, as stipulated by CL-4 standard operating procedures. The remaining supernatant was stored at -80°C for $TCID_{50}$ assays. SDS samples were loaded onto 7% SDS PAGE gels, electrophoresed and transferred as described in Section 2.12. Immunoblots were carried out as described in Section 2.13. NiV RNA was extracted from NiV infected cells by re-suspending the cell pellet in 750µl of TRIzol LS®. RNA extractions were carried out as described in Section 2.3 using cell lysates rather than supernatants and without the use of glycogen. All infectious work conducted under CL-4 conditions adhered to strict protocols stipulated by the Health Canada Laboratory Bio-safety Guidelines (www.hc-sc.gc.ca/pphb-dgspsp/publicat/lbg-ldmbl-96/index.html).

2.23 NiV Replication – Transfection and Infection

293T cells were seeded onto 35mm plates at a ratio of 1:5 24 hours before transfection. Increasing amounts of plasmid DNA was transfected into cells using Lipofectamine™ 2000, as described in Section 2.11. Table 5 provides the amount of plasmid DNA used for individual constructs throughout this thesis.

Transfection media was replaced, 24 hours post-transfection, with DMEM supplemented with 2% FBS and cells were incubated for another 24 hours.

Table 5: Transfection conditions for increasing expression of recombinant proteins into cells.

Construct Name	Amount of DNA transfected (µg)	Amount of LipofectamineTM 2000/reaction (µl)
NiV N-IRES-CMV	0.0, 0.25, 0.50, 1.0, 2.0, 4.0	5
NiV P-CMV	0.0, 0.25, 0.50, 1.0, 1.5, 2.5	5
NiV P-NiV N-CMV	0.0, 0.25, 0.50, 1.0, 2.0, 4.0	5
ΔNiV N-IRES-CMV	0.0, 0.25, 0.50, 1.0, 2.0, 4.0	5
NiV N-HA-IRES-CMV	0.0, 0.25, 0.50, 1.0, 2.0, 4.0	5
NiV N 1-1401-HA-IRES-CMV	0.0, 0.25, 0.50, 1.0, 2.0, 4.0	5
NiV N 163-1599-HA-IRES-CMV	0.0, 0.25, 0.50, 1.0, 2.0, 4.0	5
NiV N-CFP	0.0, 0.25, 0.50, 1.0, 2.0, 4.0	5
NiV N 1-162-CFP	0.0, 0.25, 0.50, 1.0, 2.0, 4.0	5
NiV N 1402-1599-CFP	0.0, 0.25, 0.50, 1.0, 2.0, 4.0	5

Cells were infected with NiV or VSV at an MOI of 1 ($2x10^6$ IFU/well), 48 hours post-transfection, as described in Section 2.22. Cell lysates and supernatants were harvested 24 hours post-infection; cell lysates were collected for protein and RNA analysis, and supernatants were collected for protein and infectivity analysis, as described in Section 2.22. All infectious work conducted under CL-4 conditions adhered to strict protocols stipulated by the Health

Canada Laboratory Bio-safety Guidelines (www.hc-sc.gc.ca/pphb-dgspsp/publicat/lbg-ldmbl-96/index.html).

2.24 Infectivity Assay – $TCID_{50}$

293T cells were seeded into 24 well dishes, 24 hours prior to infection, so that they were 80% sub-confluent at the time of infection. Infectious supernatants were removed from storage at -80°C and thawed at 37°C. Supernatants were serially diluted from 10^{-1} to 10^{-9} in Opti-MEM for NiV titres and 10^{-1} to 10^{-12} for VSV titres. 0.5mL of each dilution was adsorbed onto cells for 1 hour. Virus was removed and replaced with fresh DMEM supplemented with 2% FBS. Cells were incubated for 48 hours. The presence of cell death and/or the formation of multi-nucleated giant cells, typical NiV-induced CPE, were analyzed and calculated into $TCID_{50}$ IFU (171).

2.25 Quantitative Real-Time RT-PCR

Real-time PCR is an assay, which can quantitate the production of amplified DNA; in this case, the assay uses technology based upon the fluorochrome, SYBR green. SYBR green is able to intercalate into double-stranded DNA, and subsequently emits a fluorescent signal at 530nm. Therefore, the generation of PCR amplicons can be measured by the addition of SYBR green into the reaction mix and the increase in SYBR green emission is directly proportional to the amount of PCR products generated. This technology also includes an additional step in order to ensure specificity and sensitivity of the

results obtained: a melt curve. Once the PCR products have been generated they are heated up to 95°C slowly to determine its characteristic melting temperature, the temperature at which 50% of the DNA is in single-stranded form and 50% of the DNA is in double-stranded form. If one product is amplified during the PCR reaction, one melt peak will be visible. If non-specific products or primer dimers are formed then additional peaks will be observed, however, usually at a lower melt temperature and to a lower intensity (LightCycler® RNA Amplification Kit SYBR Green 1 Version October 2005, Roche Applied Science). One-step quantitative RT-PCR was completed using LightCycler® RNA Amplification Kit SYBR Green 1 (Roche) and SmartCycler® Real-Time PCR technology. In general, a typical 25µl reaction consisted of 5µl of Reaction Buffer, 3µl of $MgCl_2$, 0.5µl of forward primer (20mM) and 0.5µl of reverse primer (20mM), 0.5µl of Enzyme mix, 1µg of RNA, and the volume was brought up to 25µl with sterile water. See Appendix 3 for a list of primers used in these reactions. PCR reactions were quantified based on the activation of SYBR Green and standardized against the production of glyceraldehyde-3-phosphate dehydrogenase (GAPDH) DNA. General cycling conditions are outlined in Table 6.

Table 6: General thermocycling parameters for real-time RT-PCR

Number of cycles	Time	Temperature	Cycle Description
1x	1200 sec	48°C	Reverse Transcription
1x	120 sec	94°C	Denaturation and activation of polymerase
40x	15 sec 30 sec 30 sec	94°C 52°C 72°C	Denaturation Annealing Elongation
1x		60°-95°C	Melt Curve

2.26 Strand-Specific Quantitative Real-Time RT-PCR

Strand-Specific RT-PCR analysis was carried out using RNA extracted from total cell lysates. Primers were designed against the NTR between NiV G and NiV L genes (Appendix 3). RT reactions were carried out using a NiV G forward primer (Appendix 3) or a NiV L reverse primer (Appendix 3) to detect either negative-sense NiV RNA or positive-sense NiV RNA respectively, followed by real-time PCR. DNA was amplified from viral RNA by employing a strand-specific RT-PCR using Qiagen's Sensiscript® RT kit and LC-FastStart DNA Master SYBR Green 1 PCR kit (Roche) which was subsequently analyzed and quantified using SmartCycler® Real-Time PCR technology.

2.26.1 Reverse Transcription

In general, a typical RT reaction consisted of 2µl of 10X reaction buffer RT, 2µl of dNTP (5mM), 1µl of forward/reverse primer (10µM), 1µg of total RNA, 1µl of Sensiscript® Reverse Transcriptase, and sterile water was added to bring

the reaction up to 20µl. The reaction was incubated at 50°C for 1 hour and the polymerase was inactivated at 95°C for 5 min, as per the manufacturer's instructions (Sensiscript® Reverse Transcription Handbook February 2004, Qiagen). 4µl of this reaction was used to carryout quantitative real-time PCR.

2.26.2 Quantitative Real-Time PCR

A typical PCR reaction consisted of 2.5µl of 10X LightCycler® DNA Master SYBR Green I reaction mix, 0.5µl of forward primer (20µM), 0.5µl of reverse primer (20µM), 3µl of $MgCl_2$, 4µl of RT reaction and sterile water was added to bring the volume up to 25µl. General cycling conditions are outlined in Table 7. All reactions were standardized against GAPDH RNA levels using LightCycler® RNA amplification Kit SYBR Green 1 (Roche) and GAPDH primer sets (Appendix 3), as described in Section 2.25, and relative values were calculated.

Table 7: General thermocycling parameters for real-time PCR

Number of cycles	Time	Temperature	Cycle Description
1x	600 sec	95°C	Denaturation and activation of polymerase
30x	15 sec 30 sec 30 sec	95°C 50°C 72°C	Denaturation Annealing Elongation
1x		60°-95°C	Melt Curve

2.27 Northern Blots

5µg of total RNA isolated from each cell lysate was run on a 1% Agarose – 7.4% formaldehyde gel (Appendix 1). The gel was rinsed in double-distilled water (ddH_20) and soaked in 20X sodium chloride sodium citrate (SSC) buffer for 15 min (Appendix 1), transferred to a nylon membrane (Hybond N, Amersham Pharmacia Biotech) using a Vacuum blotter (Model 785 Vacuum Blotter, BioRad), UV cross-linked (UVC 500 UV Crosslinker, Hoefer) and stored at 4°C in a sealed plastic pouch until ready for use. DNA probes designed against the NiV M gene (5' NiV M/3' NiV M, Appendix 3) and the GAPDH gene (5' GAPDH/3' GAPDH, Appendix 3) were labelled with α-dATP ^{32}P (Redivue® α-dATP ^{32}P, Amersham) with the Random Primed Labelling Kit as per manufacturers instructions (Roche) using DNA templates generated by the primer sets indicated. Membranes were hybridized with the labelled probe overnight at 61°C, in a hybridization oven (Hybridiser HB-1D, Techne), and subsequently rinsed with a high salt wash buffer (2X SSC/1% SDS) and then with low salt wash buffer (0.2X SSC/1% SDS) for 20 min each at 61°C. Blots were visualized using a Typhoon 9410 Variable Mode Imager and NiV M mRNA levels were standardized against GAPDH and quantified using ImageQuant 5.2 software.

3.0 Results

3.1 Rationale and Hypothesis

NiV is a highly virulent virus, which is able to replicate to high titres and can infect a wide range of different hosts. In order to create necessary antiviral therapies it is first important to understand how the virus replicates and how the viral components work together to mediate viral replication.

It has been suggested that the N protein interacts with the P protein in the polymerase complex to mediate the formation of viral replicase, which synthesizes both the viral genome and anti-genome (78;154). I hypothesize that increased expression of recombinant NiV N proteins alone can cause the premature formation of the viral replicase complex and will subsequently disrupt normal viral replication patterns. This section has four main objectives: (1) to characterize the expression of NiV N proteins, (2) to determine the regions within the NiV N protein that are necessary for binding the NiV P protein, (3) to determine whether an imbalance in the expression levels of NiV N proteins will affect viral replication, and (4) whether the interaction between NiV N and NiV P proteins is necessary to maintain normal viral replication.

3.2 Characterization and Functional Implications of the NiV N Protein

3.2.1 Production of NiV proteins

293T cells were chosen for these studies, since they robustly express recombinant NiV proteins and they are capable of efficiently propagating NiV

(163). A NiV kinetic study was employed to assess the various stages of viral replication, to gain insights into how quickly NiV can replicate, and to determine its extent of replication in 293T cells. Additionally, this study would be useful to gain insights into the characteristics of NiV N protein expression.

In order to assess the production of viral proteins and to determine at what time point they attained their highest levels of expression, total cell extracts were assayed by immunoblot and the expression of NiV N proteins were subsequently quantified by spot densitometry. A number of time points post-infection were assessed: 3, 6, 9, 12, 18, 24, 36, and 48 hours. Viral proteins were analyzed by immunoblot in order to determine when viral protein expression is observed and which viral proteins appear the earliest. A guinea pig-derived polyclonal serum against NiV, which can detect NiV N, P, F_0, F_1 and G proteins, was used to visualize viral proteins. NiV N and P proteins were detected as early as 9 hours post-infection from cell lysates, Figure 11-upper panel. The remaining viral proteins that could be detected by the polyclonal serum (NiV G, F_o, and F_1) appeared by 18 hours post-infection, Figure 11-upper panel. NiV N protein expression was at its highest level at the last time point, 48 hours post-infection, Figure 11-lower panel.

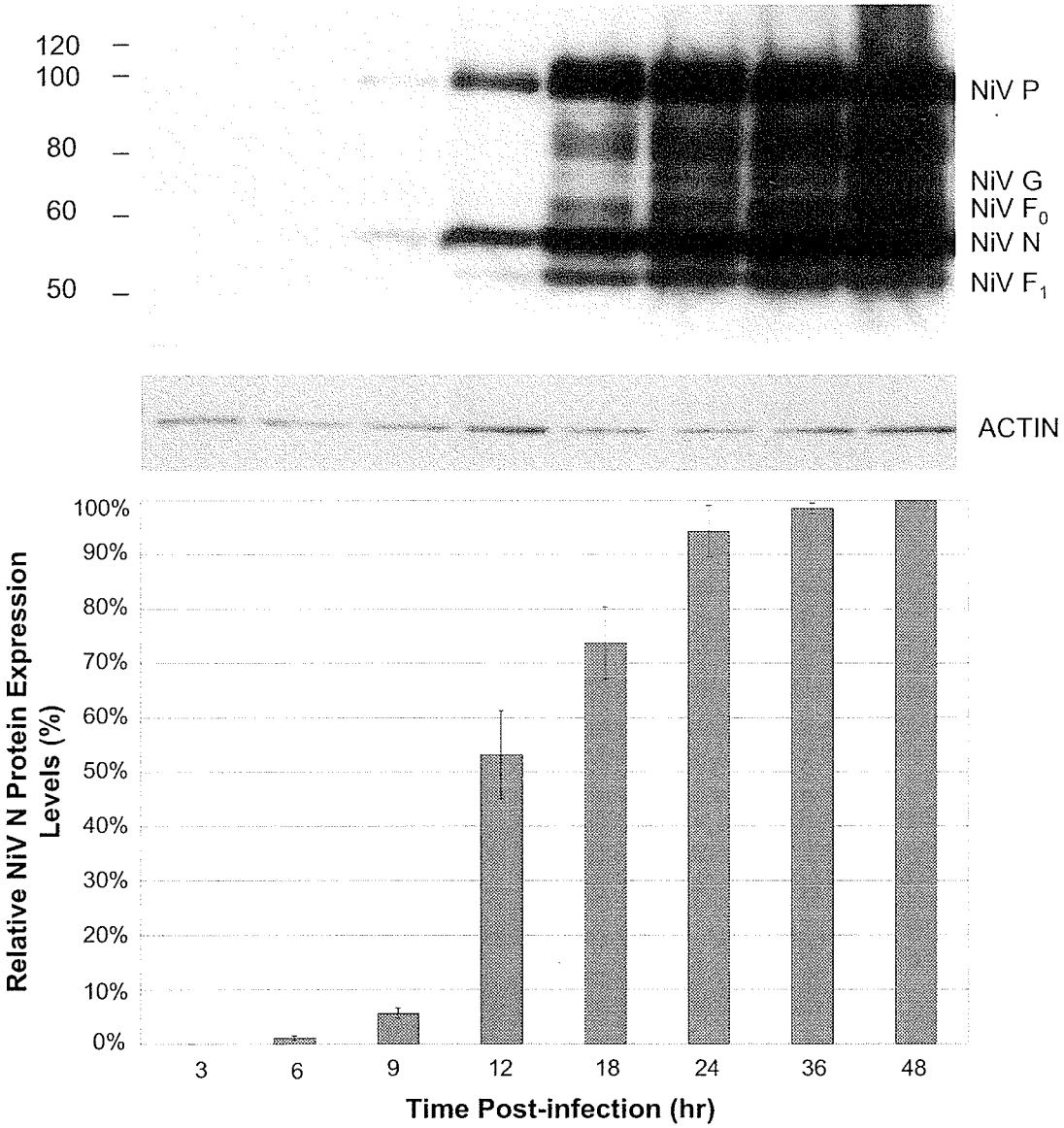

Figure 11: Kinetics Study Analyzing the Production of Viral Proteins in 293T Cells. Experiments were repeated three times. 293T cells were infected with NiV at an MOI of 1 ($2x10^6$ IFU/well) and protein cell lysates were harvested at 3, 6, 9, 12, 18, 24, 36 and 48 hours post-infection. Cell lysates were analyzed by immunoblot. Upper panel, Immunoblot- A polyclonal antibody against NiV was used to visualize the production of viral proteins. Lower panel- Protein expression, based on NiV N protein expression, was quantified by spot densitometry and AlphaEaseFC™ software. All samples were standardized against the expression of actin. Standard deviations of the mean were calculated.

Viral proteins found in the supernatant suggested the presence of viral proteins within the context of virus particles. Supernatants from NiV-infected cells were collected and viral proteins were visualized by immunoblot in order to confirm the presence of viral proteins, which were not cell-associated. NiV N and P proteins, the first proteins to appear, were barely detectable at 9 hours post-infection and by 12 hours post-infection were clearly visible, Figure 12-upper panel. The remaining viral proteins, which up until this point had not been observed by immunoblot, were present in the supernatant by 18 hours post-infection Figure 12-upper panel. NiV N proteins found in the supernatant were at the highest levels by 48 hours post-infection. Detectable levels of NiV proteins from NiV-infected cell lysates were observed slightly earlier than NiV proteins found in the supernatants. These findings suggest that viral proteins are found within the supernatant, likely in the context of the virus particle; however, it is also possible that viral proteins could be found in the supernatants due to cell death and subsequent lysis of the cell. Furthermore, it is possible that viral proteins could be secreted from the cell. Overall, viral protein expression was present at highest levels by 48 hours post infection, in both the cell lysate and the supernatant.

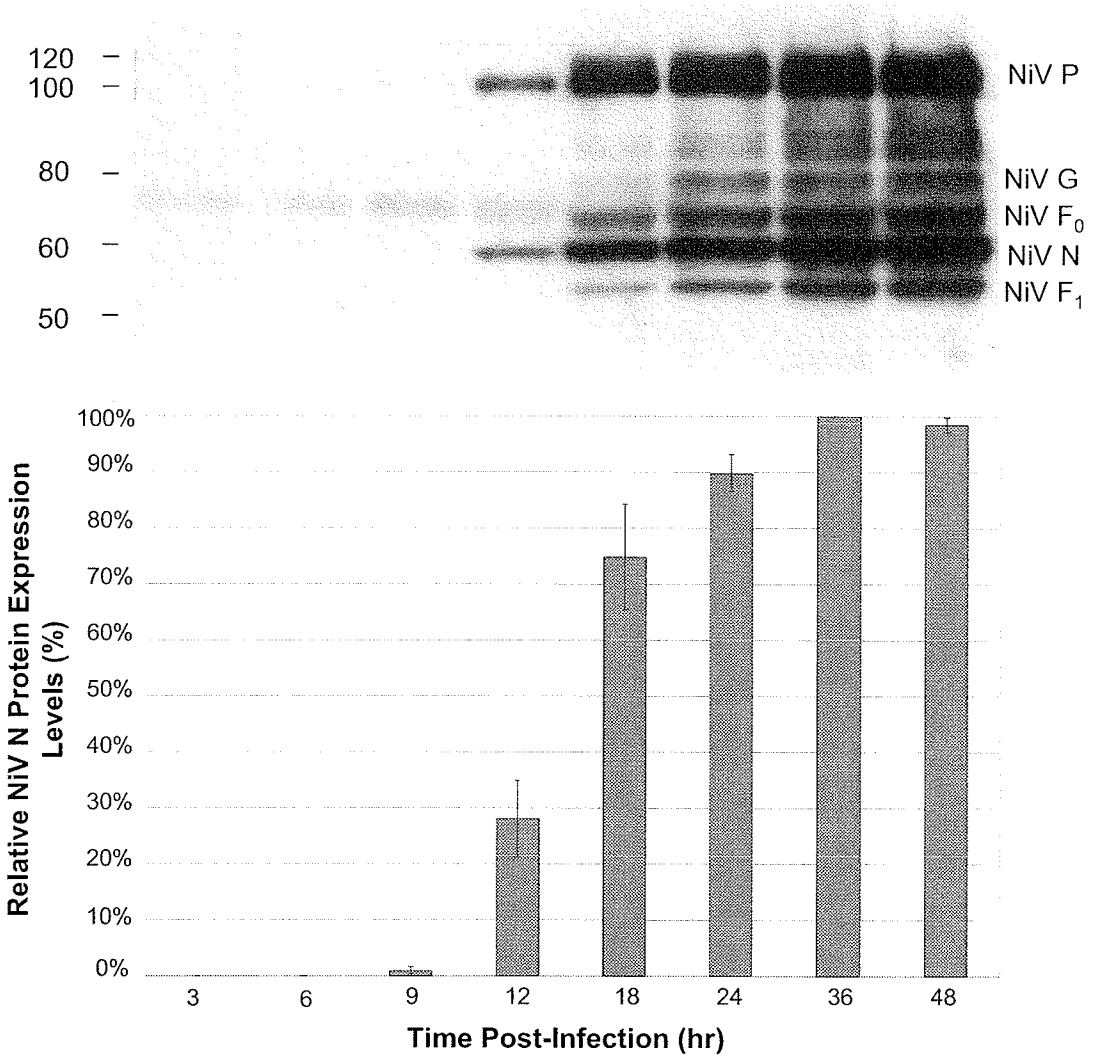

Figure 12: Kinetics Study Analyzing the Production of Viral Proteins in Cell Supernatants. Experiments were carried out in triplicate. 293T cells were infected with NiV at an MOI of 1 ($2x10^6$ IFU/well) and viral proteins were harvested from the supernatants at 3, 6, 9, 12, 18, 24, 36 and 48 hours post-infection. Supernatants were analyzed by immunoblot. Upper panel, immunoblot- A polyclonal antibody against NiV was used to visualize the production of viral proteins. Lower panel- Protein expression, based on NiV N protein expression, was quantified by spot densitometry and AlphaEaseFC™ software. Standard deviations of the mean were calculated.

3.2.2 Synthesis of NiV RNA

A prerequisite for viral protein production is the presence of viral RNA (genomic RNA and viral mRNA). Therefore, it is important to be able to detect and assess when viral RNA levels reached maximal levels. Total NiV RNA levels were assayed by real-time RT-PCR analysis using primers designed against the NiV N gene (Appendix 3). This method of analysis provided qualitative and quantitative data on when viral RNA was produced and detected. However, this assay analyzes the overall production of viral RNA and does not differentiate between production of NiV N mRNA and genomic or anti-genomic RNA. When quantified and standardized against GAPDH RNA the results demonstrated that viral RNA levels were detectable at 12 hours post-infection and increased significantly between 36 and 48 hours post-infection, Figure 13. It is unlikely that viral RNA levels would increase significantly more, since the cell monolayer was nearly destroyed by 48 hours post-infection. Other procedures may have been employed in order to distinguish between full-length genomic, anti-genomic RNA and mRNA, such as northern blots or strand-specific RT-PCR. However, these procedures were not essential for this study, since the objective of this experiment was to visualize when viral RNA levels reach maximal amounts and how this may influence the production of progeny virus.

It is evident that the components for viral replication, viral proteins and viral RNA, were present at very early time points and increased significantly between 24 and 48 hours. However, there was a discrepancy between when viral RNA and protein levels peaked, 24 hours and 48 hours respectively. This

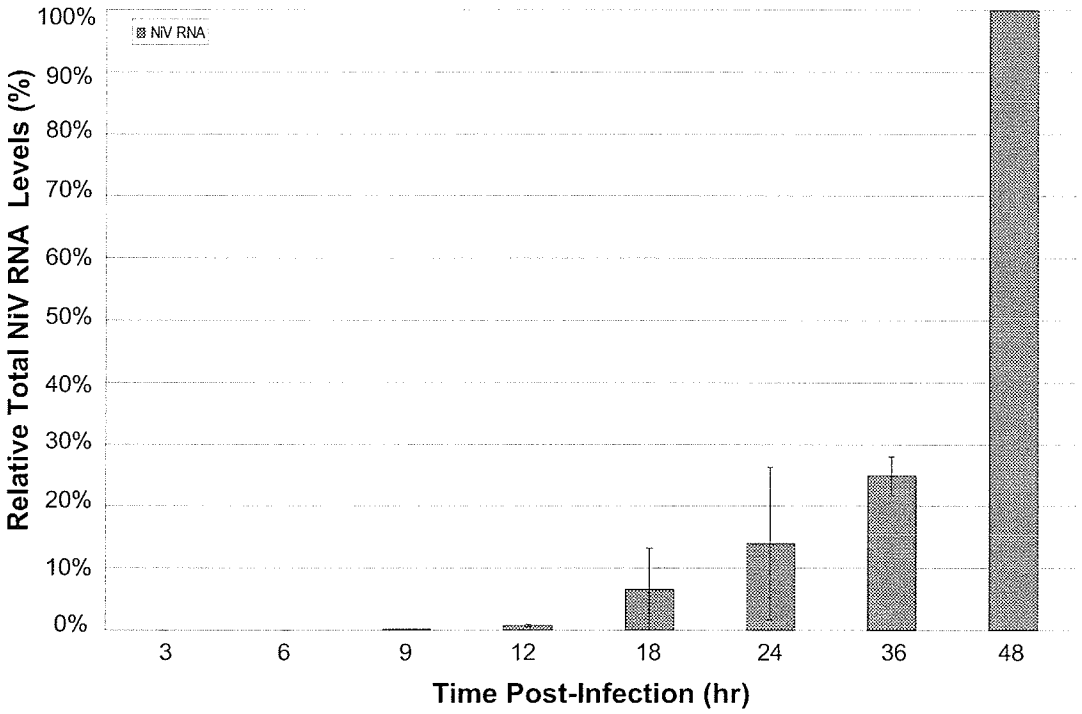

Figure 13: Kinetics Study Analyzing the Production of Total Viral RNA in 293T Cells. Experiments were repeated three times. 293T cells were infected with NiV at an MOI of 1 ($2x10^6$ IFU/well) and cell lysates were harvested at 3, 6, 9, 12, 18, 24, 36 and 48 hours post-infection. Viral RNA was quantified using Real-Time RT-PCR and Smart Cycler Technology with primers designed against the N gene. All samples were standardized against the production of GAPDH RNA. Mean and standard deviations were calculated. Standard deviations of the mean were calculated.

finding may be explained by the assay implemented to detect viral RNA. The real-time RT-PCR assay detects viral mRNA, anti-genome and genome. It could be possible that the production of viral mRNA peaked at 24 hours (when viral proteins peaked) and the production of viral genome and anti-genome continued to accumulate between 24 and 48 hours post-infection. Additionally, this discrepancy may also be attributed to the difference in sensitivity of the two assays.

3.2.3 Generation of NiV infectious particles

Upon the synthesis of viral proteins and viral genomic RNA, these viral products are assembled at the plasma membrane and are released from the cell by budding, Figure 3. The next aspect of the viral replication cycle that was analyzed was the production of progeny viruses. This is an important stage to analyze since the production of viral particles can be compared to the accumulation of viral RNA and proteins. The production of infectious virus particles was determined by $TCID_{50}$ infectivity assays. Infectious titres of $2x10^4$ $TCID_{50}$ IFU/ml were present as early as 3 hours post-infection, Figure 14. It is unlikely that any significant virus replication occurred within three hours of infection, since viral proteins and viral RNA were not produced at significant levels until 9 and 12 hours post-infection, respectively; therefore, it is likely that this value was indicative of the input virus. Over the next 36 hours, viral titres increased by 2.2-log_{10}, Figure 14.

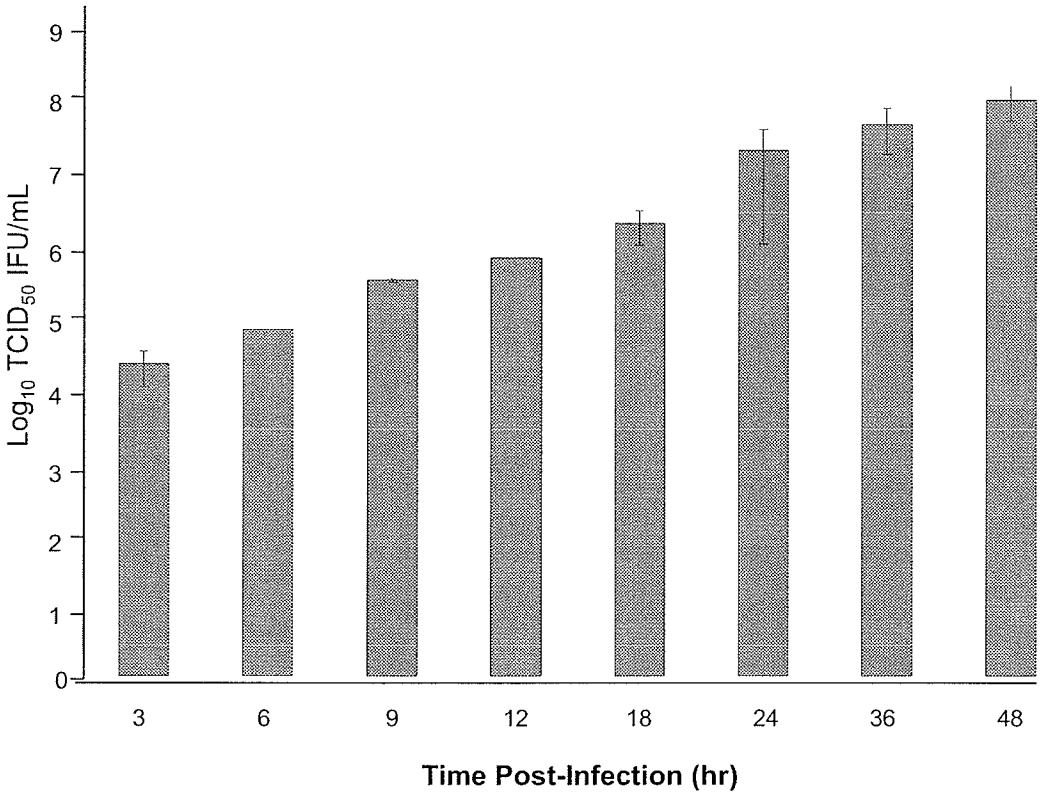

Figure 14: Kinetics Study Analyzing the Production of Progeny Virus from 293T Cells. Experiments were repeated three times. 293T cells were infected with NiV at an MOI of 1 and supernatants were harvested at 3, 6, 9, 12, 18, 24, 36 and 48 hours post-infection. Viral titres for each time point were quantified by $TCID_{50}$ in 293T cells. Standard deviations of the mean were calculated.

These findings demonstrated that by 24 hours post-infection the various viral components, viral proteins and RNA were present at sufficient amounts to mediate a significant increase in particle production (>90%). 293T cells supported NiV replication and generated typical infectious titres.

3.2.4 Expression and characterization of truncated NiV N constructs by immunoblot

NiV N and P proteins are believed to have an essential role in the synthesis of full-length viral RNA during replication. Expression of NiV N proteins may have the ability to disrupt viral replication, and this is thought to occur through the interaction between NiV N and NiV P proteins and their ability to form the replicase complex with NiV L proteins. However, before the concept of disrupting viral replication could be further assessed, it was necessary to determine the NiV P protein-binding domains found within the NiV N protein. Recombinant truncated proteins are powerful tools to evaluate various functional domains within a protein. I hypothesized that by utilizing a variety of NiV N truncated proteins, various functional domains within this protein could be identified. Although this method of identifying functional domains is a commonly used and accepted approach, it is limited by the ability of the truncated protein to maintain the same structural conformation as the full-length protein. More specifically, truncating a protein may cause alterations to the normal folding patterns of the protein. This conformational change may alter the protein's function. Therefore, the potential change in structural conformation may provide

data, which is not true of the full-length protein but rather an artefact of the truncated protein. Any changes in protein function may be artefacts of truncation and may not necessarily reflect actual functional changes in protein structure. Additionally, it must be kept in mind that a functional domain may not be limited to a single stretch of aa but may rather involve a number of different regions within the protein.

In order to identify putative regions on the NiV N protein, which are important for interacting with other viral components, various NiV N protein truncations were constructed by systematically truncating the protein from the N- or C-termini. To address the issue of structural stability of the truncated proteins, a ClustalW alignment program and a secondary structure prediction program, Jpred, were employed to analyze whether any potential structural motifs were interrupted by a truncation and whether there were any similar secondary structure motifs observed between viruses (3;4). These programs were used to compare the aa sequences between RV N, VSV N, and NiV N proteins in order to create an alignment based on their conserved sequences. Furthermore, the secondary structures of VSV N and RV N proteins, two proteins that have recently been crystallized and their tertiary structures elucidated, were also compared to the predicted secondary structures of the NiV N protein in order to determine whether NiV N proteins had any secondary structures similarities when compared to RV and VSV N proteins. The various truncations made to the NiV N protein were assessed to determine whether they could impair the formation of any potential α-helices or β-sheet motifs (3). The findings from both

prediction programs, ClustalW and Jpred, were summarized in Figure 15 and were used to determine where the truncations were located and which potential secondary structures might be interrupted. As demonstrated in Figure 15, the NiV N protein was predicted to contain a number of α-helix stretches (H). Additionally, when the locations of the truncations (denoted by vertical lines |) were taken into consideration many of the truncations were located towards the beginning or end of an α-helix stretch. The interruption of α-helices may cause structural instability. However, when the truncated proteins were individually analyzed by the Jpred software, the removal of a portion of the α-helix did not seem to inhibit the production of the remaining α-helix stretch (data not shown). Overall, the predicted structural modelling of these constructs did not indicate any obvious problems with the proposed truncations.

Truncated NiV N genes were PCR amplified using gene specific primers which also incorporated an HA epitope tag on the 3' end of the gene (Appendix 3). These amplicons were then cloned into pBK-CMV-IRES. Based on the design of the aforementioned constructs, additional smaller constructs of the NiV N gene were cloned into the vector pECFP-N1 subsequently creating an N-terminal fusion protein with CFP (Appendix 3). This fusion protein was created in order to ease the visualization of these small NiV N peptides by both IFA and immunoblot. The presence and sequence of the various NiV N gene inserts, HA-tagged and CFP-tagged, were verified by DNA sequencing.

To verify expression of the truncated NiV N proteins, cells were transfected with the various constructs and cell lysates were analyzed by


RV N
VSV N
NiV N

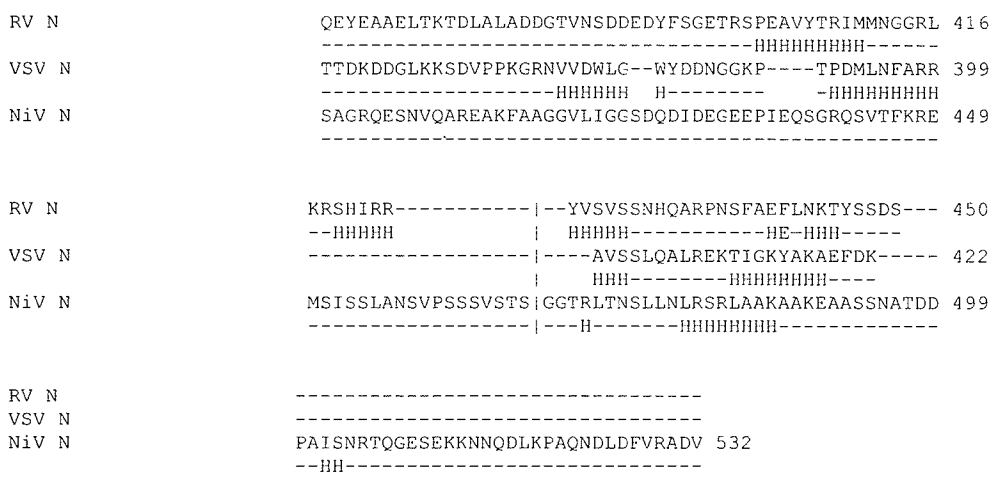

Figure 15: Secondary Structure Alignments of NiV, RV, and VSV N Proteins. A ClustalW alignment (3) was utilized to create an alignment of NiV, RV, and VSV N proteins. Jpred secondary structure prediction algorithms were used to identify potential α-helices and β-sheet regions. The results obtained from these two programs were superimposed. Letters in black represent the alignment produced from ClustalW software. Letters in red represent the Jpred secondary structure results (4), H represents helices, and E represents sheets. Vertical dashed lines represent positions within NiV N where a truncated protein was designed.

immunoblot using NiV-, HA- and/or GFP-specific antibodies (Appendix 2). The molecular weights of the truncated proteins were calculated using Compute pI/MW software (1) and compared with their observed molecular weights. Table 8 provided the predicted molecular weights and other properties for the various recombinant proteins produced.

Table 8: Protein properties of truncated NiV N constructs

Construct Name	Amino Acid Position in NiV N	Number of NiV N Amino Acids	Molecular Weight (kDa)
HA-tagged Constructs			
NiV N 1-1599-HA-IRES-CMV	1-532	532	59.2
NiV N 1-1401-HA-IRES-CMV	1-467	468	52.2
NiV N 1-1101-HA-IRES-CMV	1-367	368	41.9
NiV N 1-801-HA-IRES-CMV	1-267	268	30.6
NiV N 163-1599-HA-IRES-CMV	55-532	480	53.3
NiV N 481-1599-HA-IRES-CMV	161-532	374	41.8
NiV N 802-1599-HA-IRES-CMV	268-532	267	29.8
NiV N 163-1401-HA-IRES-CMV	55-467	414	46.3
CFP-Tagged Constructs			
NiV N 1-1599-CFP	1-532	532	83.4
NiV N 1-162-CFP	1-54	55	32.9
NiV N 163-480-CFP	55-160	108	38.5
NiV N 481-801-CFP	161-267	109	38.3
NiV N 802-1101-CFP	268-367	102	38.8
NiV N 802-1401-CFP	268-467	202	48.7
NiV N 1102-1401-CFP	368-467	162	37.4
NiV N 1102-1599-CFP	368-532	167	44.4
NiV N 1402-1599-CFP	468-532	67	33.9

Two of the truncations, NiV N 481-1599-HA and NiV N 802-1599-HA, demonstrated a slight shift in molecular weight when compared to their predicted values, Figure 16A. These constructs exhibited a 3-5 kDa and 10 kDa shift in molecular weight from their predicted values, respectively, Figure 16A. In many situations, proteins are co- or post-translationally modified thus causing an increase in the apparent molecular weight. Based on the aa sequence of the NiV N protein, Prosite protein prediction software (2) identified 25 potential phosphorylation sites, 9 possible N-myristoylation sites, and 2 potential N-linked glycosylation sites. Currently, there have been no experimental studies regarding the post-translational modifications of NiV N proteins. However, other N proteins within the order *Mononegavirales* have been shown to be phosphorylated (7;10;21;50;54;74;77;92;106;109;132;158;168-170;185) and O-linked glycosylated (94;190). These studies also demonstrated the role of these modifications in conferring protein functions. Viral proteins have also been shown to be myristoylated; however, there are no known N proteins which have been shown to have this modification (139;145;167;175). Another possible explanation for the apparent increase in molecular weight could be the presence of increased proportions of acidic residues such as glutamic acid (E) and aspartic acid (D), in these proteins. SDS is a negatively charged detergent, which binds tightly to proteins masking their intrinsic charges and creating a uniform negative charge that is roughly proportional to the protein's molecular weight. Acidic residues do not bind well to SDS due to their intrinsic negative charge and therefore, have a tendency to migrate in SDS PAGE gels more slowly. Thus, a

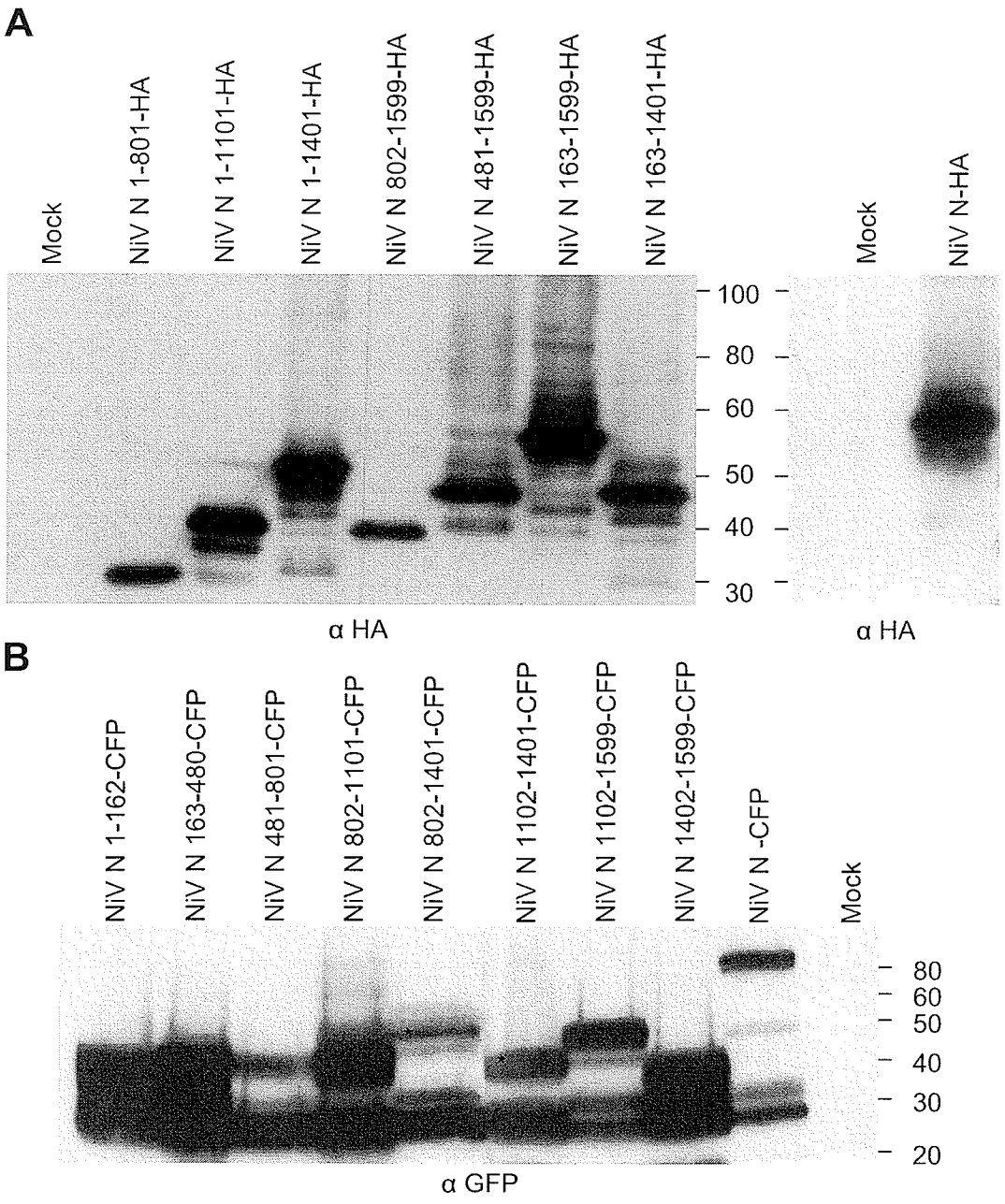

Figure 16: Expression of the Truncated NiV N Constructs by Immunoblot. Experiments were repeated at least three times. (A) 293T cells transiently expressing various truncated NiV N-HA proteins were harvested, run on a 10% SDS PAGE gel and analyzed by immunoblot. A rabbit anti-HA antibody verified expression of the various truncated NiV N-HA constructs. (B) 293T cells transiently expressing various truncated NiV N-CFP proteins were harvested, run on a 12% SDS PAGE gel and analyzed by immunoblot. A mouse anti-GFP antibody verified expression of the various truncated NiV N-CFP constructs. (*) identification of truncated proteins based on their predicted molecular weights

protein rich in acidic residues may appear to have a higher molecular weight. However, when the truncated NiV N constructs were analyzed, the composition of acidic residues remained fairly consistent at 12.0%, 11.5% and 11.7% for constructs NiV N-HA, NiV N 481-1599-HA and NiV N 802-1599-HA, respectively. In general, a number of factors may be responsible for the apparent increase in molecular weight, and it is reasonable to assume that a combination of post- or co-translational modifications of this protein were responsible for the apparent increase in molecular weight. A number of studies may be employed to assess the co/post translational modification of a protein, specifically the use of mass spectrometry as a method to detect the presence of these modifications may be useful. However, from past studies with other Paramyxoviruses, there has been no indication that the co/post translational modification of the N proteins would have any effect on their ability to bind P proteins.

Expression of the NiV N-CFP fusion proteins were visualized using a GFP-specific antibody, Figure 16B. Apart from the NiV N protein-specific bands, an additional band at approximately 27kDa was visualized in cell lysates that expressed the CFP fusion protein, Figure 16B. This band does not appear in mock transfected cells, but it does appear in all samples that have been transfected with the ECFP-N1 plasmid backbone, suggesting that this band is specific to the production of CFP but not to the production of the NiV N fusion protein. When the nucleotide sequence of the pECFP-N1 plasmid backbone was analyzed more closely, an in-frame translational start site (ATG) was found towards the beginning of the CFP gene. This indicates that if the NiV N gene

was cloned directly upstream of the CFP gene, then two proteins could be translated from this construct, a NiV N-CFP fusion protein and a separate CFP protein. The molecular weight of CFP was determined to be 27kDa, which corresponds well with the band's observed size.

Blots containing the NiV N-HA and NiV N-CFP truncated proteins were re-probed with a guinea pig-derived polyclonal NiV antiserum, Figure 17. These blots demonstrated the presence of many truncated NiV N proteins; however, not all of the truncations were detected, Figure 17. It appears that the NiV antiserum detects epitopes located in the C-terminus and under some circumstances can detect epitopes in the extreme N-terminus. Interestingly, NiV N 1-162-CFP was detected using the NiV antiserum; however, NiV N 1-801-HA and NiV N 1-1101-HA, which contain this domain, were not visualized. This could be explained by the potential masking of the epitope with addition of more of the N protein sequence to the C-terminus. Another important finding was that the additional 27kDa band, seen when expressing the NiV N-CFP fusion protein, was no longer present, Figure 17B. This suggests that the additional band seen using the GFP antibody is likely CFP or a portion of CFP. The expression of CFP in combination with the fusion protein N-CFP would likely not have a negative impact on the function of the N-CFP fusion protein, since studies have demonstrated that expression of CFP does not affect viral replication, See Section 3.2.14.

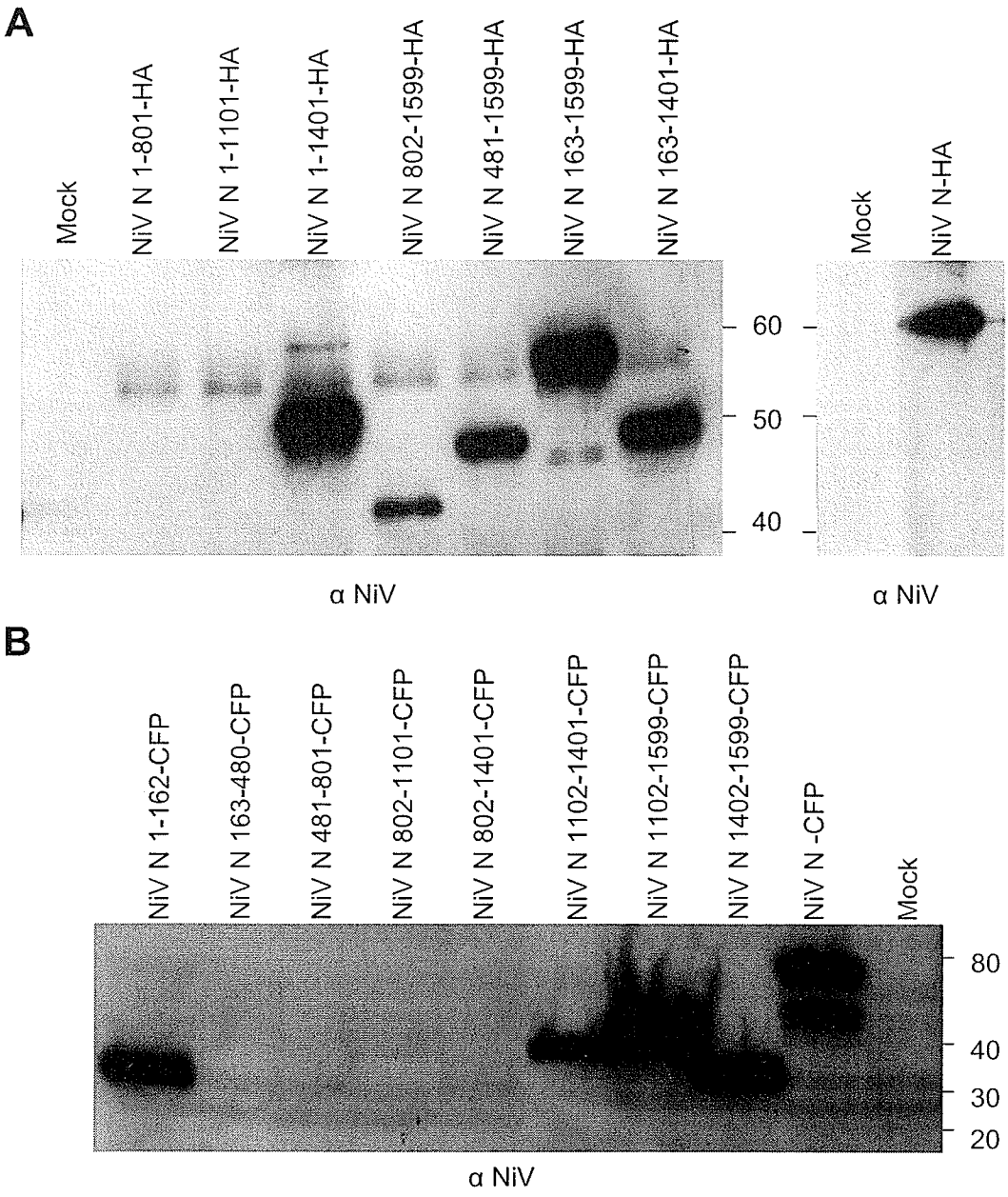

Figure 17: Detection of Truncated NiV N Constructs with NiV Specific Antibodies. (A) 293T cells transiently expressing various truncated NiV N-HA proteins were harvested, run on a 10% SDS PAGE gel and analyzed by immunoblot. A guinea pig polyclonal serum against NiV allowed for the identification of NiV N specific epitopes. (B) 293T cells transiently expressing various truncated NiV N-CFP proteins were harvested, run on a 12% SDS PAGE gel and analyzed by immunoblot. A guinea pig polyclonal serum against NiV allowed for the identification of NiV N specific epitopes.

3.2.5 Expression and characterization of truncated NiV N proteins by immunofluorescence assays

Immunoblots represent denatured proteins, which are separated based on their molecular weights whereas IFAs detect proteins in a more native state within cells. This allows the protein expression pattern and distribution within a cell to be characterized. Punctate staining is a characteristic staining pattern for NiV N proteins, which is indicative of N proteins binding viral RNA (11). More specifically, this staining pattern is representative of N protein-oligomerization and the possible formation of NC-structures through the interaction of N proteins with RNA and other N proteins. In order to assess whether the truncated proteins had this distinctive staining pattern, 293T cells were transfected with various truncated NiV N constructs and IFAs were performed 24 hours post-transfection. Although 293T cells are not ideal for IFA assays due to their natural morphology, they were still used because they were consistently employed throughout the scope of this work. Expression of NiV N proteins was visualized using a monoclonal antibody against HA, which was conjugated to an AlexaFluor®488 fluorochrome, while lamin A, a protein found on the inner leaflet of the nuclear membrane was visualized using a lamin A-specific antibody in conjunction with a secondary antibody coupled with an AlexaFluor®568 fluorochrome. Confocal microscopy was used to visualize the NiV N proteins, represented by green fluorescence, and lamin A, denoted by red fluorescence, Figure 18 and Figure 19. It should be noted that the purpose of these experiments was to visualize the expression of the NiV N proteins within cells, so

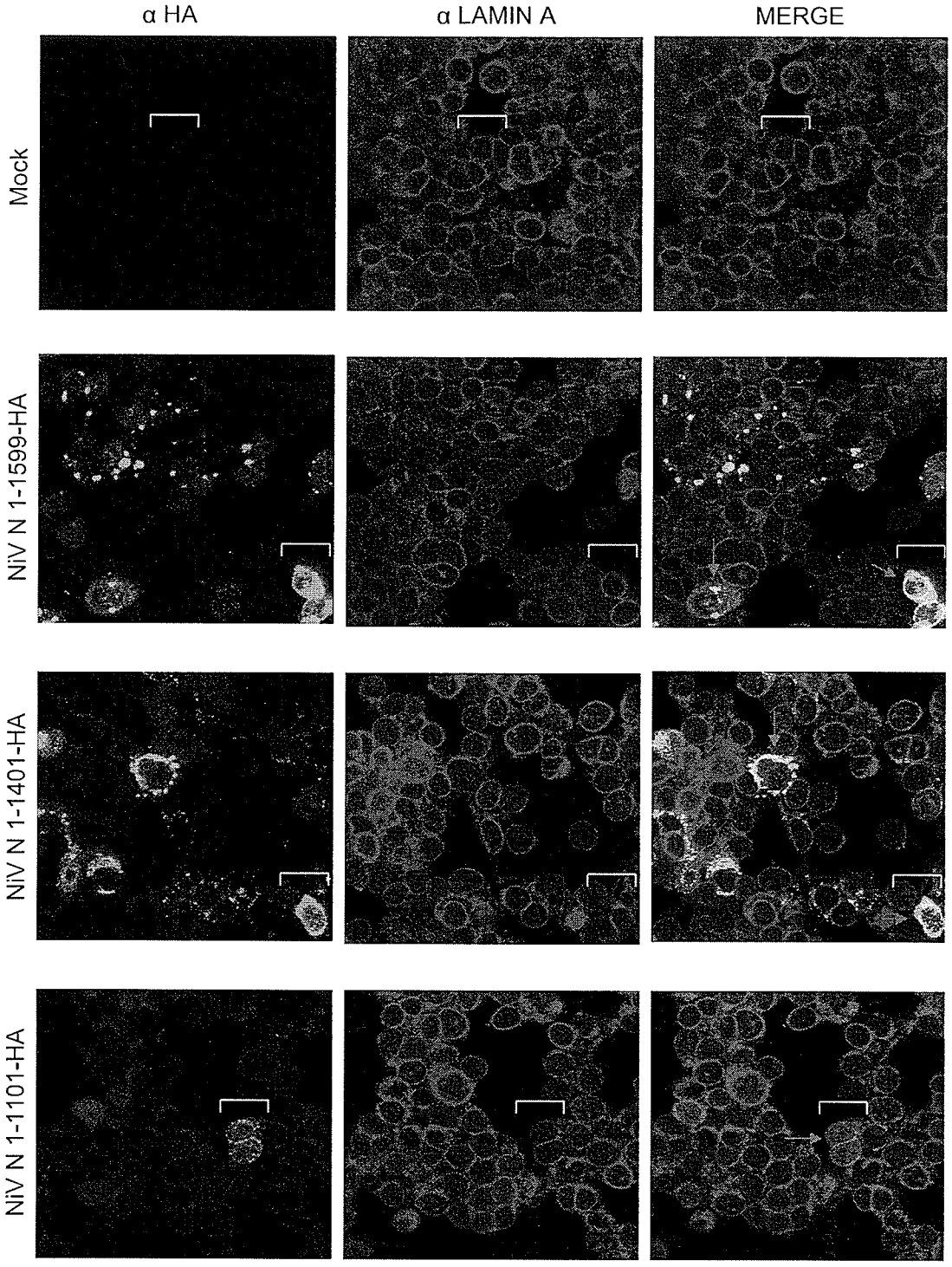
α HA
α LAMIN A
MERGE
Mock
NiV N 1-1599-HA
NiV N 1-1401-HA
NiV N 1-1101-HA

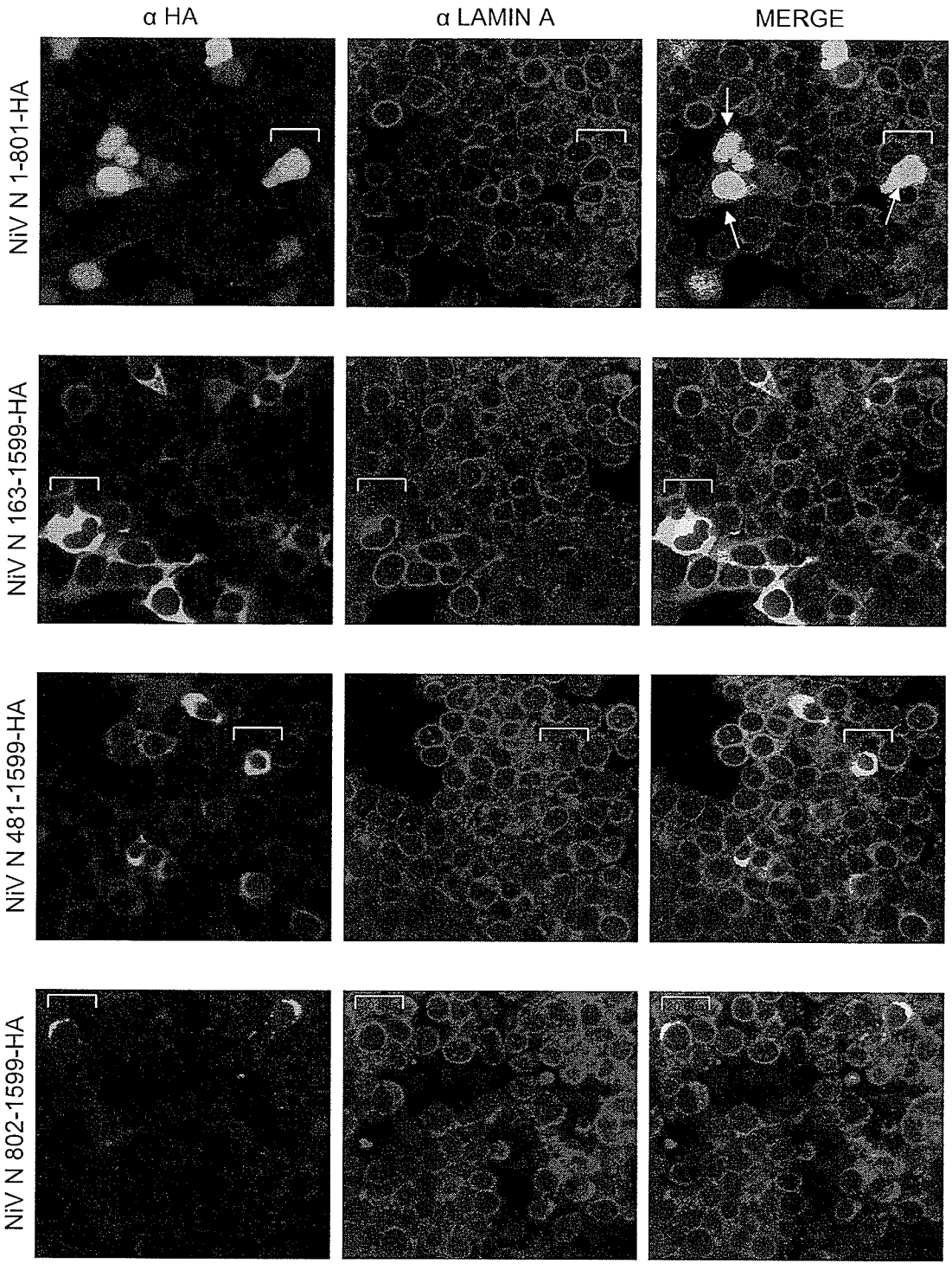
α HA
α LAMIN A
MERGE
NiV N 1-801-HA
NiV N 163-1599-HA
NiV N 481-1599-HA
NiV N 802-1599-HA

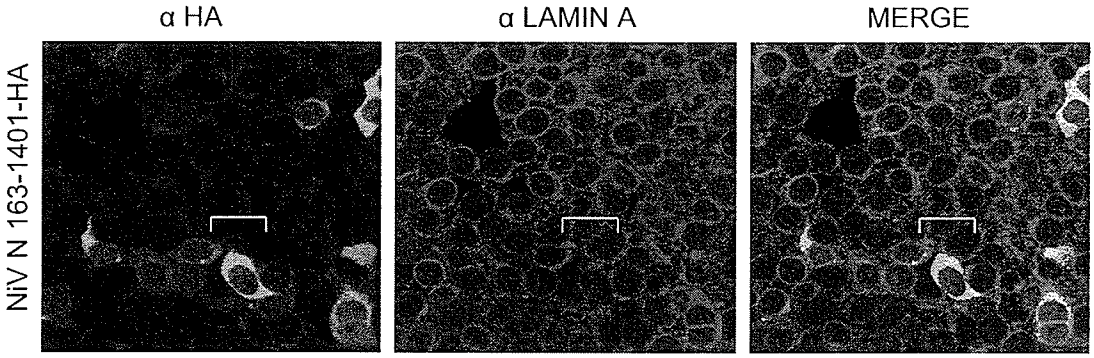

Figure 18: Expression of Truncated NiV N-HA Constructs in 293T Cells. 293T cells transiently expressing various truncated NiV N-HA proteins were analyzed by fluorescent confocal microscopy at 60x magnification employing a Z-axis slice. Cells were fixed and stained with antibodies against the HA-tag, in conjunction with an AlexaFluor®488 fluorochorome, which is represented by green fluorescence and lamin A, in conjunction with an AlexaFluor®568 fluorochrome, which is represented by red fluorescence. Co-localization between NiV N proteins and lamin A is represented by yellow fluorescence. Blue arrows indicate possible nuclear localization of NiV N proteins with punctate staining patterns. White arrows indicate possible nuclear localization of NiV N proteins with diffuse staining patterns.

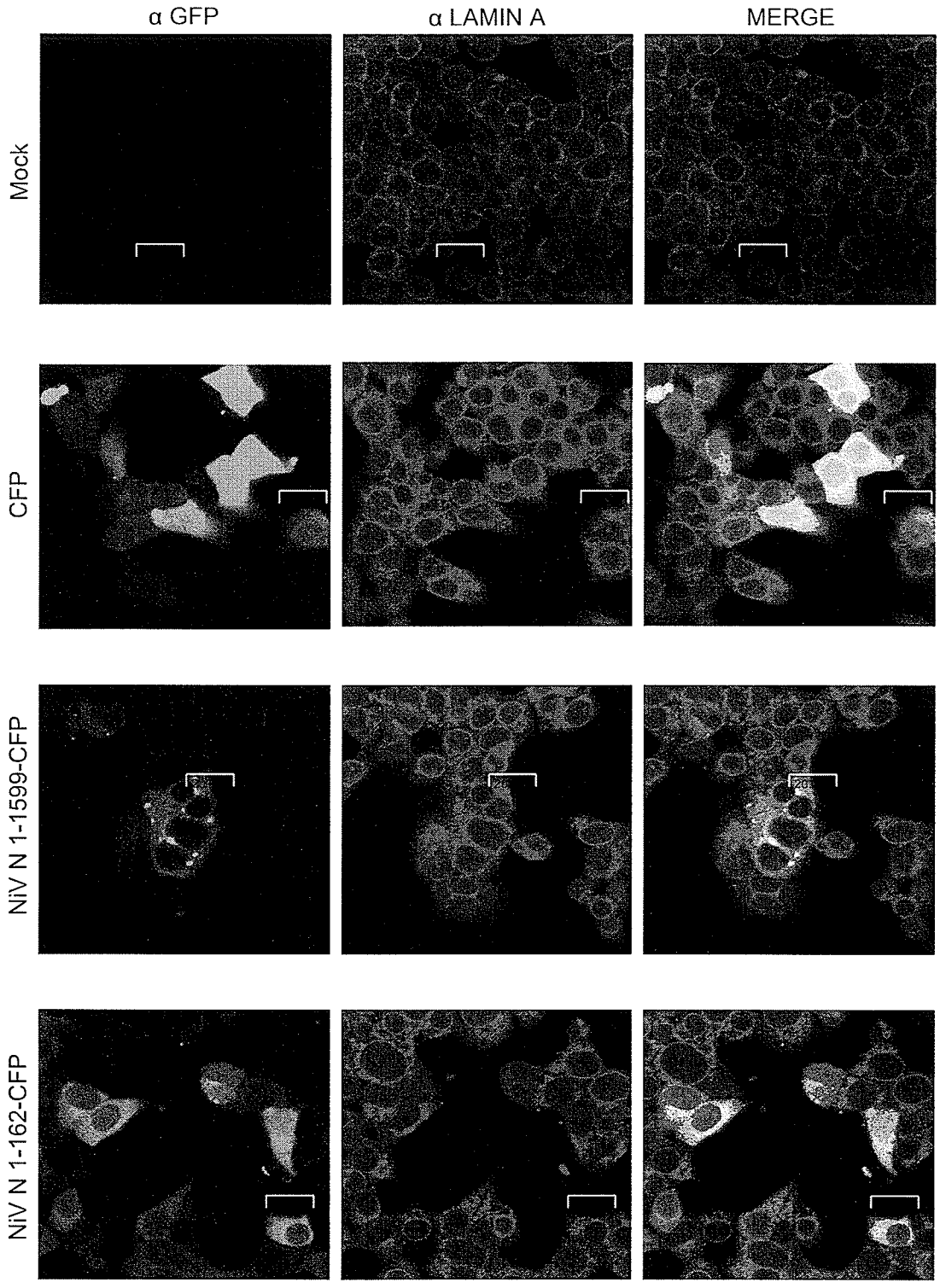
α GFP
α LAMIN A
MERGE
Mock
CFP
NiV N 1-1599-CFP
NiV N 1-162-CFP

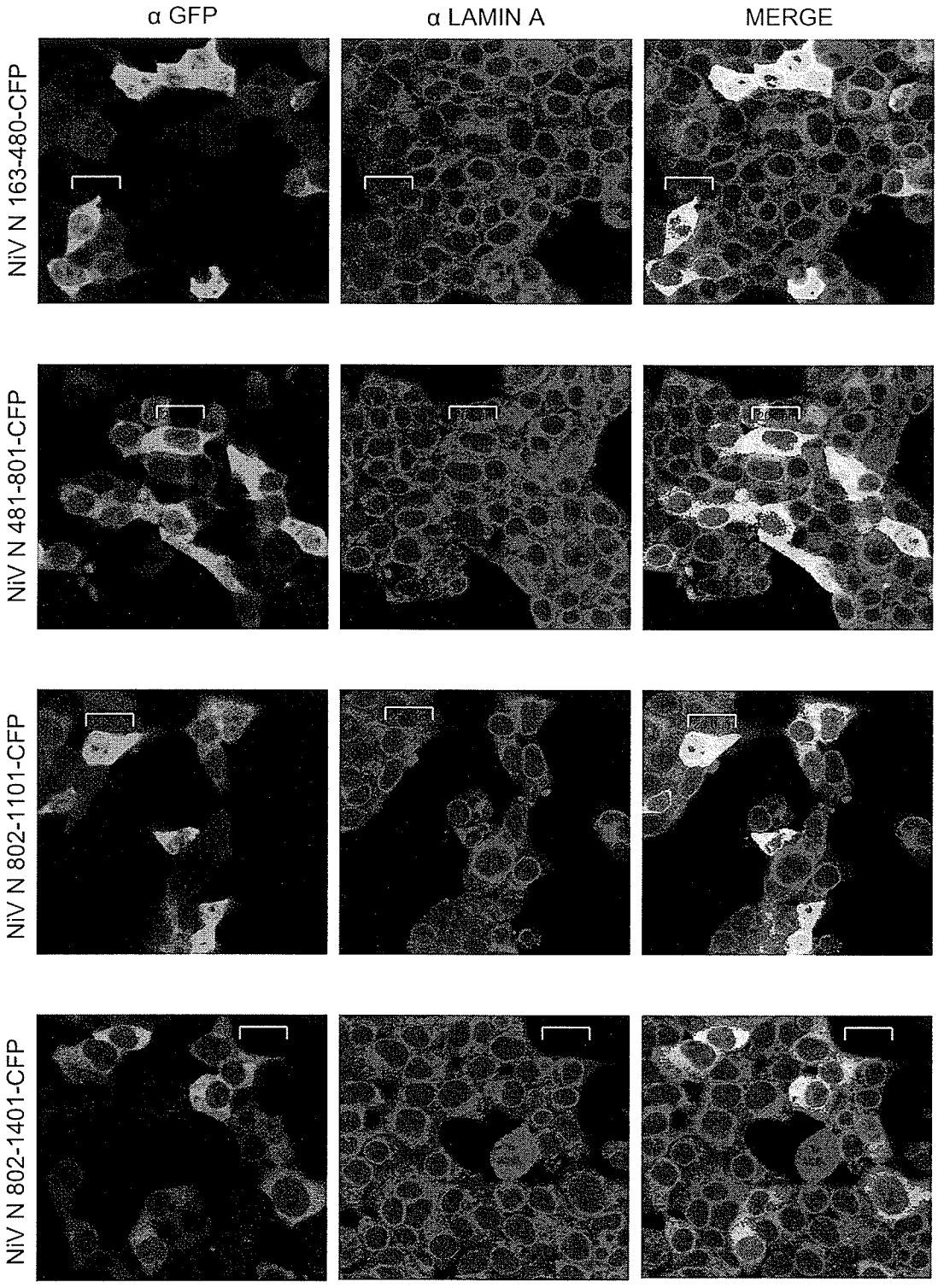
α GFP
α LAMIN A
MERGE
NiV N 163-480-CFP
NiV N 481-801-CFP
NiV N 802-1101-CFP
NiV N 802-1401-CFP

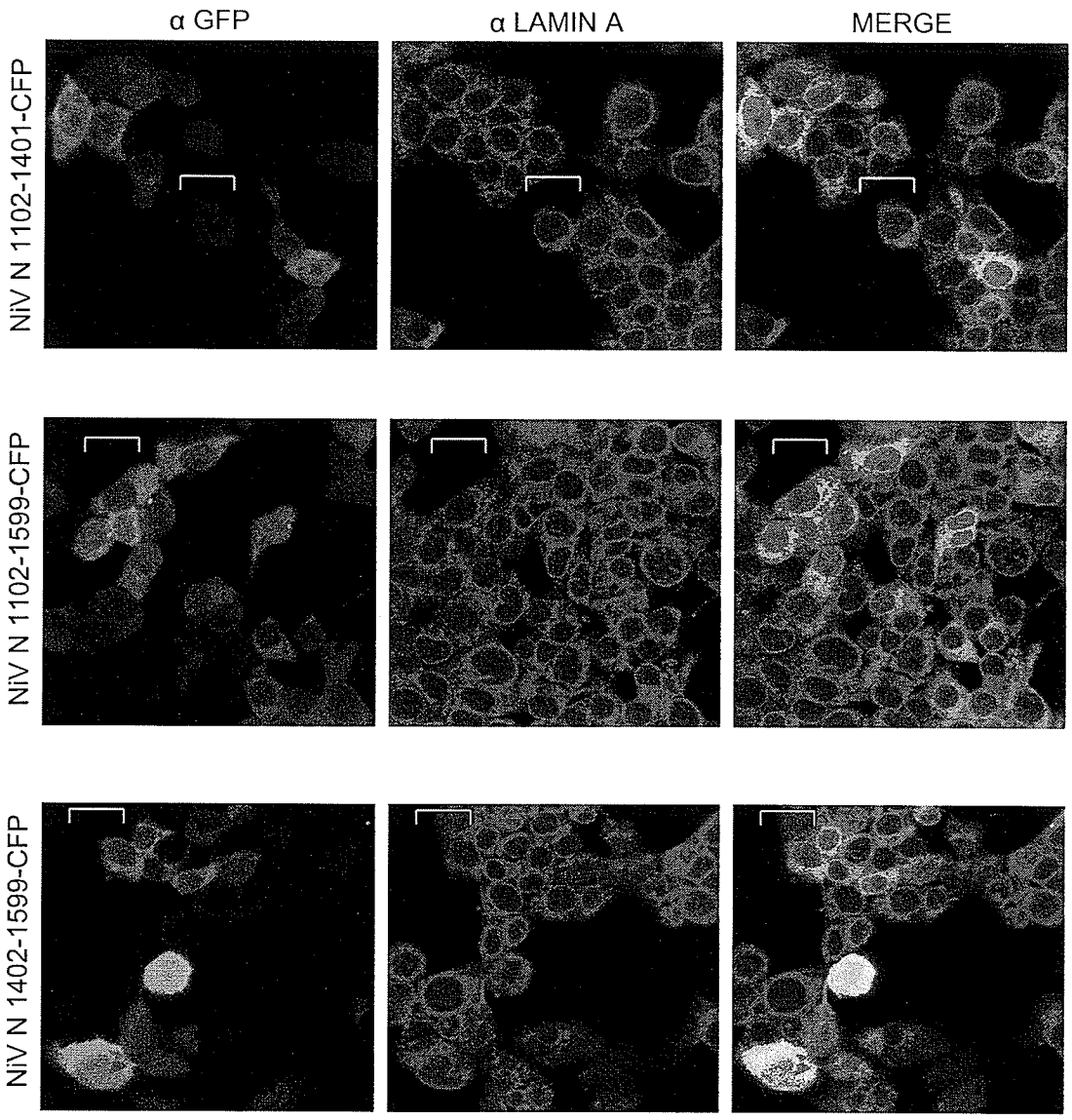

Figure 19: Expression of Truncated NiV N-CFP Constructs in 293T Cells. 293T cells transiently expressing various truncated NiV N-CFP proteins were analyzed by fluorescent confocal microscopy at 60x magnification employing a Z-axis slice. Cells were fixed and stained with antibodies against the GFP, in conjunction with an FITC fluorochorome, which is represented by green fluorescence and lamin A, in conjunction with an AlexaFluor®568 fluorochrome, which is represented by red fluorescence. Co-localization between NiV N proteins and lamin A is represented by yellow fluorescence.

the transfection protocols were not optimized for increased transfection efficiency. The positive control, full-length NiV N-1-1599-HA proteins demonstrated characteristic punctate staining, Figure 18. In addition, NiV N 1-1401-HA, NiV N 1-1101-HA and NiV N 802-1599-HA also exhibited punctate staining patterns, Figure 18. These results indicated the presence and ability of NiV N proteins to aggregate within cells, which may also include their ability to bind cellular RNA and oligomerize into NC-structures within the cytoplasm. However, constructs NiV N 163-1599-HA, NiV N 481-1599-HA and NiV N 163-1401-HA demonstrated a diffuse cytoplasmic staining, implying that these proteins did not form NiV N protein-oligomers, Figure 18. NiV N 1-801 also demonstrated diffuse staining patterns throughout the cytoplasm and the nucleus, Figure 18-white arrows. This finding suggests that the factors necessary for the predominant cytoplasmic localization of NiV N proteins were absent or non-functional in the NiV N 1-801-HA protein. This finding will be discussed more in Section 3.2.6.

The full-length NiV N-CFP construct, NiV N 1-1599-CFP, demonstrated characteristic cytoplasmic punctate staining, indicating the ability of the NiV N-CFP to oligomerize into NC-structures and that the presence of CFP did not interfere with NiV N protein-oligomerization, Figure 19. As a control, CFP was expressed within cells and its expression was visualized as a diffuse staining pattern throughout the cell, Figure 19. The truncated constructs, NiV N 1-162-CFP, NiV N 163-480-CFP, NiV N 481-801-CFP, NiV N 802-1101-CFP, NiV N 802-1401-CFP, NiV N 1102-1401-CFP, NiV N 1102-1599-CFP and NiV N 1402-

1599-CFP demonstrated diffuse staining patterns throughout the cell, but predominantly within the cytoplasm, indicating an absence of NiV N protein NC-structures, Figure 19. Unfortunately, since the NiV N-CFP constructs likely produced CFP in addition to the NiV N fusion protein, as demonstrated in Figure 16, it is difficult to analyze any potential localization into the nucleus and therefore, potential sub-cellular distribution of these proteins will not be discussed further.

These results demonstrated the presence of NiV N protein-specific punctate staining within transfected 293T cells, indicating the production of NiV N protein-oligomers. Additionally, a number of the truncated NiV N proteins were able to maintain this staining pattern and suggested that they were also capable of forming NiV N protein-oligomeric structures. NiV P proteins are thought to prevent non-specific binding of NiV N proteins to cellular RNA thereby inhibiting the formation of oligomeric structures. Therefore, the results obtained in this section could be applied to experiments in later sections to assess the ability of the NiV P protein to interact with the truncated proteins and maintain them in a soluble state. These findings also demonstrated that the NiV N protein could be found within the nucleus of cells, which will be further analyzed in the following section.

3.2.6 Localization of recombinant NiV N proteins within the nucleus of cells

A general characteristic of viruses within the order *Mononegavirales* is that they encode their own viral polymerases and does not require cellular

polymerases for viral RNA synthesis. Therefore, viral proteins are thought to be found solely in the cytoplasm of cells. However, MeV and CDV N proteins have both been shown to be present within the nucleus in various recombinant assays (162;166;202). When considering the subcellular distribution of NiV N proteins more closely, full-length NiV N proteins appeared to localize predominantly within the cytoplasm of cells. However, a fraction of NiV N proteins was expressed within the nucleus, Figure 18-black arrows. Additionally, cells expressing NiV N 1-1401 and NiV N 1-1101 also demonstrated similar punctate staining possibly within the nucleus, Figure 18-black arrows.

Two of the truncated proteins, NiV N 1-801-HA and NiV N 802-1599-HA, showed significant differences between their protein expression patterns. The construct containing the N-terminal half of the NiV N protein, NiV N 1-801-HA, displayed strong nuclear staining, while the C-terminal half of the protein localized completely within the cytoplasm of cells. These proteins were therefore analyzed more closely for their distribution within the nucleus and cytoplasm. The cytoplasm was visualized by detecting the presence of actin, which is a cytoplasmic-based protein using phalloidin (which specifically interacts with F-actin molecules) conjugated to an AlexaFluor®568 fluorochrome. The nucleus was visualized through the detection of PARP, which is a nuclear protein and has a role in DNA repair and programmed cell death, using an antibody against PARP in conjunction with a secondary antibody coupled to an AlexaFluor®647 fluorochrome. Finally, the NiV N protein was visualized using a monoclonal antibody against HA, which was coupled with an AlexaFluor®488 fluorochrome.

Controls using only secondary antibodies were used to test the specificity of the antibodies and to ensure that non-specific binding of the antibodies did not occur (data not shown). The expression of actin is represented by red fluorescence, PARP is denoted by dark blue fluorescence, and NiV N is designated by green fluorescence. Co-localization between actin and NiV N proteins is seen as yellow fluorescence and co-localization between PARP and NiV N proteins is seen as light blue fluorescence. Confocal microscopy at a magnification of 60x was utilized in order to visualize multiple cells within one field while at the same time maintaining sufficient resolution to determine the localization of proteins within the nucleus or cytoplasm. This allowed the visualization of a variety of cells, some of which may express the recombinant proteins at high levels and others at lower levels. Additionally, visualizing multiple cells with similar NiV N protein expression patterns increases the significance and relevance of the data shown.

293T cells transiently expressing full-length NiV N-HA proteins demonstrated characteristic punctate staining patterns, Figure 20. NiV N-HA sub-cellular distribution was predominantly within the cytoplasm and to a slightly lower extent within the nucleus, Figure 20-observe the punctate light blue-staining representing co-localization between NiV N proteins and PARP (black arrows). Even though only a few cells demonstrated nuclear localization of the N protein, it may be possible that only ever a small proportion of NiV N proteins gain access to the nucleus, while the majority of the N protein is found in the cytoplasm. These results also strengthen the validity of the data described in

Figure 18, which showed similar expression and sub-cellular localization patterns. The truncated proteins, NiV N 1-1401-HA, and NiV N 1-1101, previously demonstrated similar staining patterns to full-length NiV N-HA proteins, Figure 18. However, when NiV N 1-801 was analyzed more closely, it was distributed throughout the whole cell in a diffuse manner and with prominent localization within the nucleus, Figure 20. The co-localization between NiV N 1-801-HA and PARP verified its presence within the nucleus, Figure 20-observe the diffuse light blue staining patterns representing co-localization between PARP and NiV N 1-801-HA (white arrows). On the other hand, NiV N 802-1599-HA was found to be present completely within the cytoplasm and co-localized with actin, Figure 20- observe the co-localization of NiV N proteins and actin represented by yellow fluorescence. The presence of NiV N 1-801-HA within the nucleus may suggest that the N-terminal half of the protein contained a nuclear localization signal (NLS), which was responsible for the protein distribution within the nucleus. However, it must be kept in mind that even though NiV N 1-801-HA was found in the nucleus, this may be an artefact due to the truncation of the protein. It is possible that the NiV N protein does contain a NLS but is a cryptic NLS, which may or may not have biological relevance. This latter explanation may also address the finding that NiV N proteins were predominantly located within the cytoplasm. These results suggested that factors necessary for nuclear localization were absent or non-functional in the truncated NiV N 802-1599-HA protein. The presence of NiV N 802-1599-HA within the cytoplasm could be a result of several factors: (1) a nuclear export signal (NES) may be found within

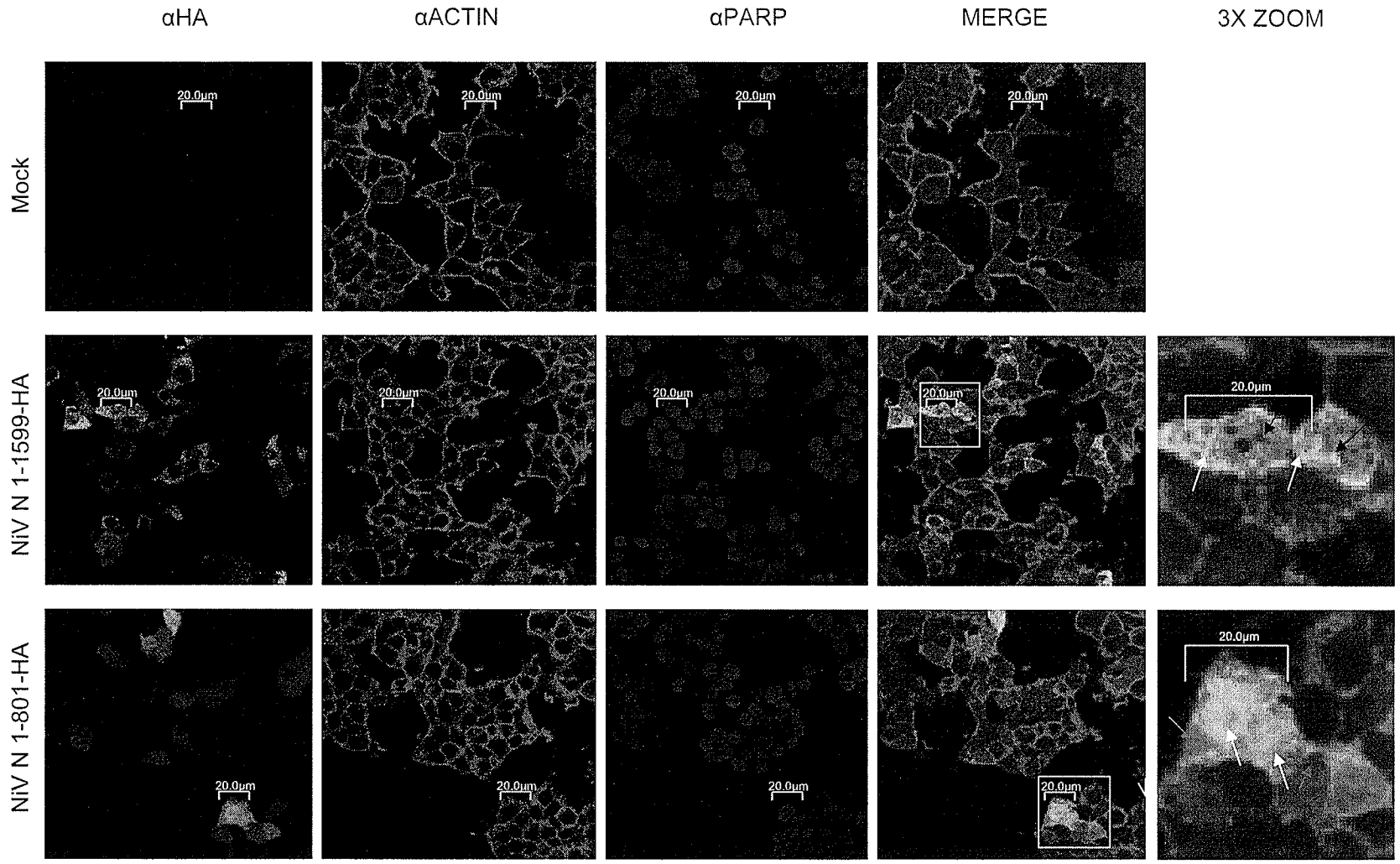
αHA
αACTIN
αPARP
MERGE
3X ZOOM
Mock
NiV N 1-1599-HA
NiV N 1-801-HA
20.0µm

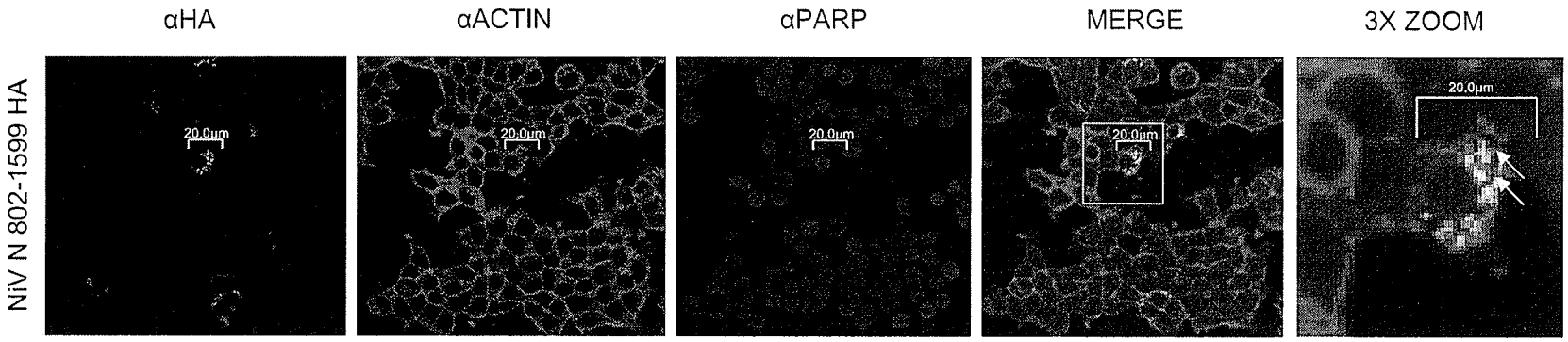

Figure 20: Analyzing the Localization Patterns of Truncated NiV N-HA Constructs. 293T cells expressing various NiV N-HA truncated proteins were analyzed by immunfluorescence assay using confocal microscopy at 60x magnification employing a Z-axis slice. Detection of NiV N proteins is represented by green, actin, a cytoplasmic protein, is represented by red, and PARP, a nuclear protein, is represented by dark blue. Co-localization between actin and NiV N proteins is represented by yellow and co-localization between NiV N proteins and PARP is represented by light blue. Regions within the white boxes are enlarged to 180x magnification in order to ease visualization of co-localization and are presented in the right-most column. Black arrows indicate nuclear localization of NiV N proteins with punctated staining patterns. White arrows indicate nuclear localization of NiV N proteins with diffuse staining patterns. Yellow arrows indicate cytoplasmic staining of NiV N proteins with punctate staining. Pink arrows indicate cytoplasmic staining of NiV N proteins with diffuse staining patterns

the C-terminal half of the protein, (2) a potential site in this region of the protein interacts with another cellular protein to retain the NiV N protein in the cytoplasm, or (3) the presence of the C-terminal half of the protein induces a structural conformation which does not favour the exposure of any potential NLS sequences. The main finding observed is that when expressed alone a small proportion of NiV N proteins are found within the nucleus of cells. Potential roles for the NiV N protein within the nucleus have yet to be elucidated. If NiV N proteins are able to localize to the nucleus, their interaction with NiV P proteins may have the ability to prevent nuclear localization and maintain the NiV N proteins in the cytoplasm for the purposes of viral replication. Therefore, by observing the ability of the NiV P protein to prevent the nuclear localization of NiV N proteins, this may provide a means to determine regions of the NiV N proteins that are necessary for binding to NiV P proteins.

3.2.7 Characterization of NiV N proteins when co-expressed with NiV P proteins within 293T cells

It has been shown that recombinantly expressed recombinant MeV or CDV N proteins were found within the nucleus of cells (112;162;166;202). Similarly, when expressed alone NiV N proteins are also within the nucleus of cells, Section 3.2.6. However, NiV N proteins are typically found within the cytoplasm during viral replication. Currently, it is unknown whether there is a nuclear presence of the NiV N protein during viral replication. Furthermore, potential functions of the NiV N protein within this sub-cellular compartment are currently

unknown. The predominant cytoplasmic localization of NiV N proteins during viral replication could be explained by its interaction with the NiV P protein. As is seen with other paramyxovirus P proteins, NiV P proteins are believed to maintain N proteins in a soluble state in the cytoplasm, so that they are available for viral encapsidation and replication (8;29;40;42;43;45;56;60;62;66;87;90;91;95;134;144;153;172;173;200;205). Therefore, a change in sub-cellular distribution may be apparent when recombinant NiV N proteins are expressed either alone or in conjunction with NiV P proteins. Furthermore, exploiting the ability of NiV P proteins to cause a change in the sub-cellular distribution of NiV N proteins may make it possible to determine regions within the NiV N protein that are necessary for the specific interaction with NiV P proteins through the co-expression of various truncated NiV N proteins and NiV P proteins. One of the hypotheses of this work suggests that expression of the NiV P protein-binding domains may have the ability to interact with the transcriptase complex and disable the functions of both the transcriptase and replicase complexes. The elucidation of the NiV P protein-binding domains within the NiV N proteins could then be used to assess this hypothesis.

Primers designed against the NiV P gene were used to amplify the NiV P ORF from NiV RNA (Appendix 3). Additionally, a FLAG-tag nucleotide sequence was incorporated onto the 5' end of the reverse primer to generate a NiV P-FLAG amplicon (Appendix 3). The FLAG-tag encodes an aspartate-rich, 8 aa sequence (DYKDDDDK). The NiV P-FLAG construct will be utilized in Section 3.2.8. Positive clones, identified through restriction enzyme digestion screens,

were subsequently sequenced, and the presence and correct sequence of the NiV P ORF was verified. NiV P protein expression was verified by transfecting 293T cells with the corresponding plasmid DNA and cell lysates were analyzed by immunoblot. The expression of NiV P proteins was verified by probing the immunoblots using NiV-specific antibodies and the observation of a 98kDa band (Figure 21, left panel), while immunoblots employing a FLAG antibody provided evidence for the presence of an in-frame FLAG-tag (Figure 21, right panel).

Fractionation experiments were preformed, where the nucleus was physically separated from the cytoplasm using a weak NP-40 lysis buffer and further analyzed by immunoblot. This study attempted to identify regions within the NiV N proteins that were able to interact with the NiV P protein by maintaining the NiV N proteins within the cytoplasm. Antibodies against a nuclear protein (histone H3), a nuclear membrane protein (lamin A), a cytoplasmic protein (actin), and a ubiquitously expressed protein (α-tubulin) (Appendix 2) were used in order to assess the efficacy of separating the cytoplasmic fraction from the nuclear fraction. The ability of this separation assay to distinguish between cytoplasmic proteins and nuclear proteins was demonstrated by immunoblot in Figure 22. Lamin A, a protein associated with the inner leaflet of the nuclear membrane, was found only within the nuclear fraction, indicating that this separation protocol appeared to contain the nuclear membrane. The detection of actin was used to confirm the presence of cytoplasmic proteins within the cytoplasmic fraction. Similarly, the ubiquitous expression of α-tubulin also

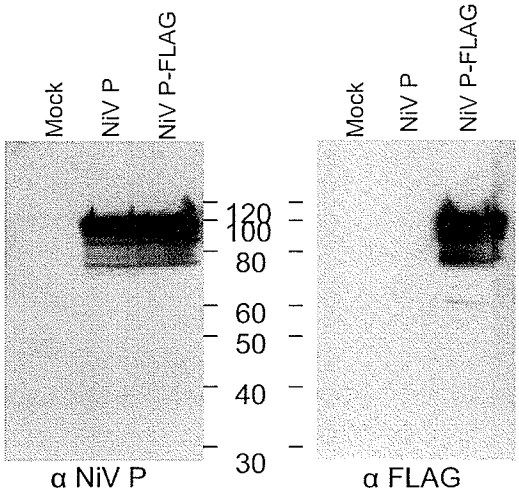

Figure 21: Expression of the NiV P-CMV and NiV P-FLAG-CMV Constructs. 293T cells were transfected with NiV P-CMV or NiV P-FLAG-CMV for 48 hours. Cell lysates were harvested and analyzed by immunoblot. A monoclonal antibody against NiV P (left panel) verified expression of the NiV P protein, while a monoclonal antibody against FLAG (right panel) verified the presence of a FLAG tag on the C-terminal end of the NiV P protein.

Protein ID	Sub-cellular Distribution	Molecular Weight	Cellular Fractionation	
			Nuclear Fraction	Cytoplasmic Fraction
Histone H3	Nuclear	17kDa	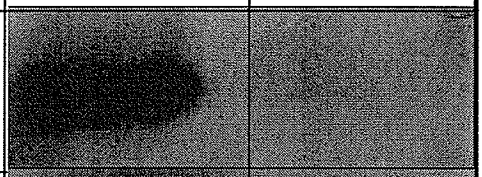	
Lamin	Inner Leaflet of the Nuclear Membrane	70kDa	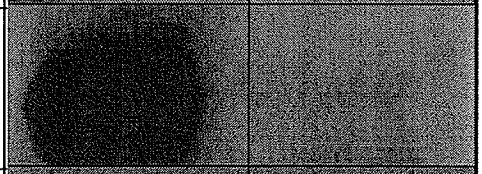	
Actin	Cytoplasmic	42kDa	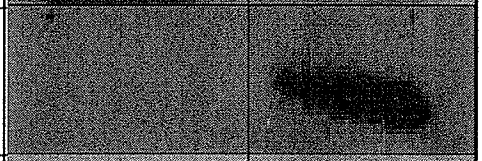	
Alpha Tubulin	Ubiquitous	50kDa	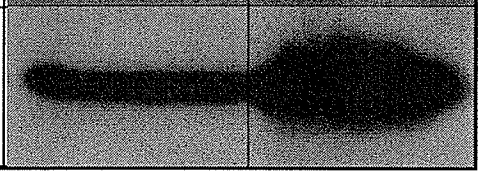	

Figure 22: Fractionation of 293T Cells into Cytoplasmic and Nuclear Fractions. 293T cells were fractionated with a weak lysis buffer and high-speed centrifugation to separate the nuclear and cellular fractions. Immunoblots using antibodies against histone H3, a small nuclear protein, lamin A, a protein found on the inner leaflet of the nuclear membrane, actin, a predominantly cytoplasmic protein and alpha tubulin, a protein expressed ubiquitously throughout the cell were used to verify the presence of various proteins within the nuclear and cytoplasmic fractions.

supported the cellular fractionation protocols, as it was found in both the nuclear and cytoplasmic fractions. Therefore, this biochemical assay provided an indirect but effective way of determining the differential localization of specific proteins between the nucleus and cytoplasm, but it could not discriminate between proteins embedded in the nuclear membrane and proteins found in the nucleus.

However, the ability of proteins to aggregate and the distribution of these aggregated proteins must also be taken into consideration. Proteins that form aggregated structures have the tendency to precipitate out of solution. Therefore, when the nuclear fraction was harvested by sedimentation, it is possible that the aggregated proteins could have been pelleted along with the nuclei. The characteristic punctate staining observed in cells expressing NiV N protein was indicative of protein aggregation and potential formation of complex NC-structures, Figure 18 and 20. Therefore, NiV N proteins may precipitate out of solution and be found within the nuclear fraction. Thus, it should be noted that the use of the term "nuclear fraction" would likely include the presence of aggregated proteins. However, it has been proposed that when NiV N proteins are co-expressed with NiV P proteins, the distribution of NiV N proteins would be maintained in a soluble fashion and will be further analyzed in Section 3.2.15. Overall, this assay may not have the potential to characterize the interaction of NiV N and NiV P proteins accurately based on their sub-cellular distribution. Nevertheless, this assay will be useful in identifying regions that are necessary for the interaction between the NiV P and N proteins to maintain NiV N proteins in a useable state for viral encapsidation and replication.

Cells were transfected with truncated NiV N constructs or co-transfected with NiV P-CMV, fractionated, brought up to equal volumes using SDS-PAGE gel loading buffer and visualized by immunoblot. Various statistical applications were employed to demonstrate whether the data obtained were meaningful and could be applied to a greater sample size. Data were analyzed using a 2-way ANOVA test in order to assess a number of variables at one time and to determine the variance between different variables. The co-expression of NiV N proteins with NiV P proteins had a significant effect on the distribution of NiV N proteins ($F=25.0259$, $P<0.0001$). The expression of various truncated proteins had a significant effect on protein distribution ($F=19.9824$, $P<0.0001$). Finally, co-expression of NiV P proteins with the various truncated proteins also had a significant impact on the distribution of the truncated proteins ($F=4.5231$, $P=0.0013$). A Tukey Post HOC test was used to compare the statistical differences between the effects that NiV P protein expression had on the distribution of the truncated NiV N proteins with the effect that NiV P protein expression had on full-length NiV N proteins. When full-length NiV N proteins were expressed alone, 72% of the protein was found in the nuclear fraction, whereas 28% of the NiV N protein was found in the cytoplasmic fraction, Figure 23. Previous IFA data demonstrated that only a limited number of cells had small amounts of NiV N proteins within the nucleus in comparison to the amount of NiV N proteins within the cytoplasm. Based on this finding it is highly probable that a large amount of aggregated NiV N proteins were harvested along with the

A

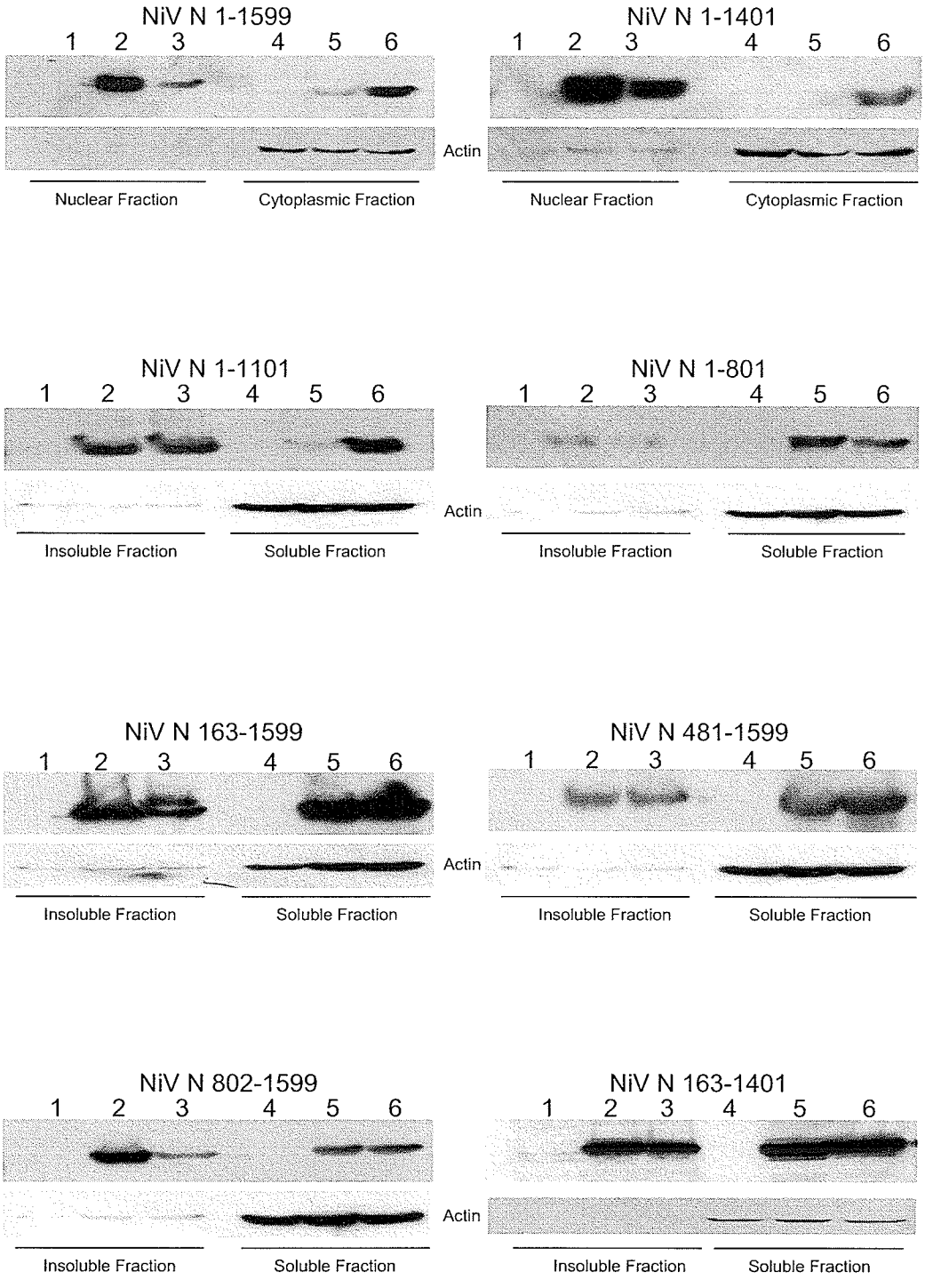
NiV N 1-1599
1 2 3 4 5 6
Actin
Nuclear Fraction
Cytoplasmic Fraction
NiV N 1-1401
1 2 3 4 5 6
Actin
Nuclear Fraction
Cytoplasmic Fraction
NiV N 1-1101
1 2 3 4 5 6
Actin
Insoluble Fraction
Soluble Fraction
NiV N 1-801
1 2 3 4 5 6
Actin
Insoluble Fraction
Soluble Fraction
NiV N 163-1599
1 2 3 4 5 6
Actin
Insoluble Fraction
Soluble Fraction
NiV N 481-1599
1 2 3 4 5 6
Actin
Insoluble Fraction
Soluble Fraction
NiV N 802-1599
1 2 3 4 5 6
Actin
Insoluble Fraction
Soluble Fraction
NiV N 163-1401
1 2 3 4 5 6
Actin
Insoluble Fraction
Soluble Fraction

B

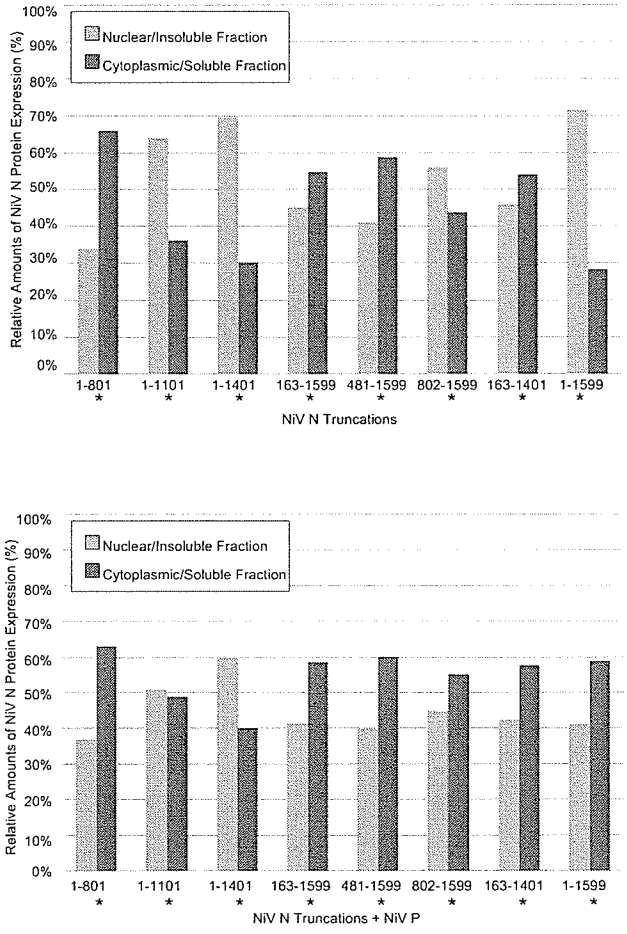

Figure 23: Fractionation of 293T Cells Expressing Truncated NiV N-HA Constructs. Experiments were repeated three times. 293T cells transiently expressing various truncated NiV N proteins or co-expressing NiV P proteins were separated into cytoplasmic/soluble and nuclear/insoluble fractions. (A) Immunoblot analysis demonstrated the cellular distribution of the truncated proteins to the cytoplasmic/soluble or nuclear/insoluble fractions. Lanes 1 and 4 are mock transfected cells (negative control), Lane 2 and 5 are cells expressing NiV N proteins, and Lane 3 are cells co-expressing NiV N and NiV P proteins. (B) Immunoblots were quantified using spot densitometry and AlphaEaseFC™ software. Standard deviations of the mean were calculated. Upper panel- demonstrated the protein distribution of cells expressing NiV N-HA constructs. Lower panel- demonstrated the protein distribution of cells expressing NiV N-HA and NiV P proteins. Values that are statistically equivalent to NiV N 1-1599 are represented by * and values that are statistically equivalent to NiV N 1-1599 + NiV P are represented by *.

nuclear fraction. As previously suggested, this assay was more indicative of the solubility of the NiV N proteins than actual sub-cellular localization of NiV N proteins within the nuclear region. In order to define the terminology of this assay more accurately, proteins found within the "cytoplasmic fraction" will more appropriately be termed the "cytoplasmic/soluble fraction", while proteins found within the "nuclear fraction" will be termed the "nuclear/insoluble fraction". When NiV N proteins were co-expressed with NiV P proteins there appeared to be a significant shift from NiV N proteins being present in the nuclear/insoluble fraction (N protein alone= 72%, N + P proteins=41%) to it being present in the cytoplasmic/soluble fraction (N protein alone= 28%, N + P proteins=59%), Figure 23. Although there was a shift, the presence of the NiV N protein in the soluble fraction was not 100%. This can be explained by two possibilities: transfected cells were not expressing both NiV N and NiV P proteins in the same cell or NiV P proteins did not have the ability to retain all of the NiV N molecules in a soluble form. This might indicate that NiV P proteins always allow a fraction of N molecules to be localized to the nuclear/insoluble fraction. In summary, when NiV N proteins are expressed alone, they are found predominantly within the nuclear/insoluble fraction. When NiV N proteins are co-expressed with NiV P proteins, the N proteins are found predominantly within the cytoplasmic/soluble fraction. These results indirectly described an interaction between the NiV N and NiV P proteins.

The truncated NiV N proteins were further analyzed with this assay to determine whether regions of the NiV N protein interacted with the NiV P protein

could be elucidated based on changes in their sub-cellular distribution and protein solubility. When expressed on its own, 70% of NiV N 1-1401-HA proteins localized to the nuclear/insoluble fraction, which was statistically equivalent to the results obtained when full-length NiV N proteins were expressed alone and localized predominantly to the nuclear/insoluble fraction, Figure 23. However, when co-expressed with NiV P proteins, 60% of NiV N 1-1401-HA proteins remained localized to the nuclear/insoluble fraction, Figure 23. These results remained statistically equivalent to results obtained with NiV N 1-1401-HA and NiV N-HA proteins when expressed independently of NiV P proteins; however, the data obtained were statistically different from data obtained with full-length NiV N proteins when co-expressed with NiV P, which demonstrated only 41% expression of NiV N proteins within the nuclear/insoluble fraction, Figure 23. These results suggest that NiV N 1-1401-HA lost the ability to interact with NiV P proteins but retained the ability to form aggregates or N protein oligomers. These results indicated that the C-terminal portion of the NiV N protein likely contained a NiV P protein-binding domain.

When NiV N protein was expressed alone, 28% of NiV N proteins were found within the cytoplasmic/soluble fraction, indicating that a fraction of the NiV N proteins were maintained in a soluble state without the presence of NiV P proteins. If the interaction between NiV N and NiV P was abolished or the ability of NiV P proteins to maintain NiV N proteins in a soluble state was disrupted, the value 28% would be the expected outcome for the localization of NiV N proteins to the cytoplasmic/soluble fraction. Any values obtained that were significantly

above 28% would be indicative of an interaction between NiV N and P proteins and a shift into the cytoplasmic/soluble fraction. When co-expressed with NiV P, NiV N 802-1599-HA demonstrated a higher amount of protein localized within the cytoplasmic/soluble fraction, 55% in comparison to the expression of NiV N-HA alone (28%), Figure 23. This finding was statistically significant, indicating that NiV N 802-1599-HA was able to interact with NiV P supporting the idea that there is a NiV P protein-binding domain found within the C-terminal end of NiV N.

The co-expression of NiV N 1-1101-HA with NiV P resulted in statistically different amounts of protein localized within the cytoplasmic/soluble fraction (49%) in comparison to the expression of NiV N-HA alone (28%), Figure 23. The difference in these results indicated that NiV N 1-1101-HA retained some ability to be distributed into the cytoplasmic/soluble fraction when co-expressed with NiV P, suggesting the presence of a possible alternative NiV P protein-binding site found within the NiV N protein. The remaining constructs did not show any statistically significant differences between the amount of protein localized within the cytoplasmic/soluble fraction and the nuclear/insoluble fraction.

The NiV N 1-801-HA, NiV N 163-1599-HA and NiV N 481-1599-HA proteins localized mainly to the cytoplasmic/soluble fraction independently of the presence of the NiV P proteins, Figure 23. These results were found to be statistically equivalent to results obtained when NiV N-HA were co-expressed with NiV P, indicating that these truncated NiV N proteins, NiV N 1-801-HA, NiV N 163-1599-HA and NiV N 481-1599-HA, retained their distribution in the cytoplasmic/soluble fraction without the assistance of the NiV P protein. When

the corresponding IFA data was taken into consideration, NiV N 1-801-HA, NiV N 163-1599-HA and NiV N 481-1599-HA stained in a diffuse pattern within the cell in contrast to the punctate staining patterns observed by NiV N-HA protein expression, Figure 18. These results imply that the factors necessary for N protein-oligomerization and aggregation were disabled. Therefore, it would be difficult to visualize an interaction between NiV N and NiV P proteins based on this solubility/protein distribution assay.

In summary, the C-terminal end of the NiV N protein was shown to be important for the interaction with NiV P proteins and its ability to maintain NiV N proteins in a soluble state. The results also suggest that there may be an additional NiV P protein-binding site located within the N-terminal half of the NiV N protein.

3.2.8 Interaction of NiV P proteins with truncated NiV N-HA proteins

A previous study has demonstrated that the C-terminal region of the NiV N protein was necessary for interacting with NiV P proteins (27). This finding has been supported by the results previously presented. Additionally, the results presented in Section 3.2.7 alluded to the possibility of an additional NiV P-protein binding domain found within the N-terminal half of the NiV N protein. In an attempt to confirm and/or extend the previous results a complementary approach was used to identify any further NiV P binding domains found within the NiV N protein. A variety of co-immunoprecipitation assays were preformed, utilizing the

expression of NiV P proteins and various truncated NiV N proteins from a mammalian expression system.

The truncated NiV N-HA proteins were immunoprecipitated by an HA affinity matrix, while the co-expressed NiV P proteins were co-immunoprecipitated through a specific interaction with the NiV N protein. The presence of immunoprecipitated and co-immunoprecipitated proteins was analyzed by immunoblot. An antibody against the HA-tag was used to visualize the presence of the truncated NiV N-HA proteins, Figure 24-upper immunoblot. The immunoblot was then stripped and re-probed with a guinea pig-derived polyclonal serum against NiV to detect the NiV P proteins, Figure 24-lower immunoblot. Mock-transfected cells, a negative control, were analyzed by immunoblot using NiV-specific or HA-specific antibodies and demonstrated that the antibodies used throughout this assay did not specifically interact with any cellular proteins, Figure 24. A second negative control, representing cells expressing NiV P proteins, showed that NiV P was not detected after immunoprecipitation, Figure 24, demonstrating that NiV P was not able to interact with the anti-HA matrix. Finally, as a positive control, cells expressing both NiV N-HA and NiV P showed the presence of both NiV P and NiV N-HA after immunoprecipitation when analyzed by immunoblot, Figure 24. This finding indicated that the NiV N-HA protein was immunoprecipitated by the anti-HA affinity matrix, while the NiV P protein was subsequently co-immunoprecipitated by interacting with the NiV N-HA protein. The remaining lanes demonstrated the presence and the ability of various truncated NiV N-HA protein to interact

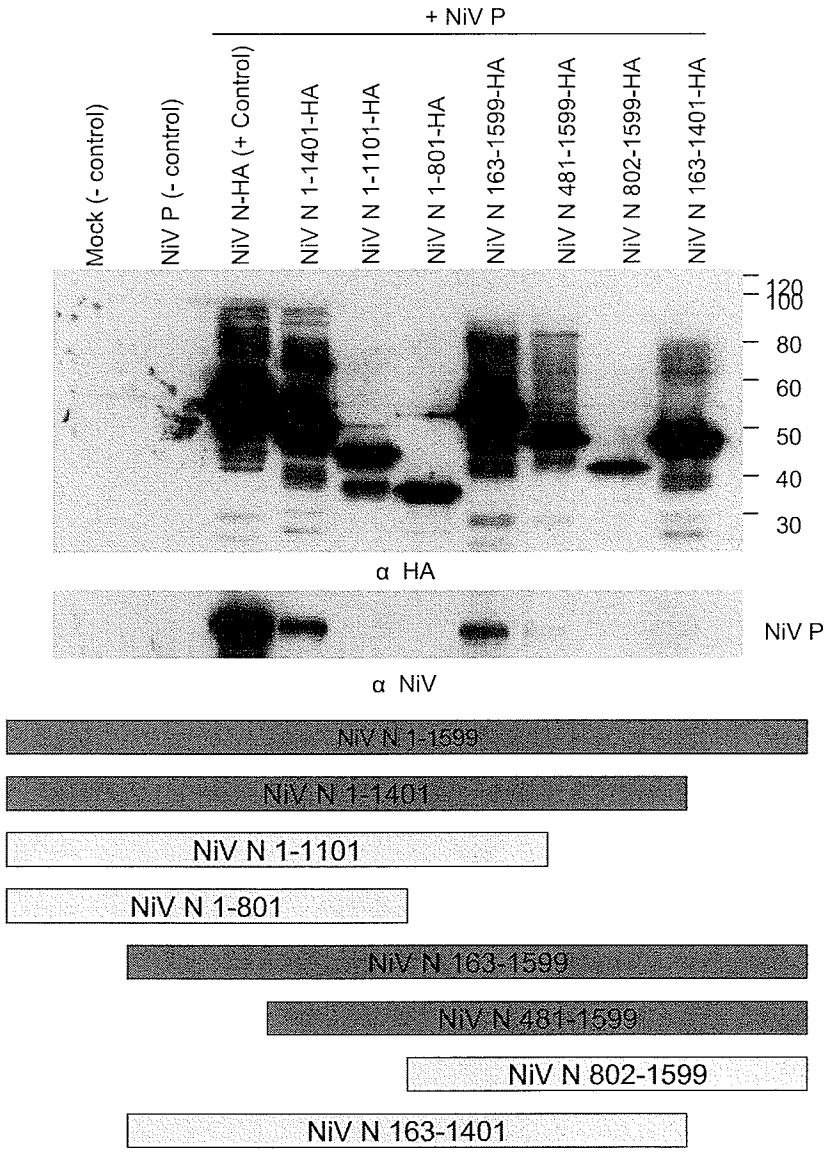

Figure 24: Anti-HA Co-immunoprecipitation Assays of NiV P and Truncated NiV N-HA Proteins. Experiments were carried out in triplicates. Co-immunoprecipitation assays utilizing cell lysates, which transiently co-expressed truncated NiV N-HA and NiV P proteins, were employed using an HA-based pull down. Upper panel- immunoblot probed against the HA-tag, verified the immunoprecipitation of all 8 NiV N-HA truncated proteins. Middle panel- the immunoblot was striped and probed for the presence of NiV P using a polyclonal serum against NiV. Lower panel- a schematic diagram of which truncated NiV N-HA constructs demonstrated the ability to interact with NiV P; Red represents a positive interaction, yellow represents a negative interaction.

specifically with NiV P, Figure 24.

In order to confirm previous results and to verify the specificity of the co-immunoprecipitation assays, an alternative set of immunoprecipitation assays were conducted. A similar experimental setup was employed as previously mentioned. A FLAG affinity matrix was used to immunoprecipitate NiV P-FLAG proteins, while truncated NiV N-HA proteins were co-immunoprecipitated through an interaction with NiV P. NiV antibodies were used to verify the presence of NiV P-FLAG (Figure 25- lower immunoblot), while an HA antibody was used to detect the presence of any co-immunoprecipitated truncated proteins (Figure 25-upper immunoblot). Table 9 summarizes the observations from the HA-based co-immunoprecipitation assays and the FLAG-based co- immunoprecipitation assays. Overall, this table compiles the experimental set up and findings using the various immunoprecipitation strategies, and distinguished between the potential and actual proteins that were co-immunoprecipitated.

The findings from these two assays demonstrated that NiV N 1-1401-HA and NiV N 163-1599-HA were able be co-immunoprecipitated with NiV P thereby indicating that they interact with NiV P. However, there was one discrepancy between the two assays, which demonstrated that NiV N 481-1599-HA was not able to be immunoprecipitated by the FLAG based pull-down. Therefore, only NiV N 1-1401-HA and NiV N 163-1599-HA were further analyzed, since NiV N 481-1599-HA was not immunoprecipitated by both assays. Examination of the co-immunoprecipitation results demonstrated that NiV N 163-1599-HA proteins were able to interact with NiV P proteins even though the N-terminal end of the

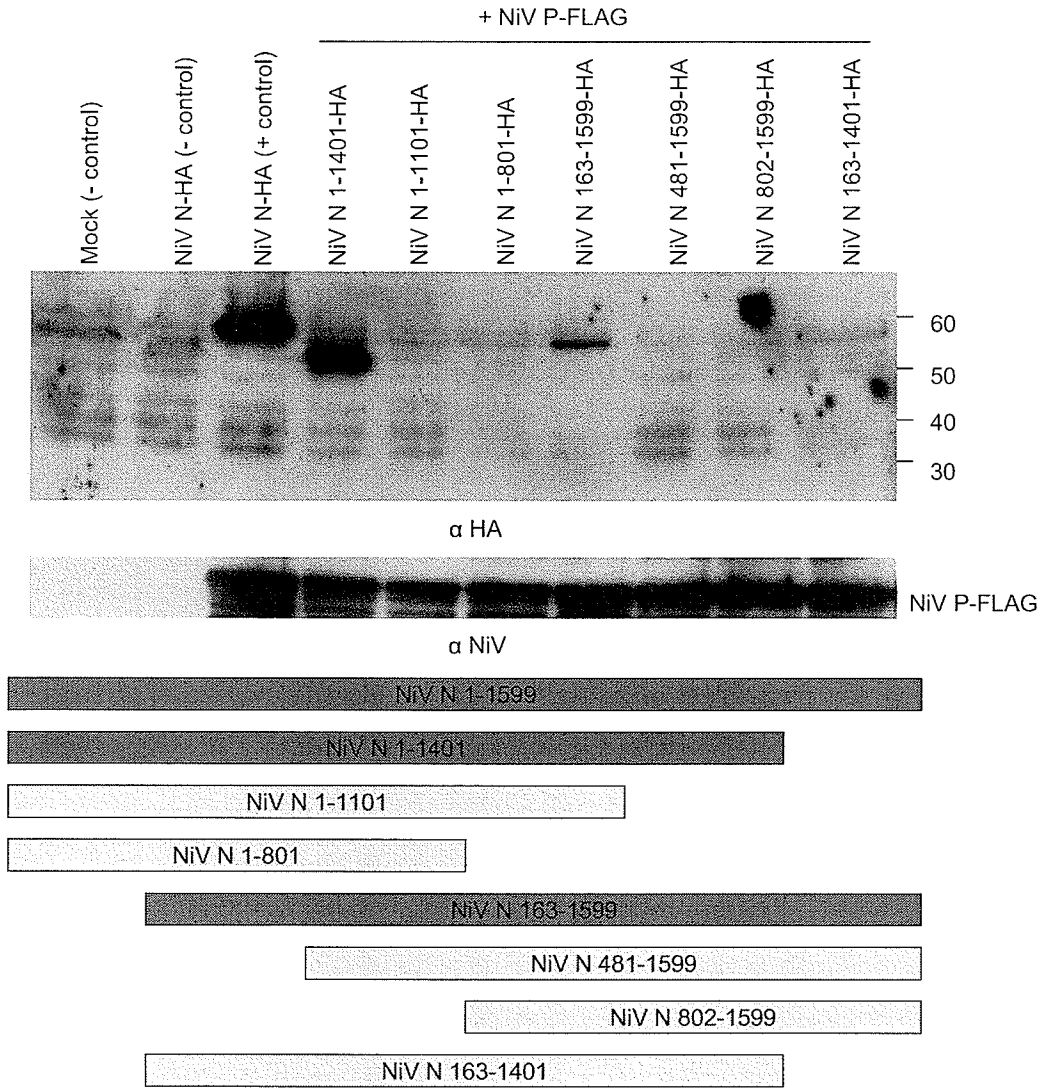

Figure 25: Anti-FLAG Co-immunoprecipitation Assays of Truncated NiV N-HA and NiV P Proteins. Experiments were repeated at least three times. Co-immunoprecipitation assays utilizing cell lysates, which transiently co-expressed various truncated NiV N-HA and NiV P proteins, were employed using a FLAG-based pull down. Upper panel- an immunoblot probed against the HA-tag, demonstrated the co-immunoprecipitation of three out of eight constructs. Middle panel- the immunoblot was striped and probed for the presence of NiV P using a polyclonal antibody against NiV, verifying that NiV P-FLAG proteins were immunoprecipitated. Lower panel- a schematic diagram of which truncated NiV N-HA constructs demonstrated the ability to interact with NiV P; Red represents a positive interaction, yellow represents a negative interaction.

Table 9: Co-immunoprecipitation assays between truncated NiV N-HA proteins and NiV P proteins

Type of Immuno-precipitation	Proteins to be Immuno-precipitated	Proteins to be Coimmuno-precipitated	Proteins Immuno-precipitated (Yes/No)	Proteins Coimmuno-precipitated (Yes/No)
NiV N-HA based Immunoprecipitation	NiV P (Negative Control)	--	No	--
	NiV N-HA	NiV P	Yes	Yes
	NiV N 1-1401-HA	NiV P	Yes	Yes
	NiV N 1-1101-HA	NiV P	Yes	No
	NiV N 1-801-HA	NiV P	Yes	No
	NiV N 163-1599-HA	NiV P	Yes	Yes
	NiV N 481-1599-HA	NiV P	Yes	Yes
	NiV N 802-1599-HA	NiV P	Yes	No
	NiV N 163-1401-HA	NiV P	Yes	No
NiV P-FLAG based Immunoprecipitation	NiV N-HA (Negative Control)	--	No	--
	NiV P-FLAG	NiV N-HA	Yes	Yes
	NiV P-FLAG	NiV N 1-1401-HA	Yes	Yes
	NiV P-FLAG	NiV N 1-1101-HA	Yes	No
	NiV P-FLAG	NiV N 1-801-HA	Yes	No
	NiV P-FLAG	NiV N 163-1599-HA	Yes	Yes
	NiV P-FLAG	NiV N 481-1599-HA	Yes	No
	NiV P-FLAG	NiV N 802-1599-HA	Yes	No
	NiV P-FLAG	NiV N 163-1401-HA	Yes	No

protein was removed. This would suggest that the N-terminal end of the protein was not important for the interactions with NiV P proteins. In the same way, the ability of NiV N 1-1401-HA proteins to interact with NiV P proteins even though the C-terminal end of the protein was removed suggests that the C-terminal end of the protein was not important for the interaction with NiV P proteins. Together this would suggest that the interacting domain would likely be found within residues 55-467. However, an alternative explanation could be that there are two separate NiV P protein-binding domains, one at each end of the NiV N protein, thus allowing each of these truncated proteins to interact with NiV P proteins. The data in Section 3.2.7 also suggested that both the N- and C-terminal ends of the NiV N protein were necessary for binding the NiV P protein, Section 3.2.7 (27). Additionally, other closely related paramyxovirus N proteins have been shown to contain two separate P protein-binding domains, typically at either end of the N protein, Section 1.7. To address this possibility, the NiV N protein was truncated from both the C- and N-terminal ends, represented by the protein NiV N 163-1401-HA. In both assays, this protein was no longer able to co-immunoprecipitate NiV P proteins, Figure 24 and Figure 25. Therefore, it is more likely that the NiV N protein contained two separate P protein-binding domains, one on the C-terminal end, aa 468-532, and another on the N-terminal end, aa 1-54. The former results agreed with results previously published by Chan *et al,* which stated that aa 469-498 are necessary for binding NiV P proteins (27). The results shown in Figure 24 and 25 provide new evidence that a potential NiV P protein-binding site may be located at the N-terminal end of the

NiV N protein. Interestingly, a number of constructs that contained one of the two predicted NiV P protein-binding domains were unable to interact with NiV P proteins in co-immunoprecipitation experiments. It is possible that these truncated proteins had an altered protein conformation that either made the NiV P protein-binding domains unavailable or the interactions between the two proteins were not strong enough to withstand the co-immunoprecipitation assay.

Overall, these results have not been able to demonstrate clearly, where a possible NiV P binding domain would be localized. Therefore, another set of truncations were employed to gain further insight into this question.

3.2.9 Interaction of NiV P proteins with truncated NiV N-CFP

The data presented in previous sections has not conclusively demonstrated that aa 1-54 and 468-532 of the NiV N protein alone are capable of binding NiV P proteins. Therefore, another series of co-immunoprecipitation assays were preformed to confirm the interaction between these two domains. In order to determine whether the N- and C-terminal ends of the NiV N protein were necessary to bind NiV P proteins a number of much larger NiV N truncations were created and fused to a C-terminal CFP tag. These constructs were used to determine whether smaller NiV N peptides were sufficient to interact with NiV P. Using a similar experimental design (see Section 3.2.8), truncated NiV N-CFP proteins were immunoprecipitated using a GFP affinity matrix while the co-expressed NiV P proteins were co-immunoprecipitated through a specific interaction with NiV N-CFP. This procedure required a slight modification in the

reagents used for the immunoblot. In order to detect the presence and the ability of the anti-GFP matrix to immunoprecipitate the truncated NiV N-CFP truncated proteins, it was necessary to use both the anti-GFP and anti-NiV antibodies simultaneously (Figure 26-upper right two panels), since the GFP antibodies were not able to detect expression of all of the truncated proteins. Some of the truncated NiV N proteins had very strong signals on the immunoblots. It is possible that the strong signals from some of these truncated proteins masked the weaker signals of other truncated proteins, thereby impairing their detection. The immunoblot was then reprobed with a monoclonal antibody against NiV P to demonstrate the ability of NiV P to interact and co-immunoprecipitate with the truncated NiV N-CFP proteins, Figure 26-lower right immunoblot. The left panel of Figure 26 shows the positive and negative controls of the assay as described in Section 3.2.8. The remaining lanes show the ability of NiV P to interact specifically with the truncated NiV N-CFP proteins, Figure 26.

In order to confirm the specificity of the previous results, complementary immunoprecipitation experiments were preformed. Using a recently developed monoclonal antibody against NiV P, a NiV P-affinity matrix was generated to immunoprecipitate NiV P proteins, while truncated NiV N-CFP proteins were co-immunoprecipitated through an interaction with NiV P. A monoclonal antibody against NiV P was used to confirm that NiV P was immunoprecipitated (Figure 27-lower right immunoblot), while the antibodies against NiV and GFP were used to demonstrate the presence of the co-immunoprecipitated proteins (Figure 27-upper right two immunoblot). The findings obtained from the GFP-based and NiV

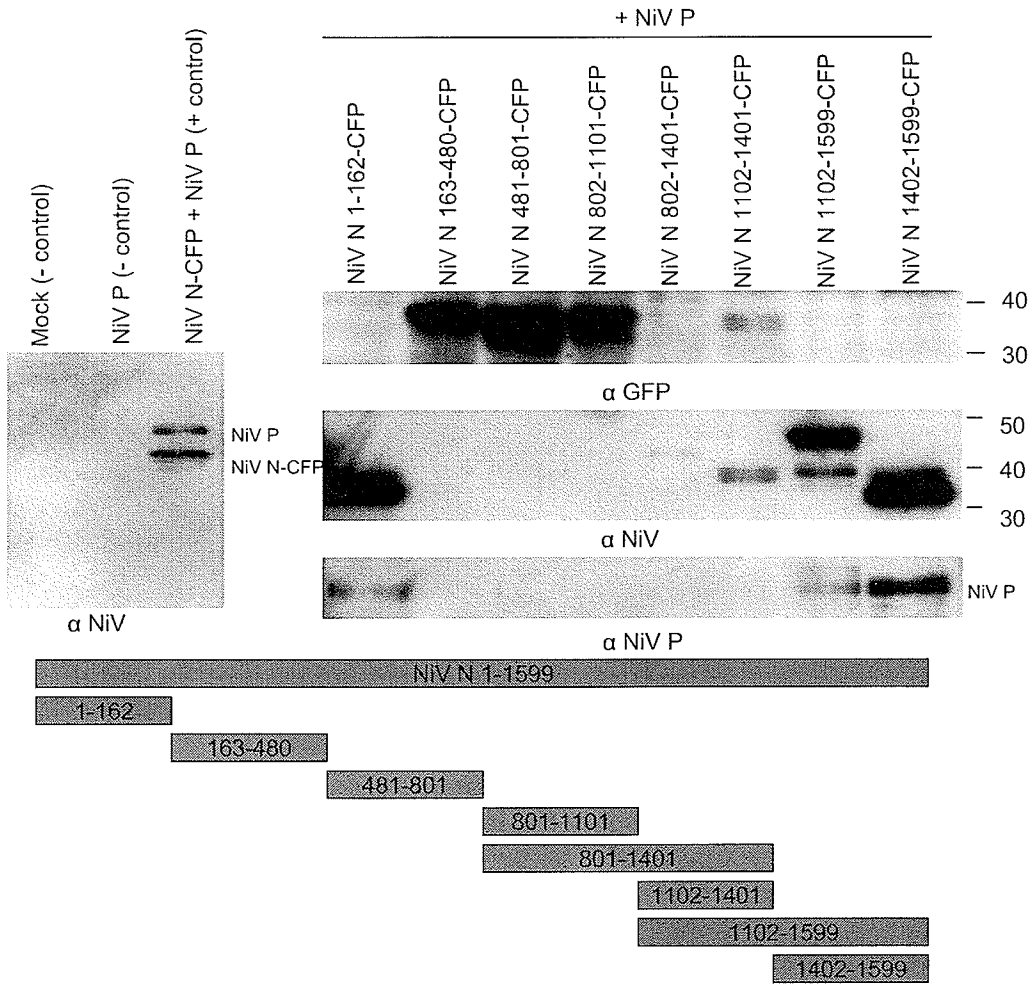

Figure 26: Anti-GFP Co-immunoprecipitation Assays of NiV P and Truncated NiV N-CFP Protiens. Experiments were repeated three times. Co-immunoprecipitation assays utilizing cell lysates, which transiently co-expressed truncated NiV N-CFP proteins and NiV P proteins, were employed using a GFP-based pull down. Left panel- immunoblot using a polyclonal antibody aginast NiV was used to verify the experimental controls. Upper right panel- an immunoblot probed with an antibody against GFP verified the immunoprecipitation of four out of eight truncated NiV N-CFP proteins. Middle right panel- the immunoblot was striped and probed using a polyclonal serum against NiV for the presence of the remaining truncated NiV N-CFP proteins. Lower right panel- the immunoblot was striped and probed with a monoclonal antibody against the NiV P protein, demonstrating the ability of two out of eight truncated N-CFP proteins to interact with NiV P proteins. The schematic diagram demonstrated which truncated NiV N-CFP proteins were able to interact with NiV P proteins; Pink represents a positive interaction, blue represents a negative interaction.

P-based co-immunoprecipitation assays are summarized in Table 10.

Using two complementary co-immunoprecipitation assays, the results confirmed that NiV N 1102-1599-CFP, NiV N 1402-1599-CFP and NiV N 1-162-CFP were able to interact with NiV P proteins and be immunoprecipitated. These data show that the NiV N protein contained two independent binding domains that were each able to bind NiV P proteins: one located between positions 1 and 54 aa (represented by construct NiV N 1-162-CFP) and another between positions 468 and 532 aa (represented by construct NiV N 1402-1599-CFP). These findings confirmed the presence of a NiV P protein-binding site located on the C-terminal end of the NiV N protein as described by Chen *et al* and indicated the presence of a novel NiV P protein-binding domain found on the N-terminus of the NiV N protein (27). These results provided the foundation to explore the functions of the NiV N and NiV P proteins during viral replication.

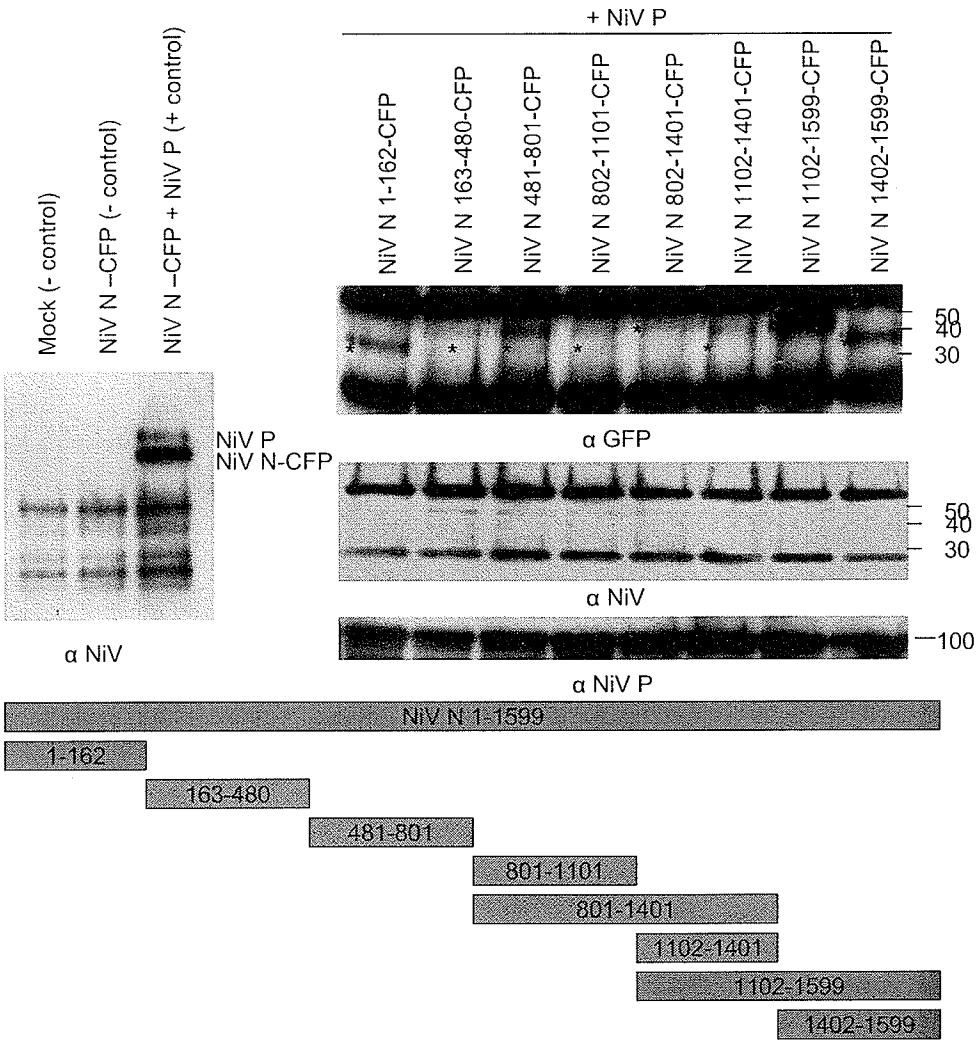

Figure 27: Anti-NiV P Co-immunoprecipitation Assays of Truncated NiV N-CFP and NiV P Proteins. Experiments were repeated three times. Co-immunoprecipitation assays utilizing cell lysate, which transiently co-expressed truncated NiV N-CFP and NiV P proteins were employed using a NiV P-based pull down. Left panel- immunoblot containing the experimental controls probed with a polyclonal antibody against NiV. Upper right panel- an immunoblot probed with an antibody against GFP demonstrated the presence of three truncated NiV N-CFP constructs, which were co-immunoprecipitated with the NiV P protein. (*) predicted location of truncated proteins based on their molecular weights. The remaining lanes are background bands. Middle right panel- the immunoblot was striped and, using a polyclonal antibody against NiV, probed for the presence of any undetected truncated NiV N-CFP proteins. Lower right panel- the immunoblot was striped and probed with a monoclonal antibody against NiV P, demonstrating the immunoprecipitation of all samples containing NiV P proteins. The schematic diagram demonstrated which truncated NiV N-CFP constructs were able to interact with NiV P proteins; Pink represents a positive interaction, blue represents a negative interaction.

Table 10: Co-Immunoprecipitation assays between truncated NiV N-CFP and NiV P proteins

Type of Immuno-precipitation	Proteins to be Immuno-precipitated	Proteins to be Coimmuno-precipitated	Proteins Immuno-precipitated (Yes/No)	Proteins Coimmuno-precipitated (Yes/No)
NiV N-CFP based Immunoprecipitation	NiV P (-) Control	--	No	--
	NiV N-CFP	NiV P	Yes	Yes
	NiV N 1-162-CFP	NiV P	Yes	Yes
	NiV N 163-480-CFP	NiV P	Yes	No
	NiV N 481-801-CFP	NiV P	Yes	No
	NiV N 802-1101-CFP	NiV P	Yes	No
	NiV N 802-1401-CFP	NiV P	Yes	No
	NiV N 1102-1401-CFP	NiV P	Yes	No
	NiV N 1102-1599-CFP	NiV P	Yes	Yes
	NiV N 1402-1599-CFP	NiV P	Yes	Yes
NiV P- based Immunoprecipitation	NiV N-CFP (-) Control	--	No	--
	NiV P	NiV N-CFP	Yes	Yes
	NiV P	NiV N 1-162-CFP	Yes	Yes
	NiV P	NiV N 163-480-CFP	Yes	No
	NiV P	NiV N 481-801-CFP	Yes	No
	NiV P	NiV N 802-1101-CFP	Yes	No
	NiV P	NiV N 802-1401-CFP	Yes	No
	NiV P	NiV N 1102-1401-CFP	Yes	No
	NiV P	NiV N 1102-1599-CFP	Yes	Yes
	NiV P	NiV N 1402-1599-CFP	Yes	Yes

3.2.10 Increased expression of NiV N proteins correlates with reduced levels of viral mRNA production

Based on the "two polymerase entry model" the increased availability of N proteins can skew the balance between transcriptase and replicase formation towards the increased production of a replicase (78;154). However, the precise mechanism (or mechanisms) for the interaction between NiV N proteins and the polymerase complex are not fully understood. By establishing an experimental system that provided increasing amounts of NiV N protein in cells prior to NiV challenge, it might be possible to disable the transcriptase complex and subsequently cause an overall reduction of viral RNA. The proposed mechanism by which viral RNA synthesis could be disabled depends on the ability of the NiV N protein to interact with the transcriptase complex to cause the premature formation of the viral replicase complex. By analogy to the current model for VSV replication, NiV N could interact with the transcriptase complex by binding to NiV P (78;154). The premature formation of a viral replicase would disable viral transcription and subsequently halt viral translation. Therefore, by preventing the production of essential viral proteins required to mediate the production of viral RNA, the assembly of virions would be inhibited. I hypothesize that the interaction between NiV N and NiV P is an essential factor in abrogating viral replication specifically at the level of viral RNA synthesis. Moreover, it is possible that the recombinant expression of NiV N has the ability to transform viral transcriptases into viral replicases. This would result in a decrease in viral mRNA synthesis, which would then partially explain the mechanism behind the

impairment of viral replication. However, before examining the role that the interaction between NiV N and NiV P have in abrogating viral replication, it was first necessary to determine whether recombinant NiV N was capable of impairing viral replication.

In an attempt to increase the expression of recombinant NiV N proteins, an IRES, a nucleotide sequence that directs cap-independent translation of the ORF, was cloned directly upstream of the NiV N ORF of the NiV N-CMV construct previously created (Appendix 3). In order to assess whether the IRES had a positive impact on recombinant NiV N protein expression, 293T cells were transfected with either NiV N-CMV or NiV N-IRES-CMV and analyzed by immunoblot. The signals were quantified by spot densitometry and standardized against the expression of actin before comparison. The addition of an IRES upstrem of the NiV N gene was able to boost NiV N protein expression by approximately 20%, Figure 28.

293T cells were transfected with NiV-N-IRES-CMV. The efficiency of transfection was determined by flow cytometry. Approximately 80-90% of cells were positive for NiV expression (data not shown). To determine whether the use of increasing amounts of plasmid DNA during transfections correlated with an increase in NiV N protein expression, immunoblots were preformed and the protein signals were quantified. It was observed that increasing amounts of input plasmid DNA resulted in an increased amount of recombinant protein expression (Figure 29); similar to what has been observed for other N proteins (141). To determine whether increased expression of NiV N proteins inhibited viral

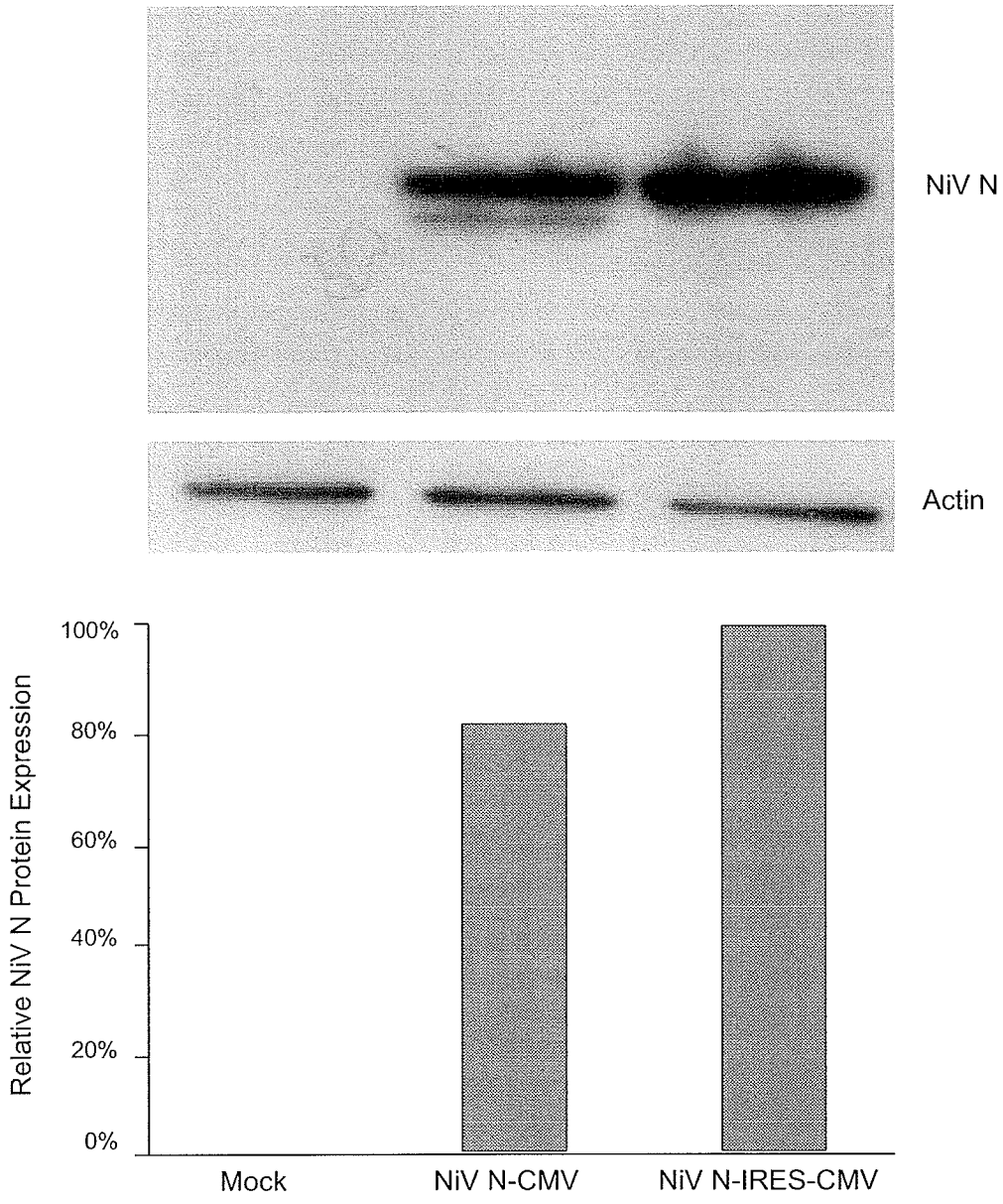

Figure 28: Enhancing the Expression Levels of Recombinant NiV N Proteins. The presence of a IRES in the vector NiV N-IRES-CMV was able to enhance expression of NiV N in comparion to NiV N-CMV. Samples were quantified using spot densitometry and AlphaEaseFC™ software.

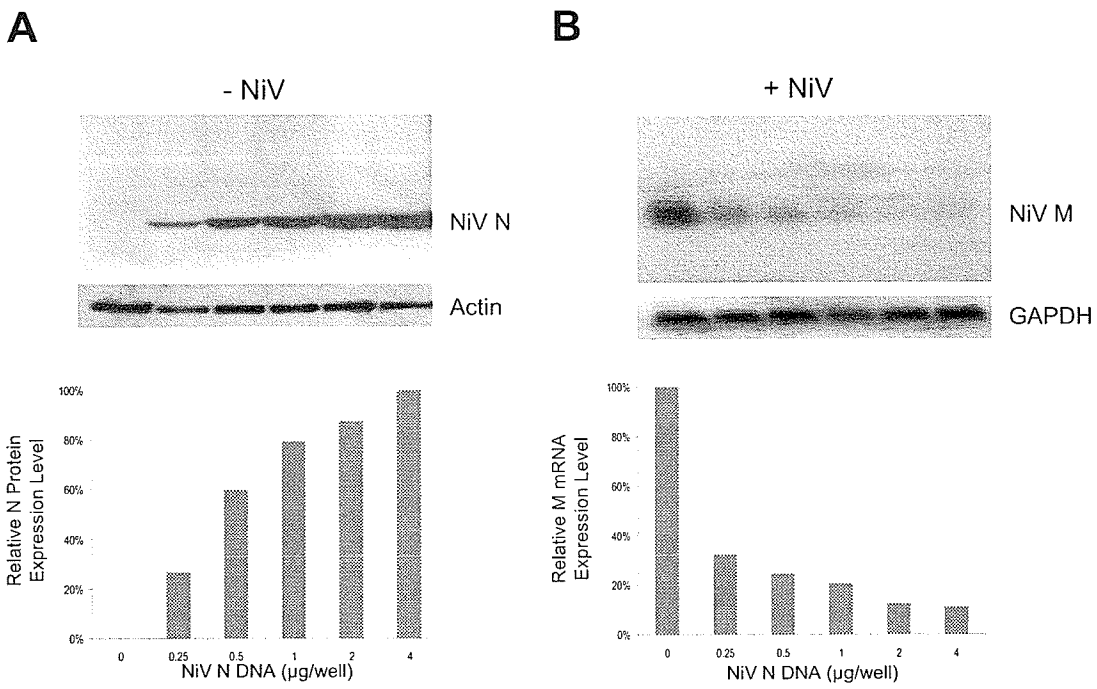

Figure 29: Analysis of NiV Transcription as Expression Levels of NiV N Proteins Increase. Experiments were carried out in triplicate. 293T cells were transfected with increasing amounts of NiV N-IRES-CMV plasmid DNA. (A) Upper panel- immunoblot analysis using a monoclonal antibody against NiV N, demonstrated increased expression of NiV N proteins. Lower panel - immunoblots were quantified using AlphaEaseFC^{TM} software and standardized against actin. (B) Following transfection, cells were infected with NiV at an MOI of 1 ($2x10^6$ IFU/well) for 24 hours. RNA was extracted from NiV infected cell lysates and analyzed by northern blot. Upper panel - a DNA probe designed against the M gene was used to detect NiV M mRNA. Lower panel - the autoradiogram was subjected to phosphoimager analysis, quantified using ImageQuant software and standardized against GAPDH. Standard deviations of the mean were calculated.

transcription, cells transiently expressing various concentrations of NiV N proteins were infected with NiV at an MOI of 1 ($2x10^6$ IFU/well) and incubated for 24 hours. Total RNA extracted from these cells was analyzed by northern blot using a DNA probe designed against the NiV M ORF to detect NiV M transcripts. This probe had the potential to recognize NiV M mRNA, NiV anti-genome and genome. However, bands representing synthesized NiV M mRNA were discriminated from full-length anti-genomes or genomes based on size. A probe was designed to detect the presence of GAPDH RNA, which was used as an internal standard for quantification. Cells expressing high levels of NiV N showed a 74% decrease in NiV M mRNA compared to cells that did not express any recombinant NiV N (Figure 29B, compare NiV M band intensities in right lane and right column with band intensities in left lane and left column). These results demonstrated that increasing NiV N protein levels had a detrimental effect on viral mRNA synthesis, while cellular GAPDH mRNA production was not affected, indicating a specific inhibitory interaction on viral RNA.

3.2.11 Viral protein production was reduced in the presence of recombinant NiV N protein

To determine whether viral protein expression was inhibited due to the increased expression of recombinant NiV N, cell lysates were harvested for immunoblot analysis. A guinea pig-derived polyclonal antibody against NiV was used to detect NiV proteins. Detection of cellular actin was used as a quantitative standard. Cells expressing high levels of NiV N proteins

demonstrated a 98% decrease in NiV P protein expression levels, in comparison to cells that did not express any recombinant NiV N proteins (Figure 30, compare NiV P bands intensities in the right lane and right column with band intensities in the left lane and left column). The overall expression levels of NiV N remained high because of the expression of recombinant NiV N proteins, data not shown. Since recombinant NiV N protein expression remained consistently high, this indicated that a total shutdown of cellular protein translation did not occur but rather that viral protein expression was specifically targeted. To assess specifically whether expression of recombinant NiV N remained at high levels while viral protein expression (including virally expressed NiV N) decreased, similar experiments were carried out using a NiV N construct, NiV-N-HA-IRES-CMV. Cells were transfected with increasing amounts of NiV N-HA-IRES-CMV plasmid DNA and subsequently infected with NiV. Cell lysates were harvested and viral protein production was analyzed by immunoblot. Reduced expression of NiV proteins was observed as the amount of recombinant NiV N-HA expression increased, Section 3.2.20. Furthermore, this blot was probed with an antibody against the HA-tag (Appendix 2) to determine the expression of recombinant NiV N proteins. Increased expression levels of recombinant NiV N-HA was maintained as the expression levels of other viral proteins decreased, Section 3.2.20. This experiment showed that increasing levels of the recombinant NiV N protein was associated with a significant reduction of viral protein expression.

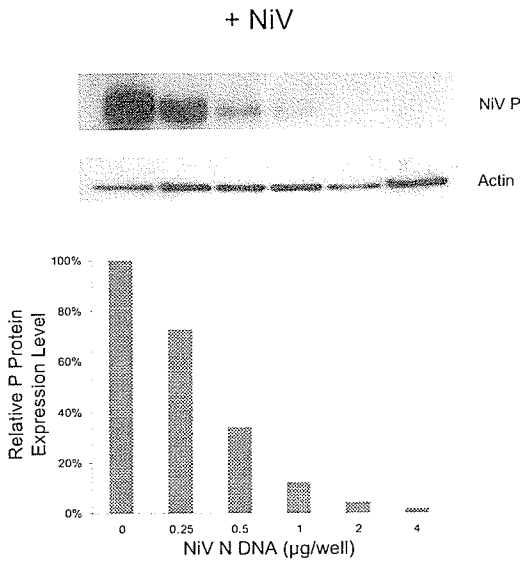

Figure 30: Analysis of NiV Translation as Expression Levels of NiV N Proteins Increase. Experiments were repeated three times. 293T cells expressing increasing amounts of NiV N proteins were infected with NiV at an MOI of 1 ($2x10^6$ IFU/well) for 24 hours. Cell lysates were harvested and analyzed by immunoblot. Upper panel- Using a guinea pig polyclonal antibody against NiV, immunoblot analysis demonstrated a reduction in viral protein expression. Lower panel- immunoblots were quantified using AlphaEaseFC™ software and standardized against actin. For all experiments, standard deviations of the mean were calculated.

3.2.12 Increased expression of recombinant NiV N proteins correlated with lower levels of full-length genomic RNA production.

To determine the impact that increasing expression of NiV N had on viral genomic RNA production, total cellular RNA was extracted from cells that transiently expressed increasing concentrations of NiV N proteins and were subsequently infected with NiV. One-step real-time RT-PCR analysis using a primer set targeting the NTR of the NiV G and NiV L genes (Appendix 3) showed that NiV RNA (viral mRNA, full-length genomic and anti-genomic RNA) was reduced by approximately 90% when expression levels of recombinant NiV N proteins were high (Figure 31A, compare the relative levels of viral RNA in cells expressing high levels of NiV N protein, right point, and with cells expressing no recombinant NiV N protein, left point). Viral mRNA was believed to be the most prominent species of RNA detected during NiV replication and a decrease in mRNA synthesis would likely be manifested as a reduction in total viral RNA present. Therefore, to look more closely at whether the increased expression of NiV N proteins had an affect on genome replication, the accumulation of genomic and/or anti-genomic RNA was analyzed. Strand-specific reverse transcription was carried out using a forward primer designed in the NiV G gene for detection of negative-sense full-length genome, or a reverse primer designed in the NiV L gene for detection of positive-sense viral RNA representing both viral mRNA and anti-genome coupled with the use of a primer set designed within the NTR of the NiV G and NiV L genes and real-time PCR (Appendix 3). A 94% decrease in

A

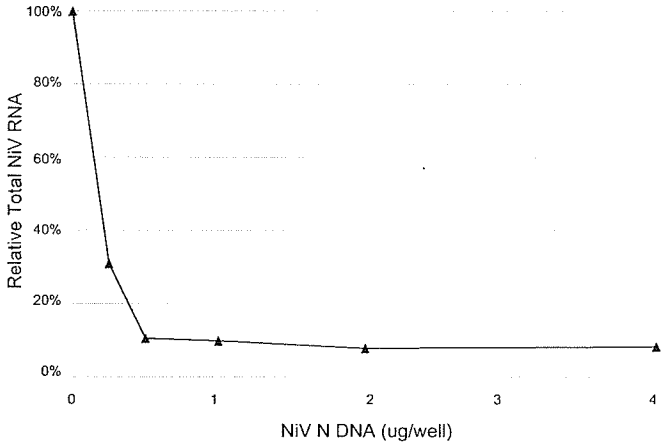

B

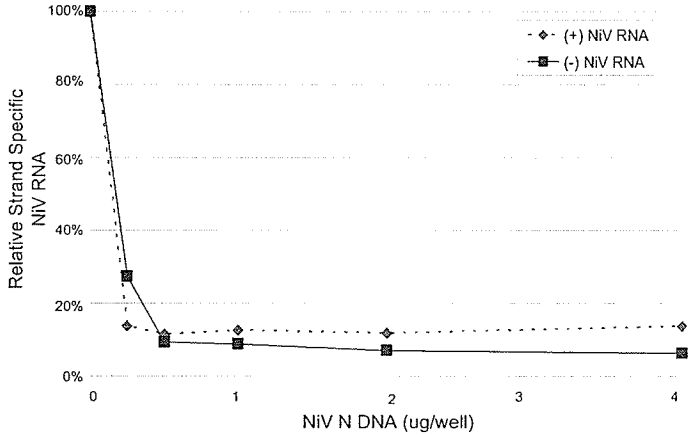

Figure 31: Analysis of Viral RNA by Real-Time RT-PCR. Experiments were carried out in triplicate. Cells expressing increasing amounts of NiV N were infected with NiV at an MOI of 1 ($2x10^6$ IFU/well) for 24 hours. RNA was extracted from cell lysates. A primer set designed in the non-translated region between the NiV G and NiV L genes was designed to detect NiV RNA. (A) One-step RT-PCR was carried out using real-time SmartCycler technology. Each reaction was quantified and standardized against GAPDH. (B) Strand-specific reverse transcription was done using a forward primer designed in the NiV G gene to detect negative-sense NiV genome (■) or a reverse primer designed in the NiV L gene to detect positive-sense NiV RNA (▲). Real-time PCR was carried out using SmartCycler technology. Each reaction was quantified and standardized against GAPDH. For all experiments, standard deviations of the mean were calculated.

production of viral genome (Figure 31B, compare relative values between the ■ left point and the ■ right point) and an 86% decrease in positive strand viral RNA (Figure 31B, compare relative RNA values between the ▲ left point and the ▲ right point) was observed in cells expressing high levels of recombinant NiV N in comparison to cells that did not express any recombinant NiV N. Overall, synthesis of all viral RNA (positive-sense RNA and negative-sense genomic RNA) was reduced in the presence of elevated expression of recombinant NiV N proteins.

3.2.13 Production of infectious NiV was reduced in the presence of increased NiV N protein expression levels.

$TCID_{50}$ infectivity assays were used to determine viral titres of cells expressing increasing amounts of NiV N proteins, which were then exposed to NiV. Cells that did not express recombinant NiV N proteins produced viral titres of $5.2x10^6$ $TCID_{50}$ IFU/ml (Figure 32, left lane). In contrast, cells expressing high levels of recombinant NiV N proteins showed reduced viral titres of $2.8x10^2$ $TCID_{50}$ IFU/ml, (Figure 32, right lane). Overall, a 4-log_{10} decrease in viral titres was observed between cell that did not express any recombinant NiV N proteins and cells expressing high levels of recombinant NiV N proteins. Decreased levels of viral mRNA transcripts and viral protein expression likely explain the observed low *de novo* generation of NiV infectivity. Since the expression of NiV N proteins appeared to be responsible for the abrogation of viral replication, a number of controls were put in place in order to assess whether the NiV N

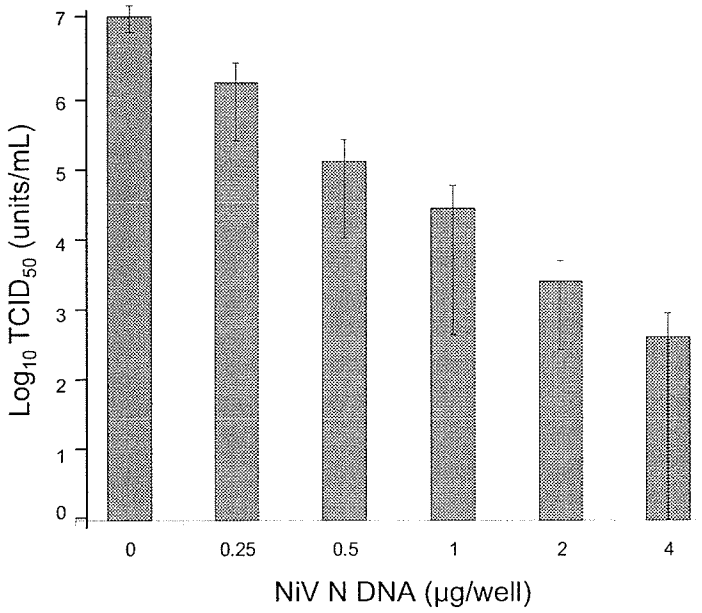

Figure 32: Comparison of NiV Titres Between Cells Expressing Increasing Amounts of Recombinant NiV N Proteins. Viral titrations were done in triplicate in three separate experiments. Supernatants were harvested from 293T cells which transiently expressed recombinant NiV N proteins and were previously infected with NiV. Serial dilutions from 10^{-1} to 10^{-9} were adsorbed for 1 hour onto fresh 293T cells and $TCID_{50}$ viral titres were calculated 48 hours post-infection. Standard deviations of the mean were calculated.

protein had a direct role in impairing viral replication.

3.2.14 The expression of recombinant NiV N proteins was responsible for the reduction in viral translation.

To test whether other components of the RNP complex were capable of causing reduced levels of NiV protein production, NiV N-IRES-CMV was substituted with NiV P-CMV. 293T cells were transfected with increasing amounts of NiV P-CMV and infected with NiV at an MOI of 1 ($2x10^6$ IFU/well). Viral protein production was quantified and standardized against the expression of actin. Immunoblots using a polyclonal antibody against NiV were used to determine the expression of the NiV P protein, which increased with increasing amounts of transfected plasmid DNA (Figure 33-upper panel). A monoclonal antibody against NiV N proteins was used to visualize any changes of NiV N protein expression levels during viral replication. Immunoblot analysis demonstrated a steady level of NiV N protein expression in all samples, indicating that as levels of recombinant NiV P proteins expression increased there was no detectable effect on the expression of other NiV proteins (Figure 33-lower panel, compare NiV N protein expression in the right column with expression levels in the left column). Similar results were obtained when NiV N was substituted with another viral protein, such as the NiV F protein, or other proteins such as CFP (data not shown). In contrast to NiV N protein expression, increasing expression of recombinant NiV P proteins, did not appear to modify

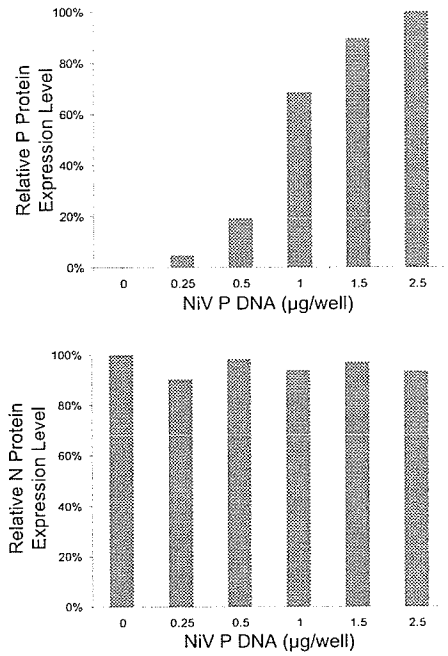

Figure 33: Analysis of NiV Translation as Expression Levels of NiV P Proteins Increase. Experiments were repeated three times. 293T cells expressing increasing amounts of NiV P proteins were infected with NiV N at an MOI of 1 (2x106 IFU/well) for 24 hours. Cells were harvested and analyzed by immunoblot. Upper panel – A polyclonal antibody against NiV was used to detect NiV P proteins. Immunoblots were standardized against actin and quantified using AlphaEaseFCTM software. Lower panel - A monoclonal antibody against NiV N was used to analyze expression of NiV N to determine changes in NiV protein expression levels. immunoblots were quantified using AlphaEaseFCTM software and standardized against actin. For all experiments, standard deviations of the mean were calculated.

the expression levels of NiV gene products suggesting that the impairment of viral replication was specific to the expression of NiV N.

3.2.15 The solubility of NiV N proteins

Paramyxovirus N proteins have been shown to bind non-specifically to cellular RNA and to form "false" NC-structures when expressed alone (8;12;53;98;123;130). NiV N has been shown to form these same structures as well (57;181). The presence of "false" NC-structures in cells prior to NiV infection could explain the apparent decrease in viral replication and production of progeny viruses. It is possible that the polymerase complexes from the incoming virus could be attracted to these "false" NC-structures and diverted from "true" NC-structures. This could cause an overall reduction in the synthesis of viral RNA. The ability of NiV N to bind cellular RNA, when expressed alone and form NC-like structures has yet to be fully understood. To determine whether recombinantly expressed NiV N proteins possessed the ability to form "false" NC-structures, cells transfected with NiV N-IRES-CMV were disrupted with an NP-40 lysis buffer and analyzed by negative staining electron microscopy. Figure 34 shows the presence of herringbone structures or NC-like structures in cells expressing NiV N proteins alone. These structures were not present in mock-transfected cells (data not shown). This result suggested that NiV N was able to self-assemble and form "false" NC-structures. However, these experiments do not confirm that NiV N proteins were bound to cellular RNA.

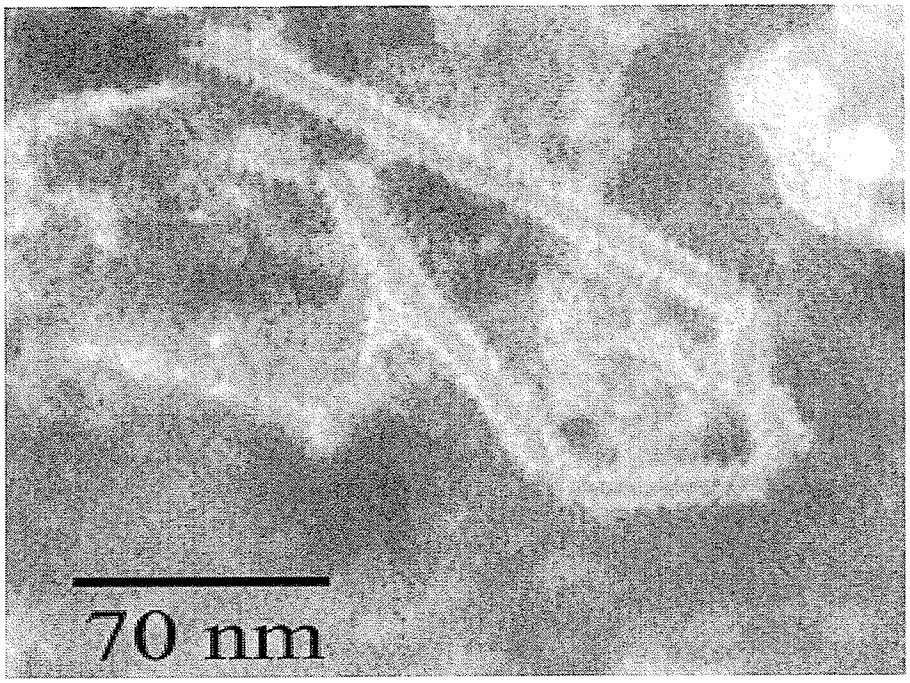

Figure 34: Visualization of Herringbone Structures by Electron Microscopy. Experiments were repeated three times. 293T cells expressing recombinant NiV N proteins were distrupted in an NP-40 lysis buffer. Supernatants were used to visualize the production of nucleocapsid-like structures by electron microscopy.

The role of the P protein in replication provides some insight into the potential recruitment of polymerase complexes to "false" NC-structures. The P proteins of other negative-stranded RNA viruses bind the N proteins and maintain them in a soluble state, thereby preventing non-specific binding of cellular RNAs (42;173;200). The P protein is also believed to act as a chaperone for the N protein, sequestering it to appropriate sites of virus replication where it can recognize the viral RNA template (42;75;91;173;200). Therefore, the co-expression of NiV N and NiV P could prevent the formation of N protein aggregates and the non-specific binding of cellular RNA, by making the N protein soluble and available for viral replication and "true" NC formation.

To address this issue, a dual promoter construct was created, which expresses both NiV N and NiV P. Construct NiV P-NiV N-CMV was created by amplifying the CMV promoter, the NiV N gene and the SV40 poly(A) tail, from the NiV N-CMV construct (Appendix 3), and cloning it downstream of the NiV P gene and SV40 poly(A) tail of the NiV P-CMV construct, Figure 9. DNA sequencing was used to verify the sequence of the NiV P and NiV N ORFs from any positive clones. Expression of NiV N and NiV P was verified by immunoblot using a guinea pig-derived polyclonal serum against NiV, Figure 35. Positive controls were represented by the expression of either NiV N or NiV P proteins individually, Figure 35. Expression of the NiV P-NiV N-CMV construct was verified by the presence of two NiV protein bands, one representing NiV P proteins and the other representing NiV N proteins. Expression of NiV N and P from this construct was also determined by fluorescent confocal microscopy to ensure co-expression

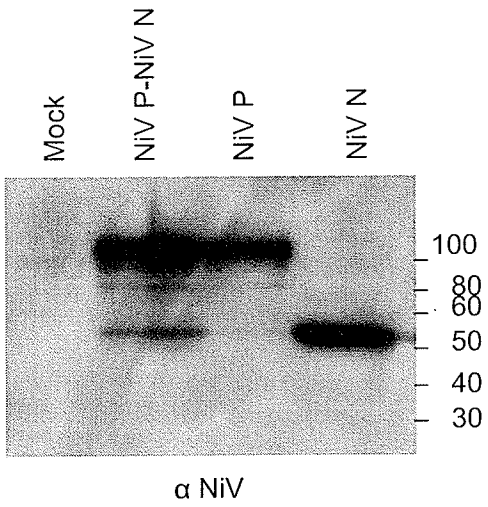

Figure 35: Expression of the NiV P-NiV N-CMV construct. 293T cells transiently expressing either, NiV N, NiV P or NiV N and NiV P together, were harvested and analyzed by immunoblot. Using a polyclonal antibody against NiV, immunoblot verified the expression of NiV N and/or NiV P. The lane containing mock transfected cells acts as a negative control. The lanes individually expressing NiV N or NiV P proteins are positive controls, while cells transfected with NiV P-NiV N-CMV demonstrate the expression of both NiV N and NiV P proteins.

of the proteins (Figure 36), as well as the predicted co-localization due to the previously interaction observed between these proteins, Figure 24-27. Cells expressing NiV N proteins alone were visualized using a mouse monoclonal antibody conjugated to a FITC fluorochrome, Figure 36- NiV N proteins are represented by green staining. When the NiV N protein was expressed in cells alone, it was observed in a characteristic punctate staining pattern, implying N-protein oligomerization, Figure 36 (11). Cells expressing NiV P proteins alone were visualized by using a mouse monoclonal antibody against the NiV P protein in conjunction with a secondary antibody conjugated to an AlexaFluor®568 fluorochrome, Figure 36 – NiV P proteins are represented by red staining. In addition, the monoclonal antibody against NiV P proteins did not cross-react with NiV N, nor did the monoclonal antibody against NiV N cross-react with NiV P, Figure 36. Finally, cells transfected with NiV P-NiV N-CMV demonstrated clear expression of both NiV N and NiV P as well as co-localization between NiV N and NiV P (Figure 36, co-localization between NiV N and NiV P proteins was represented by yellow staining). Additionally, there seemed to be a redistribution of NiV N from a punctate staining pattern to a diffuse staining pattern when co-expressed with NiV P, indicating that NiV P maintained NiV N in a soluble state (Figure 36, compare cells expressing NiV N proteins alone to cells expressing both NiV N and NiV P proteins).

In order to more directly assess the solubility of the NiV N protein, cells expressing NiV N or NiV N in conjunction with NiV P were lysed, clarified and centrifuged through a 20% sucrose cushion. Proteins found within the

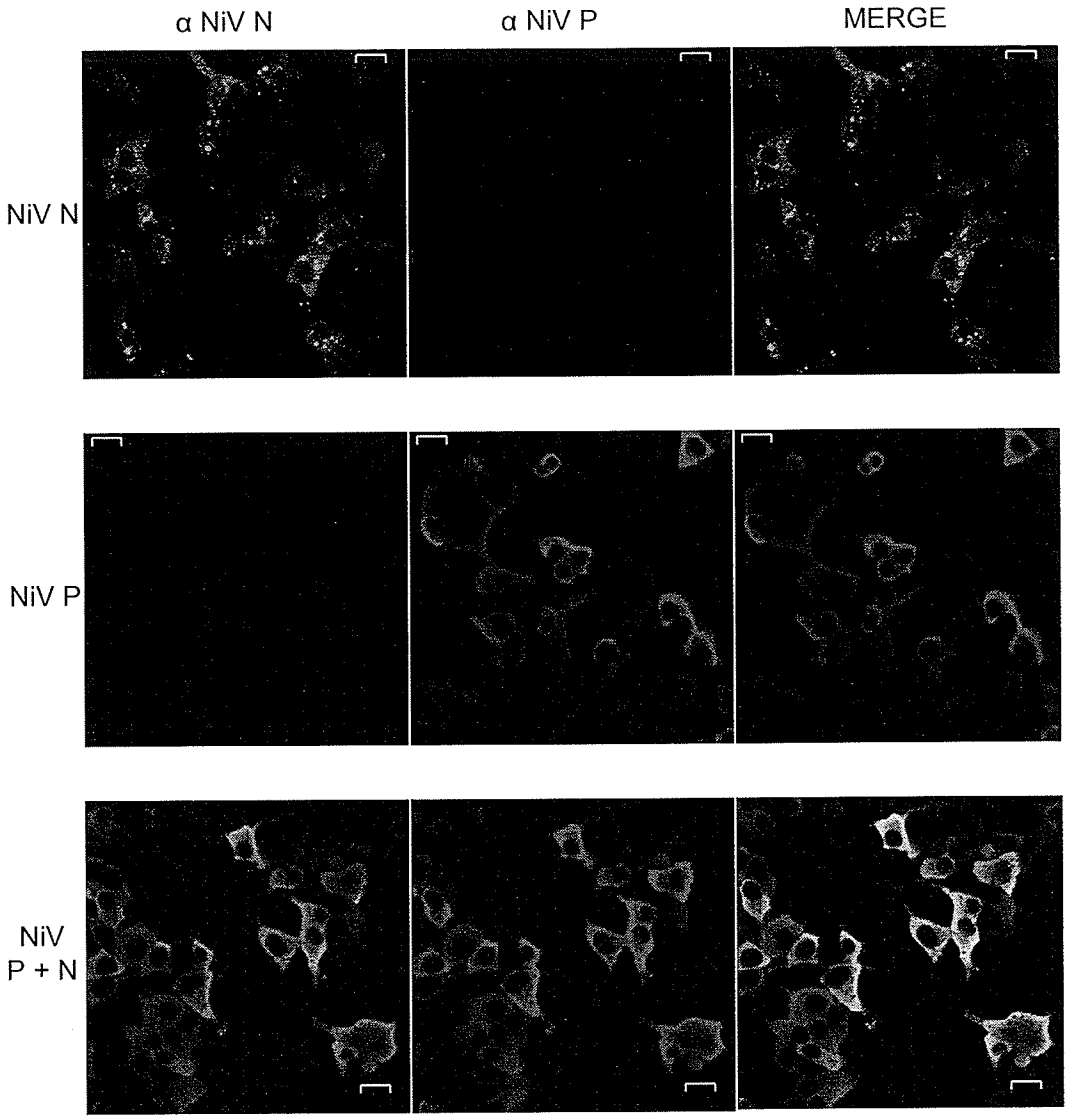

Figure 36: Visualization of NiV N and NiV P Proteins in 293T Cells. 293T cells expressing constructs NiV N-IRES-CMV, NiV P-CMV or NiV P-NIV N-CMV were analyzed by fluorescent confocal microscopy at a 60x magnification employing a Z-axis slice. A monoclonal antibody against NiV N conjugated with a FITC fluorochrome were used to detect NiV N proteins and are represented by green. A monoclonal antibody against NiV P used in conjunction with a secondary antibody containing an AlexaFluor®568 fluorochrome were used to detect NiV P proteins and are represented by red. Co-localization between NiV N and NiV P proteins is represented by yellow.

supernatant were considered soluble, while proteins found in the protein pellet were considered insoluble or aggregated. Immunoblots demonstrated that when NiV N was expressed alone, it was distributed predominantly within the insoluble fraction, indicating that it was found in an aggregated form, Figure 37. A small proportion of NiV N was found in the soluble fraction, Figure 37. However, when NiV N was co-expressed with NiV P, NiV N was redistributed to the soluble fraction, while there were no detectable levels of NiV N in the insoluble fraction, Figure 37. These results indicated that NiV N was predominantly insoluble when expressed alone, but was maintained in the soluble fraction in the presence of NiV P. Taken together, these experiments, shown in Figures 36 and 37 clearly demonstrate the ability of the NiV P to maintain NiV N in a soluble state.

3.2.16 Simultaneous expression of NiV N and NiV P proteins caused an overall decrease of NiV replication.

Section 3.2.15 demonstrated the ability of NiV P proteins to maintain NiV N proteins in a soluble state. Therefore, the use of the NiV P-NiV N-CMV construct was used to answer the question of whether the impairment of NiV replication could be attributed to the recruitment of the viral polymerase towards "false" NC-structures. To study the effect that simultaneous expression of both the NiV N and NiV P proteins had on viral replication, 293T cells were transfected with increasing amounts of NiV P-NiV N-CMV plasmid DNA and were subsequently infected with NiV. All stages of the viral replication pathway were analyzed: viral transcription, translation, replication, and production of progeny viruses. A 75%

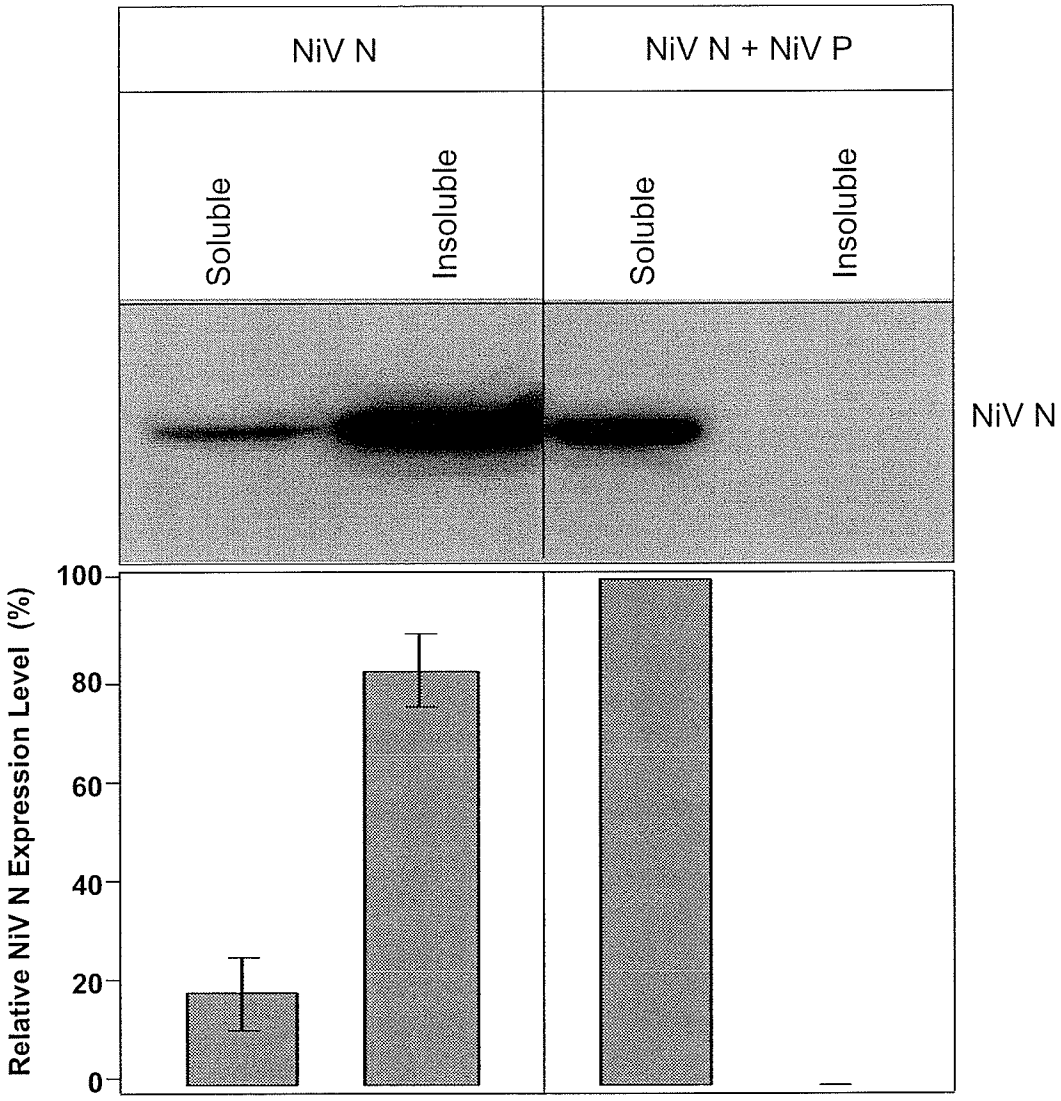

Figure 37: The Solubility of NiV N Proteins. Experiments were repeated three times. 293T cells transiently expressing NiV N proteins alone or both NiV N and NiV P proteins were lysed with an NP-40 lysis buffer. Supernatants added to a 20% sucrose cushion and underwent ultracentrifugation at 130,000xg for 1 hour at 4°C. Samples from the supernatant (soluble fraction) and the pellet (insoluble fraction) were visualized by immunoblot using a monoclonal antibody against NiV N. Expression of NiV N proteins was quantified using AlphaEase™ software. For all experiments, standard deviations of the mean were calculated.

decrease in the expression of the NiV F_0 protein (Figure 38C, compare expression levels between the right column and the left column), an 88% decrease in the amount of NiV M mRNA (Figure 38B, compare transcription levels in the left lane and left column with the right lane and right column), and a 78% overall decrease in the presence of viral genome (Figure 38D, compare the presence of genomic RNA levels between the right and left points) was observed in cells expressing both recombinant NiV N and NiV P. NiV-infected cells not expressing any recombinant NiV N and NiV P produced viral titres of $4.67x10^6$ $TCID_{50}$ IFU/ml, whereas cells expressing NiV N and P at high levels produced viral titres of $8.7x10^3$ $TCID_{50}$ IFU/ml, Figure 38E. This represents a decrease in viral titres of approximately 2.5-log_{10} (Figure 38E, compare values in the right column with values in the left column). Similar results were observed when NiV N alone or NiV N and P proteins together were expressed; i.e. general inhibition of viral replication at all stages of the replication cycle (Section 3.2.10-3.2.13).

Although NiV N, when co-expressed with NiV P was able to reduce viral replication, it was only able to cause a 2.5-log_{10} reduction in viral titres, whereas when NiV N was expressed alone it was able to impair the production of progeny viruses by 4-log_{10} (Section 3.2.13). The expression levels of NiV N were compared between cells transfected with NiV N-IRES-CMV or NiV P-NiV N-CMV, and cells infected with NiV, Figure 39. When 4µg of NiV P-NiV N-CMV were transfected into cells, NiV N expression was comparable to the expression levels obtained when 0.25µg of NiV N-IRES-CMV was compared, cells transfected with 0.25µg of NiV N-IRES-CMV plasmid DNA resulted in a decrease in production of

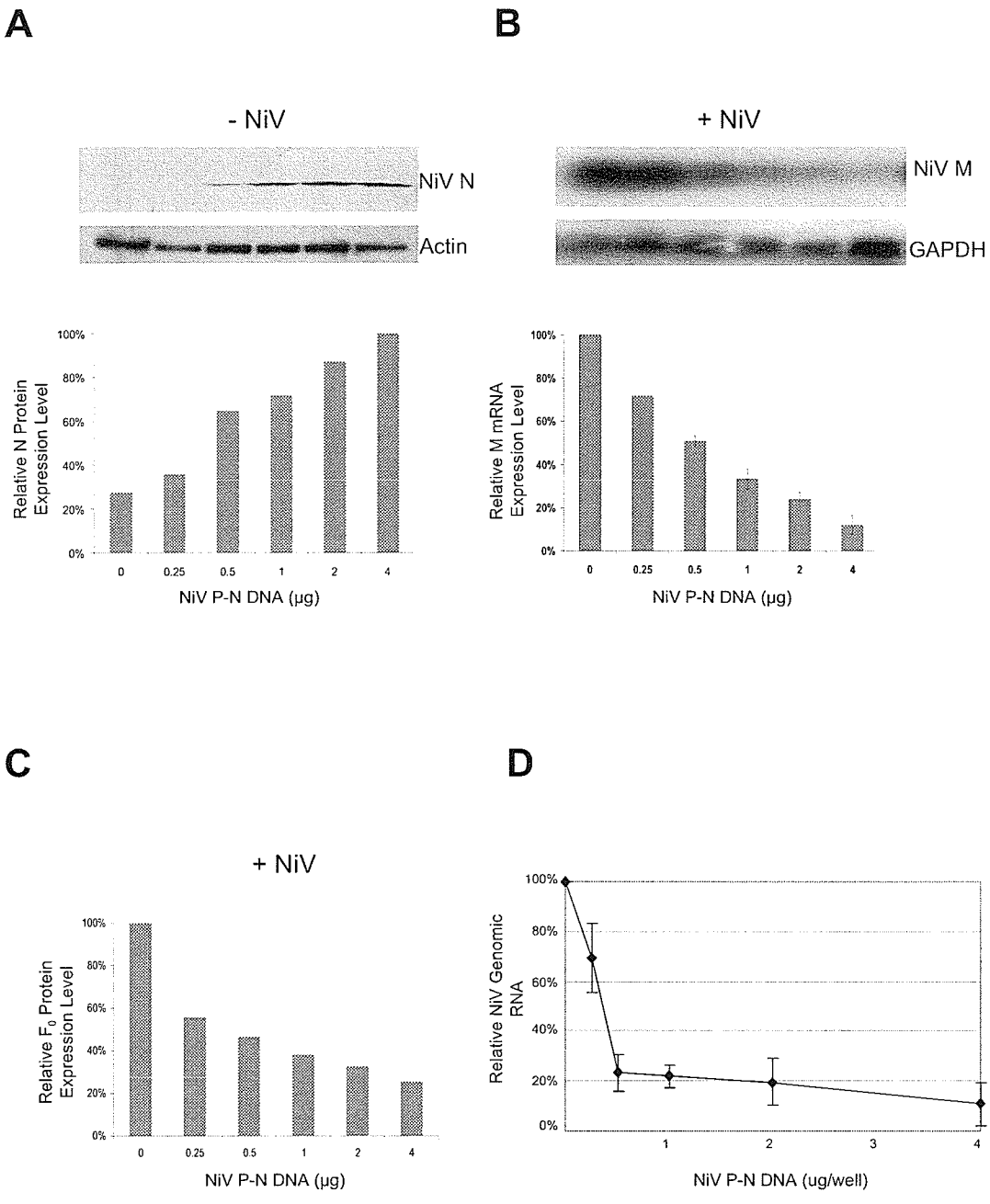
A
B
- NiV
+ NiV
NiV N
Actin
NiV M
GAPDH
Relative N Protein Expression Level
100%
80%
60%
40%
20%
0%
0
0.25
0.5
1
2
4
NiV P-N DNA (µg)
Relative M mRNA Expression Level
NiV P-N DNA (µg)
C
D
+ NiV
Relative F0 Protein Expression Level
NiV P-N DNA (µg)
Relative NiV Genomic RNA
1
2
3
4
NiV P-N DNA (ug/well)

E

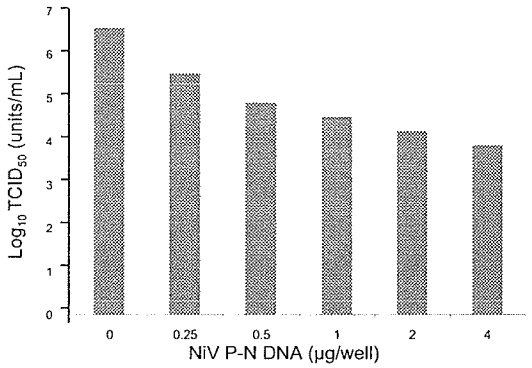

Figure 38: Analysis of NiV replication when Recombinant NiV N and NiV P Proteins Simultaneously Increase. Experiments were carried out in triplicate. 293T cells expressing both NiV N and NiV P proteins were infected with NiV at an MOI of 1 ($2x10^6$ IFU/well) for 24 hours. (A) Cell lysates were harvested prior to infection and analyzed by immunoblot. Upper panel- immunoblot analysis using a monoclonal antibody against NiV N, demonstrated increased expression of NiV N protein. Lower panel - immunoblots were quantified using AlphaEaseFC™ software and standardized against actin. (B) Total RNA was extracted from cells lysates and analyzed the presence of NiV M mRNA by northern blot. Upper panel - a DNA probe designed against the NiV M gene detected NiV M mRNA. Lower panel - the autoradiogram was subjected to phosphoimager analysis, quantified using ImageQuant software and standardized against GAPDH. (C) Cell lysates were harvested post-infection and analyzed by immunoblot. Using a polyclonal guinea pig antibody against NiV, the expression of F_0 was determined. Immunoblots were quantified using AlphaEaseFC™ software and standardized against actin. (D) Total RNA was extracted from cell lysates and used to analyze the presence of genomic NiV RNA. Strand-specific reverse transcription employed a forward primer designed in the NiV G gene to detect negative-sense NiV genome. Real-time PCR was carried out using SmartCycler technology and a primer set designed within the NTR of the NiV G and NiV L gene. Each reaction was quantified and standardized against GAPDH. (E) Supernatants were harvested from cells post-infection and serially diluted from 10^{-1} to 10^{-9}. Dilutions were adsorbed for 1 hour onto fresh 293T cells and $TCID_{50}$ viral titres were calculated 48 hours post-infection. For all experiments, standard deviations of the mean were calculated.

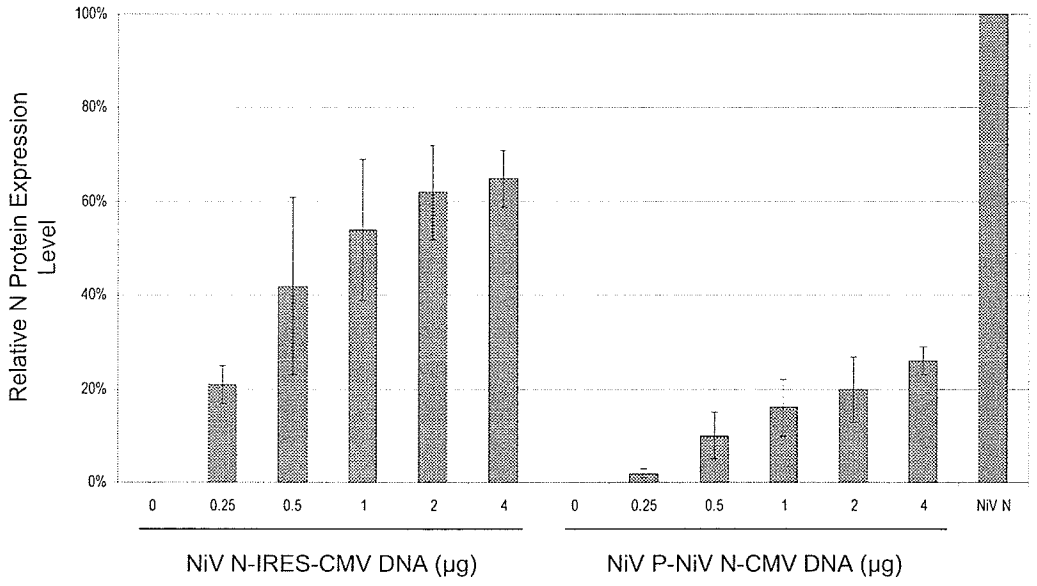

Figure 39: A Comparative Analysis of NiV N Protein Expression. Experiments were carried out in triplicate. 293T cells transiently expression NiV N proteins alone, or together with NiV P proteins were harvested and analyzed by immunoblot. A monoclonal antibody against the NiV N protein was used to detect the expression levels of NiV N proteins between recombinant NiV N proteins and viral NiV N proteins. Immunoblots were quantified using AlphaEaseFC™ software and standardized against actin. Standard deviations of the mean were calculated.

progeny virus by 0.76-$\log_{10}$ whereas (Figure 32), cells transfected with 4.0µg of NiV P-NiV N-CMV resulted in a decrease in viral titres of 2.5-$\log_{10}$ (Figure 38). These results demonstrated a clear difference between in the ability of NiV N to abrogate viral replication when expressed at similar levels. More specifically, NiV N, which was co-expressed with NiV P, were able to inhibit viral replication to a higher degree than when NiV N was expressed on its own. In general, the variation between the reduction in viral titres with and without the expression of NiV P proteins was attributed to the overall weaker expression of NiV N proteins when using the dual promoter system in comparison to the expression of NiV when using the NiV N-IRES-CMV construct.

3.2.17 Recombinant NiV N mRNA was not sufficient for the decrease in viral proteins, mRNA and full-length genome

To address the possibility of whether recombinant NiV N mRNA (rather than the N protein) had a role in causing the reduction of NiV replication, the construct ΔNiV N-IRES-CMV, a transcriptionally active but translationally inactive NiV N construct, was produced by site-directed mutagenesis. Translational 'ATG' start sites were mutated to 'TTG', diagrammatically represented in Figure 40A (Appendix 3). Changes to the nucleotide sequence were verified by DNA sequencing. RNA was extracted from cell lysates and analyzed by northern blot in order to verify the presence of NiV N mRNA, while protein cell lysates were collected for visualization of the NiV N protein by immunoblot. Using a DNA probe designed against the NiV N ORF, northern blot analysis was able to detect

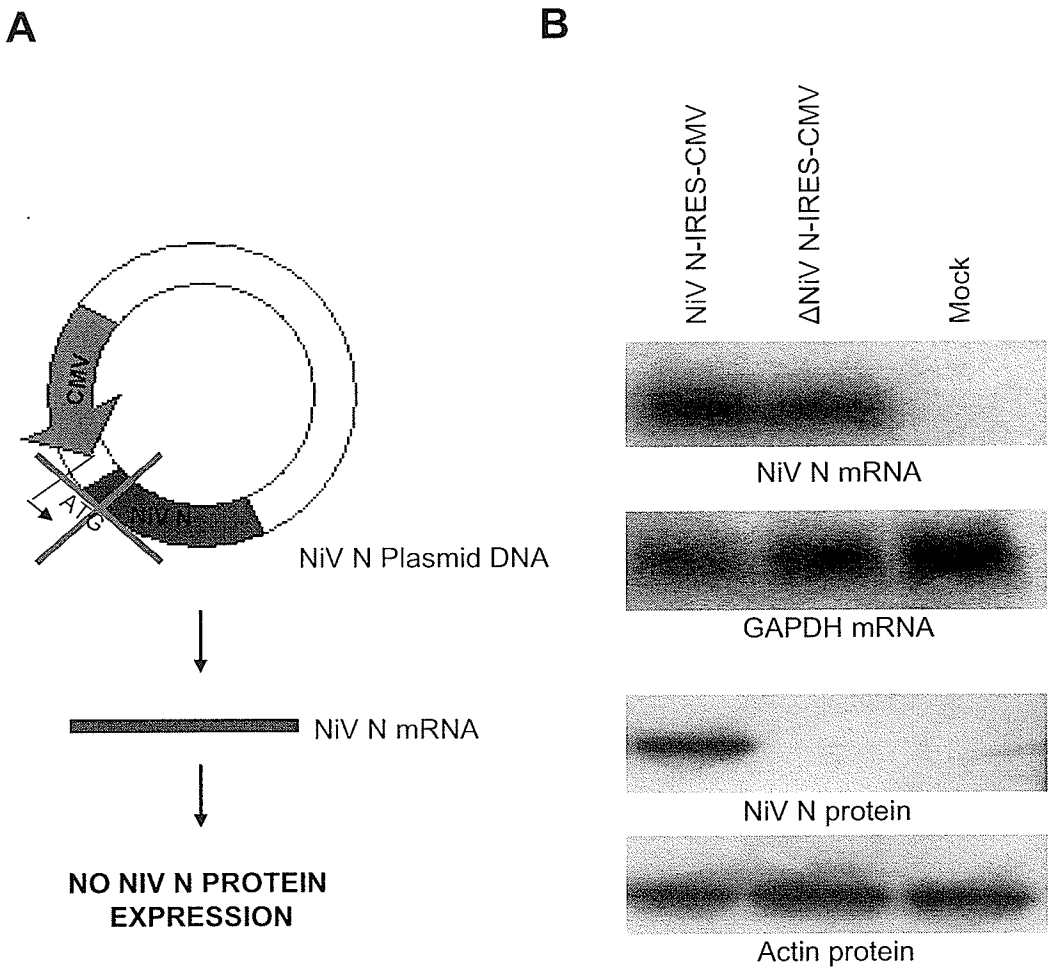

Figure 40: Expression of the ΔNiV N-IRES-CMV construct. Site directed mutagenesis was employed to remove the ATG start codon from the NiV N-IRES-CMV construct. (A) A schematic diagram of the construct is presented, where the ATG start site is removed thus producing a plasmid, which is able to synthesize NiV N mRNA but is unable to produce NiV N proteins. (B) Northern blots, using a DNA probe designed against the NiV N ORF, and immunoblots, using a monoclonal antibody against NiV N, were used to verify the ability of the constructs to produce NiV N mRNA and NiV N proteins, respectively.

the presence of NiV N mRNA from cells transfected with either ΔNiV N-IRES-CMV or NiV N-IRES-CMV, Figure 40B. Immunoblot analysis demonstrated that cells transfected with NiV N-IRES-CMV, the positive control, were able to express NiV N proteins (Figure 40B- left lane) whereas NiV N proteins was not detected in lysates from cells transfected with ΔNiV N-IRES-CMV (Figure 40B-middle lane). Mock transfected cells acted as a negative control for the production of NiV N mRNA and proteins (Figure 40B-right lane).

293T cells were transfected with increasing amounts of the ΔNiV N-IRES-CMV and were subsequently infected with NiV. Immunoblot analysis did not demonstrate any significant changes in the levels of viral translation between cells expressing high levels of recombinant ΔNiV N transcripts and cells expressing no recombinant ΔNiV N transcripts (Figure 41, compare NiV P protein intensity in the right lane and right column with protein intensity in the left lane and left column). Strand-specific real-time RT-PCR analysis was employed to detect negative-sense viral genome and positive-sense viral RNA. No significant changes in production of full-length viral genome or positive-sense viral RNA was observed between cells, which contained high amounts of the ΔNiV N-IRES-CMV construct versus cells that did not contain any ΔNiV N-IRES-CMV plasmid DNA (data not shown). These results demonstrated that the increase in recombinant NiV N mRNA did not silence transcription and translation of NiV genes nor did it hinder replication of full-length viral genome. These results indicated that the shutdown of viral replication was specific for the presence of recombinant NiV N protein.

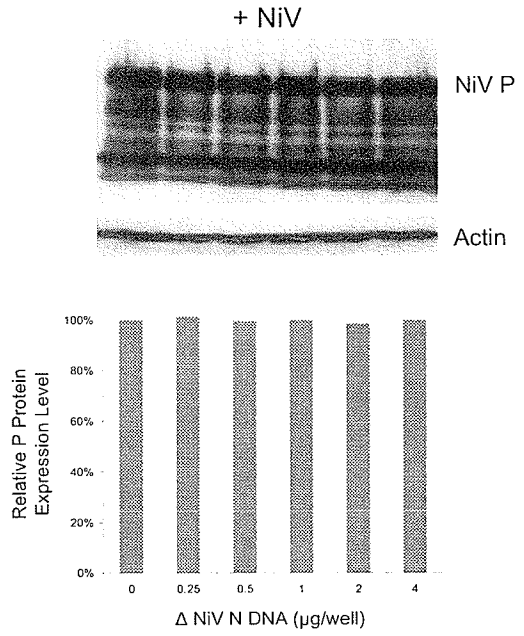

Figure 41: Analysis of NiV Replication as NiV N mRNA Increased. Experiments were carried out in triplicate. (A) 293T cells were transfected with increasing amounts of ΔNiV N-IRES-CMV, a plasmid that is transcriptionally-active but translationally-inactive, and infected with NiV at an MOI of 1 ($2x10^6$ IFU/well) for 24 hours. Upper panel- cell lysates were analyzed by immunoblot using a polyclonal guinea pig antibody against NiV was used to detect the presence of NiV proteins. Lower panel- samples were quantified using AlphaEaseFC™ software based on the expression of the NiV P protein and standardized against actin. Standard deviations of the mean were calculated.

3.2.18 Increased expression of the NiV N protein did not affect VSV replication in 293T cells.

NiV replication was impaired with increasing expression levels of NiV N proteins. This finding may be the consequence of NiV N proteins creating an overall cytotoxic environment within cells or activating the innate immune response, such as interferon (IFN) α/β production. In order to address the question of whether cells expressing increasing levels of NiV N proteins generated an antiviral state or an overall general toxic environment, cells expressing increasing levels of NiV N proteins were infected with VSV at an MOI of 1 ($2x10^6$ PFU/well). VSV is a virus known to be highly sensitive to the IFN response and the subsequent production of an antiviral state (51;52;142;174;206). Immunoblot analysis using a monoclonal antibody against the VSV G protein (Sigma®) demonstrated that the level of VSV G expression was consistent regardless of whether cells expressed high amounts of NiV N or not (Figure 42A, compare the VSV G protein intensity in the left lane and left column with the protein intensity in the right lane and right column). These results were supported by $TCID_{50}$ viral titre analysis, which showed that there were no differences in the VSV titres between cells expressing recombinant NiV N proteins and cells which did not (Figure 42B, compare viral titres in the right column with viral titres in the left column). These results revealed that the cellular environment supported VSV replication regardless of pre-existing expression of recombinant NiV N.

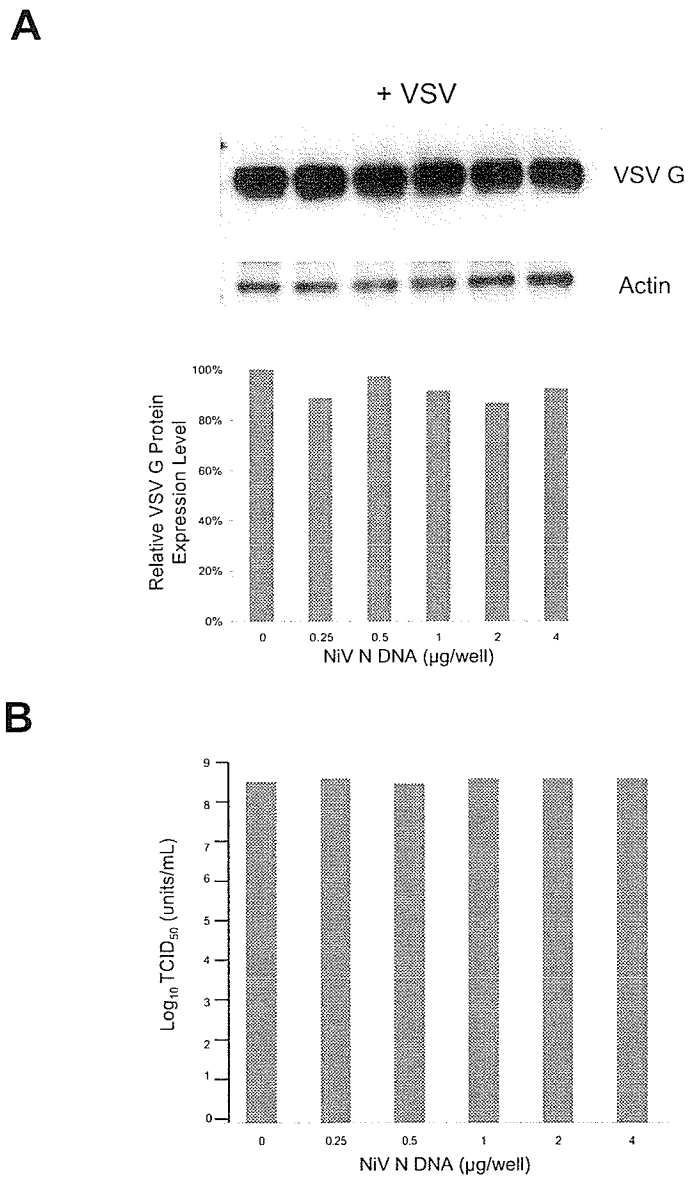

Figure 42: The Effect of Increasing Amounts of NiV N Proteins on VSV Replication. Experiments were repeated three times. Cells expressing increasing levels of NiV N were subsequently infected with VSV at an MOI 1 ($2x10^6$ IFU/well) for 24 hours. (A) Upper panel- total cell lysates were analyzed by immunoblot using a monoclonal antibody targeted against the VSV G protein. Lower panel- samples were quantified using AlphaEaseFC™ software and standardized against actin. (B) Supernatants were harvested and adsorbed for 1 hour onto fresh 293T cells. $TCID_{50}$ viral titres were calculated 48 hours post-infection. Viral titrations were done in triplicate. For all experiments, standard deviations of the mean were calculated.

3.2.19 Recombinant expression of NiV N proteins did not inhibit receptor-mediated fusion.

Expression of recombinant NiV N proteins did not seem to inhibit normal cellular functions such as RNA transcription and protein translation, based on GAPDH mRNA and Actin protein levels respectively. However, it could be speculated that the recombinant expression of NiV N proteins could interfere with some stage of virus entry, possibly by interacting with cellular receptors during transport to the cell surface. A previous study with MeV demonstrated that MeV N proteins were able to enter late endosomes, where they were able to interact with cell surface proteins, and were transported back to the cell surface before coming in contact with the lysosomes (119). Similarly, processing of NiV F proteins by Cathepsin L is believed to occur in late endosomes, and these endosomes are believed to be recycled back to the cell surface allowing activated NiV F to interact with the NiV G protein (49). Although this is an unlikely event for NiV N proteins, it could be used to explain the overall impairment of viral replication with increasing amounts of NiV N protein expression. To address this question, a receptor-mediated fusion assay was utilized. This system focused on the recombinant expression of NiV F and G proteins and subsequent formation of multi-nucleated giant cells or syncytia (15;16;163;178). The main mechanism behind viral entry into a cell was based on the ability of the virus to bind to cellular receptors on the cell surface and fuse the viral envelope with the cellular membrane. Currently, there is no evidence that NiV particles gain access to cells through cell-mediated endocytosis.

Furthermore, there is evidence that indicates that endocytosis has no role during NiV infection (49). Although this study did not utilize a virus-based assay to demonstrate receptor-mediated fusion, the NiV F and G protein-mediated fusion assay assesses the ability of NiV N to inhibit the production of multi-nucleated giant cells (syncytia), which would be a consequence of NiV F and G protein-mediated membrane fusion and the main mechanism behind viral entry. As a positive control for fusion, cells expressing CFP were mixed with cells expressing NiV F and G proteins. 24 hours post-transfection cells were analyzed by fluorescent microscopy and diffuse CFP staining was seen throughout the large syncytia (Figure 43B). The results indicated that cells expressing CFP were able to fuse with cells expressing NiV F and G proteins. Cells expressing the recombinant NiV N-CFP fusion protein were mixed with cells expressing recombinant NiV F and G proteins. Figure 43D shows that cells, which were expressing NiV N-CFP were readily able to fuse and form syncytia with cells expressing NiV F and G proteins. Expression of NiV N proteins caused a punctate staining pattern and was apparent within the multi-nucleated giant cells. In support of these findings, cells expressing increasing amounts of NiV N proteins demonstrated massive syncytia formation throughout the cell population, indicating that cells expressing NiV N proteins were infected by NiV (data not shown). Since this mechanism of fusion was required for viral entry into a cell, these results suggested that expression of recombinant NiV N proteins did not block viral entry.

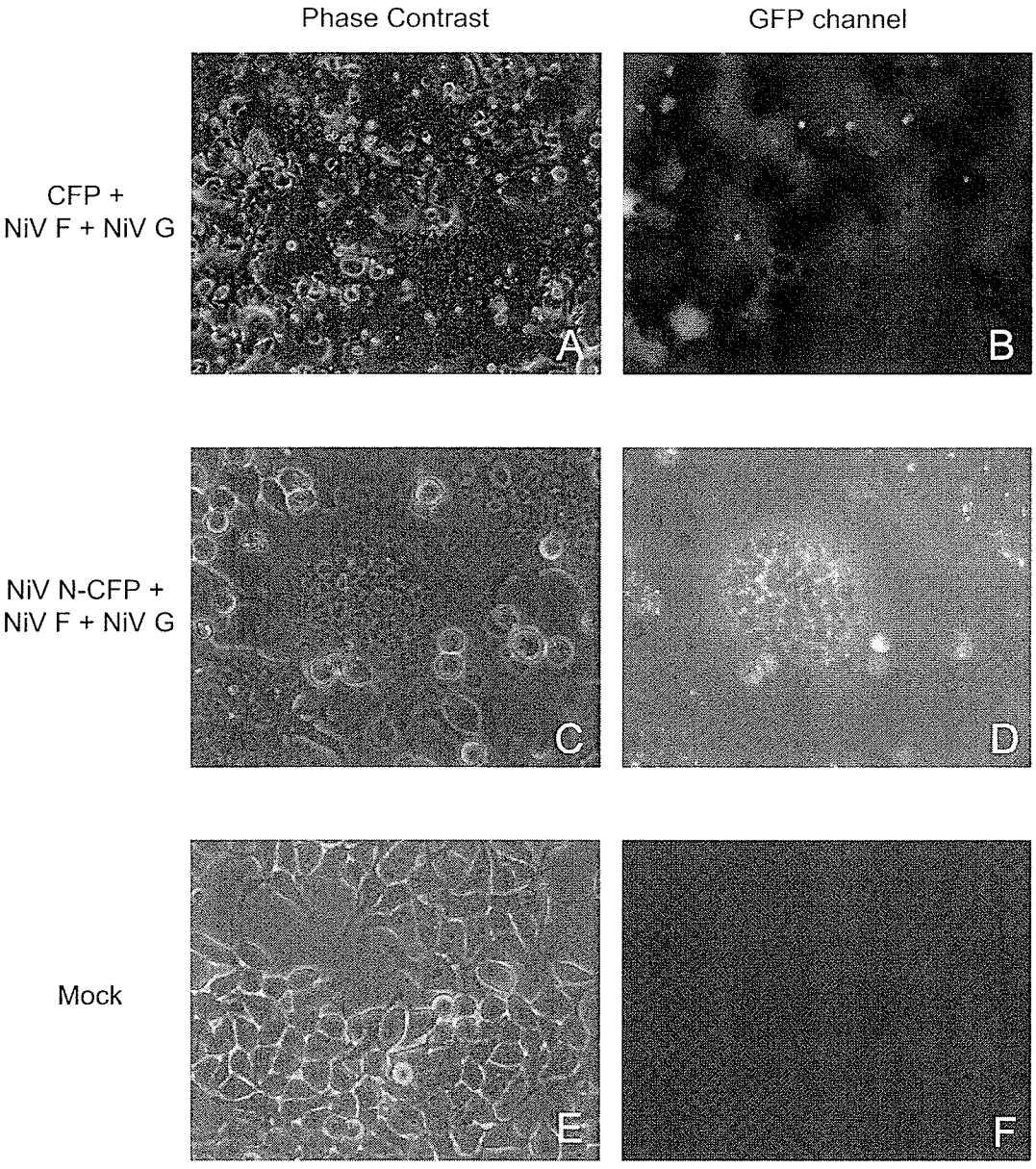

Figure 43: Analysis of NiV F and G Protein-Mediated Fusion in the Presence of Recombinant NiV N Proteins. Experiments were repeated three times. 293T cells transiently expressed either, NiV F and G proteins, NiV N-CFP or CFP. Cells expressing CFP were mixed with cells expressing NiV F and G (A and B) or cells expressing NiV N-CFP were mixed with cells expressing NiV F and G (C and D) and further incubated for 24 hours. The ability of cells expressing NiV N-CFP or CFP to fuse with cells expressing NiV F and G proteins was visualized by the presence of fluorescent multi-nucleated giant cells using fluorescent microscopy at a magnification of 32X.

3.2.20 Truncated NiV N-HA proteins containing either of the functional NiV P protein-binding domains were essential for the reduced levels of viral replication

A variety of controls has supported the hypothesis that the NiV N protein may interact with the NiV P protein in order to mediate the impairment of viral replication. It has been suggested that recombinant NiV N was responsible for the abrogation of viral replication due to its potential to convert the NiV transcriptases into replicases. It was believed that the transcriptase complex was comprised of the NiV L and the NiV P proteins, while the production of the viral replicase was thought to occur through the interaction of the NiV N protein with the transcriptase complex via binding to the NiV P protein. The NiV P protein-binding domains found within the NiV N protein have been described in prior sections, Section 3.2.8 and 3.2.9. Therefore, to determine whether the presence of either of the NiV P protein-binding domains found on the NiV N protein had any effect of viral replication, a series of experiments were carried out using constructs NiV N 1-1401-HA, NiV N 163-1599-HA, NiV N 1-162-CFP and NiV N 1402-1599-CFP. The data from these experiments would determine whether the interaction between NiV N and P is essential for the abrogation of viral replication. Furthermore, it will also determine whether the NiV P protein-binding domains found within the NiV N protein alone are responsible for the abrogation of viral replication.

The first set of truncated proteins analyzed contained an HA-tag on the C-terminal end of the protein. NiV N 1-1401-HA is a truncated protein deficient in

the C-terminal NiV P-protein binding domain, NiV N 163-1599-HA is a truncated protein deficient in the N-terminal NiV P protein-binding domain, and NiV N 163-1401-HA is a truncated protein deficient in both NiV P protein-binding domains. To ensure that the addition of an HA-tag did not affect the ability of the proteins to function in viral replication, NiV N-HA was used as a positive control. Every experiment had its own set of internal negative controls.

Cells were transfected and subsequently infected with virus before being analyzed by immunoblot for the expression of viral proteins. A guinea pig-derived polyclonal antibody against NiV was used to visualize the production of NiV P proteins, while an antibody against the HA-tag was used to visualize the recombinantly expressed HA-tagged NiV N proteins. Immunoblots were quantified and standardized against actin. A correlation between the amount of transfected plasmid DNA and expression of recombinant NiV N-HA proteins was observed, Figure 44A. Cells expressing high levels of recombinant NiV N-HA proteins showed a 77% reduction in viral translation of NiV P in comparison to cells not expressing any recombinant NiV N-HA (Figure 44B, top left panel-compare NiV P protein band intensities in the right lane and right column with band intensities in the left lane and left column). Similarly, when NiV N 163-1599-HA proteins was expressed at high levels, the expression of NiV P was inhibited by 55% in comparison to cells that did not express any recombinant proteins (Figure 44B, top middle panel-compare protein intensity in right lane and right column with the protein intensity in left lane and left column). Cells expressing high amounts of NiV N 1-1401-HA proteins demonstrated a

A

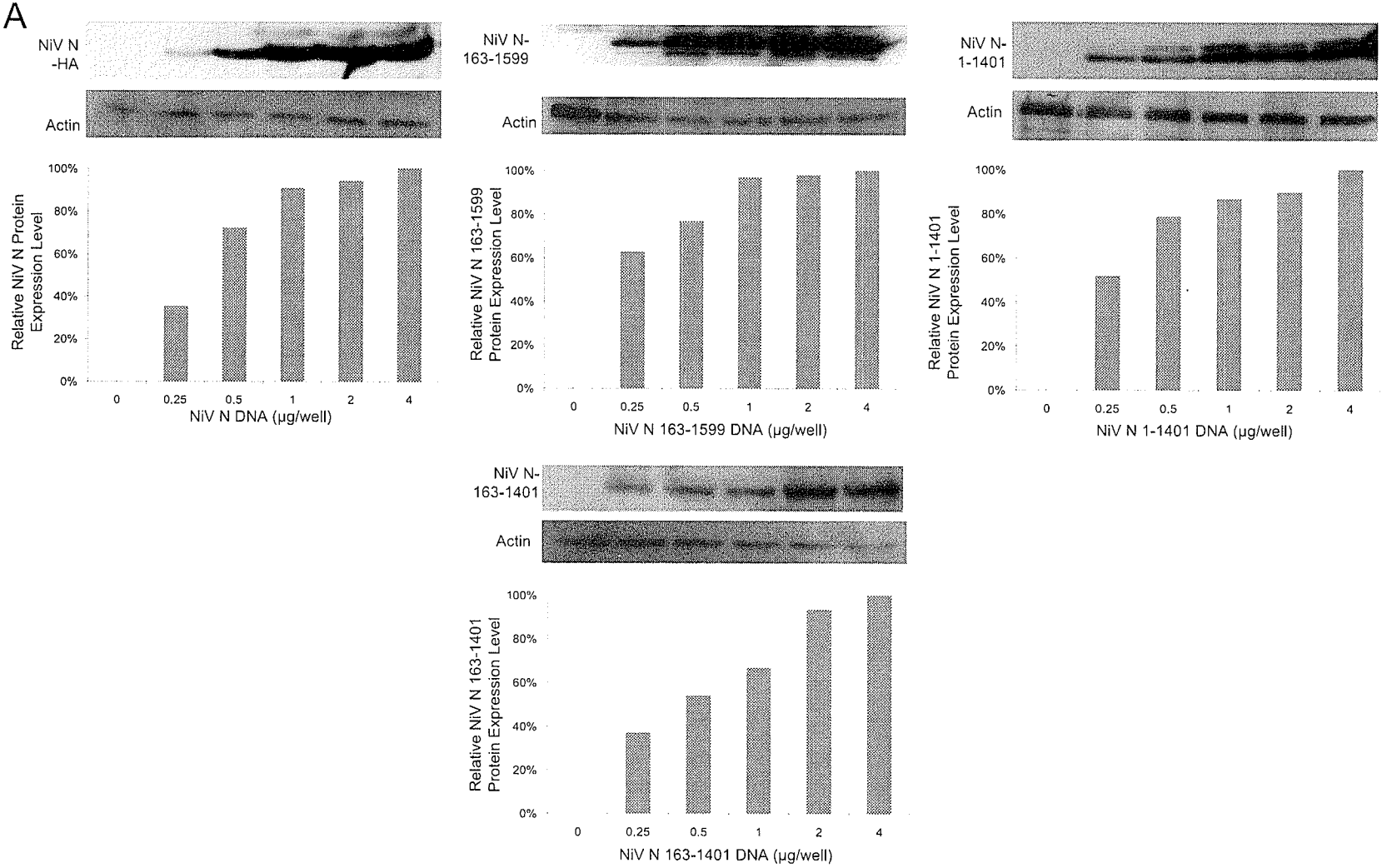
NiV N -HA
Actin
Relative NiV N Protein Expression Level
100%
80%
60%
40%
20%
0%
0
0.25
0.5
1
2
4
NiV N DNA (µg/well)
NiV N-163-1599
Actin
Relative NiV N 163-1599 Protein Expression Level
NiV N 163-1599 DNA (µg/well)
NiV N-1-1401
Actin
Relative NiV N 1-1401 Protein Expression Level
NiV N 1-1401 DNA (µg/well)
NiV N-163-1401
Actin
Relative NiV N 163-1401 Protein Expression Level
NiV N 163-1401 DNA (µg/well)

B

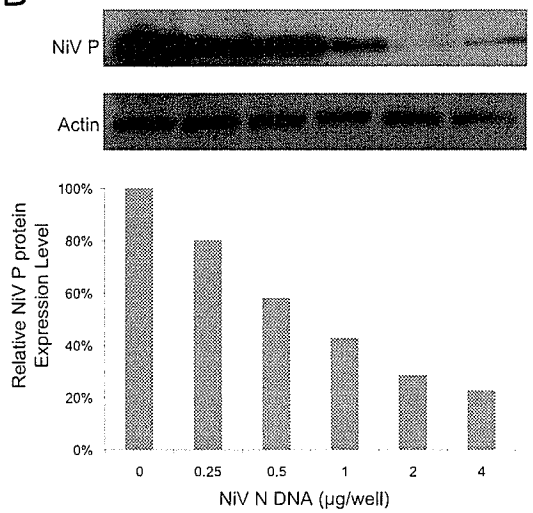
NiV P
Actin
Relative NiV P protein Expression Level
100%
80%
60%
40%
20%
0%
0
0.25
0.5
1
2
4
NiV N DNA (µg/well)

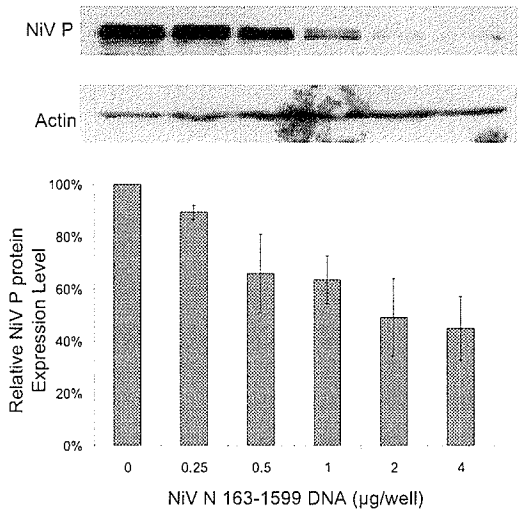
NiV P
Actin
Relative NiV P protein Expression Level
100%
80%
60%
40%
20%
0%
0
0.25
0.5
1
2
4
NiV N 163-1599 DNA (µg/well)

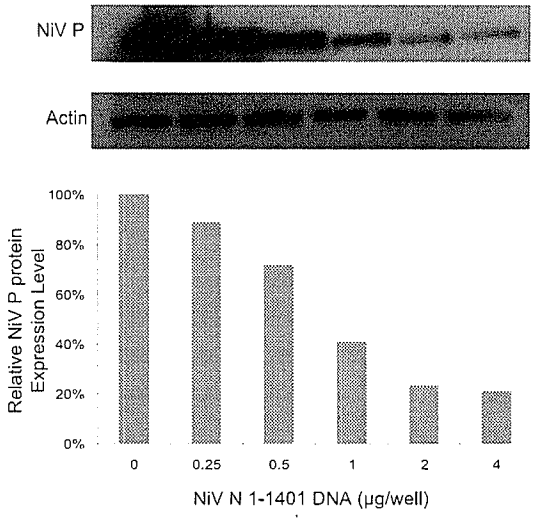
NiV P
Actin
Relative NiV P protein Expression Level
100%
80%
60%
40%
20%
0%
0
0.25
0.5
1
2
4
NiV N 1-1401 DNA (µg/well)

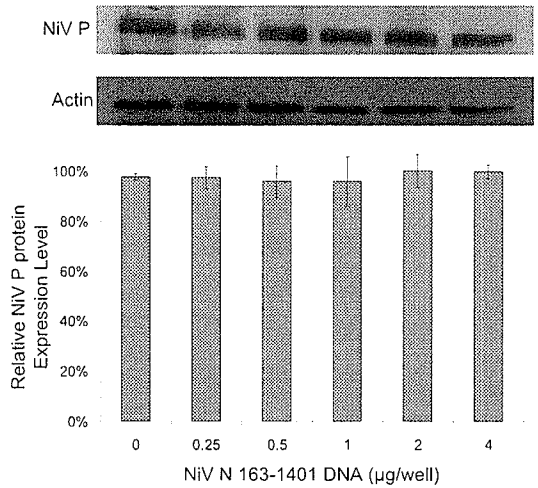
NiV P
Actin
Relative NiV P protein Expression Level
100%
80%
60%
40%
20%
0%
0
0.25
0.5
1
2
4
NiV N 163-1401 DNA (µg/well)

C

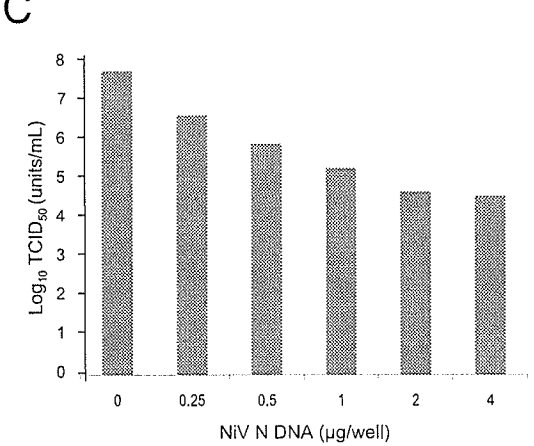
Log10 TCID50 (units/mL)
0
1
2
3
4
5
6
7
8
0
0.25
0.5
1
2
4
NiV N DNA (µg/well)

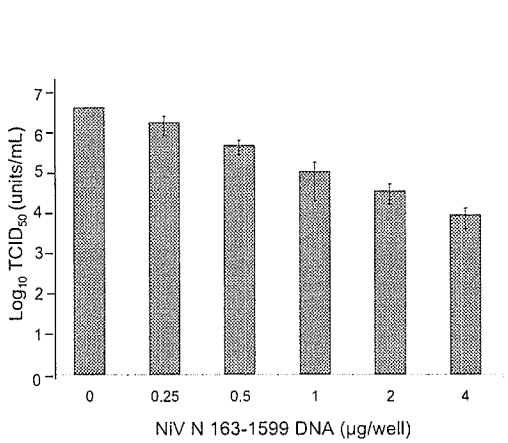
Log10 TCID50 (units/mL)
0
1
2
3
4
5
6
7
0
0.25
0.5
1
2
4
NiV N 163-1599 DNA (µg/well)

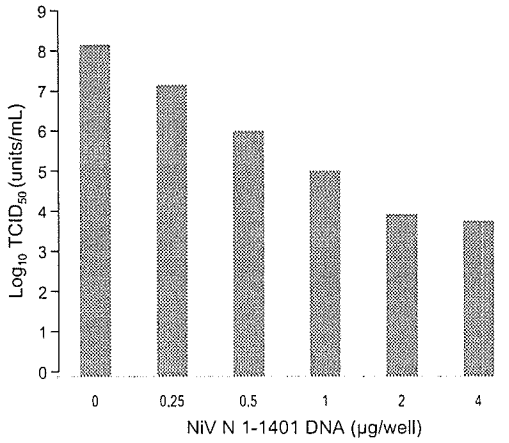
Log10 TCID50 (units/mL)
0
1
2
3
4
5
6
7
8
9
0
0.25
0.5
1
2
4
NiV N 1-1401 DNA (µg/well)

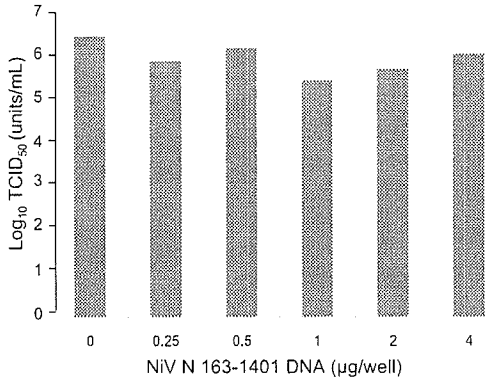
Log10 TCID50 (units/mL)
0
1
2
3
4
5
6
7
0
0.25
0.5
1
2
4
NiV N 163-1401 DNA (µg/well)

Figure 44: Analysis of NiV Replication as Expression Levels of Truncated NiV N-HA Protein Increase. All experiments were carried out in triplicate and standard deviations of the mean were calculated. 293T cells transiently expressing increased amounts of various truncated NiV N-HA proteins were infected with NiV at an MOI of 1 ($2x10^6$ IFU/well) for 24 hours. Upper left panel represents cells expressing NiV N-HA, upper middle panel represent cells expressing NiV N 163-1599-HA, upper right panel represent cells expressing NiV N 1-1401-HA and lower middle panel represents cells expressing NiV N 163-1401-HA. (A) Cell lysates were harvested and analyzed by immunoblot using an antibody against the HA-tag. Immunoblot analysis demonstrated an increase in truncated NiV N-HA protein expression as amounts of transfected plasmid DNA increased. Immunoblots were quantified using AlphaEaseFC™ software and standardized against the expression of actin. (B) Cell lysates were harvested and analyzed by immunoblot using a polyclonal antiserum against NiV. Immunoblot analysis demonstrated the expression levels of NiV P proteins. Immunoblots were quantified using AlphaEaseFC™ software and standardized against the expression of actin. (C) Supernatants were harvested and serial dilutions from 10^{-1} to 10^{-9} were adsorbed for 1 hour onto fresh 293T cells, and $TCID_{50}$ viral titres were calculated 48 hours post-infection. Viral titrations were done in triplicate.

suppression of NiV P expression by 79% in comparison to cells, which did not express any recombinant protein (Figure 44B, top right panel-compare protein intensity between right lane and right column and left lane and left column). However, cells expressing increasing amounts of NiV N 163-1401-HA demonstrated no significant changes in NiV P protein expression levels when viral protein levels were assessed (Figure 44B, bottom panel-compare the protein intensity between all lanes and columns).

The ability of cells expressing various amounts of recombinant NiV N-HA to produce progeny virus was assessed by $TCID_{50}$ assays. Cells expressing high levels of NiV N-HA proteins demonstrated a 3.2-log_{10} decrease in viral titres in comparison to cells not expressing any recombinant proteins (Figure 44C, top left panel-compare the viral titres between the right and left columns). Cells transiently expressing high levels of NiV N 163-1599-HA demonstrated a 3.2-log_{10} decrease in infectious titres observed in contrast to cells that did not express any recombinant proteins (Figure 44C, top middle panel-compare the viral titres between the right and left columns). Similarly, there was a reduction in viral titres of 4.4-log_{10} between cells that did not express any recombinant proteins and cells expressing high amounts of NiV N 1-1401-HA (Figure 44C, top right panel-compare the viral titres between the right and left columns). In contrast, when viral titres were compared between cells expressing recombinant NiV N 163-1401-HA and cells not expressing any recombinant proteins, viral titres varied within 1-log_{10} of each other (Figure 44C, bottom panel-compare the viral titres between all columns). These results demonstrated that a recombinant

protein deficient in both NiV P binding domains did not have an adverse effect on NiV titres.

These results demonstrate an overall dysfunction in viral replication when increased amounts of recombinant NiV N-HA proteins containing one or both NiV P protein-binding domains were present in cells. However, when both of the NiV P protein-binding domains were removed from the NiV N protein, there was no detectable effect on viral replication. These results suggest that the interaction between NiV N and NiV P proteins was essential to the abrogation of NiV replication.

3.2.21 Truncated NiV N-CFP proteins containing either of the functional NiV P binding domains were able to impair viral replication

The previous results demonstrated the importance of the NiV P protein-binding domains in the disruption of viral replication. The experiments described in this section were designed to determine whether the expression of the recombinant NiV P protein-binding domains alone, NiV N 1-162-CFP or NiV N 1402-1599-CFP, could have any effect on viral replication. The recombinant NiV N 1-162-CFP protein contained the N-terminal NiV P protein-binding domain, while the protein NiV N 1402-1599-CFP contained the C-terminal NiV P protein-binding domain.

Cells were transfected with the truncated NiV N-CFP constructs and were subsequently infected with NiV, as previously described. Cell lysates were analyzed by immunoblot to visualize the expression of the viral and recombinant

proteins, as previously described. A guinea pig-derived polyclonal antibody against NiV was used to visualize the presence of the NiV P protein, while an antibody against GFP was used to visualize the presence of the recombinant NiV N-CFP proteins. As a positive control, it was necessary to confirm whether the recombinant protein, NiV N-CFP, was able to inhibit viral replication. The results of these experiments demonstrated that cells expressing high levels of NiV N-CFP had a 55% lower level of NiV P protein expression in comparison to cells expressing no recombinant proteins (Figure 45B, left panel-compare NiV P protein band intensities in right lane and right column with band intensities in left lane and left column). When the truncated proteins were assessed by immunoblot, cells transiently expressing NiV N 1-162-CFP demonstrated an 80% reduction in NiV P protein expression between cells expressing high amounts of NiV N 1-162-CFP and cells not expressing any recombinant proteins (Figure 45B, middle panel-compare protein intensities between right lane and right column with protein intensities from left lane and left column). Cells transiently expressing NiV N 1402-1599-CFP demonstrated a 61% reduction in NiV P protein expression between cells expressing high amounts of NiV N 1401-1599-CFP in comparison to cells not expressing any recombinant NiV N proteins (Figure 45B, right panel-compare protein intensities in right lane and right column to protein intensities in left lane and left column). These results demonstrated that the regions containing the NiV P protein-binding domains from the NiV N protein were capable of abrogating viral translation.

A

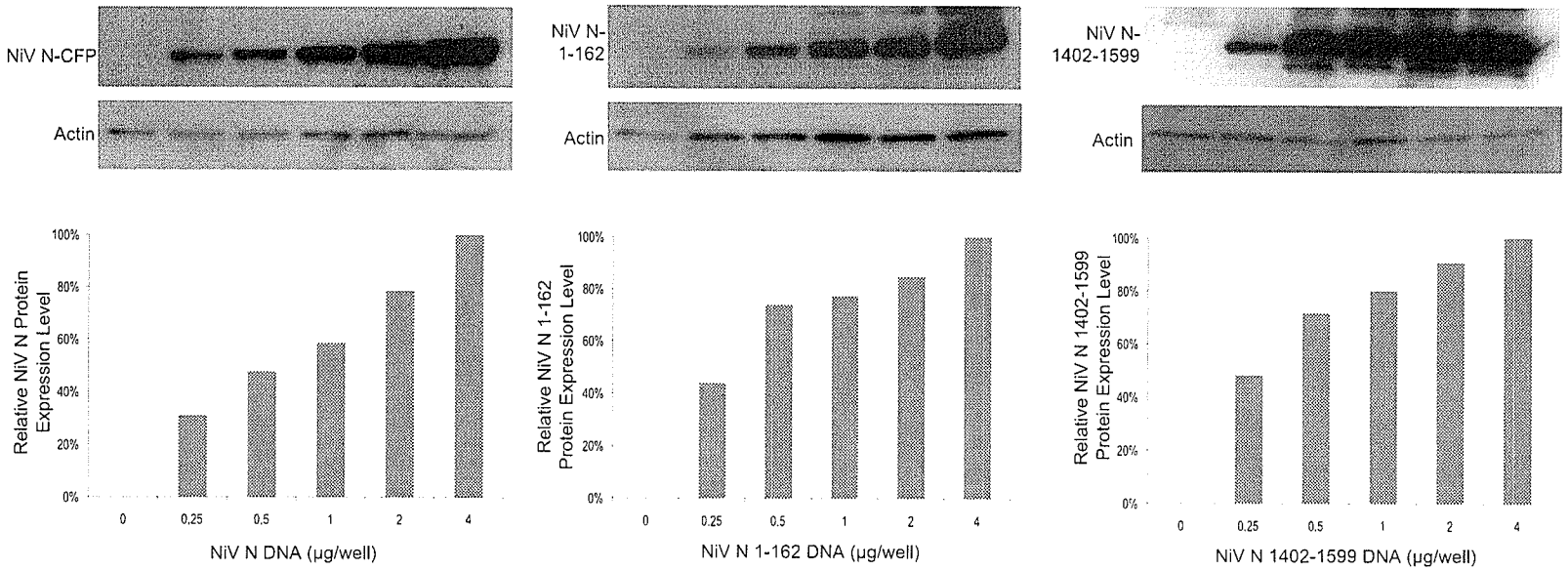
NiV N-CFP
Actin
NiV N-1-162
Actin
NiV N-1402-1599
Actin
Relative NiV N Protein Expression Level
100%
80%
60%
40%
20%
0%
0
0.25
0.5
1
2
4
NiV N DNA (µg/well)
Relative NiV N 1-162 Protein Expression Level
NiV N 1-162 DNA (µg/well)
Relative NiV N 1402-1599 Protein Expression Level
NiV N 1402-1599 DNA (µg/well)

B

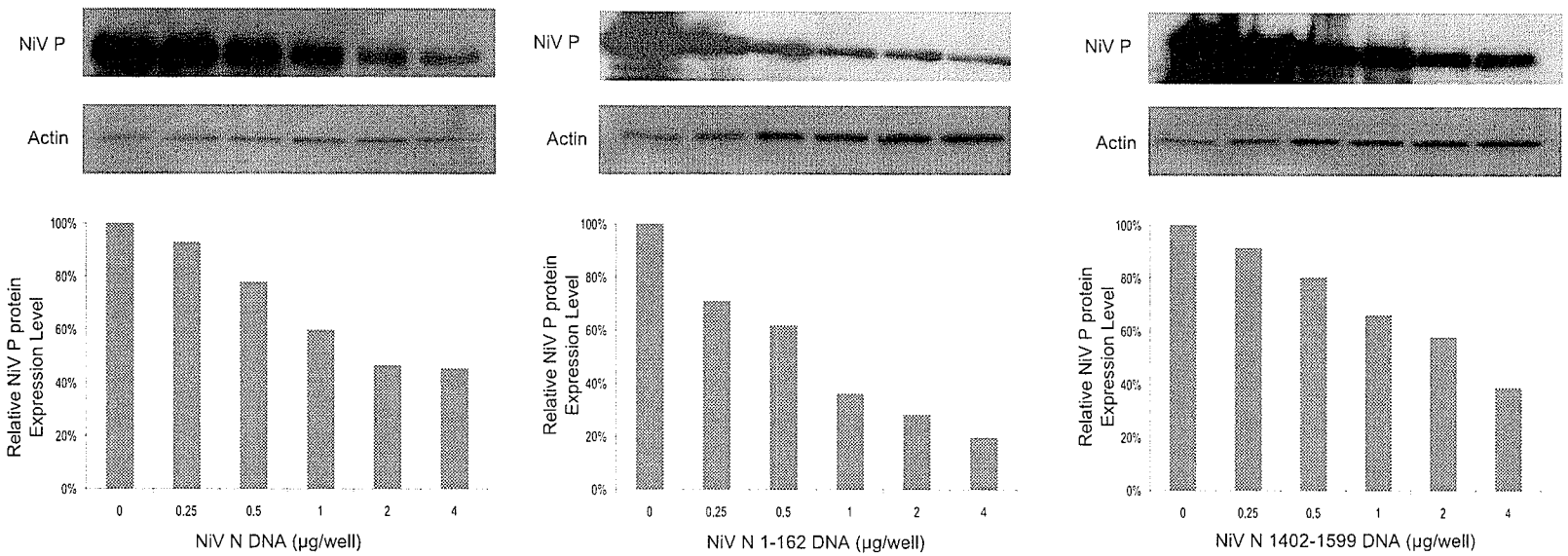
NiV P
Actin
Relative NiV P protein Expression Level
100%
80%
60%
40%
20%
0%
0
0.25
0.5
1
2
4
NiV N DNA (µg/well)
NiV P
Actin
Relative NiV P protein Expression Level
100%
80%
60%
40%
20%
0%
0
0.25
0.5
1
2
4
NiV N 1-162 DNA (µg/well)
NiV P
Actin
Relative NiV P protein Expression Level
100%
80%
60%
40%
20%
0%
0
0.25
0.5
1
2
4
NiV N 1402-1599 DNA (µg/well)

C

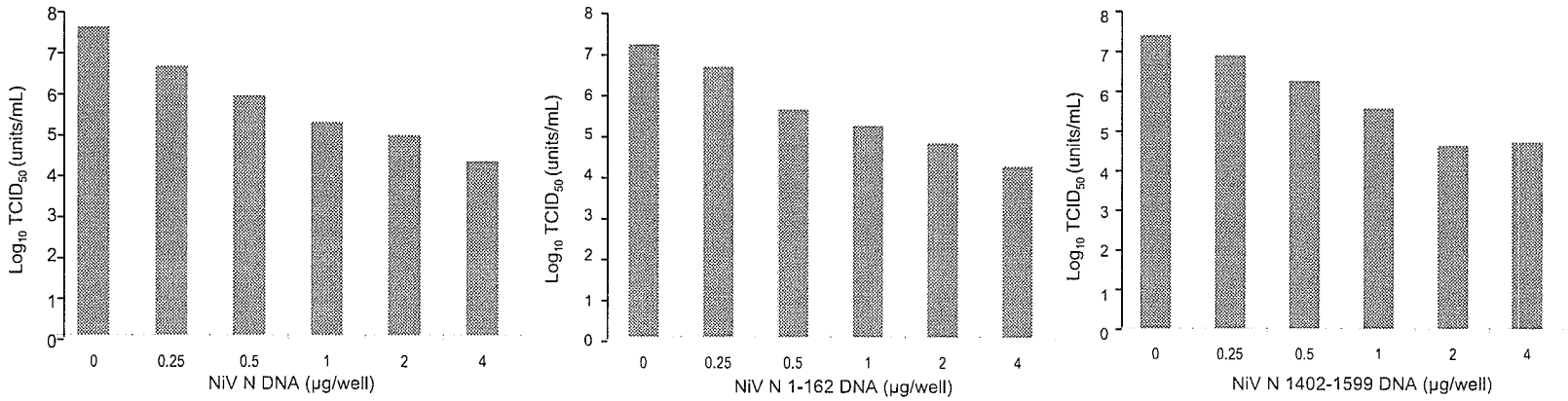

Figure 45: Analysis of NiV Replication as Expression Levels of Truncated NiV N-CFP Protein Increase. All experiments were carried out in triplicate and standard deviations of the mean were calculated. 293T cells transiently expressing increased amounts of various truncated NiV N-CFP proteins were infected with NiV at an MOI of 1 ($2x10^6$ IFU/well) for 24 hours. Left panel represents cells expressing NiV N-CFP, middle panel represent cells expressing NiV N 1-162-CFP, and right panel represent cells expressing NiV N 1402-1599-CFP. (A) Cell lysates were harvested and analyzed by immunoblot using an antibody against GFP to detect the CFP fusion tag. Immunoblot analysis demonstrated an increase in truncated NiV N-CFP protein expression as amounts of transfected plasmid DNA increased. Immunoblots were quantified using AlphaEaseFC™ software and standardized against the expression of actin. (B) Cell lysates were harvested and analyzed by immunoblot using a polyclonal antiserum against NiV. Immunoblot analysis demonstrated the expression levels of NiV P proteins. Immunoblots were quantified using AlphaEaseFC™ software and standardized against the expression of actin. (C) Supernatants were harvested and serial dilutions from 10^{-1} to 10^{-9} were adsorbed for 1 hour onto fresh 293T cells, and $TCID_{50}$ viral titres were calculated 48 hours post-infection. Viral titrations were done in triplicate.

When viral titres were assayed, cells expressing high levels of NiV N-CFP, showed a 3.2-$\log_{10}$ decrease in viral titres in comparison to cells not expressing additional recombinant proteins (Figure 45C, left panel-compare viral titre between the right and left columns). Cells expressing high amounts of NiV N 1-162-CFP demonstrated a 3.1-$\log_{10}$ decrease in viral titres when compared to cells not expressing any recombinant proteins (Figure 45C, middle panel-compare viral titre between the right and left columns). Similarly, a 2.7-$\log_{10}$ reduction of viral titres was observed between cells expressing and not expressing NiV N 1402-1599 recombinant proteins (Figure 45C, right panel-compare viral titre between the right and left columns). These results confirmed the influence that a peptide encoding one of the two NiV P protein-binding sites of NiV N could abrogate viral replication. These findings suggested that there was a dysfunction in the proper production of the viral polymerase complexes and that the interaction between NiV N and NiV P proteins was likely responsible for this inhibition.

4.0 Discussion

The NiV N protein is critical fro the process of viral replication. However, a balance between viral protein expression and production of viral RNA is essential in the maintenance of NiV replication. The central findings presented in this study clearly demonstrate that by providing increasing levels of the NiV N protein alone NiV replication was suppressed in a dose-dependent manner. Furthermore, the NiV P protein-binding sites found within the NiV N protein alone were sufficient to suppress viral replication, while other portions of the NiV N protein were not. From the results obtained, a model for the suppression of NiV replication by the presence of recombinant NiV N proteins was developed. It is believed that the recombinant expression of NiV N proteins caused the premature formation of the viral replicase by binding to the transcriptase complex through an interaction with the NiV P protein, thus causing a suppression of viral transcription and subsequent viral replication.

4.1 Eliminating Factors which could be Responsible for the Suppression of Viral Replication

The results obtained throughout this thesis supported the idea that viral replication was disabled in response to the recombinant expression of NiV N. The proposed mechanism for this inhibition is that the recombinant NiV N proteins may have the ability to prematurely convert the transcriptase complexes into replicase complexes. This conversion would prevent the production of viral mRNA, but the newly formed replicase complex should be competent for the

production of viral genome and anti-genome. However, the transformation of the transcriptase complex into a replicase complex would have a negative effect on viral transcription and subsequent viral protein production, thereby causing a decrease in viral replication. However, it was still possible that the disruption of viral replication could also be due to several alternative explanations. These alternatives may involve factors that interfered with specific aspects of viral replication or those that initiated various host responses as a result of excess expression of the NiV N protein.

4.1.1 The host's response to increased expression of NiV N proteins

Innate immunity is the first response by the host against foreign pathogens. Upon viral infection of a naïve host, an immediate non-specific attack is mounted by the host in response to the invading pathogen. This triggers the activation of a number of response pathways, which converge upon the production of IFN. The presence of IFN also promotes the production of IFN-stimulated genes, which help to establish an antiviral environment (28). RNA viruses have the ability to stimulate the IFN response through the interaction of various viral moieties, such as double-stranded RNA, with toll-like receptors (101). Once activated, these receptors proceed to activate the IFN pathway.

One possibility is that the IFN pathway was activated in response to increased expression of NiV N proteins in 293T cells. Other viral N proteins, such as the MeV N protein and the VSV N protein, have been shown to have a role in activating various stages of the IFN pathway (118;182;183). Additionally,

the production of "false" NC-structures has been suggested to be a possible initiation factor of the IFN response (182). Therefore, the formation of "false" NC-structures by the NiV N protein could have played a role in activating the host's innate immune responses. However, when recombinant NiV N proteins were maintained in a soluble state by co-expression with NiV P, NiV N were still capable of inhibiting viral replication, Section 3.2.15. Therefore, it was unlikely that the formation of "false" NC-structures and activation of the innate immune response was the mechanism responsible for the impairment of viral replication in this experimental setup.

Presently, it is not understood whether NiV N proteins have the ability to trigger the IFN response. However, 293T cells are thought to be deficient in the ability to respond to IFN (Personal Communication with Hana Weingartl); therefore, the establishment of an antiviral state in 293T cells is unlikely. Nevertheless, control experiments using VSV, a virus known to be highly sensitive to the establishment of an antiviral state (51;52;122;142;174;206), demonstrated that cells expressing increased levels of NiV N did not impair the ability of VSV to replicate normally. This indicated that mechanisms of the innate immune response were not triggered in this experimental setup. Additionally, the ability of VSV to replicate normally in cells also indicated that vital cellular functions were not hampered by the over-expression of NiV N proteins. More specifically, the cellular components necessary for viral translation were not consumed by the expression of recombinant NiV N proteins, thereby allowing other viral proteins to be synthesized.

4.1.2 The response of NiV replication to excess amounts of NiV N mRNA

RNA interference is an effective way of inhibiting viral replication and has been developed as an antiviral strategy. In this technique, small interfering RNAs and short hairpin RNAs directed against a specific component of the viral genome have been effective at inhibiting viral replication from a variety of viruses (5;22;68;72;99;113). Additionally, the presence of larger RNA sequences, such as viral genes, have also been demonstrated to interfere with viral replication. The presence of N genes for a variety of RNA viruses demonstrated an inhibitory effect on viral replication. A study with Rift Valley Fever Virus (RVFV) has determined that the presence of the RVFV N RNA molecules were able to inhibit the production of progeny viruses independent of the expression of the RVFV N proteins (13). Similar studies with LaCrosse virus and Dengue virus also demonstrated viral interference induced by RNA molecules based on the N gene (63;138;151;152). In the same way, it is possible that the NiV N RNA produced from the NiV N-IRES-CMV construct was capable of interfering with viral replication. However, studies utilizing a transcriptionally-active but translationally-inactive NiV N construct indicated that the inhibition of NiV replication was specifically mediated by the expression of the NiV N proteins and not the NiV N mRNA. Therefore, NiV N RNA did not appear to contribute to the impairment of viral replication. This finding does not rule out the possibility that RNA molecules designed against the NiV N gene could have a role in interfering with viral replication. However, RNA interference does not seem to be

responsible for the decrease in viral replication observed within this experimental setup.

4.1.3 NiV replication in response to increased expression of viral proteins

Since NiV N mRNA did not seem to have a negative effect on viral replication, it was clear that the presence of the NiV N proteins was necessary to impair viral replication. Recent studies with BDV have demonstrated that expression of recombinant BDV N, P or X proteins, all of which are components of the BDV RNP complex, were capable of abrogating viral replication (69).

Altering the levels of the RNP components in a viral system could have adversely effect the balance between viral transcription and genome synthesis. As previously mentioned, the expression of N proteins was needed for the transformation of the transcriptase complex into the replicase complex. This process must therefore be regulated to prevent a disruption of viral replication. Therefore, an over-expression of BDV N proteins would be expected to inhibit viral replication and would further be supported by the findings observed with NiV N proteins.

Unlike what had been observed for NiV, the other components of the RNP complex, BDV X and P were also able to inhibit viral replication. It is possible that the effect observed by the BDV X and P employed alternative mechanisms of inhibition, which were responsible for the impairment of viral replication. The BDV X protein is believed to negatively regulate the viral polymerase through an interaction with BDV P; the mechanisms behind this regulation are unclear (147).

Therefore, since expression of BDV X has the ability to inhibit the polymerase function, it would be expected that increased expression of the X protein would likely impair virus replication. Nevertheless, paramyxoviruses do not have an X protein or a known equivalent protein as a component of their RNP complex, so the effect that the X protein could have on viral replication it is not likely a factor with respect to the findings observed within this thesis. Based on the model for VSV, the role of the P protein during viral replication is to act as a co-factor for the L protein, and to maintain N proteins in a soluble state so that they are available for viral replication. Insufficient levels of P proteins will have a negative effect on viral replication. However based on the current theories of replication, increased levels of the P protein would not be expected to interfere with the production of viral RNA. Unlike the NiV N proteins, which were shown to inhibit viral transcription (Section 3.2.10), the P proteins were not expected to inhibit a specific aspect of viral replication. Instead, it was possible that the increased expression of the BDV P proteins had an indirect negative effect on viral replication, by possibly activating a host response. However, the effect that increasing the expression of BDV P proteins had on viral replication, and possibly the host response, may not be applicable for other viruses. NiV P proteins were expressed at high levels in 293T cells and did not have any negative effects on viral replication, suggesting that viral replication was not affected nor was an inhibitory host response initiated and that the inhibition of NiV replication is a direct result of the increased expression of the NiV N protein.

4.1.4 NiV F and G protein-mediated fusion in the presence of recombinant NiV N proteins

Viral entry is the first stage at which viral replication could be disrupted. If the cellular receptors, which allow the attachment of NiV to the cell membrane were blocked viral replication could also be subsequently impaired. Receptor-mediated viral interference has been demonstrated for NiV by the expression of recombinant NiV G proteins (163). It has been described that cells stably expressing NiV G proteins were resistant to infection at the level of viral entry (163). These authors suggested that the recombinant NiV G protein was able to occupy the viral receptors preventing the virus from binding and entering cells (163). It could be possible that NiV N proteins could similarly interact with the cellular receptors (ephrin B2 and ephrin B3) and subsequently block viral entry. Previous studies with MeV, have demonstrated that MeV N proteins can be found on the surface of cells associated with cell surface proteins (119). There are a number of possibly ways that NiV N proteins could interact with cellular receptors to inhibit viral entry. NiV N proteins could interact with newly synthesized cellular receptors within the cell and prevent them from being transported to the cell surface. NiV N proteins could interact with newly synthesized cellular receptors within cells and this complex could be transported to the surface of the cell, while the presence of the NiV N protein may block the docking sites for viral entry. For these two scenarios to occur NiV N proteins would have to be shunted through the secretory pathway, which is unlikely since NiV N proteins have not been shown to be targeted towards the endoplasmic

reticulum (ER) or golgi. However, studies specifically looking at whether NiV N proteins are targeted to the ER/golgi have not been done. The final possibility could be that NiV N proteins interacted with surface proteins or was secreted from cells using an alternative pathway. Then it may be possible that NiV N proteins could interact with cellular receptors found on the surface of adjacent cells thereby blocking viral attachment and entry. Other viral N proteins have demonstrated their ability to interact with proteins on the cell surface. For example, MeV N proteins have been shown to be released from cells and capable of binding two distinct surface proteins on cells: FcγRII, which has a speculated role in immunosuppression and a new cellular receptor termed "the nucleoprotein receptor" (108;155). Therefore, it could be possible that NiV N proteins bound to the cellular receptor and blocked the ability of the virus to attach to cells, thereby causing the reduction in viral replication. If viral entry were inhibited at increasing levels of NiV N proteins, this would be observed by a dose-dependent reduction in viral replication. Results demonstrated that in the presence of excess amounts of NiV N proteins NiV F and G protein-mediated fusion was not inhibited. Since NiV N proteins did not inhibit NiV F and G-mediated fusion, the viral core was likely delivered into cells containing excess amounts of N protein. These findings suggested that instead of interfering with viral entry the NiV N protein must be interfering with a later stage of viral replication.

4.1.5 The effect of "false" NC-structures have on NiV replication

It has been commonly observed that paramyxovirus N proteins cause a punctate staining pattern in cells when visualized by IFA (8;11). This staining pattern is indicative of the ability of N proteins to encapsidate RNA, whether cellular or viral RNA, and form elongated NC-structures (8). Encapsidation of the viral genome is mediated through an interaction between the N protein and its corresponding P protein (42;173;200). P proteins are believed to maintain N proteins in a soluble form by directing them towards binding viral RNA and preventing non-specific binding to cellular RNA (42;75;91;173;200). Therefore, the production of NC-structures is likely representative of targeted binding of viral RNA. The findings in this thesis demonstrated that cells expressing recombinant NiV N proteins were capable of forming herringbone structures, which resembled typical NC-structures. It could be speculated that the incoming viral polymerase might be recruited towards "false" NC-structures and away from replication of the "true" NC-structures, thereby causing a reduction in viral replication. This question was addressed by maintaining NiV N proteins in a soluble state through the co-expression of NiV P proteins. It was observed that when NiV N was maintained in a soluble state by co-expression with NiV P, NiV N was able to suppress viral replication to similar levels as NiV N when expressed alone. These findings indicated that the recruitment of the viral polymerase towards "false" NC-structures was not the main mechanism for the suppression of viral replication. Instead it is likely that the production of "false" NC-structures rendered the N protein unavailable to interfere with viral replication. It was found

that when maintained in a soluble state, the weak expression of NiV N proteins was capable of inhibiting viral replication to the same extent as when NiV N proteins were expressed alone and at higher levels. These results suggested that by maintaining NiV N proteins in a soluble state it was more effective at disrupting viral replication. Therefore, it is possible that when NiV N is found in "false" NC-structures, it was effectively rendered unavailable and incapable of interacting with the transcriptase to cause the premature formation of the replicase and the subsequent abrogating of viral replication.

4.1.6 The disruption of viral replication

Several lines of evidence indicated that the functions of the polymerase complex were compromised by over-expression of the NiV N protein. It was demonstrated that viral replication was impaired at all stages of the replication pathway when recombinant NiV N proteins were over-expressed.

It has been suggested that as NiV N protein levels increase in an infected cell, the production of viral genomic RNA would begin (103;110;188). As expected, the results presented in this work demonstrated that the synthesis of viral mRNA was suppressed by increasing amounts of the NiV N proteins, which was indicative of low or non-existing presence of the viral transcriptase. Therefore, it was thought that with increasing levels of NiV N protein, the production of viral genomic RNA would accumulate, rather than viral transcripts. However, experimental results showed only low levels of viral full-length RNA found in cells expressing high amounts of N or N and P proteins. Since viral

transcription was disabled and the production of viral proteins was subsequently diminished, the viral L proteins needed to synthesize viral genomic RNA were not produced and therefore were not available to propagate the production of full-length RNA. The synthesis of viral full-length RNA was observed at low levels likely due to the pre-existing viral polymerase and genomic RNA, which were introduced during infection. From these results, the following hypothesis was proposed to explain the observed impairment of viral replication, Figure 46. Prior to infection, NiV N proteins were recombinantly expressed in cells. Upon viral attachment to the cellular receptors and release of the viral RNP into cells, the transcriptase complexes became saturated with recombinant NiV N proteins creating a functional replicase complex through the interaction of the NiV N proteins with the NiV P protein. This replicase complex was deficient in synthesizing viral transcripts but it was able to synthesize full-length viral RNA. Nevertheless, the synthesis of viral genome would be disabled due to the lack of available viral proteins, such as the NiV L proteins, which are essential for the synthesis of full-length viral RNA. Therefore, full-length viral RNA was produced at minimal levels, while only the polymerase complexes present from the input virus were available for the synthesis of mRNA. Additionally, virus assembly and egress would also be inhibited due to the lack of viral proteins, such as the NiV M protein, which is responsible for viral budding and plays an important role in virus assembly. During a normal infection, the process of transcription and synthesis of viral genome are regulated based on the availability of NiV N proteins during the viral life cycle. However, upon the addition of NiV N proteins, the production

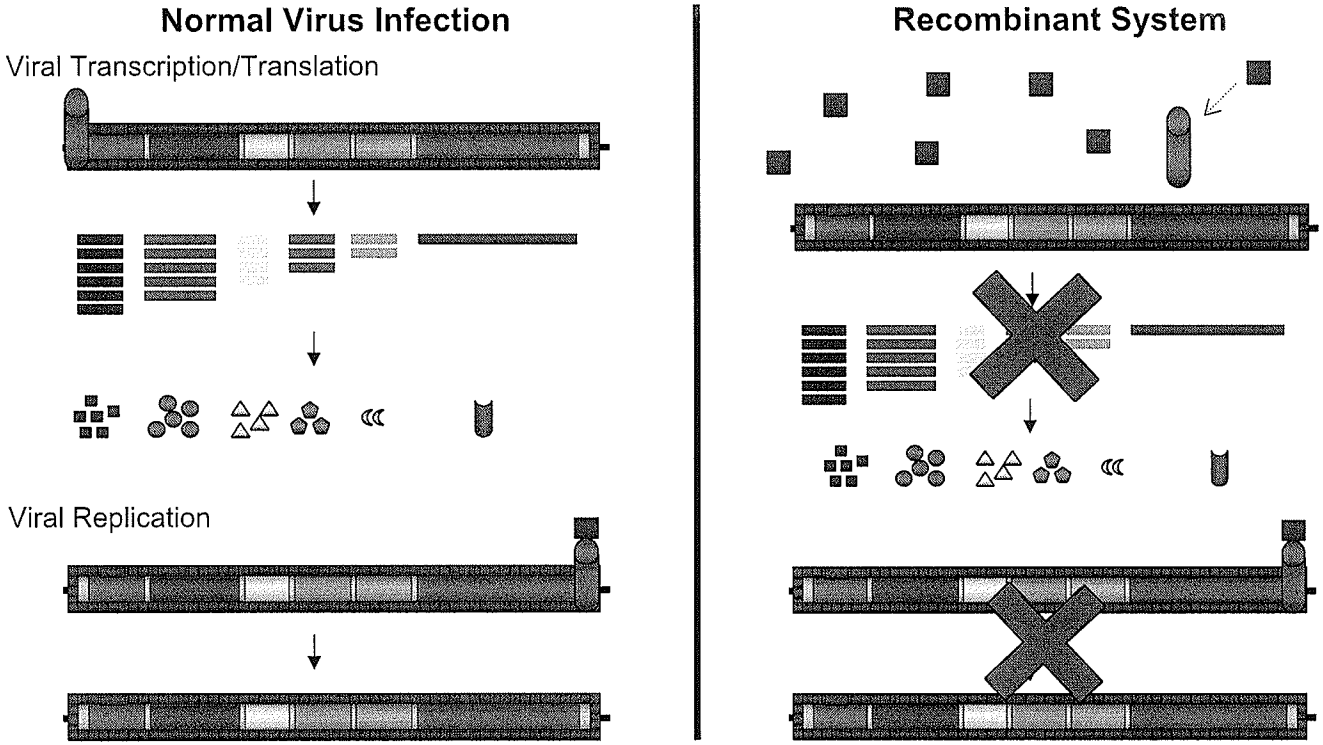

Figure 46: Proposed Mechanisms Driving the Reduction of NiV Replication. Left Side – during normal viral replication, the incoming RNP complex allows for the synthesis viral mRNA by the transcriptase complex, subsequently leading to production of viral proteins. Once the proteins needed to synthesize the viral genome are produced, the NiV N protein binds to the transcriptase complex forming a viral replicase complex. This complex mediates the production of viral full-length RNA. Right side – upon release of the viral RNP into cells, the preexisting recombinant NiV N proteins are able to bind to the viral transcriptase and convert it into a viral replicase, leading to the inhibition in viral transcription and therefore a halt in viral translation. The viral replicase is able to synthesize viral full-length RNA, however, the lack of viral proteins presents prevents the propagation of viral (anti-) genome. Therefore, the amount of full-length viral RNA is suppressed. Overall, the preexisting expression of recombinant NiV N causes an abrogation of both viral transcription and synthesis of viral (anti-)genome.

of viral RNA was disrupted. The shutdown of all viral RNA production caused a suppression of viral replication and production of progeny virus.

4.2 NiV P-Binding Domains Within the NiV N Protein Mediate Viral Interference

The interaction between the NiV N protein and NiV P protein has two main functions during the synthesis of viral RNA: (1) viral genome encapsidation and (2) formation of the viral replicase complex. The primary hypothesis in this thesis is that pre-existing recombinant NiV N proteins can interact with the NiV transcriptase complexes to create NiV replicase complexes prematurely, thus causing the termination of viral replication. The formation of the viral replicase is believed to occur through an interaction between the NiV N protein and the NiV P protein of the transcriptase complex (78). Therefore, the elucidation of the NiV P protein-binding domains found on the NiV N protein provided a useful tool to confirm whether the interaction between NiV N and NiV P proteins was essential to the impairment of viral replication or whether the NiV N protein was interacting with the polymerase complex in a different manner. Two separate NiV P protein-binding domains were identified on the NiV N protein, one at the extreme N-terminus (aa 1-54) and the other at the extreme C-terminus (aa 468-532). These results supported a previous study, which identified a NiV P protein-binding domain within the C-terminal end of NiV N (27). However, the results presented here demonstrate the presence of an additional NiV P protein-binding domain within the N-terminal end of the NiV N protein. If impairment of viral replication

occurs by the premature production of the viral replicase complex, when expressed in cells, the NiV P protein-binding domains within the NiV N protein may be capable of similarly disabling viral replication. The small NiV N peptides encompassing the NiV P protein-binding sites alone might occupy the NiV N protein-binding site on the NiV P protein of the transcriptase complex and prevent full-length NiV N proteins from binding. Binding of these peptides may not convert the transcriptase complex into a functional replicase complex, but may likely have the ability to disable the functions of the polymerase. By expressing various truncated NiV N proteins, it was confirmed that the NiV P protein-binding domains were essential in suppressing viral replication. The presence of one of the two NiV P protein-binding sites from the NiV N protein was sufficient to cause a similar decrease in viral replication as was seen with full-length NiV N proteins. Removal of both of the NiV P protein-binding domains rendered the truncated NiV N protein unable to interfere with viral replication. These results suggested that the presence of the NiV P protein-binding domains found within the NiV N protein were capable of interfering with the functions and/or formation of the viral polymerases.

The presence of the N-terminal NiV P protein-binding domain correlated with a greater reduction in viral translation when compared to the presence of the C-terminal NiV P protein-binding domain. The C-terminal NiV P protein-binding domain did not have as much of a dramatic effect on viral translation; instead, it was capable of suppressing the production of progeny viruses at comparable levels. These results suggested that the N-terminal NiV P protein-binding

domain of the NiV N protein might be more efficient at creating a replicase complex, thereby disabling the transcriptase and subsequent production of viral proteins, and abrogating the production of infectious virus. While the C-terminal NiV P protein-binding domain did not have the ability to disable the transcriptase complex to the same extent as the N-terminal domain, it is possible that the C-terminal domain was able to compromise the function of the viral replicase or render it non-functional. This possibility would explain how viral translation was not greatly reduced, but viral titres were reduced to the same extent as when full-length NiV N was expressed in cells. Overall, it was observed that the NiV P protein-binding domains found within the NiV N protein were essential for the disruption of viral replication, while other components of the NiV N protein were not capable of impairing viral replication. However, it remains unclear whether the truncated NiV N proteins/peptides were able to form a functional replicase complex, as would be expected with the presence of full-length NiV N protein.

The C-terminal NiV P binding domain has the ability to interact with the NiV N protein-binding site found on the transcriptase, but it was not able to reduce viral translation to the same extent as the N-terminal domain. Therefore, it is not understood whether this region was important for the conversion of the transcriptase into the replicase or whether it was simply occupying the NiV N binding site and preventing full-length NiV N from binding and forming a functional replicase complex. Data from the fractionation/solubility studies also indicated that the C-terminal NiV P protein-binding site was important for maintaining NiV N in a soluble form, while the N-terminal NiV P protein-binding

domain did not have such a significant role. The removal of the C-terminal NiV P protein-binding site from the NiV N protein prevented NiV P proteins from being able to retain the truncated NiV N protein in a soluble form. These results imply that this site was essential for viral encapsidation. The production and encapsidation of viral genomic RNA is a highly dynamic process and the presence of two NiV P protein-binding domains found within the NiV N protein could have two separate roles during the viral life cycle. It is hypothesized that the main function of the N-terminal domain of the NiV N protein is responsible for the formation of the replicase complex, while the main function of the C-terminal domain of the NiV N protein is to interact with NiV P to maintain NiV N proteins in a soluble state thereby directing them towards viral encapsidation.

4.3 Additional Factors which may Enhance the NiV N-Mediated Impairment of Viral Replication.

This body of work proposed that the formation of a premature replicase complex plays a major role in the suppression of viral replication. This is dependent upon the interaction between the NiV N protein and the NiV P protein of the transcriptase complex. Although the proposed mechanism, that the premature formation of the replicase was believed to be the dominant mechanism behind the abrogation of viral replication, other factors may play a role.

When the production of progeny viruses was compared to the number of cells initially infected, the data obtained from this study indicated that when cells

transiently expressed NiV N proteins more that 99% of cells were resistant to replicating NiV. However, only 80-90% of cells were shown to be transfected (flow cytometry data not shown) and expressing NiV N proteins; therefore, additional factors likely aided in the ability of the NiV N protein to mediate the impairment of viral replication in the 10-20% of non-transfected cells. One possible explanation could be that NiV N proteins are secreted from cells and taken up by naïve cells to mount their protective affects. It is possible that NiV N proteins could adopt similar strategies of MeV N proteins. MeV N proteins have been shown to enter the late endocytic pathway, where they were subsequently found on the cell surface and secreted into the cell supernatant (119). Furthermore, these N proteins were internalized by naïve cells (108;119;155). Therefore, if NiV N proteins could be secreted from cells and taken up into new cells, they could have the potential to interact with the incoming viral transcriptases to cause a similar disruption in viral replication as previously observed. This could also explain how cells, which were not expressing NiV N was resistant to viral replication.

Although the innate immune response likely did not play a role in the inhibition of NiV replication, the inability of these remaining cells to support viral replication could be explained by the ability of the NiV N proteins to activate some sort of specific cell-mediated resistance against NiV in neighbouring cells. Similar to other paramyxoviruses N proteins, NiV N proteins were present within the nucleus of cells (202). In order to gain access to the nucleus the NiV N protein must have interacted with a specific carrier protein. Therefore, the

interaction between NiV N proteins and carrier proteins may have had a significant role in the disruption of viral replication. One approach for identifying these interacting cellular partners could be elucidated by employing an immunoprecipitation assay of NiV N proteins coupled with mass spectrometry analysis. Currently, NiV N proteins have only been visualized within the nucleus in a recombinant expression system, and should be confirmed by visualization of NiV N proteins within the context of the virus. This may be difficult since it is likely that the presence of the other viral components, such as the NiV P protein, will prevent NiV N proteins from entering the nucleus because of its attempts to maintain NiV N proteins in a soluble state for viral encapsidation in the cytoplasm. Nevertheless, it is not impossible that NiV N proteins could localize to the nucleus, since the N proteins of closely related viruses such as MeV have been found in the nucleus in both viral and recombinant systems (157;162;166;202). It has been speculated that nuclear localization of morbillivirus N proteins correlated with viral persistence and pathogenesis (157;162;166;202). However, their role in the nucleus has not been specifically elucidated. Similarly, the presence of NiV N proteins within the nucleus could have a role in NiV pathogenesis and/or persistence. On the other hand, expression of NiV N proteins within the nucleus may have a beneficial role to the host, such as stimulating various host responses, which may further aid in the suppression of viral replication.

Overall, the interaction of NiV N proteins with cellular proteins and their role in the nucleus could be a factor in the impairment of viral replication. Upon

identification of the cellular transport partner(s), transgenic cell lines could be established which are deficient in the expression of these specific proteins. Further experiments could be conducted in order to determine a potential mechanism for how NiV N proteins localize to the nucleus. For example, it could be determined whether the presence of this cellular protein correlated with viral persistence. Additionally, the life cycle of NiV could be compared between cells expressing this cellular protein and cells deficient in this cellular protein to gain insights on why the NiV N protein may be targeted to the nucleus. Finally, it could be determined whether transient expression of NiV N proteins in these cells would still have the same negative effect on viral replication as was seen in the experiments in this thesis. These examples of experiments could be used to elucidate the role of the NiV N protein within the nucleus.

4.4 Targets for the Creation of Antiviral Substances and Future Work

The results presented in this thesis showed how NiV N proteins and smaller NiV N peptides were capable of interfering with viral replication. These results pave the way for the future development of antiviral molecules designed to disrupt the interactions between components of the polymerase complexes, specifically the NiV N and NiV P proteins. Antiviral therapies for other negative-stranded viruses have mainly focused on interfering with virus-mediated entry and the roles of the surface glycoproteins. Studies on human parainfluenza virus 3 (HPIV3) and NDV have demonstrated that Zanamivir, a compound originally developed as a neuraminidase inhibitor for influenza virus, has the ability to

inhibit HPIV3 and NDV neuraminidase function, while receptor-mediated binding was also inhibited for HPIV3 (148;149). Small molecule inhibitors have also been shown to disrupt viral entry by inhibiting the function of the F protein for MeV and respiratory syncytial virus (RSV) (96;146). Interfering with viral RNA synthesis has been another targeted area for various antiviral systems. Studies with rhabdoviruses have demonstrated that S-adenosylhomocysteine hydrolase inhibitors can prevent the capping function needed to synthesize viral mRNA and have suggested that these techniques could be applied to other members of the order *Mononegavirales* (47;48). Other techniques utilizing RNA interference methods have been able to significantly affect viral replication and reduced RSV titres in cell culture, as well as a variety of animal models (37;38;111;199). Currently, antiviral therapies targeted towards the viral polymerase of negative-stranded RNA viruses have not been extensively studied. However, one new trend in antiviral therapy design is towards the interference of protein-protein interactions of multimeric polymerase complexes (70). Recently, a paper focusing on the influenza A virus, a segmented negative-stranded RNA virus belonging to the family *Orthomyxoviridae,* showed that a small peptide encoding the polymerase acidic protein binding site found within the polymerase basic 1 protein was able to disrupt viral replication, possibly by interrupting the formation of the polymerase complex (70). In a similar manner, this thesis has demonstrated that the expression of a small peptide encoding the NiV P protein-binding domain within the NiV N protein, a component of one of the polymerase complexes, has the ability to disable the formation of a functional replicase

polymerase complex. Therefore, in the same way, the NiV P protein-binding domains found within the NiV N protein could also be further analyzed for its antiviral potential and production of future therapeutics. These data using influenza A correlated nicely with the results in this thesis. These two systems have a similar mechanism of viral abrogation, which indicates that interfering with protein-protein interactions of multimeric polymerase complexes may provide a profitable approach to designing novel antiviral therapies. However, before reaching the stage of creating synthetic molecules to interfere with viral replication, a number of further experiments should be carried out.

Currently, it has not been directly shown whether the NiV N protein was able to interact with the viral transcriptase to form a viral replicase. Observing the interaction between the NiV N proteins or peptides and the transcriptase complex is critical to confirming the proposed mechanism of inhibition of viral replication. Currently, there are no tools to detect the NiV L protein by immunoblot. Therefore, cells transiently expressing NiV N-HA proteins could be infected with NiV and an HA-based radio-immunoprecipitation assay employed in order to detect the presence of NiV L proteins and the other components of the replicase complex. Upon demonstrating the production of a transcriptase or replicase, these complexes should be purified and assessed for their ability to produce viral RNA. Secondly, providing structural information of the NiV N protein through X-ray crystallography or NMR studies would provide important evidence to understand the various structural domains that the NiV N protein contains and provide deeper insights into how the NiV N protein interacts with

other N proteins and with RNA. Furthermore, visualizing the interactions between full-length NiV N protein or the smaller NiV N peptides and NiV P proteins, using similar NMR or X-ray crystallography studies, would provide insights into the interaction between the NiV N and NiV P proteins and whether there are any specific structural domains responsible for these interactions. Additionally, this information would also aid in the design of various synthetic molecules, which would be capable of interfering with the interaction between NiV N and NiV P proteins. Finally, applying the same experimental setup as described within this thesis to other paramyxoviruses and negative-stranded viruses would be a useful approach in determining whether viral replication can be abrogated in a similar fashion.

The work presented in this thesis provides insights into NiV replication, which specifically focused on the interactions between NiV N and NiV P proteins and the various functions that the NiV N protein may have in viral replication. These findings may also be applicable to the replication strategies of other paramyxoviruses and negative-stranded RNA viruses. The significant decrease in viral replication observed in these studies provides an intriguing starting point for the development of antiviral therapeutics that target the interaction betweent the N and P proteins.

5.0 References

1. Expasy-Compute pI/MW tool. 2007.
2. Expasy - Prosite. 2007.
3. ClustalW. 2007.
4. Jpred. 2007.
5. **Adelman, Z.N., I. Sanchez-Vargas, E.A. Travanty, J.O. Carlson, B.J. Beaty, C.D. Blair, and K.E. Olson**. 2002. RNA silencing of dengue virus type 2 replication in transformed C6/36 mosquito cells transcribing an inverted-repeat RNA derived from the virus genome. J Virol **76**:12925-33.
6. **Albertinin, A., A. Wernimont, T. Muziol, R. Ravelli, C. Clapier, G. Schoehn, W. Weissenhorn, and R. Ruigrok**. 2006. Crystal structure of the Rabies virus nucleoprotein-RNA complex. Science **313**:360-363.
7. **Anzai, J., F. Takamatsu, K. Takesuchi, T. Kohno, K. Morimoto, H. Goto, N. Minamoto, and A. Kawai** . 1997. Identification of a phosphatase-sensitive epitope of rabies virus nucleoprotein which is recongized by a monoclonal antibody 5-2-26. Microbiol. Immunol. **41**:229-240.
8. **Banerjee, A., P. Masters, T. Das, and D. Chattopadhyay**. 1989. Specific interaction of vesicular stomatitis virus nucleocapsid protein (N) with the phosphoprotein (NS) prevents its binding with non-specific RNA., p. 121-128. In AnonymousGenetics and Pathogenicity of Negative Strand Viruses. Elsevier, Amsterdam.
9. **Bankamp, B., S.M. Horikami, P.D. Thompson, M. Huber, M. Billeter, and S.A. Moyer**. 1996. Domains of the measles virus N protein required for binding to P protein and self assembly. Virology **216**:272-277.
10. **Becker, S., S. Huppertz, H. Klenk, and H. Feldmann**. 1994. The nucleoprotein of Marburg virus is phosphorylated. J. Gen. Virol. **75**:809-818.
11. **Berhane, Y., J.D. Berry, C. Ranadheera, P. Marszal, B. Nicolas, X. Yuan, M. Czub, and H. Weingartl**. 2006. Production and characterization of monoclonal antibodies against binary ethylenimine inactivated Nipah virus. J Virol Methods **132**:59-68.

12. **Bhella, D., A. Ralph, L. Murphy, and R. Yeo**. 2002. Significant differences in nucleocapsid morphology within the *Paramyxoviridae*. J. Gen. Virol. **83**:1831-1839.

13. **Billecocq, A., M. Vazeille-Falcoz, F. Rodhain, and M. Bouloy**. 2000. Pathogen-specific resistance to Rift Valley fever virus infection is induced in mosquito cells by expression of the recombinant nucleoprotein but not NSs non-structural protein sequences. J Gen Virol **81**:2161-6.

14. **Bonaparte, M.I., A.S. Dimitrov, K.N. Bossart, G. Crameri, B.A. Mungall, K.A. Bishop, V. Choudhry, D.S. Dimitrov, L.F. Wang, B.T. Eaton, and C.C. Broder**. 2005. Ephrin-B2 ligand is a functional receptor for Hendra virus and Nipah virus. Proc Natl Acad Sci U S A **102**:10652-7.

15. **Bossart, K.N., L.F. Wang, B.T. Eaton, and C.C. Broder**. 2001. Functional expression and membrane fusion tropism of the envelope glycoproteins of Hendra virus. Virology **290**:121-35.

16. **Bossart, K.N., L.F. Wang, M.N. Flora, K.B. Chua, S.K. Lam, B.T. Eaton, and C.C. Broder**. 2002. Membrane fusion tropism and heterotypic functional activities of the Nipah virus and Hendra virus envelope glycoproteins. J Virol **76**:11186-98.

17. **Bourhis, J.-M., V. Receveur-Brechot, M. Oglesbee, X. Zhang, M. Buccellato, H. Darbon, B. Canard, S. Finet, and S. Longhi**. 2005. The intrinsically disordered C-terminal domain of the measles virus nucleoprotein interacts with the C-terminal domain of the phosphoprotein via two distinct sites and remains predominantly unfolded. Protein Science **14**:1975-1992.

18. **Box, G.E.P. and D.R. Cox**. 1964. An analysis of transformations. Journal of Royal Statistical Society Series B **26**:211-246.(Abstract)

19. **Buchholz, C.J., C. Retzler, H.E. Homann, and W.J. Neubert**. 1994. The carboxy-terminal domain of Sendai virus nucleocapsid protein is involved in complex formation between phosphoprotein and nucleocapsid-like particles. Virol. **204**:770-776.

20. **Buchholz, C., D. Spehner, R. Drillien, W. Neubert, and H. Homann**. 1993. The conserved N-terminal region of Sendai virus nucleocapsid protein NP is required for nucleocapsid assembly. J. Virol. **67**:5803-5812.

21. **Campbell, J., S. Cosby, J. Scott, B. Rima, S. Martin, and M. Appel**. 1980. A comparison of measles virus and canine distemper virus polypeptides. J. Gen. Virol. **48**:

22. **Caplen, N.J., Z. Zheng, B. Falgout, and R.A. Morgan**. 2002. Inhibition of viral gene expression and replication in mosquito cells by dsRNA-triggered RNA interference. Mol Ther **6**:243-51.

23. **Cattaneo, R., G. Rebmann, A. Schmid, K. Baczko, V. ter Meulen, and M.A. Billeter**. 1987. Altered transcription of a defective measles virus genome derived from a diseased human brain. EMBO J **6**:681-8.

24. **Centers for Disease Control and Prevention**. 1999. Outbreak of Hendra-like virus - Malaysia and Sinagpore, 1998-1999. MMWR Morb Mortal Wkly Rep. **48**:265-269.

25. **Centers for Disease Control and Prevention**. 1999. Update: outbreak of Nipah virus - Malaysia and Singapore, 1999. MMWR Morb Mortal Wkly Rep. **48**:335-337.

26. **Cevik, B., J. Kaesberg, S. Smallwood, J.A. Feller, and S.A. Moyer**. 2004. Mapping the phosphoprotein binding sites on Sendai virus NP protein assembled into nucleocapsids. Virol. **325**:216-224.

27. **Chan, Y.P., C.L. Koh, S.K. Lam, and L.F. Wang**. 2004. Mapping of domains responsible for nucleocapsid protein-phosphoprotein interaction of Henipaviruses. J Gen Virol **85**:1675-84.

28. **Chehadeh, W., S. Chabou, C. Fontier, G. Alm, G. Lion, L. Bocket, P. Wattre, and D. Hober**. 2000. In HIV-1 infected patients, plasma levels of HIV-1 RNA are inversely correlated with IFN alpha responsiveness of whole-blood cultures to Sendai virus. Journal of Clinical Virology **16**:123-128.

29. **Chenik, M., K. Chebli, Y. Gaudin, and D. Blondel**. 1994. *In vivo* interaction of rabies virus phosphoprotein (P) and nucleoprotein (N): existence of two N-binding sites on P protein. J. Gen. Virol. **75**:2889-2896.

30. **Chua, K.B., C.L. Koh, P.S. Hooi, K.F. Wee, J.H. Khong, B.H. Chua, Y.P. Chan, M.E. Lim, and S.K. Lam**. 2002. Isolation of Nipah virus from Malaysian Island flying-foxes. Microbes Infect **4**:145-51.

31. **Chua, K.B., L.F. Wang, S.K. Lam, G. Crameri, M. Yu, T. Wise, D. Boyle, A.D. Hyatt, and B.T. Eaton**. 2001. Tioman virus, a novel paramyxovirus isolated from fruit bats in Malaysia. Virology **283**:215-29.

32. **Chua, KB., WJ. Bellini, PA. Rota, BH. Harcourt, A. Tamin, SK. Lam, TG. Ksiazek, PE. Rollin, SR. Zaki, W. Sheih, CS. Goldsmith, DJ. Gubler, JT. Roehrig, B. Eaton, AR. Gould, J. Olson, H. Field, P.**

Daniels, AE. Ling, CJ. Peters, LJ. Anderson, and BW. Mahy. 2000. Nipah virus: a recently emergent deadly paramyxovirus. Science. **288**:1432-1435.

33. **Chua, KB., KJ. Goh, KT. Wong, A. Kamarulzaman, PS. Tan, TG. Ksiazek, SR. Zaki, G. Paul, SK. Lam, and CT. Tan**. 1999. Fatal encephalitis due to Nipah virus among pig-farmers in Malaysia. Lancet. **354**:1257-1259.

34. **Chuang, J.L. and J. Perrault**. 1997. Initiation of vesicular stomatitis virus mutant polR1 transcription internally at the N gene in vitro. J Virol **71**:1466-75.

35. **Ciancanelli, M.J. and C.F. Basler**. 2006. Mutation of YMYL in the Nipah Virus Matrix Protein Abrogates Budding and Alters Subcellular Localization. J Virol **80**:12070-8.

36. **Coronel, E., K. Murti, T. Takimoto, and A. Portner**. 1999. Human parainfluenza virus type 1 matrix and nucleoprotein genes transiently expressed in mammalian cells induce the release of virus-like particles containing nucleocapsid-like structures. J. Virol. **73**:7035-7038.

37. **Cramer, H.** 2005. Antisense approaches for inhibiting respiratory syncytial virus. Expert Opin Biol Ther **5**:207-20.

38. **Cramer, H., J.R. Okicki, M. Kuang, and Z. Xu**. 2005. Targeted therapy of respiratory syncytial virus by 2-5A antisense. Nucleosides Nucleotides Nucleic Acids **24**:497-501.

39. **Curran, J., R. Boeck, and D. Kolakofsky**. 1991. The Sendai virus P gene expresses both an essential protein and an inhibitor of RNA synthesis by shuffling modules via mRNA editing. EMBO J **10**:3079-3085.

40. **Curran, J., H. Homann, C. Buchcholz, S. Rochat, W. Neubert, and D. Kolakofsky**. 1993. The hypervariable C-terminal tail of the Sendai paramyxovirus nucleocapsid protein is required for template function but not for RNA encapsidation. J. Virol. **67**:4358-4364.

41. **Curran, J., J. Marq, and D. Kolakofsky**. 1992. The Sendai virus nonstructural C protein specifically inhibit viral mRNA synthesis. Virology **189**:647-656.

42. **Curran, J., JB. Marq, and D. Kolakofsky**. 1995. An N-terminal domain of the Sendai paramyxovirus P protein acts as a chaperone for the NP protein during the nascent chain assembly step of genome replication. J Virol. **69**:849-855.

43. **Das, T. and A. Banerjee**. 1992. Role of the phosphoprotein (P) in the encapsidation of presynthesized and de novo synthesized vesicular stomatitis virus RNA by the nucleocapsid protein (N) in vitro. Cell. Mol. Biol. **38**:17-26.

44. **Das, T., AK. Gupta, PW. Sims, CA. Gelfand, JE. Jentoft, and AK. Banerjee**. 1995. Role of cellular casein kinase II in the function of the phosphoprotein subunit of RNA polymerase of vesicular stomatitis virus. J Biol Chem. **270**:24100-24107.

45. **Davis, N., H. Arnheiter, and G. Gertz**. 1986. Vesicular stomatitis virus N and NS proteins form multiple complexes. J. Virol. **59**:751-754.

46. **De, B., A. Lesoon, and A. Banerjee**. 1991. Human parainfluenza virus type 3 transcription in vitro: role of cellular actin in mRNA synthesis. J. Virol. **65**:3268-3275.

47. **De Clercq, E.** 2005. John Montgomery's legacy: carbocyclic adenosine analogues as SAH hydrolase inhibitors with broad-spectrum antiviral activity. Nucleosides Nucleotides Nucleic Acids **24**:1395-415.

48. **De Clercq, E., G. Andrei, J. Balzarini, P. Leyssen, L. Naesens, J. Neyts, C. Pannecouque, R. Snoeck, C. Ying, D. Hockova, and A. Holy**. 2005. Antiviral potential of a new generation of acyclic nucleoside phosphonates, the 6-[2-(phosphonomethoxy)alkoxy]-2,4-diaminopyrimidines. Nucleosides Nucleotides Nucleic Acids **24**:331-41.

49. **Diederich, S., L. Thiel, and A. Maisner**. 2008. Role of endocytosis and cathepsin-mediated activation in Nipah virus entry. Virology

50. **Dietzschold, B., M. Lafon, H. Wang, L. Otvos, E. Celis, W. Wunner, and H. Koprowski**. 1987. Localization and immunological characterization of antigenic domains of rabies virus internal N and NS proteins. Virus Res. **9** :

51. **Durbin, J.E., R. Hackenmiller, M.C. Simon, and D.E. Levy**. 1996. Targeted disruption of the mouse Stat1 gene results in compromised innate immunity to viral disease. Cell **84**:443-50.

52. **Durbin, R.K., S.E. Mertz, A.E. Koromilas, and J.E. Durbin**. 2002. PKR protection against intranasal vesicular stomatitis virus infection is mouse strain dependent. Viral Immunol **15**:41-51.

53. **Egelman, E.H., S.S. Wu, M. Amrein, A. Portner, and G. Murti**. 1989. The Sendai virus nucleocapsid exists in at least four different helical states. J Virol **63**:2233-43.

54. **Elliott, L., M. Kiley, and J. McCormick**. 1985. Descriptive analysis of Ebola virus proteins. Virology **147**:169-176.

55. **Emerson, S.U.** 1982. Reconstitution studies detect a single polymerase entry site on the vesicular stomatitis virus genome. Cell **31**:635-42.

56. **Errington, W. and P. Emmerson**. 1997. Assembly of recombinant Newcastle disease virus nucleocapsid protein into nucleocapsid-like structures is inhibited by the phosphoprotein. J. Gen. Virol. **78**:2335-2339.

57. **Eshaghi, M., W.S. Tan, S.T. Ong, and K. Yusoff**. 2005. Purification and characterization of Nipah virus nucleocapsid protein produced in insect cells. J Clin Microbiol **43**:3172-7.

58. **Field, H., P. Young, J.M. Yob, J. Mills, L. Hall, and J. Mackenzie**. 2001. The natural history of Hendra and Nipah viruses. Microbes Infect **3**:307-14.

59. **Field, H.E., P.C. Barratt, R.J. Hughes, J. Shield, and N.D. Sullivan**. 2000. A fatal case of Hendra virus infection in a horse in north Queensland: clinical and epidemiological features. Aust Vet J **78**:279-80.

60. **Fooks, A., J. Stephenson, A. Warnes, A. Dowsett, B. Rima, and G. Wilkinson**. 1993. Measles virus nucleocapsid protein expressed in insect cells assembles into nucleocapsid-like structures. J. Gen. Virol. **74**:1439-1444.

61. **Freed, E.O.** 2002. Viral late domains. J Virol **76**:4679-87.

62. **Fu, Z., Y. Zheng, W. Wunner, H. Koprowski, and B. Dietzschold**. 1994. Both the N- and the C-terminal domains of the nominal phosphoprotein of rabies virus are involved in binding to the nucleoprotein. Virol. **200**:590-597.

63. **Gaines, P.J., K.E. Olson, S. Higgs, A.M. Powers, B.J. Beaty, and C.D. Blair**. 1996. Pathogen-derived resistance to dengue type 2 virus in mosquito cells by expression of the premembrane coding region of the viral genome. J Virol **70**:2132-7.

64. **Gao, Y. and J. Lenard**. 1995. Cooperative binding of multimeric phosphoprotein (P) of vesicular stomatitis virus to polymerase (L) and template. J Virol. **69**:7718-7723.

65. **Gao, Y. and J. Lenard**. 1995. Multimerization and transcriptional activation of the phosphoprotein (P) of vesicular stomatitis virus by casein kinase-II. EMBO J. **14**:1240-1247.

66. **Garcia, J., B. Garcia-Barreno, A. Vivo, and J. Melero**. 1993. Cytoplasmic inclusions of respiratory syncytial virus-infected cell formation on inclusion-bodies in transfected cells that co-express the nucleoprotein, the phosphoprotein and the 22K protein. Virology **195**:243-247.

67. **Garoff, H., R. Hewson, and D. Opstelten**. 1998. Virus maturation by budding. Microbiol. Mol. Biol. Rev. **62**:

68. **Ge, Q., M.T. McManus, T. Nguyen, C.H. Shen, P.A. Sharp, H.N. Eisen, and J. Chen**. 2003. RNA interference of influenza virus production by directly targeting mRNA for degradation and indirectly inhibiting all viral RNA transcription. Proc Natl Acad Sci U S A **100**:2718-23.

69. **Geib, T., C. Sauder, S. Venturelli, C. Hassler, P. Staeheli, and M. Schwemmle**. 2003. Selective virus resistance conferred by expression of Borna disease virus nucleocapsid components. J Virol **77**:4283-90.

70. **Ghanem, A., D. Mayer, G. Chase, W. Tegge, R. Frank, G. Kochs, A. Garcia-Sastre, and M. Schwemmle**. 2007. Peptide-mediated interference with influenza A virus polymerase. J Virol **81**:7801-4.

71. **Ghildyal, R., M. Murray, N. Vardaxis, and J. Meanger**. 2002. Respiratory syncytial virus matrix protein associates with nucleocapsids in infected cells. J. Gen. Virol. **83**:753-757.

72. **Gitlin, L., S. Karelsky, and R. Andino**. 2002. Short interfering RNA confers intracellular antiviral immunity in human cells. Nature **418**:430-4.

73. **Goh, K.J., C.T. Tan, N.K. Chew, P.S. Tan, A. Kamarulzaman, S.A. Sarji, K.T. Wong, B.J. Abdullah, K.B. Chua, and S.K. Lam**. 2000. Clinical features of Nipah virus encephalitis among pig farmers in Malaysia. N Engl J Med **342**:1229-35.

74. **Gombart, A., A. Hirano, and T. Wong**. 1995. Nucleoprotein phosphorylated on both serine and threonine is preferentially assembled ino the nucleocapsids of measles virus. Virus. Res. **37**:

75. **Green, T., S. Macpherson, S. Qiu, J. Lebowitz, G. Wertz, and M. Luo**. 2000. Study of the assembly of vesicular stomatitis virus N protein: role of the P protein. J. Virol. **74**:9515-9524.

76. **Green, T., X. Zhang, G. Wertz, and M. Luo**. 2006. Structure of the vesicular stomatitis virus nucleoprotein-RNA complex. Science **313**:357-360.

77. **Grubman, M., C. Mebus, B. Dale, M. Yamanaka, and T. Yilma**. 1988. Analysis of the polypeptides synthesized in rinderpest virus-infected cells. Virology **163**:261-267.

78. **Gupta, A.K., D. Shaji, and A.K. Banerjee**. 2003. Identification of a novel tripartite complex involved in replication of vesicular stomatitis virus genome RNA. J Virol **77**:732-8.

79. **Halpin, K., P.L. Young, H. Field, and J.S. Mackenzie**. 1999. Newly discovered viruses of flying foxes. Vet Microbiol **68**:83-7.

80. **Halpin, K., P.L. Young, H.E. Field, and J.S. Mackenzie**. 2000. Isolation of Hendra virus from pteropid bats: a natural reservoir of Hendra virus. J Gen Virol **81**:1927-32.

81. **Hanna, J.N., W.J. McBride, D.L. Brookes, J. Shield, C.T. Taylor, I.L. Smith, S.B. Craig, and G.A. Smith**. 2006. Hendra virus infection in a veterinarian. Med J Aust **185**:562-4.

82. **Harcourt, B.H., L. Lowe, A. Tamin, X. Liu, B. Bankamp, N. Bowden, P.E. Rollin, J.A. Comer, T.G. Ksiazek, M.J. Hossain, E.S. Gurley, R.F. Breiman, W.J. Bellini, and P.A. Rota**. 2005. Genetic characterization of Nipah virus, Bangladesh, 2004. Emerg Infect Dis **11**:1594-7.

83. **Harcourt, B.H., A. Tamin, K. Halpin, T.G. Ksiazek, P.E. Rollin, W.J. Bellini, and P.A. Rota**. 2001. Molecular characterization of the polymerase gene and genomic termini of Nipah virus. Virology **287**:192-201.

84. **Harcourt, B.H., A. Tamin, T.G. Ksiazek, P.E. Rollin, L.J. Anderson, W.J. Bellini, and P.A. Rota** . 2000. Molecular characterization of Nipah virus, a newly emergent paramyxovirus. Virology **271**:334-49.

85. **Harty, R.N. and P. Palese**. 2002. Measles virus phosphoprotein (P) requires the NH_2- and COOH-terminal domains for interactions with the nucleoprotein (N) but only the COOH terminus for interactions with itself. J. Gen. Virol. **76**:2863-2867.

86. **Homann, H.E., P.H. Hofschneider, and W.J. Neubert**. 1990. Sendai virus gene expression in lytically and persistently infected cells. Virology **177**:131-40.

87. **Homann, H., W. Willenbrink, C. Buchholz, and W. Neubert**. 1991. Sendai virus protein-protein interactions studied by a protein-blotting protein-overlay technique: mapping of domains on NP protein required for binding to P protein. J. Virol. **65**:1304-1309.

88. **Hooper, P.T., P.J. Ketterer, A.D. Hyatt, and G.M. Russell**. 1997. Lesions of experimental equine morbillivirus pneumonia in horses. Vet Pathol **34**:312-22.

89. **Hooper, P.T., H.A. Westbury, and G.M. Russell**. 1997. The lesions of experimental equine morbillivirus disease in cats and guinea pigs. Vet Pathol **34**:323-9.

90. **Horikami, S.M., J. Curran, D. Kolakofsky, and S.A. Moyer**. 1992. Complexes of Sendai virus NP-P and P-L proteins are required for defected interfering particle genome replicaiton in vitro. J.Virol. **66**:4901-4908.

91. **Howard, M. and G. Wertz**. 1989. Vesicular stomatitis virus RNA replication: a role for the NS protein. J. Gen. Virol. **70**:2683-2694.

92. **Hsu, C. and D. Kingsbury**. 1982. Topography of phosphate residues in sendai virus proteins. Virology **120**:225-234.

93. **Hsu, V.P., M.J. Hossain, U.D. Parashar, M.M. Ali, T.G. Ksiazek, I. Kuzmin, M. Niezgoda, C. Rupprecht, J. Bresee, and R.F. Breiman**. 2004. Nipah virus encephalitis reemergence, Bangladesh. Emerg Infect Dis **10**:2082-7.

94. **Huang, Y., R. Romito, B. De, and A. Banerjee**. 1993. Characterization of the in vitro system for the synthesis of mRNA from human respiratory syncytial virus. Virol. **193**:862-867.

95. **Huber, M., R. Cattaneo, P. Spielhofer, C. Orvell, E. Norrby, M. Messerli, J.-C. Perriard, and M. Billeter**. 1991. Measles virus phosphoprotein retains the nucleocapsid protein in the cytoplasm. Virology **185**:

96. **Huntley, C.C., W.J. Weiss, A. Gazumyan, A. Buklan, B. Feld, W. Hu, T.R. Jones, T. Murphy, A.A. Nikitenko, B. O'Hara, G. Prince, S. Quartuccio, Y.E. Raifeld, P. Wyde, and J.F. O'Connell**. 2002. RFI-641, a potent respiratory syncytial virus inhibitor. Antimicrob Agents Chemother **46**:841-7.

97. **Jack, P.J., D.B. Boyle, B.T. Eaton, and L.F. Wang**. 2005. The complete genome sequence of J virus reveals a unique genome structure in the family Paramyxoviridae. J Virol **79**:10690-700.

98. **Juozapaitis, M., R. Slibinskas, J. Staniulis, T. Sakaguchi, and K. Sasnauskas**. 2005. Generation of Sendai virus nucleocapsid-like particles in yeast. Virus Res **108**:221-4.

99. **Kapadia, S.B., A. Brideau-Andersen, and F.V. Chisari**. 2003.

Interference of hepatitis C virus RNA replication by short interfering RNAs. Proc Natl Acad Sci U S A **100**:2014-8.

100. **Kato, A., K. Kiyotani, M.K. Hasan, T. Shioda, Y. Sakai, T. Yoshida, and Y. Nagai**. 1999. Sendai virus gene start signals are not equivalent in reinitiation capacity: moderation at the fusion protein gene. J Virol **73**:9237-46.

101. **Katze, M., Y. He, and M. Gale Jr**. 2002. Viruses and interferon, a fight for supremacy. Nature Reviews Immunology **2**:675-687.

102. **Kho, C.L., W.S. Tan, B.T. Tey, and K. Yusoff**. 2004. Regions on nucleocapsid protein of Newcastle disease virus that interact with its phosphoprotein. Arch. Virol. **149**:997-1005.

103. **Kingsbury, DW.** 1974. The molecular biology of paramyxoviruses. Med Microbiol Immunol (Berl). **160**:73-83.

104. **Kingston, R., D. Hamel, L. Gay, F. Dahlquist, and B. Matthews**. 2004. Structural basis for the attachment of a paramyxoviral polymerase to its template. PNAS **101**:8301-8306.

105. **Kingston, R., W. Baase, and L. Gay**. 2004. Characterization of nucleocapsid binding by the measles virus and mumps virus phosphoproteins. J. Virol. **78**:8630-8640.

106. **Komada, H., M. Tsurudome, H. Bando, M. Nishio, A. Yamada, M. Hishiyama, and Y. Ito**. 1989. Virus specific polypeptides of human parainfluenza virus type 4 and their synthesis in infected cells. Virology **171**:254-259.

107. **Krug, R., M. Shaw, B. Broni, G. Shapiro, and O. Haller**. 1985. Inhibition of influenza viral mRNA synthesis in cells expressing the interferon-induced Mx gene product. Journal of Virology **56**:201-206.

108. **Laine, D., M.-C. Trescol-Biemont, S. Lonhi, G. Libeau, J. Marie, P.-O. Vidalain, O. Azocar, A. Diallo, B. Canard, C. Rabourdin, and H. Valentin**. 2003. Measles virus (MV) nucleoprotein binds to a novel cell surface receptor distinct from FcγRII via its C-terminal domain: role in MV-induced immunosupression. . J. Virol. **77**:11332-11346.

109. **Lamb, R. and PW. Choppin**. 1977. The synthesis of Sendai virus polypeptides in infected cells. III. Phosphorylation of polypeptides. Virology **81**:382-397.

110. **Lamb, R. and D. Kolakofsky**. 2001. Paramyxoviridae: The viruses and their replication, p. 1305-1340. In B. eds. Fields, D. Knipe, P.

Howley, and D. Griffin (eds.), Fields' Virology. Lippincott Williams and Wilkins, Philadelphia.

111. **Leaman, D.W.** 2005. 2-5A antisense treatment of respiratory syncytial virus. Curr Opin Pharmacol **5**:502-7.

112. **Lee, C., D. Hodgins, J.G. Calvert, S.K. Welch, R. Jolie, and D. Yoo**. 2006. Mutations within the nuclear localization signal of the porcine reproductive and respiratory syndrome virus nucleocapsid protein attenuate virus replication. Virology **346**:238-50.

113. **Lee, N.S., T. Dohjima, G. Bauer, H. Li, M.J. Li, A. Ehsani, P. Salvaterra, and J. Rossi**. 2002. Expression of small interfering RNAs targeted against HIV-1 rev transcripts in human cells. Nat Biotechnol **20**:500-5.

114. **Lehle, C., G. Razafitrimo, J. Razainirina, N. Andriaholinirina, S.M. Goodman, C. Faure, M.C. Georges-Courbot, D. Rousset, and J.M. Reynes**. 2007. Henipavirus and Tioman virus antibodies in pteropodid bats, Madagascar. Emerg Infect Dis **13**:159-61.

115. **Lim, C.C., W.L. Lee, Y.S. Leo, K.E. Lee, K.P. Chan, A.E. Ling, H. Oh, A.P. Auchus, N.I. Paton, F. Hui, and P.A. Tambyah**. 2003. Late clinical and magnetic resonance imaging follow up of Nipah virus infection. J Neurol Neurosurg Psychiatry **74**:131-3.

116. **Lindman, H.** 1974. Analysis of variance in complex experimental designs. W. H. Freeman & Co., San Francisco.

117. **Luby, S.P., M. Rahman, M.J. Hossain, L.S. Blum, M.M. Husain, E. Gurley, R. Khan, B.N. Ahmed, S. Rahman, N. Nahar, E. Kenah, J.A. Comer, and T.G. Ksiazek**. 2006. Foodborne transmission of Nipah virus, Bangladesh. Emerg Infect Dis **12**:1888-94.

118. **Marcus, P.I. and M.J. Sekellick**. 1980. Interferon induction by viruses. III. Vesicular stomatitis virus: interferon-inducing particle activity requires partial transcription of gene N. J Gen Virol **47**:89-96.

119. **Marie, J.C., F. Saltel, J.M. Escola, P. Jurdic, T.F. Wild, and B. Horvat**. 2004. Cell surface delivery of the measles virus nucleoprotein: a viral strategy to induce immunosuppression. J Virol **78**:11952-61.

120. **Markwell, M. and C. Fox**. 1980. Protein-protein interactions within paramyxoviruses identified by native disulphide bonding or reversible chemical cross-linking. J. Virol. **33**:152-166.

121. **Mebatsion, T., M. Koenig, and K. Conzelmann**. 1996. Budding of rabies virus particles in the absence of the spike glycoprotein. Cell

84:941-951.

122. **Meraz, M.A., J.M. White, K.C. Sheehan, E.A. Bach, S.J. Rodig, A.S. Dighe, D.H. Kaplan, J.K. Riley, A.C. Greenlund, D. Campbell, K. Carver-Moore, R.N. DuBois, R. Clark, M. Aguet, and R.D. Schreiber**. 1996. Targeted disruption of the Stat1 gene in mice reveals unexpected physiologic specificity in the JAK-STAT signaling pathway. Cell **84**:431-42.

123. **Meric, C., D. Spehner, and V. Mazarin**. 1994. Respiratory syncytial virus nucleocapsid protein (N) expressed in insect cells forms nucleocapsid-like structures. Virus Res **31**:187-201.

124. **Middleton, D.J., C.J. Morrissy, B.M. van der Heide, G.M. Russell, M.A. Braun, H.A. Westbury, K. Halpin, and P.W. Daniels**. 2007. Experimental Nipah virus infection in pteropid bats (Pteropus poliocephalus). J Comp Pathol **136**:266-72.

125. **Middleton, D.J., H.A. Westbury, C.J. Morrissy, B.M. van der Heide, G.M. Russell, M.A. Braun, and A.D. Hyatt**. 2002. Experimental Nipah virus infection in pigs and cats. J Comp Pathol **126**:124-36.

126. **Morgan, E. and D. Kingsbury**. 1984. Complete sequence of the Sendai virus NP gene from a cloned insert. Virology **135**:279-287.

127. **Morita, E. and W.I. Sundquist**. 2004. Retrovirus budding. Annu Rev Cell Dev Biol **20**:395-425.

128. **Mungall, B.A., D. Middleton, G. Crameri, J. Bingham, K. Halpin, G. Russell, D. Green, J. McEachern, L.I. Pritchard, B.T. Eaton, L.F. Wang, K.N. Bossart, and C.C. Broder**. 2006. Feline model of acute nipah virus infection and protection with a soluble glycoprotein-based subunit vaccine. J Virol **80**:12293-302.

129. **Murray, K., P. Selleck, P. Hooper, A. Hyatt, A. Gould, L. Gleeson, H. Westbury, L. Hiley, L. Selvey, B. Rodwell, and a.l. et**. 1995. A morbillivirus that caused fatal disease in horses and humans. Science **268**:94-7.

130. **Myers, T.M., S. Smallwood, and S.A. Moyer**. 1999. Identification of nucleocapsid protein residues required for Sendai virus nucleocapsid formation and genome replication. J. Gen. Virol. **80**:1383-1391.

131. **Nagai, Y., H. Ogura, and H.-D. Klenk**. 1976. Studies on the assembly of the envelope of Newcastle disease virus. Virology **69**:523-538.

132. **Naruse, H., Y. Nagai, T. Yoshida, M. Hamaguchi, T. Matsumoto, S.**

Isomura, and S. Suzuki. 1981. The polypeptides of mumps virus and their synthesis in infected chick embryo cells. Virology **112**:119-130.

133. **Negrete, O.A., E.L. Levroney, H.C. Aguilar, A. Bertolotti-Ciarlet, R. Nazarian, S. Tajyar, and B. Lee**. 2005. EphrinB2 is the entry receptor for Nipah virus, an emergent deadly paramyxovirus. Nature **436**:401-5.

134. **Nishio, M., M. Tsurudome, M. Kawano, N. Watanabe, S. Ohgimoto, M. Ito, H. Komada, and Y. Ito**. 1996. Interaction between nucleocapsid protein (NP) and phosphoprotein (P) of human parainfluenza virus type 2: one of the two NP binding sites on P is essential for granule formation. J. Gen. Virol. **77**:2457-2463.

135. **Nishio, M., M. Tsurudome, M. Kawano, N. Watanabe, S. Ohgimoto, M. Ito, H. Komada, and Y. Ito**. 1999. Mapping of domains on the human parainfluenza virus type 2 nucleocapsid protein (NP) required for NP-phosphoprotein or NP-NP interaction. J. Gen. Virol. **80**:2017-2022.

136. **O'Sullivan, J.D., A.M. Allworth, D.L. Paterson, T.M. Snow, R. Boots, L.J. Gleeson, A.R. Gould, A.D. Hyatt, and J. Bradfield**. 1997. Fatal encephalitis due to novel paramyxovirus transmitted from horses. Lancet **349**:93-5.

137. **Olson, J.G., C. Rupprecht, P.E. Rollin, U.S. An, M. Niezgoda, T. Clemins, J. Walston, and T.G. Ksiazek**. 2002. Antibodies to Nipah-like virus in bats (Pteropus lylei), Cambodia. Emerg Infect Dis **8**:987-8.

138. **Olson, K.E., S. Higgs, P.J. Gaines, A.M. Powers, B.S. Davis, K.I. Kamrud, J.O. Carlson, C.D. Blair, and B.J. Beaty**. 1996. Genetically engineered resistance to dengue-2 virus transmission in mosquitoes. Science **272**:884-6.

139. **Pal, R., M.S. Reitz Jr, E. Tschachler, R.C. Gallo, M.G. Sarngadharan, and F.D. Veronese**. 1990. Myristoylation of gag proteins of HIV-1 plays an important role in virus assembly. AIDS Res Hum Retroviruses **6**:721-30.

140. **Paterson, D.L., P.K. Murray, and J.G. McCormack**. 1998. Zoonotic disease in Australia caused by a novel member of the paramyxoviridae. Clin Infect Dis **27**:112-8.

141. **Pattnaik, A. and GW. Wertz**. 1991. Cells that express all five proteins of vesicular stomatitis virus from cloned cDNAs support replication, assembly and budding of defective interfering particles. Proc Natl

Acad Sci USA. **88**:1379-1383.

142. **Pavlovic, J., T. Zurcher, O. Haller, and P. Staeheli** . 1990. Resistance to influenza virus and vesicular stomatitis virus conferred by expression of human MxA protein. J Virol. **64**:3370-3375.

143. **Peluso, R. and S. Moyer**. 1984. Vesicular stomatitis virus proteins required for the in vitro replication of defective interfering particle genome RNA, p. 153-160. In AnonymousNonsegmented negative strand viruses. Academic Press Inc., New York, N.Y.

144. **Peluso, R. and S. Moyer**. 1988. Viral proteins required for the *in vitro* replication of vesicular stomatitis virus defective interfering particles genome RNA. Virology **162**:369-376.

145. **Perez, M., D.L. Greenwald, and J.C. de la Torre**. 2004. Myristoylation of the RING finger Z protein is essential for arenavirus budding. J Virol **78**:11443-8.

146. **Plemper, R.K., K.J. Erlandson, A.S. Lakdawala, A. Sun, A. Prussia, J. Boonsombat, E. Aki-Sener, I. Yalcin, I. Yildiz, O. Temiz-Arpaci, B. Tekiner, D.C. Liotta, J.P. Snyder, and R.W. Compans**. 2004. A target site for template-based design of measles virus entry inhibitors. Proc Natl Acad Sci U S A **101**:5628-33.

147. **Poenisch, M., G. Unterstab, T. Wolff, P. Staeheli, and U. Schneider**. 2004. The X protein of Borna disease virus regulates viral polymerase activity through interaction with the P protein. J Gen Virol **85**:1895-8.

148. **Porotto, M., P. Carta, Y. Deng, G.E. Kellogg, M. Whitt, M. Lu, B.A. Mungall, and A. Moscona**. 2007. Molecular determinants of antiviral potency of paramyxovirus entry inhibitors. J Virol **81**:10567-74.

149. **Porotto, M., M. Fornabaio, O. Greengard, M.T. Murrell, G.E. Kellogg, and A. Moscona**. 2006. Paramyxovirus receptor-binding molecules: engagement of one site on the hemagglutinin-neuraminidase protein modulates activity at the second site. J Virol **80**:1204-13.

150. **Portner, A. and K. Murti**. 1986. Localization of P, NP, and M proteins on Sendai virus nucleocapsid using immunogold labeling. Virology **150**:469-478.

151. **Powers, A.M., K.I. Kamrud, K.E. Olson, S. Higgs, J.O. Carlson, and B.J. Beaty**. 1996. Molecularly engineered resistance to California serogroup virus replication in mosquito cells and mosquitoes. Proc

Natl Acad Sci U S A **93**:4187-91.

152. **Powers, A.M., K.E. Olson, S. Higgs, J.O. Carlson, and B.J. Beaty**. 1994. Intracellular immunization of mosquito cells to LaCrosse virus using a recombinant Sindbis virus vector. Virus Res **32**:57-67.

153. **Precious, B., D. Young, A. Bermingham, R. Fearns, M. Ryan, and R. Randall**. 1995. Inducible expression of the P, V, NP genes of the paramyxovirus SV5 in cell-lines and an examination of NP:P and NP:V interactions. J. Virol. **69**:8001-8010.

154. **Qanungo, K.R., D. Shaji, M. Mathur, and A.K. Banerjee**. 2004. Two RNA polymerase complexes from vesicular stomatitis virus-infected cells that carry out transcription and replication of genome RNA. Proc Natl Acad Sci U S A **101**:5952-7.

155. **Ravanel, K., C. Castelle, T. Defrance, T. Wild, D. Charron, Lotteau V, and C. Rabourdin-Combe**. 1997. Measles virus nucleocapsid protein binds to FcγRII and inhibits human B-cell antibody production. J. Exp. Med. **186**:269-278.

156. **Reynes, J.M., D. Counor, S. Ong, C. Faure, V. Seng, S. Molia, J. Walston, M.C. Georges-Courbot, V. Deubel, and J.L. Sarthou**. 2005. Nipah virus in Lyle's flying foxes, Cambodia. Emerg Infect Dis **11**:1042-7.

157. **Robbins, S.J. and F. Rapp**. 1982. Restriction of virus-specific protein synthesis in a persistent paramyxovirus infection. Arch Virol **71**:85-91.

158. **Robbins, S. and R. Brussell**. 1979. Structural phosphoproteins associated with purified measles virions and cytoplasmic nucleocapsids. Intervirology **12**:96-102.

159. **Rudolph, M., I. Kraus, A. Dickmanns, M. Eickmann, W. Garten, and R. Ficner**. 2003. Crystal structure of the Borna disease virus nucleoprotein. Struct. **11**:1219-1226.

160. **Ryan, K. and D. Kingsbury**. 1988. Carboxyl-terminal region of Sendai virus P protein is required for binding to viral nucleocapsids. Virology **167**:106-112.

161. **Sanderson, C.M., H.H. Wu, and D.P. Nayak**. 1994. Sendai virus M protein binds independently to either the F or the HN glycoprotein in vivo. J Virol **68**:69-76.

162. **Sato, H., M. Masuda, R. Miura, M. Yoneda, and C. Kai**. 2006. Morbillivirus nucleoprotein possesses a novel nuclear localization

signal and a CRM1-independent nuclear export signal. Virology **352**:121-30.

163. **Sawatsky, B., A. Grolla, N. Kuzenko, H. Weingartl, and M. Czub**. 2007. Inhibition of henipavirus infection by Nipah virus attachment glycoprotein occurs without cell-surface downregulation of ephrin-B2 or ephrin-B3. J Gen Virol **88**:582-91.

164. **Selvey, L.A., R.M. Wells, J.G. McCormack, A.J. Ansford, K. Murray, R.J. Rogers, P.S. Lavercombe, P. Selleck, and J.W. Sheridan**. 1995. Infection of humans and horses by a newly described morbillivirus. Med J Aust **162**:642-5.

165. **Sendow, I., H.E. Field, J. Curran, Darminto, C. Morrissy, G. Meehan, T. Buick, and P. Daniels**. 2006. Henipavirus in Pteropus vampyrus bats, Indonesia. Emerg Infect Dis **12**:711-2.

166. **Shin, Y.S., T. Mori, K. Tomonaga, K. Iwatsuki, C. Kai, and T. Mikami**. 1997. Expression of the nucleocapsid protein gene of the canine distemper virus. J Vet Med Sci **59**:51-3.

167. **Shiraishi, T., S. Misumi, M. Takama, I. Takahashi, and S. Shoji**. 2001. Myristoylation of human immunodeficiency virus type 1 gag protein is required for efficient env protein transportation to the surface of cells. Biochem Biophys Res Commun **282**:1201-5.

168. **Smith, G. and LE. Hightower**. 1981. Identification of the P proteins and other disulfide-linked and phosphorylated proteins of Newcastle disease virus. J. Virol. **37**:256-267.

169. **Sokol, F. and H. Clark**. 1973. Phosphoproteins, structural components of rhabdoviruses. Virology **52**:246-263.

170. **Sokol, F. and H. Koprowski**. 1975. Structure-function relationships and mode of replication of animal rhabdoviruses. Proc. Natl. Acad. Sci. U.S.A **72**:933-936.

171. **Spearman, C.** 1908. The method of right and wrong cases (constant stimuli) with Gauss formulae. Brit. J. Psychol. **2**:227

172. **Spehner, D., R. Drillien, and P.M. Howley**. 1997. The assembly of the measles virus nucleoprotein into nucleocapsid-like particles is modulated by the phosphoprotein. Virol. **232**:260-268.

173. **Spehner, D., A. Kirn, and R. Drillien**. 1991. Assembly of nucleocapsidlike structures in animal cells infected with a vaccinia virus recombinant encoding the Measles virus nucleoprotein. J Virol. **65**:6296-6300.

174. **Staeheli, P. and J. Pavlovic**. 1991. Inhibition of vesicular stomatitis virus mRNA synthesis by human MxA protein. J Virol. **65**:4498-4501.

175. **Strecker, T., A. Maisa, S. Daffis, R. Eichler, O. Lenz, and W. Garten**. 2006. The role of myristoylation in the membrane association of the Lassa virus matrix protein Z. Virol J **3**:93

176. **Stricker, R., G. Mottet, and L. Roux**. 1994. The Sendai virus matrix protein appears to be recruited in the cytoplasm by the viral nucleocapsid to function in viral assembly and budding. J Gen Virol **75 (Pt 5)**:1031-42.

177. **Takimoto, T., K.G. Murti, T. Bousse, R.A. Scroggs, and A. Portner**. 2001. Role of matrix and fusion proteins in budding of Sendai virus. J Virol **75**:11384-91.

178. **Tamin, A., B.H. Harcourt, T.G. Ksiazek, P.E. Rollin, W.J. Bellini, and P.A. Rota**. 2002. Functional properties of the fusion and attachment glycoproteins of Nipah virus. Virology **296**:190-200.

179. **Tan, C.T., K.J. Goh, K.T. Wong, S.A. Sarji, K.B. Chua, N.K. Chew, P. Murugasu, Y.L. Loh, H.T. Chong, K.S. Tan, T. Thayaparan, S. Kumar, and M.R. Jusoh**. 2002. Relapsed and late-onset Nipah encephalitis. Ann Neurol **51**:703-8.

180. **Tan, C.T. and K.T. Wong**. 2003. Nipah encephalitis outbreak in Malaysia. Ann Acad Med Singapore **32**:112-7.

181. **Tan, W.S., S.T. Ong, M. Eshaghi, S.S. Foo, and K. Yusoff**. 2004. Solubility, immunogenicity and physical properties of the nucleocapsid protein of Nipah virus produced in Escherichia coli. J Med Virol **73**:105-12.

182. **tenOever, B.R., M.J. Servant, N. Grandvaux, R. Lin, and J. Hiscott**. 2002. Recognition of the measles virus nucleocapsid as a mechanism of IRF-3 activation. J Virol **76**:3659-69.

183. **tenOever, BR., S. Sharma, W. Zou, Q. Sun, N. Grandvaux, I. Julkunen, H. Hemmi, M. Yamamoto, S. Akira, WC. Yeh, R. Lin, and J. Hiscott**. 2004. Activation of TBK1 and IKKvarepsilon kinases by vesicular stomatis virus infection and the role of viral ribonucleoprotein in the development of interferon antiviral immunity. J Virol. **78**:10636-10649.

184. **Uppal, P.K.** 2000. Emergence of Nipah virus in Malaysia. Ann N Y Acad Sci **916**:354-7.

185. **Vainiopaa, R., B. Ziola, and A. Salmi**. 1978. Measles virus polypeptides

in purified virions and in infected cells. Acta. Pathol. Microbiol. Scand. [B] **86B**:379-385.

186. **Vidal, S. and D. Kolakofsky**. 1989. Modified model for the switch from Sendai virus transcription to replication. J Virol **63**:1951-8.

187. **Vulliemoz, D. and L. Roux**. 2001. 'Rule of Six': how does the Sendai virus RNA polymerase keep count? J. Virol. **75**:4506-4518.

188. **Wagner, RR. and JK. Rose**. 1996. Rhabdoviridae: the viruses and their replication. p. 1121-1136. In B.N. Fields, D.M. Knipe, and P.M. Howley (eds.), Lippincott-Raven Press, Philadelphia, Pa.

189. **Wang, L.F., M. Yu, E. Hansson, L.I. Pritchard, B. Shiell, W.P. Michalski, and B.T. Eaton**. 2000. The exceptionally large genome of Hendra virus: support for creation of a new genus within the family Paramyxoviridae. J Virol **74**:9972-9.

190. **Watanabe, S., T. Noda, and Y. Kawaoka**. 2006. Functional mapping of the nucleoprotein of Ebola virus. J. Virol. **80**:3743-3751.

191. **Weingartl, H., S. Czub, J. Copps, Y. Berhane, D. Middleton, P. Marszal, J. Gren, G. Smith, S. Ganske, L. Manning, and M. Czub**. 2005. Invasion of the central nervous system in a porcine host by nipah virus. J Virol **79**:7528-34.

192. **Westbury, H.A.** 2000. Hendra virus disease in horses. Rev Sci Tech **19**:151-9.

193. **Westbury, H.A., P.T. Hooper, S.L. Brouwer, and P.W. Selleck**. 1996. Susceptibility of cats to equine morbillivirus. Aust Vet J **74**:132-4.

194. **Whelan, S.P. and G.W. Wertz**. 2002. Transcription and replication initiate at separate sites on the vesicular stomatitis virus genome. Proc Natl Acad Sci U S A **99**:9178-83.

195. **Williamson, M.M., P.T. Hooper, P.W. Selleck, H.A. Westbury, and R.F. Slocombe**. 2001. A guinea-pig model of Hendra virus encephalitis. J Comp Pathol **124**:273-9.

196. **Wong, K.T., I. Grosjean, C. Brisson, B. Blanquier, M. Fevre-Montange, A. Bernard, P. Loth, M.C. Georges-Courbot, M. Chevallier, H. Akaoka, P. Marianneau, S.K. Lam, T.F. Wild, and V. Deubel**. 2003. A golden hamster model for human acute Nipah virus infection. Am J Pathol **163**:2127-37.

197. **Wong, S.C., M.H. Ooi, M.N. Wong, P.H. Tio, T. Solomon, and M.J. Cardosa**. 2001. Late presentation of Nipah virus encephalitis and

kinetics of the humoral immune response. J Neurol Neurosurg Psychiatry **71**:552-4.

198. **Wright, P.J., G. Crameri, and B.T. Eaton**. 2005. RNA synthesis during infection by Hendra virus: an examination by quantitative real-time PCR of RNA accumulation, the effect of ribavirin and the attenuation of transcription. Arch Virol **150**:521-32.

199. **Xu, Z., M. Kuang, J.R. Okicki, H. Cramer, and N. Chaudhary**. 2004. Potent inhibition of respiratory syncytial virus by combination treatment with 2-5A antisense and ribavirin. Antiviral Res **61**:195-206.

200. **Yang, J., DC. Hooper, WH. Wunner, H. Koprowski, B. Dietzschold, and ZF. Fu**. 1998. The specificity of rabies virus RNA encapsidation by nucleoprotein. Virology. **242**:107-117.

201. **Yob, J.M., H. Field, A.M. Rashdi, C. Morrissy, B. van der Heide, P. Rota, A. bin Adzhar, J. White, P. Daniels, A. Jamaluddin, and T. Ksiazek**. 2001. Nipah virus infection in bats (order Chiroptera) in peninsular Malaysia. Emerg Infect Dis **7**:439-41.

202. **Yoshida, E., Y.S. Shin, K. Iwatsuki, T. Gemma, N. Miyashita, K. Tomonaga, N. Hirayama, T. Mikami, and C. Kai**. 1999. Epitopes and nuclear localization analyses of canine distemper virus nucleocapsid protein by expression of its deletion mutants. Vet Microbiol **66**:313-20.

203. **Yoshida, T., Y. Nagai, K. Maeno, M. Iinuma, M. Hamaguchi, T. Matsumoto, S. Nagayoshi, and M. Hoshino**. 1979. Studies on the role of M protein in virus assembly using a ts mutant of HVJ (Sendai virus). Virology **92**:139-154.

204. **Yoshida, T., Y. Nagai, S. Yoshii, K. Maeno, T. Matsumoto, and M. Hosino**. 1976. Membrane (M) protein of HVJ (Sendai virus): its role in virus assembly. Virology **71**:143-161.

205. **Zhao, H. and A. Banerjee**. 1995. Interaction between the nucleocapsid protein and the phosphoprotein of human parainfluenza virus 3. J. Biol. Chem. **270**:12485-12490.

206. **Zurcher, T., J. Pavlovic, and P. Staeheli**. 1992. Mechanism of human MxA protein action: variants with changed antiviral properties. EMBO J. **11**:1657-1661.

6.0 Appendices

Buffer Recipes

Solutions for chemical treatment of *E.coli* Top 10 cells

Solution A

10mM $MnCl_2$
50mM $CaCl_2$
10mM MES pH 6.3
Adjust volume with sterile water, filter sterilize and store at 4°C.

Solution B

85ml of Solution A
15ml of glycerol
Filter sterilize and store at 4°C.

6x DNA Gel Loading buffer

30% Glycerol (dissolved in water)
0.25% Bromophenol Blue

SOC medium

20 g Bacto Tryptone
5 g Bacto Yeast Extract
2 ml 5M NaCl
2.5 ml M KCl
10 ml 1M MgCl2
10 ml 1M MgSO4
20 ml 1M Glucose
900 ml water
Adjust to 1000 ml

LB Broth

10 g tryptone
5 g yeast extract
10 g NaCl
Adjust volume to 1000 ml

4X SDS Gel Loading Buffer

20 ml 1M Tris-HCL (pH 7.5)
40 ml 10% SDS
35 ml Glycerol
0.5g Bromophenol Blue
Adjust volume to 100 ml with Water
Before using add BME to a final concentration of 10% per sample

SDS PAGE Gel Recipes (total volume = 10mL)

7% (w/w) Resolving Gel
- 5.7 ml Sterile Water
- 1.7 ml 40% Acrylamide (w/w)*
- 2.5 ml 1.5M Tris-HCL pH 8.8
- 100 µl 10% SDS
- 50 µl 10% Ammonium Persulfate
- 10 µl TEMED

10% (w/w) Resolving Gel
- 4.9 ml Sterile Water
- 2.5 ml 40% Acrylamide (w/w)*
- 2.5 ml 1.5M Tris-HCL pH 8.8
- 100 µl 10% SDS
- 50 µl 10% Ammonium Persulfate
- 10 µl TEMED

12% (w/w) Resolving Gel
- 4.3 ml Sterile Water
- 3.0 ml 40% Acrylamide (w/w)*
- 2.5 ml 1.5M Tris-HCL pH 8.8
- 100 µl 10% SDS
- 50 µl 10% Ammonium Persulfate
- 10 µl TEMED

4% (w/w) Stacking Gel
- 6.4 ml Sterile Water
- 1.0 ml 40% Acrylamide (w/w)*
- 2.5 ml 0.5M Tris-HCL pH 6.8
- 100 µl 10% SDS
- 50 µl 10% Ammonium Persulfate
- 10 µl TEMED

*37.5:1 (w/w)ratio of acrylamide to N,N'-methylene bis-acrylamide

Transfer Buffer
- 2.9 g Tris-Base
- 1.47 g Glycine
- 2 ml 10% SDS
- 100 ml Methanol
- Adjust volume to 500 ml with Water

Stripping buffer

125 ml 1M Tris-HCL (pH 6.7)
40 ml 10% SDS solution
Adjust volume to 200 ml
Before using add 0.7% BME

Cell fractionation Lysis Buffer

0.1 M HEPES
0.05 M Ammonium Chloride
7 mM Potassium Chloride
4.5 mM Magnesium Acetate
Dissolve in Water
0.25% NP-40
0.01% Aprotinin

NP-40 Lysis Buffer

50 mM Tris-HCL (pH 7.5)
150 mM NaCl
0.1% NP-40
Just before use for every 10 ml of buffer:
Add 1 µl Aprotinin
100 µl 100mM PMSF (dilute in isopropanol)

Immunoprecipitation Equilibration Buffer

20 mM Tris-HCL (pH 7.5)
100 mM NaCl
0.1 mM EDTA

5X Formaldehyde Gel Running Buffer

0.1 M MOPS (pH 7.0)
40 mM Sodium Acetate
5 mM EDTA (pH 8.0)
0.1% DEPC

Preparing RNA Samples for Electrophoresis

5 µg RNA (approximately 4 µl)
2 µl 5x Formaldehyde Gel Running Buffer
4 µl Formaldehyde
10 µl Formamide
Heat samples at 65°C for 15 minutes
Add 2 µl of Formaldehyde Gel Loading Buffer

1% Agarose-Formaldehyde Gel

For 50ml mini gel:

- 0.5 g Agarose
- 31 ml DEPC Treated Water
- 10 ml 5X Formaldehyde Gel Running Buffer
- 9 ml 37% Formaldehyde

Formaldehyde gel loading buffer

- 50% Glycerol (dissolved in water)
- 1 mM EDTA (pH 8.0)
- 0.25% Bromophenol Blue
- 0.1% DEPC

20X SSC buffer

- 175.3 g NaCl
- 88.2 g Sodium Citrate
- 800 ml Water
- Adjust pH to 7.0
- Adjust volume to 1000 ml

Summary of primary and secondary antibodies

Antibody	Company	Source	Method	Dilution	Uses
Primary Antibodies					
Anti HA	Sigma®	rabbit	Immunoblot	1:500	Section 3, 6, 7
Anti HA	Sigma®	mouse	IFA	1:100	Section 3
Anti HA – AlexaFluor® 488	Invitrogen™	mouse	IFA	1:100	
Anti NiV	In House	guinea pig	Immunoblot IFA	1:1000 1:100	Section 3, 4, 5, 6, 7
Anti NiV N	In House	mouse	Immunoblot IFA	1:5000 1:200	Section 3, 5, 6
Anti NiV N – FITC	In House	mouse	IFA	1:100	Section 3
Anti NiV P	In House	mouse	IFA Immuno-precipitation Immunoblot	1 :100 5 µg 1 :1000	Section 3, 6
Anti GFP	Santa Cruz	mouse	Immunoblot	1:2500	Section 3, 6, 7
Anti GFP FITC conjugated	Santa Cruz	mouse	IFA	1 :100	Section 3
Anti FLAG HRP conjugated	Sigma®	mouse	Immunoblot	1:5000	Section 6
Anti FLAG	Sigma®	mouse	Immuno-precipitation	4.9µg	Section 6
Anti Lamin A	Sigma®	rabbit	IFA Immunoblot	1 :100 1 :500	Section 3, 6
Anti Actin	Sigma®	mouse	Immunoblot	1:1000	Section 4, 5, 7
Anti VSV G	Sigma®	Rabbit	Immunoblot	1 :10 000	Section 5
Anti PARP	R&D laboratory	Goat	IFA	1 :100	
Phalloidin-AlexaFluor® 568	Invitrogen™		IFA	1 :40	

Secondary Antibodies					
Anti rabbit HRP conjugated	Sigma®	goat	Immunoblot	1:10 000	Section 3, 6
Anti mouse HRP conjugated	KPL®	goat	Immunoblot	1:10 000	Section 3, 5, 6, 7
Anti guinea pig HRP conjugated	Sigma®	goat	Immunoblot	1:10 000	Section 3, 4, 5, 6, 7
Anti rabbit Alexa Fluor® 568 conjugated	Invitrogen™	goat	IFA	1:100	Section 3
Anti mouse Alexa Fluor® 488 conjugated	Invitrogen™	goat	IFA	1:100	Section 3
Anti Goat AlexaFluor® 647	Invitrogen™	chicken	IFA	1:100	

Summary of primers:

Blue: Restriction enzymes incorporated into primers

Stop codons or Start codons incorporated into primers to create a fusion protein

Purple: Nucleotides incorporated into primers to create in frame fusion proteins

Pink: Tags incorporated into primers

Primer Name	Use	Primer Sequence (5' to 3') and Features	Method	Notes
Section 3.2.2				
5' GAPDH		ACCATCTTCCAGGAGCGAGA	Real Time RT-PCR	
3' GADPH		TCATGGATGACCTTGGCCAG	Real Time RT-PCR	
5' Ndiag		ATCAATCGTGGTTATCTTGA	Real Time RT-PCR	
3' Ndiag		CAGCCGAGTTCTGCAACTTGATC	Real Time RT-PCR	
Section 3.2.4				
CR144 Fwd	Clone NiV N ORF into pBK-CMV-IRES with a C-terminal HA-tag	AATGCTAGCATGAGTGATATCTTTGAAGAG *Nhe1*	PCR	
CR113 rev		ATTGGATCC AGCATAATCTGGAACATCATATGGATA *BamHI* HA-TAG CACATCAGCTCTGACGAAATCAAGG	PCR	
CR169-tag rev	Clone NiV N 1-801 into pBK-CMV-IRES with a C-terminal HA-tag	AATGGATCC AGCATAATCTGGAACATCATATGGATA *BamHI* HA-TAG GAATCCTGCCATACCAGTTTCC	PCR	Use with forward primer CR144
CR170-tag rev	Clone NiV N 1-1101 into pBK-CMV-IRES with a C-terminal HA-tag	AATGGATCC AGCATAATCTGGAACATCATATGGATA *BamHI* HA-TAG TGCTGATTTTTGGCCTAGTCTG	PCR	Use with forward primer CR144

CR171-tag rev	Clone NiV N 1-1401 into pBK-CMV-IRES with a C-terminal HA-tag	AATGGATCC AGCATAATCTGGAACATCATATGGATA *BamHI* HA-TAG GGATGTGCTCACAGAACTGCTC	PCR	Use with forward primer CR144
CR172 fwd	Clone NiV N 802-1599 into pBK-CMV-IRES with a C-terminal HA-tag	ATTGCTAGC TTCGCAACCATCAGATTCGGG *Nhe1*	PCR	Use with reverse primer CR113
CR173 fwd	Clone NiV N 481-1599 into pBK-CMV-IRES with a C-terminal HA-tag	ATTGCTAGC CTGGTCTCTGCAGTTATCACC *Nhe1*	PCR	Use with reverse primer CR113
CR174 fwd	Clone NiV N 163-1599 into pBK-CMV-IRES with a C-terminal HA-tag	ATTGCTAGC GCACTTGATGTGATTAGATCTCCG *Nhe1*	PCR	Use with reverse primer CR113
CR186	Clone NiV N 163-1401 into pBK-CMV-IRES with a C-terminal HA-tag	AATGGATCC AGCATAATCTGGAACATCATATGGATA *BamHI* HA-tag GGATGTGCTCACAGAACTGCTC	PCR	Use with CR174
CR110 fwd	Clone NiV N ORF into pECFP-N1	ATTGCTAGCATGAGTGATATCTTTGAAG *Nhe1*	PCR	Creates a fusion protein with CFP
CR111 rev		AATGGTACCTGCACATCAGCTCTGACG *Kpn1*	PCR	
CR176 rev	Clone NiV N 1-162 into pECFP-N1	AATGGATCCGCAAACAATGTTAGTTCCCATCTGAG *BamHI*	PCR	Use with CR144 GC insertion creates a fusion protein with CFP
CR194 fwd	Clone NiV N 163-480 into pECFP-N1	ATTGGATCCCGGGTGCTCATGTCTGTTATCC *BamHI*	PCR	Use with CR174 GC insertion creates a fusion protein with CFP

CR187 fwd	Clone NiV N 481-801 into pECFP-N1	ATTGCTAGCATGCTGGTCTCTGCAGTTATCAC *Nhe1*	PCR	GC insertion creates a fusion protein with CFP
CR188 rev		ATTGGATCCGCGAATCCTGCCATACCAGTTTC *BamHI*	PCR	GC insertion creates a fusion protein with CFP
CR178 rev	Clone NiV N 802-1101 into pECFP-N1	AATGGATCCGCTGCTGATTTTTGGCCTAGTCTG *BamHI*	PCR	Use with CR172 GC insertion creates a fusion protein with CFP
CR189 rev	Clone NiV N 802-1401 into pECFP-N1	AATGGATCCGCGGATGTGCTCACAGAACTGC *BamHI*	PCR	Use with CR172 GC insertion creates a fusion protein with CFP
CR180 fwd	Clone NiV N 1402-1599 into pECFP-N1	ATTGCTAGCATGGGTGGGACCAGATTGACTAATTC *Nhe1*	PCR	
CR181 rev		AATGGATCCGCCACATCAGCTCTGACGAAATC *BamHI*	PCR	GC insertion creates a fusion protein with CFP
CR183 fwd	Clone NiV N 1102-1599 into pECFP-N1	ATTGCTAGCATGCGTCACCATGCTGGAGGAATTG *Nhe1*	PCR	Use with CR181
	Clone NiV N 1102-1401 into pECFP-N1		PCR	Use with CR183 and CR189
Nseq1	Sequences NiV N	CAGCCGAGCTTACGGCCTAC	Sequencing	
Nseq1R		GTAGGCCGTAAGCTCGGCTG	Sequencing	
Nseq2		GATGAGTATTTCATCCCTTG	Sequencing	
Nseq2R		CAAGGGATGAAATACTCATC	Sequencing	
RP001 fwd	Sequences in pECFP-N1	GATCTCGAGCTCAAGCTTCG	Sequencing	
RP004 rev		GATCAGTTATCTAGATCCGG	Sequencing	
M13 fwd	Sequences in pCR®-Blunt II-Topo®	CTGGCCGTCGTTTTAC	Sequencing	
M13 rev		CAGGAAACAGCTATGA	Sequencing	

CMV fwd	Sequences in the CMV promoter	CGCAAATGGGCGGTAGGCGTG	Sequencing	
Lac Z rev	Sequences in the Lac Z gene	CTGCAAGGCGATTAAGTTGG	Sequencing	
N 163-1401 mut2	Mutagenesis primers for N 163-1401	CATAATCTGGAACATCATATGGATAGGATGTGCTCACAGAACTG	Mutagenesis	Inserts GGAT
N 163-1401 mut2R		CAGTTCTGTGAGCACATCCTATCCATATGATGTTCCAGATTATG	Mutagenesis	
N1102-1401 mut1	Mutagenesis primers for N 1102-1401	CAGTTCTGTGAGCACATCCCGGGATCCACCGGTCGCCACC	Mutagenesis	Change G → C
N1102-1401 mut1R		GGTGGCGACCGGTGGATCCCGGGATGTGCTCACAGAACTG	Mutagenesis	
Section 3.2.7				
CR010 fwd	Clone NiV P ORF into pBK-CMV	GCTAGCTCATCCAATGGATAAATTGGAACT *Nhe 1*	RT-PCR	
CR011 rev		CTCGAGTTCAGTGATCAAATATTACCGTCA *Xho 1*	RT-PCR	
CR190 fwd	Clone NiV P ORF into pBK-CMV with a C-terminal FLAG tag	ATTGCTAGCATGGATAAATTGGAACTAGTC *Nhe 1*	PCR	
CR191 rev		ATTCTCGAG CTTGTCGTCGTCGTCCTTGTAGTC *Xho1* FLAG tag AATATTACCGTCAATGATGTC	PCR	
Pseq1	Sequences NiV P	GCAGTACCGTTCACTCTGAG	Sequencing	
Pseq1R		CTCAGAGTGAACGGTACTGC	Sequencing	
Pseq2		GCAAGGGAAAGATGCTCAGC	Sequencing	
Pseq2R		GCTGAGCATCTTTCCCTTGC	Sequencing	
Pseq3		GAGATCCCAAAGATCATCAA	Sequencing	

Pseq3R		TTGATGATCTTTGGGATCTC	Sequencing	
Pmut1	Mutagenesis primers for NiV P	GATCAAACAAAAGCCTGGGAAGATTTTCTGC	Mutagenesis	Changes A → T
Pmut1R		GCAGAAAATCTTCCCAGGCTTTTGTTTGATC	Mutagenesis	
Pmut2		GGAACTATTGGAAAGAGAGTGTCGAACACC	Mutagenesis	Changes T → A
Pmut2R		GGTGTTCGACACTCTCTTTCCAATAGTTCC	Mutagenesis	
Pmut3		CCCATTAAAAAGGGCACAGACGCGAAATATCC	Mutagenesis	Deletes 2 nucleotides
Pmut3R		GGATATTTCGCGTCTGTGCCCTTTTTAATGGG	Mutagenesis	
PFLAG mut 1	Mutagenesis primers for NiV P-FLAG	CGACACTGATCGCTTGAATTATCACGCAGATCATTTAG	Mutagenesis	Changes C → T
PFLAG mut 1R		CTAAATGATCTGCGTGATAATTCAAGCGATCAGTGTCG	Mutagenesis	
Section 3.2.10				
5' IRES	IRES template	CTTAATCTAGAGATTGGGGCAGGGTGGAGAGGTGGGCTCTTCC TGCTT *Xba 1* CCCACTCATCTTATAGCTTTCTTTCCCC	N/A	
3' IRES	IRES template	ATCTGCTAGCCTGTGATATCCTTTCCTCCTTGGTTTGGATCTCGA ATTCG *Nhe1* GATCTGGGGAAAGAAAGCTATAAGAT	N/A	
IRES fwd	Clone IRES into NiV N-CMV	CTTAATCTAGAGATTGGGGC *Xba 1*	PCR	Xba1 and Nhe 1 digestion produce compatible cohesive ends
IRES rev		ATCTGCTAGCCTGTGATATCC *Nhe 1*	PCR	
5' GAPDH		ACCATCTTCCAGGAGCGAGA	Real Time RT-PCR and PCR	PCR product is used to create probes for Northern blots
3' GADPH		TCATGGATGACCTTGGCCAG	Real Time RT-PCR and PCR	

5' N probe		TGAGAATCCTCAAAACTGCT	PCR	PCR product is used to create probes for Northern blots
3' N probe		ATGAACTTCCTTACTGATAG	PCR	
5' M probe		GTTCTCTCAACATCTTCAAC	PCR	PCR product is used to create probes for Northern blots
3' M probe		GACATCAAGAGTATTTCAAG	PCR	
Section 3.2.12				
NiV G fwd		CTCTTGAAGAATAAGATTTG	Reverse Transcription	
NiV L rev		GGCTGATTGTGTCTCAATTG	Reverse Transcription	
NiV G-L fwd		GAATGTTAAATTTAATAGTTC	Real Time PCR	
NiV G-L rev		CAGTCTATGGTCAATTGAATG	Real Time PCR	
Section 3.2.15				
CR215 fwd	Clone NiV N-CMV into NiV P-CMV	ATTACGCGTTAAGATACATTGATG *Mlu1*	PCR	Creates a dual promoter vector expressing NiV N and NiV P
CR216 rev		ATTACGCGTATGCATTAGTTATTAATAGTAATC *Mlu1*	PCR	
Section 3.2.17				
N mut 4	Mutagenesis primers for Δ NiV N ORF	GCCTCTTCAAAGATATCACTCTAGCTAGCTGATATCCTTTCCTC	Mutagenesis	Removes 1st start codon
N mut 4R		GAGGAAAGGATATCAGCTAGCTAGAGTGATATCTTTGAAGAGGC	Mutagenesis	
N mut 5		GAAAGCAGCTCCAACTTTCAGTGACTCGGCAGCACTCGGAG	Mutagenesis	Removes 2nd start codon
N mut 5R		CTCCGAGTGCTGCCGAGTCACTGAAAGTTGGAGCTGCTTTC	Mutagenesis	

2 Log DNA Ladder
New England BioLabs® Inc.

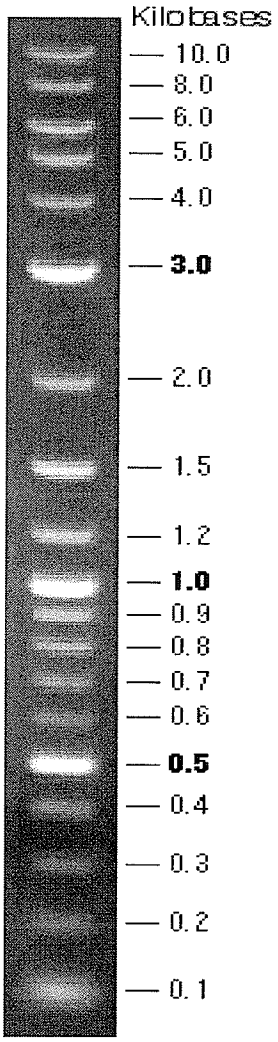

Magic Mark XP™
Western Protein Standard
Invitrogen™

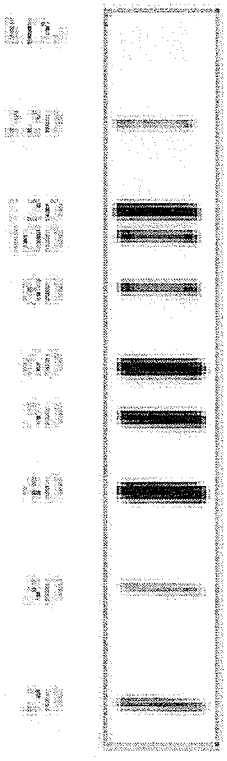

See Blue® Plus2
Prestained Standard
Invitrogen™